

An investigation of the mechanism of chelate formation at group 6  
metal carbonyl centres

by

Celia V Gallagher BSc

for

Dr Conor Long

A thesis submitted for the Degree of Doctor of Philosophy

Dublin City University  
School of Chemical Sciences

September 1993

### **Declaration**

I hereby certify that this material, which I now submit for assessment on the programme of study leading to the award of Doctor of Philosophy is entirely my own work and has not been taken from the work of others save and to the extent that such work has been cited and acknowledged within the text of my work

Signed Celia V. Gallagher

Date 29/9/93

Celia V Gallagher

## Acknowledgments

I would like to thank my supervisor, Dr Conor Long, for his help, patience and understanding (especially about all that broken glassware) for the period of time I spent in D C.U. I would also like to thank Dr D. A. Morton-Blake in Trinity College for the CNDO calculations and Dr R. A Howie for collecting the data used in the crystal structure determination Thanks to the technical staff -Mick, Veronica, Fiontan, Damien and Morris- for all their help

Thanks to the C.L R G past -Graham, Barry, Gerry- and present - Irene, Mick, Maureen, Mary, Ciara- and to all my fellow postgrads especially those in lab AG07 (Albert's group) There are a number of people that I am grateful to for making my stay in D C U enjoyable -Veronica, Barry, Diana, Mary, Ciaran, Carol I would also like to thank Patrick Cahill for all the printing, Patxi Saez de Vitteri for his help with the infrared files and Dr Venita Hanratty for the loan of her books

Finally, I would like to thank my family- Margaret, Neil, Dermot, Martin- and especially Mum and Dad for their support There are not enough words to express my gratitude to my family who were always there for me even when they wanted to run away.

## Table of contents

	Page
Title page	i
Declaration	ii
Acknowledgements	iii
Table of Contents	iv
Dedication	ix
Abstract	x

## Chapter 1

Introduction	1
1.1 Historical background	2
1.2 Structure and bonding	3
1.3 The substitution reactions of the $M(CO)_5(L)$ complexes	8
1.4 The substitution reactions of $M(CO)_5(L)$	11
1.5 The substitution reactions of the $M(CO)_4(L)$ complexes	14
1.6 The detection, isolation and characterisation of some $M(CO)_5(L)$ complexes	16
1.7 The isolation of a novel ligand bridged metal carbonyl complex	18
1.8 References	20

## Chapter 2

CNDO calculations	23
2.1 Introduction	24
2.2 Results and discussion	27
2.2.1 Monitoring the formation of $(Cr(CO)_5)_2(dmbpy)$ at 273K, in toluene solution by infrared spectroscopy	27
2.2.2 CNDO calculations for 2,2'-bipyridine and 2,2'-bipyridinium <sup>2+</sup>	31

2.2.3 CNDO calculations using dimethyldimine and dimethyldiminium	38
2.3 Summary	42
2.4 References	45

## Chapter 3

<b>The isolation, characterisation and reaction of a series of <math>M(CO)_5(L)</math> complexes in the solid and solution state</b>	<b>47</b>
3.1 Introduction	48
3.2 Results and discussion	51
3.2.1 The synthesis and characterisation of $(Cr(CO)_5)_2(dphbpy)$ ( $dphbpy = \mu$ -4,4'-diphenyl-2,2'-bipyridine) and its reactions in solution and solid state	51
3.2.1.1 The preparation of $(Cr(CO)_5)_2(dphbpy)$	51
3.2.1.2 The characterisation of $(Cr(CO)_5)_2(dphbpy)$ by infrared and UV-visible spectroscopy	52
3.2.1.3 The reactions of $(Cr(CO)_5)_2(dphbpy)$ in the solid state, as monitored by infrared spectroscopy	57
3.2.1.4 The reactions of $(Cr(CO)_5)_2(dphbpy)$ in toluene solution, in the absence and presence of excess ligand, as monitored by infrared spectroscopy	59
3.2.1.5 The reaction of $(Cr(CO)_5)_2(dphbpy)$ in toluene solution, in the absence and presence of excess ligand, as monitored by UV-visible spectroscopy	64
3.2.1.6 The reaction of $(Cr(CO)_5)_2(dphbpy)$ in CO saturated toluene, as monitored by UV-visible spectroscopy	70
3.2.1.7 The activation parameters for the formation of $Cr(CO)_4(dphbpy)$ in the absence and presence of excess ligand	73
3.2.1.8 Summary	79

3 2.2 The synthesis and characterisation of the $M(CO)_5(bpa)$ ( $M = Cr$ or $W$ , $bpa = bis\text{-}picolyamine$ ) complexes and their reactions in solution	82
3 2.2 1 The preparation of the $M(CO)_5(bpa)$ complexes	82
3.2 2.2 The characterisation of $M(CO)_5(bpa)$ by infrared, UV-visible and $^1H$ n.m.r. spectroscopy	84
3.2.2.3 The reactions of the $M(CO)_5(bpa)$ complexes in the solid state	89
3 2.2 4 The reactions of the $M(CO)_5(bpa)$ complexes in toluene solution, in the absence and presence of excess ligand, as monitored by infrared spectroscopy	92
3.2 2 5 The reactions of the $M(CO)_5(bpa)$ complexes in toluene solution, in the absence and presence of excess ligand, as monitored by UV-visible spectroscopy	99
3.2.2.6 The reactions of the $M(CO)_5(bpa)$ complexes in CO saturated toluene, as monitored by UV-visible spectroscopy	108
3.2.2 7 The activation parameters for the formation of the $M(CO)_4(bpa)$ species from $M(CO)_5(bpa)$ , in the absence and presence of excess ligand	112
3 2 2 8 Summary	122
3.2 3 The synthesis and characterisation of $Cr(CO)_5(ampy)$ ( $ampy = 2\text{-aminomethylpyridine}$ ) and its reactions in solution and the solid state	125
3 2.3 1 The preparation of $Cr(CO)_5(ampy)$	125
3 2 3 1 The characterisation of $Cr(CO)_5(ampy)$ using infrared and UV-visible spectroscopy	126
3.2 3.2 The reactions of $Cr(CO)_5(ampy)$ in the solid state	131
3 2 3 4 The reactions of $Cr(CO)_5(ampy)$ in toluene solution, in the absence and presence of excess ligand, as monitored by infrared spectroscopy	134
3.2.3.5 The reactions of $Cr(CO)_5(ampy)$ in toluene solution, in the absence and presence of excess ligand, as monitored by UV-visible spectroscopy	138

3.2.3.6 The attempts at observing the proposed equilibrium process of the $\text{Cr}(\text{CO})_5(\text{ampy})$ complex in the presence of excess ligand, as monitored by $^1\text{H}$ n.m.r. spectroscopy	144
3.2.3.7 The reaction of $\text{Cr}(\text{CO})_5(\text{ampy})$ in CO saturated toluene, as monitored by UV-visible spectroscopy	146
3.2.3.8 The determination of the activation parameters for the formation of $\text{Cr}(\text{CO})_4(\text{ampy})$ in the absence of excess ligand	148
3.2.3.9 Summary	151
3.2.4 The synthesis and characterisation of the $\text{M}(\text{CO})_5(\text{bipyam})$ ( $\text{M} = \text{Cr}$ or $\text{W}$ , $\text{bipyam} = 2,2'$ -dipyridylamine) complexes and their reactions in the solid state and solution.	154
3.2.4.1 The preparation of the $\text{M}(\text{CO})_5(\text{bipyam})$ complexes	154
3.2.4.2 The characterisation of the $\text{M}(\text{CO})_5(\text{bipyam})$ complexes by infrared and UV-visible spectroscopy	155
3.2.4.3 The reactions of $\text{M}(\text{CO})_5(\text{bipyam})$ in the solid state	159
3.2.4.4 The reactions of $\text{M}(\text{CO})_5(\text{bipyam})$ in solution	161
3.2.4.5 Summary	167
3.2.5 The synthesis and characterisation of $\text{Cr}(\text{CO})_4(\text{phen})$ ( $\text{phen} = 1,10$ -phenanthroline)	169
3.2.5.1 The preparation of $\text{Cr}(\text{CO})_4(\text{phen})$	169
3.2.5.2 The characterisation of $\text{Cr}(\text{CO})_4(\text{phen})$ by infrared and UV-visible spectroscopy	171
3.2.5.3 The addition of a solution of phen in toluene to a sample of $\text{Cr}(\text{CO})_5(\text{cis-cyclo-octene})$ at 273K, as monitored by infrared spectroscopy	173
3.2.5.4 Summary	175
3.3 Summary	176
3.4 Experimental	179
3.4.1 Materials	179

3 4 2 Equipment	179
3 4 2.1 Infrared spectral studies	179
3 4.2.2 UV-visible spectral studies	181
3.4.2 3 NMR spectral studies	182
3 4.2 4 Thermogravimetric analysis	182
3 4.2.5 Photolysis experiments	182
3 4.2.6 The determination of the activation parameters	183
3 4.3 The synthesis of the $(M(CO)_5)_x(L)$ ( $M = Cr$ or $W$ , $x = 1$ or $2$ ; $L =$ dphbpy, bpa, ampy or bipyam)	184
3.4 3 1 The synthesis of $(Cr(CO)_5)_2(dphbpy)$	184
3 4.3.2 The synthesis of $M(CO)_5(bpa)$ ( $M = Cr$ or $W$ )	184
3.4 3 3 The synthesis of $Cr(CO)_5(ampy)$	185
3 4.3 4 The synthesis of $M(CO)_5(bipyam)$ ( $M = Cr$ or $W$ )	185
3.4.4 The synthesis of $M(CO)_x(L)$ ( $M = Cr$ or $W$ , $x = 3$ or $4$ , $L =$ dphbpy, bpa, ampy or phen)	186
3 4 4 1 The synthesis of $M(CO)_x(L)$ ( $M = Cr$ or $W$ ; $x = 3$ or $4$ , $L =$ dphbpy, bpa or ampy)	186
3.4 4.2 The synthesis of $W(CO)_4(bpa)$	187
3 4 4.3 The synthesis of $Cr(CO)_4(phen)$	187
3.5 References	188

## Chapter 4

### The molecular structure determination of $W(CO)_5(bipyam)$ and infrared spectroscopic analysis of the complex in the solid and solution state

4.1 Introduction	192
4.2 Results and discussion	196
4.2.1 Data collection for $W(CO)_5(bipyam)$	196



4.2.2 The molecular structure of $\text{W}(\text{CO})_5(\text{bipyam})$	203
4.3 Summary	208
4.4 References	210
 Appendix A	 211
 Appendix B	 214

## **Dedication**

For Mum and Dad

# **An investigation of the mechanism of chelate formation at group 6 metal carbonyl centres.**

**Celia V. Gallagher BSc.**

## **Abstract**

The reactions of  $M(CO)_5(S)$  ( $M = Cr$  or  $W$ ,  $S =$  solvent) with a series of ligands,  $L$ , ( $L =$  *dmf*), were investigated. In each case the appropriate chelate  $M(CO)_4(L)$  compounds were formed. The intermediates,  $M(CO)_5(L)$ , were also isolated and characterised by infrared, UV-visible and  $^1H$  nmr spectroscopy. The activation parameters for the formation of the  $M(CO)_4(L)$  species were determined, where possible. The subsequent reactions of the  $M(CO)_5(L)$  intermediates were investigated and a mechanism for the chelate formation is proposed.  $W(CO)_5(2,2'$ -bipyridylamine) was synthesised and structurally characterised by single crystal X-ray diffraction as a model for the monodentately coordinated *dmf* compounds.

An investigation into the effect of conformational change on the  $pK_a$  of the conjugate acid of 2,2'-bipyridine and related ligands was also conducted. Complete neglect of differential overlap (CNDO) calculations revealed that, for non-polar media, there was an increase in  $pK_a$  of the conjugate acid of 2,2'-bipyridine when the angle ( $\theta$ ) between the pyridine rings was in the range  $105^\circ$ - $120^\circ$ . In polar media the  $pK_a$  of the conjugate acid of 2,2'-bipyridine was at a maximum when the ligand adopted the *cis* conformation ( $\theta = 0^\circ$ ). This study was also extended to include the conjugate acid of the dimethyldmfe ligand. The results showed that, for non-polar media, there was an increase in the  $pK_a$  of the conjugate acid of the dimethyldmfe ligand when the angle between the two nitrogens was in the range of  $90^\circ$ - $105^\circ$ . In polar media this angle was revealed to be in the range of  $75^\circ$ - $105^\circ$ .

## **Chapter 1**

### **Introduction**

## 1.1 Historical background

In the last 40 years organometallic compounds have become the subject of general interest and the field is now recognised as an independent branch of chemistry. An independent development, which remained unknown to most chemists until much later, was the synthesis of metal derivatives in which an unsaturated organic compound was bonded to a transition metal. The preparation of the platinum complex of ethylene,  $\text{K}^+[\text{C}_2\text{H}_4\text{PtCl}_3]^-$ , by W. C. Zeise in 1827 marked the birth of transition metal organometallic chemistry. The importance of these compounds was not recognised until after 1950, when their structures were adequately explained. The first metal carbonyl compound, iron pentacarbonyl, was synthesised in 1890 by L. Mond<sup>1</sup> in England. The carbonyls of cobalt (1910), molybdenum (1910), chromium (1926), tungsten (1928), ruthenium (1938) and iridium (1940) were subsequently prepared<sup>2</sup>.

In recent years transition metal organometallic chemistry has become an extremely important area of chemistry, principally due to the utility of members of this class of compounds for catalysing or assisting the transformation of organic substrates<sup>3</sup>. The metal carbonyl compounds have been studied extensively and their use in homogenous catalytic processes is a continuing area of investigation, because of the ease of removal of a carbonyl group, by thermal or photochemical means, to yield a vacant coordination site on the metal centre. It has been suggested that the ability to generate a vacant coordination site is the most important property of a homogeneous catalyst<sup>4</sup>. From the industrial point of view, heterogeneous systems have greater practical advantages over homogeneous ones, notably because of the ease of separation of products from any excess of reactants and from the catalyst. However, a number of homogeneous processes have been developed, because they may give much higher selectivity in reactions, as they operate under milder conditions of temperature and pressure or because of other technical advantages<sup>5</sup>. In 1963 Karl Ziegler and

Guilio Natta were awarded the Nobel Prize for Chemistry in recognition of the development of a class of catalysts. The catalyst was made by treating  $\text{TiCl}_4$  with  $\text{Al}(\text{C}_2\text{H}_5)_3$  and was used in the production of polyethylene. The impetus for the discovery was the lack of raw materials during World War II which led to the need for alternative, synthetic replacements.

The thermal chemistry of group 6 metal carbonyl compounds was well established before recent interest in the photochemical reactivity was stimulated, because of the possibility of more efficient generation of coordinately unsaturated metal carbonyl compounds. The advent of laser flash photolysis, photodiode-array UV-visible spectroscopy and Fourier-transform infrared techniques has heightened this interest because such techniques are suited to the study of such reactive intermediates.

## 1.2 Structure and bonding

From the beginning metal carbonyls raised difficult problems for the current bonding theory. Their unusual properties and stoichiometries for metal compounds could not be accounted for as, their compositions were apparently not related to the formal valency, as it was then understood. A typical transition metal has  $(n + 1)s$ ,  $(n + 1)p$  and  $(n)d$  orbitals and the number of electrons needed to reach the ideal configuration is 18. Organometallic compounds tend to react in such a way as to obtain the favoured 18-electron configuration, including the formation of multiple metal-metal bonds when necessary. To explain the bonding in metal carbonyl compounds a brief discussion of the bonding between carbon monoxide (CO) and a transition metal is presented.

Carbon monoxide is the most important  $\pi$ -bonding ligand. It has a filled  $\sigma$  orbital and two filled  $\pi$  orbitals, localised mainly between carbon and oxygen. It also

possesses two lone pairs of electrons localised on the carbon and oxygen atoms, but directed away from the molecule. The spatial extent of the carbon lone pair is greater than that of the oxygen lone pair, because of the electronegativity difference between carbon and oxygen. CO also possesses two mutually perpendicular  $\pi$  antibonding ( $\pi^*$ ) orbitals, directed away from the CO internuclear region and these two orbitals are empty in the ground state. The filled orbitals are localised to a greater extent on oxygen than carbon and the empty  $\pi^*$  orbitals are more localised on carbon. When CO is bonded to a single transition metal, the M-C-O linkage is linear. If the z direction is chosen as the internuclear axis then the  $d_{z^2}$ ,  $d_{xz}$  and  $d_{yz}$  orbitals of the metal have the correct symmetry to interact with the carbon lone pair, the  $\pi_x^*$  and  $\pi_y^*$  orbitals (Figure 1.2.1)

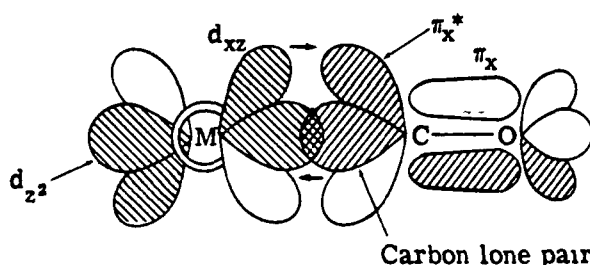


Figure 1.2.1 The M-CO bonding

The net effect of the bonding is that CO donates electron density to the metal in a  $\sigma$  fashion from its carbon lone pair and accepts electron density from the metal in a  $\pi$  fashion into its  $\pi^*$  orbitals. Thus, CO is classified as a  $\sigma$ -donor,  $\pi$ -acceptor ligand. It is the  $\sigma$  bonding which contributes mainly to the total bond energy but the  $\pi$  bonding has important ramifications.

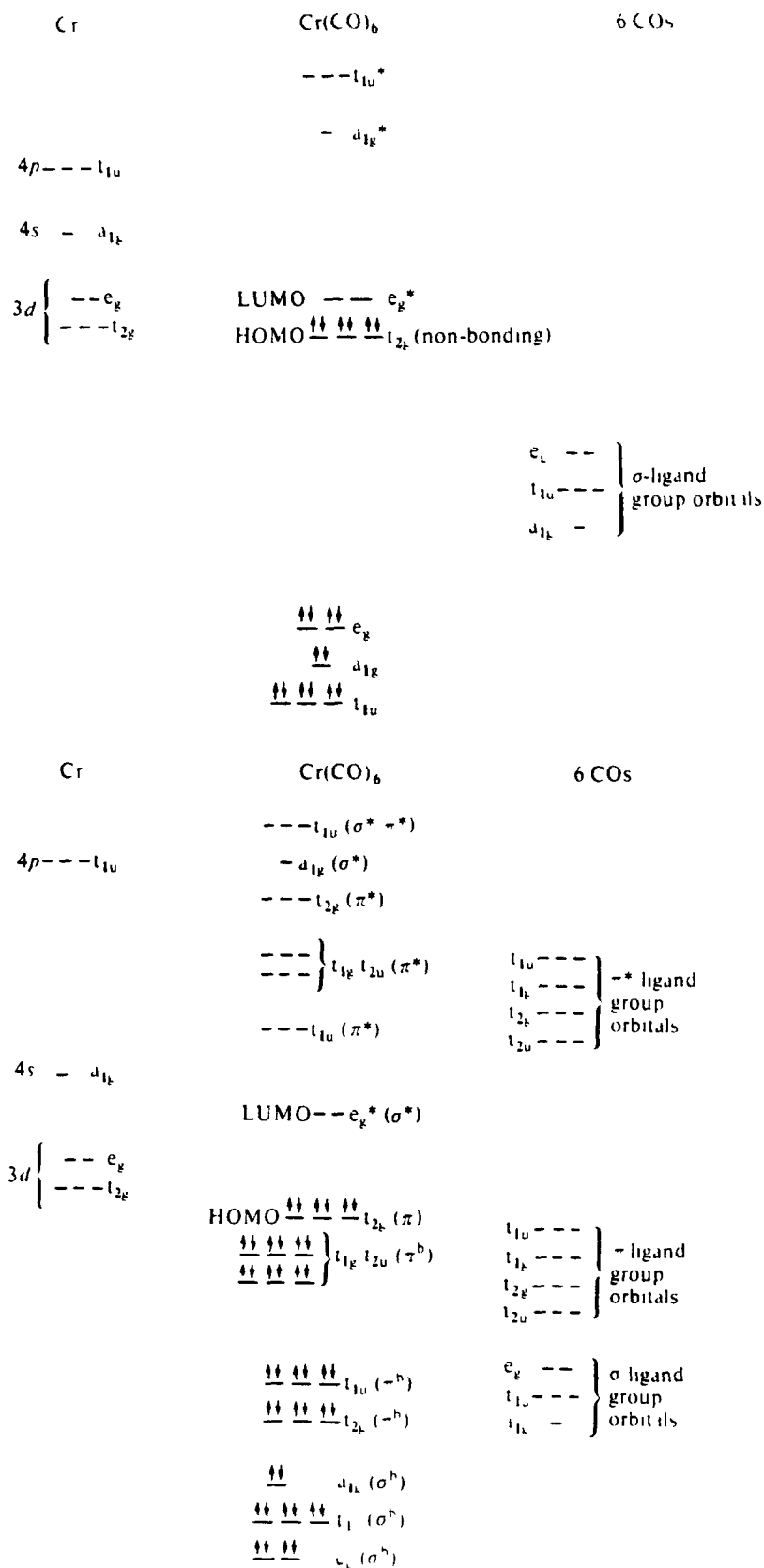


Figure 1.2.2. (a) The MO description of the bonding in Cr(CO)<sub>6</sub>, neglecting π interactions and (b) including π interactions



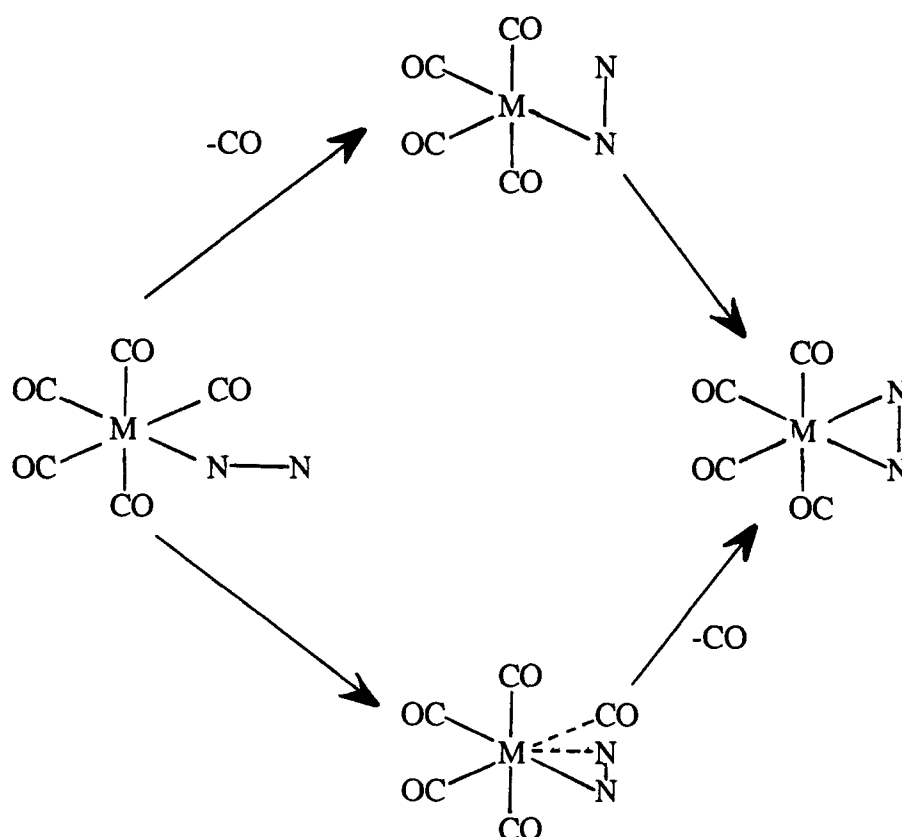
Both interactions weaken the C-O bond, although the  $\pi$  interaction has the greater effect because it directly populates a CO antibonding orbital. It is this ability of CO to accept electron density from the metal which enables the stabilisation of metals in low oxidation states

The molecular orbital view of the bonding in  $\text{Cr}(\text{CO})_6$  is presented in a simplified manner in Figure 1.2.2(a). This model assumes that the CO is a  $\sigma$ -donor molecule, and shows six  $\sigma$  bonds for  $\text{Cr}(\text{CO})_6$  with the six Cr 3d electrons in a non-bonding  $t_{2g}$  orbital. Figure 1.2.2(b) presents the molecular orbital equivalent of the valence bond description. By including the  $\text{Cr-CO}\pi^*$  interaction, the three formerly non-bonding Cr  $t_{2g}$  HOMOs (Highest Occupied Molecular Orbitals) have become strongly bonding, which corresponds to the back donation of electrons shown in Figure 1.2.1. The energy difference between the HOMO and the LUMO (Lowest Unoccupied Molecular Orbital) is increased over that exhibited in Figure 1.2.2, and greatly stabilises  $\text{Cr}(\text{CO})_6$ .

We are currently interested in the mechanism of chelate formation at group 6 metal carbonyl centres. Two possible pathways exist for the process of ring closure in chelation reactions involving bidentate ligands (Scheme 1.2.1). A sixteen valence electron species is formed as the intermediate stage of the upper process while the intermediate stage of the lower process involves a twenty valence electron species. Although a great deal is now known about ligand substitution chemistry of low valent transition metal centres and the formation of chelate products, our knowledge of the structure and reactivity of their reaction intermediates is still limited. Information about the nature of ligand substitution reactions at low valent transition metal centres is useful in systematic organometallic synthesis and in the design of homogenous catalytic processes.

Many studies on the mechanism of chelate forming reactions have been performed using diimine ligands and we have been particularly interested in the mechanism of chelate formation at  $\text{Cr}(\text{CO})_6$  centres and in part  $\text{W}(\text{CO})_6$  centres. The diimine class of ligands such as 2,2'-bipyridine and 1,10-phenanthroline, are very efficient chelating ligands resultant from a balance between their  $\sigma$ -donor and  $\pi$ -acceptor properties and their chelating ability.

Scheme 1 2 1: The two possible pathways that exist for the mechanism of ring closure in chelation reactions involving bidentate ligands



N—N= diimine bidentate ligand

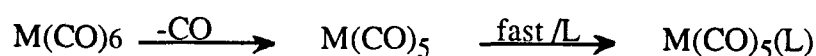
### 1.3 The substitution reactions of the $M(CO)_6$ complexes.

The substitution reactions of  $M(CO)_6$ , which may occur under thermal and/or photochemical conditions, are thought to occur *via* three distinct mechanisms, a dissociative ligand independent path, an associative ligand dependant path or an interchange ligand dependant pathway which involves ligand attack at the metal. A two term rate law governs the substitution reactions of metal hexacarbonyls (equation 1.3.1)

$$-\frac{d[M(CO)_6]}{dt} = k_1[M(CO)_6] + k_2[M(CO)_6][L]$$

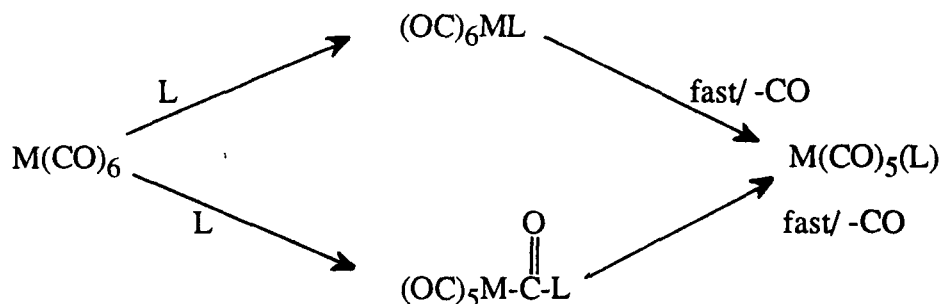
equation 1 3 1

The ligand independent path,  $k_1$ , is consistent with a dissociative route<sup>7</sup> to form a five coordinate intermediate as the rate determining step (equation 1.3 2), while the ligand dependant path is described by  $k_2$ . The associative route<sup>7</sup>, with rate constant  $k_2$ , could involve attack of the ligand at either the carbonyl carbon or metal of  $M(CO)_6$ , (Scheme 1.3.1). The contribution of the  $k_2$  term to the overall rate depends upon the nature of L. One factor that would influence operation of either a dissociative or interchange process is the greater possibility of a sixteen electron intermediate state, as opposed to a twenty electron intermediate state of an associative mode.

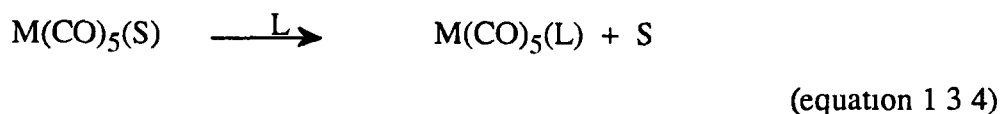
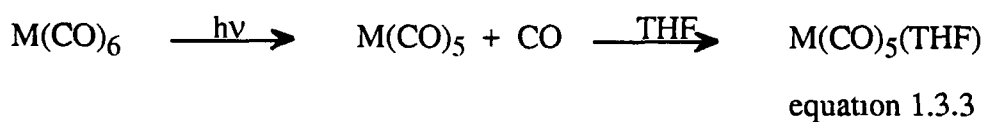


(equation 1 3.2)

Scheme 1 3 1 The two pathways for forming the  $M(CO)_5(L)$  complex



The primary photoproduct, formed upon photolysis of  $M(CO)_6$  has been identified as  $M(CO)_5$ <sup>8</sup> and it seems that this is quite likely the primary product of thermal reactions also Dahlgren and Zink<sup>5</sup> obtained experimental evidence that the primary photochemical process of  $M(CO)_6$  is dissociative in nature In the presence of a donor solvent such as tetrahydrofuran (THF) the solvent acts as a nucleophile and forms a solvent stabilised complex with the coordinately unsaturated pentacarbonyl species (equation 1 3 3) In solvents with poor donor ability, experiments indicate that the  $M(CO)_5$  intermediate is quite reactive Flash photolysis studies show that in CO saturated cyclo-hexane, the rate constant for the recombination of  $Cr(CO)_5$  with CO is approximately  $3 \times 10^6 \text{ mol}^{-1} \text{ dm}^3 \text{ s}^{-1}$



In the presence of a nucleophile the solvent molecule can be displaced, the stronger incoming ligand can displace the solvent because of the weakness of the interaction between the metal pentacarbonyl fragment and solvent (equation 1 3 4)

The substitution of group 6 metal carbonyls with  $\sigma$ -donor ligands results in the displacement of a maximum of three carbonyl ligands. A minimum of three carbonyl ligands must remain to accept electron density from the metal since the  $\sigma$ -donor ligands cannot help decrease the electron build up on the metal. The  $\sigma$ -donor/ $\pi$ -acceptor ligands, like CO, have the capacity to donate electrons to the metal and accept electrons back from the metal into  $\pi^*$  orbitals. The  $\sigma$ -donor/ $\pi$ -acceptor ligands are sometimes capable of substituting for more than three carbonyls. The dimeric ligands, which are of considerable interest to our work, are weaker  $\pi$ -acceptors than CO, but yet are strong  $\sigma$ -donors and can displace CO. These ligands accept  $\pi$  electron density from the metal into the C=N  $\pi^*$  orbitals.

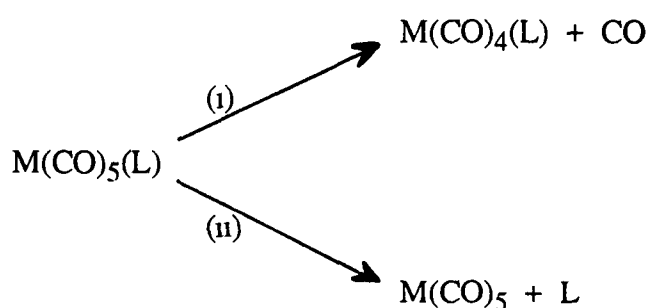
Early work<sup>10</sup> on the substitution of CO from  $M(CO)_6$  by a ligand, L, (L =  $As(C_6H_5)_3$ ,  $P(OC_6H_5)_3$ ,  $P(OCH_2)_3CC_2H_5$ ,  $P(OC_2H_5)_3$  or  $P(\eta-C_4H_9)$ ) led to assumptions that the actual size of the metal influences the effectiveness of the various pathways for carbonyl substitution. It was observed that, upon changing from Cr to W, the dissociative process became less important and the associative path appeared to increase in importance. This was concluded from a comparison of rates for both pathways and the increase in ratio was consistent with the increase in atomic radii from Cr to W. Recent work<sup>11</sup> yielded similar results which anticipated that an interchange pathway may be operative for Mo, as opposed to a dissociative mode relative to Cr. Other work on the substitution reactions of group 6 metal carbonyls observed that the displacement of CO from  $Cr(CO)_6$  by pyridine, which is a weak  $\pi$ -acceptor ligand, allows more Cr-CO  $\pi$ -bonding<sup>12</sup>. This results in an increase in Cr-CO bond strength and thus pyridine could stabilise the transition state in the proposed CO dissociation mechanism.

Although the majority of group 6 metal carbonyl complexes proceed *via* a ligand independent path, as the concentration of the entering ligand and/or

polarity of the solvent is increased the second order reaction becomes more important. Increasing nucleophilicity and  $\pi$ -acceptor ability of the incoming ligand also appear to favour the second order reaction<sup>12</sup>. There is evidence that implies both paths of Scheme 1 3.1 are important for strong nucleophiles. The upper path could proceed *via* an associative or interchange process, but as the associative process would involve a 20 valence electron intermediate, the interchange process is more probable<sup>7,13</sup>.

#### 1.4 The substitution reactions of $M(CO)_5(L)$ ( $M = Mo, Cr, or W$ )

In order to gain an insight into the factors governing the formation of  $M(CO)_4(L)$  from  $M(CO)_5(L)$ , it is necessary to understand the substitution reactions of the  $M(CO)_5(L)$  complexes. Monosubstituted complexes of the type,  $M(CO)_5(L)$ , exhibit reactivity patterns similar to those of the metal hexacarbonyls. These properties are however altered to some extent with the presence of one or more non-carbonyl ligands. The photolysis of  $M(CO)_5(L)$  complexes may result in the loss of either CO or L (Scheme 1 4 1). In the presence of added L the upper path could generate *cis* or *trans* ( $M(CO)_4(L)_2$ ), while the lower path would simply regenerate  $M(CO)_5(L)$ <sup>6</sup>.



(Scheme 1 4 1)

The upper path (i) becomes more important as the strength of the M-L bond increases, despite excitation energies being sufficiently high to result in the loss of CO or L. Thus, for strong ligands (good  $\sigma$ -donor/ $\pi$ -acceptor) complete replacement of the

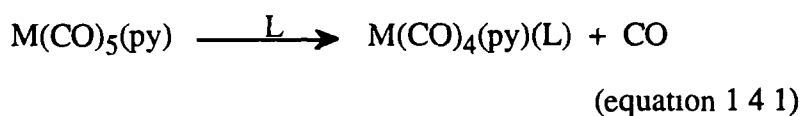
carbonyl ligands may occur, while for ligands such as THF (11),  $M(CO)_5(THF)$ , is virtually the only product. Thermal reactions of group 6 carbonyl derivatives often follow kinetics similar to those of the photolysis reactions above. The nature of the ligand, L, in the  $M(CO)_5(L)$  complexes greatly influences the reaction rate, especially the magnitude of  $k_1$ , the rate constant for the ligand independent path. In virtually all cases the rate of the substitution reaction is greater when L is any ligand other than CO<sup>13,14</sup>. The ligands with good  $\sigma$ -donor but poor  $\pi$ -acceptor ability exhibit significantly faster rates than the ligands closer to CO in bonding, the  $\pi$ -acceptor ligands<sup>12</sup>. The rate law for the substitution reactions of  $M(CO)_5(L)$  complexes, presented in equation 1 4 2, is similar to the rate law for the substitution reactions of the parent hexacarbonyls

$$\frac{-d[M(CO)_5(L)]}{dt} = k_1 [M(CO)_5(L)] + k_2 [M(CO)_5(L)][L']$$

equation 1 4 2

The labilising of  $M(CO)_5(L)$  by L is invariably of the carbonyl ligands *cis* to L, thus the incoming ligand is initially in the *cis* position. The *cis* labilisation could be resultant from the strengthening of the M-CO bond *trans* to L, particularly for poor  $\pi$ -acceptor ligands<sup>16,17</sup>. Angelici<sup>12</sup> divided ligands into two categories of labilising and non-labilising ligands based on their effect on M-CO bonding compared to that of the parent hexacarbonyl. The former have donor atoms which are H, N, O, or the halogens, while donor atoms of non-labilising atoms are P, As, Sb, Mn, and Au. Dobson has offered evidence that halides, and to a lesser extent other ligands, cause relatively more rapid dissociation of *cis* CO compared with *trans* CO groups<sup>18,19</sup>. Studies of the exchange of  $^{13}CO$  with  $Mn(CO)_5(Br)$  or  $Re(CO)_5(Br)$ , which proceed by dissociative CO loss, have shown that CO is lost preferentially from the *cis* position<sup>15</sup>. The substitution reactions of  $M(CO)_5(A)$  by a ligand L<sup>12</sup> were studied and when A is a labilising ligand, such as pyridine, the M-CO bonds *trans* to pyridine are

strengthened, while the M-CO bond *cis* to pyridine is labilised. This results in a greater ease of replacement of CO by an incoming ligand L, and the formation of *cis*-M(CO)<sub>4</sub>(A)(L) (equation 1.4.1)



The rate of CO replacement in this case is more rapid than for that of the parent hexacarbonyl<sup>12</sup>. When the A of M(CO)<sub>5</sub>(A) is a non-labilising ligand such as P(OR)<sub>3</sub>, which is a weaker  $\pi$ -acceptor than CO, substitution by L usually occurs at a position *trans* to the bound ligand. The rate of substitution in this case is approximately the same as that observed for M(CO)<sub>6</sub> itself<sup>12</sup>. The formation of an initial specific product, because of the use of a labilising or non-labilising ligand, may be altered by rearrangement to form a more thermodynamically stable compound<sup>20</sup>.

There have been a number of investigations performed on the effect of the basicity of the ligand on the rate of substitution of the M(CO)<sub>5</sub>(L) complexes. An early study<sup>21</sup>, which investigated the rates and mechanisms of amine displacement from W(CO)<sub>5</sub>(Am) with a series of phosphine and phosphite ligands. The results showed that, with the exception of pyridine, the rates of dissociation of the amine increased with increasing pK<sub>a</sub> value of the amine. Darensbourg and Brown<sup>22</sup> studied the decomposition of the Mo(CO)<sub>5</sub>(Am) complex in the absence and presence of phosphine ligands. They discovered that the rate of reaction was found to depend on the concentration of the nucleophile and increased in the order of increasing nucleophilicity: (η-C<sub>4</sub>H<sub>9</sub>)<sub>3</sub>P > (CH<sub>3</sub>O)<sub>3</sub>P > (C<sub>6</sub>H<sub>5</sub>O)<sub>3</sub>P > PF<sub>3</sub>, which is also the order of increasing pK<sub>a</sub> value of the free ligand.



Connor *et al*<sup>23</sup> have studied the chelation reaction of the  $M(CO)_5(L)$  complexes ( $L = Ph_2PCH_2CH_2CH_2PPh_2$  (dpp),  $Ph_2PCH_2CH_2PPh_2$  (dpe),  $Ph_2PCH_2PPh_2$  (dpm),  $Me_2PCH_2CH_2PMe_2$  (dmpe)) On changing the metal from Cr to W<sup>24</sup> a marked difference in the rate of chelation was observed In the case of the  $M(CO)_5(dpe)$  complex the rate increased by a factor of 85. The rate of chelation also decreased with increasing chain length, implying the greater ease of formation of a four membered ring compared to that of a five or six membered ring The mechanism of chelate formation was thought to be a concerted process, where the stretching of an M-CO bond must be accompanied by the appearance of an incoming ligand in the right orientation Factors that increase the probability of this occurrence increase the rate of the chelation reaction

### 1.5 The substitution reactions of the $M(CO)_4(L)$ complexes.

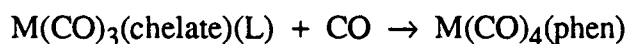
The substitution reactions of the  $M(CO)_4(\text{chelate})$  complexes have been studied by a number of workers<sup>11,25-29</sup> In general, the reactions of the  $M(CO)_4(\text{chelate})$  complexes with a ligand L results in one of three complexes: (i)  $M(CO)_3(L)(\text{chelate})$ , (ii)  $M(CO)_4(L)_2$ , (iii)  $M(CO)_3(L)_3$  The formation of a particular type of compound is dependant upon the nature of the chelating ligand, as the stronger ligands (bpy, phen) tend to be retained and  $M(CO)_3(L)(\text{chelate})$  complexes formed. Weaker ligands, such as norbornadiene, are displaced and the resultant complex is  $M(CO)_4(L)_2$

$$\text{Rate} = (k_1 + k_2 [L])(M(CO)_4(\text{chelate}))$$

equation 1 5.1

The rate law for such reactions may be generalised as that in equation 1 5.1 The reaction may proceed via one of three mechanisms<sup>12</sup> (i) associative ( $M = Mo$  or  $W$ ), (ii) dissociative or (iii) chelate ring opening When the chelated ligand is a diimine,

such as bpy or phen, the dissociation of CO forms a five coordinate intermediate, which reacts with L to form the product. Evidence strongly indicates that dissociation occurs from carbonyl ligands *cis* to the chelated bpy or phen<sup>27,30-32</sup>. Similarly, substitution may occur in the opposite direction, indicating the reversibility<sup>20</sup> of the reaction, as shown in equation 1.5.2



equation 1.5.2

Angelici and Graham<sup>25,27</sup> investigated the reaction of  $\text{Cr}(\text{CO})_4(\text{chelate})$  (chelate = bpy, 4,4'-dimethyl-2,2'-bipyridine (dmbpy), phen or substituted phen) with L (L =  $\text{P}(\text{OC}_2\text{H}_5)_3$ ,  $\text{P}(\text{OCH}_2)_3$  and  $\text{P}(\text{O}_3\text{C}_6\text{H}_9)_3$ , which yielded the *cis*- $\text{M}(\text{CO})_3(\text{L})(\text{chelate})$  complex. When M = Mo or W,<sup>33,26</sup> there were two additional products,  $\text{M}(\text{CO})_4(\text{L})_2$  and  $\text{M}(\text{CO})_3(\text{L})_3$ . For M = Cr, it was found that the reaction proceeded *via* a first order rate law which was found to decrease with increasing  $\text{pK}_a$  values of the bound ligand, within each group of ligands. For M = Mo or W, it was found that the first order rate constant,  $k_1$ , decreased as the  $\text{pK}_a$  value of the bound ligand increased. The second order rate constant, for M = Mo or W, was found to increase with increasing  $\text{pK}_a$  values of the chelated ligand.

These studies show that bpy, phen, and other ligands that are weaker  $\pi$ -acceptors than CO labilise octahedral carbonyl complexes towards dissociative loss of the ligands that are in a *cis* position. The loss of a CO from a *cis* position does not necessarily result in a *fac* geometry for the product  $\text{M}(\text{CO})_3(\text{chelate})(\text{L})$ , as the five coordinate intermediate is often partially fluxional and in several cases fully fluxional on the time scale of the substitution reaction<sup>32</sup>.

## 1.6 The detection, isolation and characterisation of some $M(CO)_5(L)$ complexes.

The advent of rapid spectroscopic techniques facilitated the study of the  $M(CO)_5(L)$  ( $L$ = bidentate ligand) complexes, generated by photochemical means, and the monitoring of subsequent thermal products. A number of workers investigated the photolysis of  $M(CO)_6$ <sup>34-36</sup> in the presence of a large excess of diimine ligand, and identified  $M(CO)_5(L)$  as the intermediate in the chelation process, where a potentially chelating ligand is coordinated in a monodentate manner. The subsequent reaction of the  $M(CO)_5(L)$  complexes to form the appropriate  $M(CO)_4(L)$  complexes was rapid and earlier attempts at isolating the  $M(CO)_5(L)$  intermediate left the mechanism of subsequent chelation unclear.

Early work by Wrighton<sup>34</sup> *et al* involved the application of rapid-scan Fourier-transform infrared spectroscopy to characterise the monodentately coordinated intermediate in the photochemical formation of  $M(CO)_4(4,4'$ -dialkyl-2,2'-bipyridine) from  $M(CO)_6$ . The identification of the  $M(CO)_5(4,4'$ -dialkyl-2,2'-bipyridine) intermediate was based on its similarity to the  $M(CO)_5(2$ -phenylpyridine) and  $M(CO)_5(py)$  complexes. The rate constant for CO displacement in the Mo complex, to form the chelated species, was found to be at least 50 times faster than the corresponding W species, while the Cr species was found to react at approximately the same rate. This ordering of reactivity,  $Mo > W \approx Cr$ , is consistent with the known thermal labilities for the hexacarbonyls of this triad<sup>37</sup>.

Much work has been performed by Lees<sup>38</sup> *et al*, who initially studied the reaction kinetics and behaviour of  $M(CO)_5(L)$  intermediates, produced in the photolysis of  $M(CO)_6$  solutions, containing the 1,4-di-*tert*-butyl-1,4-azabutadiene (1,4-dab) ligand. The identification of the  $M(CO)_5(L)$  complexes was based on its similarity to the  $M(CO)_5(piperidine)$  and  $M(CO)_5(py)$  complexes. It was proposed that the

mechanism of chelate formation occurred *via* a CO extrusion process. The rate of reaction for the formation of the chelate product was determined by following the growth of the MLCT absorption of the  $M(CO)_4(1,4\text{-dab})$  complex, which was given to be a relatively slow first order process. From a comparison of chelation rates for a series of ligands it was observed that the order of the rate of chelation appeared to be dependant on steric constraints  $\text{phen} > \text{bpy} > 1,4\text{-dab}$ . A later study on the kinetics and mechanism of a photoinitiated  $W(CO)_5(L)$  intermediate ( $L = 2\text{-pyridinal-imine}$ )<sup>39</sup>, yielded similar results. The rate data obtained in this study implied that a substantial contribution to the CO extrusion reaction is made by the associating ligand when it is already coordinated in a monodentate fashion.

The isolation of a number of stable  $M(CO)_5(L)$  intermediates was surprising in light of the fact that many workers assumed the mechanism of chelate formation to be rapid. Three such intermediates ( $L = \text{dipyridylmethane}$ <sup>40</sup> (dpym, Figure 1 6.1),  $\text{dipyndylethane}$ <sup>40</sup> (dpve, Figure 1 6 2) and  $\text{ethyldiamine}$ <sup>41</sup> (en)), the first of their type were isolated and characterised and their subsequent reaction to form the  $M(CO)_4(L)$  species monitored. The  $Mo(CO)_5(dpym)$  intermediate formed the  $Mo(CO)_4(dpym)$  chelate at room temperature but the chelates for Cr and W of the same ligand were only observed after further irradiation. However, the  $M(CO)_5(dpve)$  intermediates did not form the  $M(CO)_4(dpve)$  chelate products even after further irradiation. Isolation of these species shows that the reactions of these types of complexes do not necessarily proceed *via* a spontaneous ring closure mechanism. The absence of chelation was attributed to poor  $\sigma$ -overlap between the  $\sigma$ -orbital of the uncoordinated nitrogen atom and the metal d-orbital in  $M(CO)_5(\text{dipyridylalkane})$ . Apparently, addition of bridging carbon atoms in bpy to yield the dpym and dpve ligands results in a substantial reduction in metal-nitrogen overlap. The stability of the  $M(CO)_5(en)$  complexes was attributed to the reduction of ligand-orbital overlap that is necessary to bring about chelation and to the diminished affinity of the ligand electrons

for the metal centre. The en ligand, unlike the bpy ligand, is able to undergo free rotation about the C-N bond and thus, when it attains a *cis* geometry the overlap of the N lone pair with the metal centre may be poor



Figure 1.6.1  
dipyritylmethane

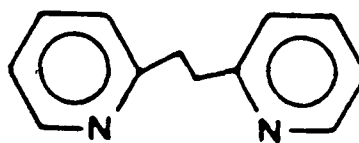


Figure 1.6.2  
dipyritylethane

### 1.7 The isolation of a novel ligand bridged metal carbonyl complex.

Recently, a number of ligand bridged metal complexes ( $L = \text{bpy}^{42}$ ,  $\text{dmbpy}^{43}$ ) have been isolated  $(\text{Cr}(\text{CO})_5)_2(L)$ . These complexes were prepared using equimolar amounts of a novel  $\text{Cr}(\text{CO})_5$  transfer reagent,  $\text{Cr}(\text{CO})_5(\text{cis-cyclo-octene})^{44}$  and ligand. The isolation of these complexes was attributed to their insolubility in the solvent employed during the reaction. The structure of the  $(\text{Cr}(\text{CO})_5)_2(\text{dmbpy})$  was the first of its type to be determined by single crystal diffraction<sup>45</sup>. However, soon after this publication the molecular structure of  $(\text{PPN})_2[\text{Pt}(\text{C}_6\text{F}_5)_3(\mu\text{-}2,2'\text{-bpy})\text{Pt}(\text{C}_6\text{F}_5)_3]^{46}$  was determined, where bpy acts as bridge. It was observed that upon heating, these  $(\text{Cr}(\text{CO})_5)_2(L)$  complexes generated not only the  $\text{M}(\text{CO})_4(L)$  chelate product, but also the parent hexacarbonyl. The regeneration of the parent hexacarbonyl had previously been noted by other workers<sup>22-24</sup>, but this was suppressed by the addition of excess ligand. In the case of the  $(\text{Cr}(\text{CO})_5)_2(L)$  complexes the addition of excess ligand

resulted in a doubling of the formation of the chelate species while regenerating the parent hexacarbonyl in the presence of CO saturated solvent.

In most of the experiments described thus far there have been a number of questions raised

- (i) the early experiments involving the photolysis of the  $M(CO)_6$  complexes had a large excess of  $M(CO)_6$  present, such that not all reacted,
- (ii) the ligand was always present in a large excess, up to a 100 fold excess,
- (iii) the mechanism of ring closure was assumed to occur *via* an intramolecular CO extrusion process, but the evolution of CO was never detected,
- (iv) the formation of the ligand bridged metal carbonyl complexes was attributed to the insolubility of the complexes, but it may be possible that these complexes have an integral role in the mechanism of chelate formation

In an effort to gain a better understanding of the subsequent reaction of the  $M(CO)_5(L)$  complexes to form the  $M(CO)_4(L)$  species, we have attempted to isolate a series of  $M(CO)_5(L)$  complexes and monitor the ensuing chelate forming reaction. We have also attempted to repeat the preparation of the ligand bridged metal carbonyl complexes in a more polar solvent to determine whether or not solvent polarity plays a role in the formation of these complexes.

## 1.8 References

- 1 Mond, L , Langer, C., Quincke, F *J Chem Soc* 1890, **57** 749
- 2 Haiduc, I , Zuckerman, J J *Basic Organometallic Chemistry* Walter de Gruyter, Berlin, New York, 1985
- 3 Geoffroy, G L , Wrighton, M S *Organometallic Photochemistry* Academic Press, New York, 1979
- 4 Huuheey, J E *Inorganic Chemistry Principles of Structure and Reactivity* Harper International Edition (third edition), Harper and Row Publishers, New York, 1978
- 5 Cotton, F. A , Wilkinson, G *Advanced Inorganic Chemistry* Cotton, John Wiley and Sons, New York, 1980
- 6 Wilkinson, G , Stone, F G A , Abel, E W *Comprehensive Organometallic Chemistry The Synthesis, Reactions and Structures of Organometallic Chemistry* Vol 3 Pergamon Press, Oxford, 1982
- 7 Howell, J A S., Burkinshaw, P M *Chem Rev* 1983, **83** 557
- 8 (a) Simon, D , Peters, K S *Chem Phys Letts* 1985, **98** 53  
(b) Simon, D., Xie, X *J Phys Chem* 1989, **93** 291.  
(c) Kelly, J M , Long, C , Bonneau, R *J Phys Chem* 1983, **87** 3344.  
(d) Strohmeier, W *Agnew Chem Internat edit* 1964, 3, **11** 730
- 9 Dahlgren, R M , Zink, J I *Inorg Chem* 1977, 16, **12** 3154
- 10 Graham, J R , Angelici, R J *Inorg Chem* 1967, **6** 2082
- 11 Dobson, G R *Acc Chem Res* 1976, **9**.300
- 12 Angelici, R J *Organomet Chem Revs* 1968, **3** 173
- 13 Tolman, C A *Chem Soc Rev* 1972, **1** 337
- 14 Awad, H H , Dobson, G R , Dobson, C B , Leipoldt, J G., Schneider, K., van Eldik, R , Wood, H E *Inorg Chem* 1989, **28** 1654
- 15 Atwood, J D , Brown, T L *J Am Chem Soc* 1976, **98** 3160.

- 16 Atwood, J. D., Brown, T L *J Am Chem Soc* 1976, **98** 3150
- 17 Atwood, J D., Brown, T L *J Am Chem Soc* 1976, **98** 3155
- 18 (a) Dobson, G. R , Brown, R A *J Inorg Nucl Chem* 1972, **34**: 2785.  
(b) Brown, R A., Dobson, G R. *Inorg Chim Acta* 1972, **6** 65.
- 19 Dobson, G R *Ann N Y Acad Sci* 1974, **239** 237.
- 20 Dobson, G. R., Smith, L A H. *Inorg Chem* 1970, **9**. 1001.
- 21 Ingemanson, C M , Angelici, R. J *Inorg Chem* 1968, **12**· 2646.
- 22 Darensbourg, D. J , Brown, T L *Inorg Chem* 1968, 1679
- 23 Connor, J. A , Day, J P., Jones, E M., Mc Ewen, G. K *J Chem Soc., Dalton Trans* 1973, 347
- 24 (a) Connor, J A., Hudson, G A *J Organomet Chem* 1974, **73**. 351  
(b) Connor, J A., Riley, P. J *J Organomet Chem* 1975, **94** 55.
- 25 Angelici, R J., Graham, J R *J Am Chem Soc* 1965, **24**· 5586
- 26 Angelici, R J , Graham, J R *J Am Chem Soc* 1965, **24** 5590
- 27 Graham, J R., Angelici, R J *Inorg Chem* 1967, **6**· 988
- 28 Dobson, G R , Faber, G C *Inorg Chim Acta* 1970, **4** 87
- 29 Dobson, G R., Rettenmaier A J *Inorg Chim Acta* 1972, **6**: 507
- 30 Dokiya, M , Johnston, R D , Basolo, F *Inorg Chem* 1970, **9** 996
- 31 Cohen, M A , Brown, T L *Inorg Chem* 1976, **15** 1417
- 32 Dobson, G R , Asali, K J *J Am Chem Soc* 1979, **101** 5433
- 33 Graham, J R , Angelici, R J *Inorg Chem* 1967, **6**· 2082
- 34 Wrighton, M S., Kazlauskas, R J *J Am Chem Soc* 1982, **104** 5784
- 35 Oishi, S *Organometallics* 1988, **7**, **6** 1237
- 36 Kalyanasundaram, K *J Phys Chem* 1988, **92** 2219
- 37 Darensbourg, D J *J Adv Organomet Chem* 1982, **21** 113



- 38 (a) Schadt, M J , Lees, A J *J Am Chem Soc* 1986, **25** 672  
 (b) Schadt, M J , Gresalfi, N J , Lees, A J *J Chem Soc Chem Commun* 1984, 506  
 (c) Schadt, M J., Gresalfi, N J , Lees, A. J *Inorg Chem* 1985, **24** 2942.
- 39 Chan, L., Lees, A. J *Inorg Chim Acta* 1986, **113**. L3.  
 Chan, L., Lees, A. J *J Chem Soc , Dalton Trans* 1987, 513  
 Drolet, D. P., Chan, L., Lees, A. J *Organometallics* 1988, **7**:2502.
- 40 Marx, D E , Lees, A J. *Organometallics* 1986, **5**. 2072.
- 41 Marx, D E., Lees, A. J *Inorg Chem* 1987, **26**: 2254
- 42 Creaven, B. S *Photochemical, Thermal and Spectroscopic studies of Metal Carbonyl Complexes* Ph.D Thesis, Dublin City University, 1989.
- 43 Creaven, B S , Grevels, F-W , Long, C *Inorg Chem* 1989, **28** 2231
- 44 Grevels, F-W , Skibbe, V *J Chem Soc Chem Commun* 1984, 681
- 45 Creaven, B S., Long, C , Howie, R A , Mc Quillan, G. P., Low, J. *Inorg Chim Acta* 1989, **157**. 151.
- 46 Uson, R , Fornies, J., Tomas, M , Casas, J M., Fortuno, C *Polyhedron* 1989, **8**. 2209

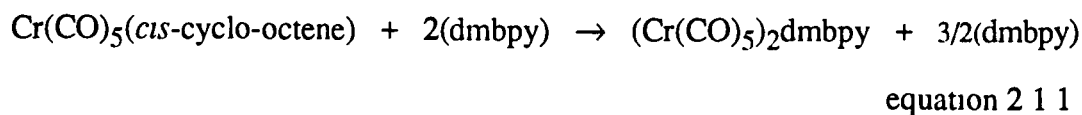
## **Chapter 2**

### **Complete Neglect of Differential Overlap - Calculations**

## 2.1. Introduction

The mechanism of formation of  $M(CO)_4(L)$   $M = Cr, Mo$  or  $W$ ,  $L =$  diamine ligands, from  $M(CO)_6$  and  $L$  has been the subject of numerous investigations. As reviewed in Chapter 1, there are a number of questions remaining unanswered in previous investigations. The first metal carbonyl complex, which contained a potentially chelating bidentate ligand coordinated in a monodentate fashion, was  $M(CO)_5(en)$  ( $en =$  ethylenediamine)<sup>1</sup>. The apparent stability of these complexes was surprising in light of the fact that some workers indicated a rapid mechanism of ring closure for the  $en$  ligand<sup>2</sup>. Since then numerous metal complexes have been isolated where a potentially chelating bidentate ligand is coordinated in a monodentate manner<sup>3</sup>.

Much work has been performed on the mechanism of chelate formation at group 6 metal carbonyl centres employing 2,2'-bipyridine ( $bpy$ ) ligands<sup>3,4</sup>. In these investigations the chelated complex, in which the ligand coordinates in a bidentate manner, was the only complex isolated. An intermediate in which the ligand coordinated in a monodentate fashion was, however, detected. Recent investigations<sup>5</sup> into chelation mechanisms employed  $Cr(CO)_5(cis\text{-cyclo-octene})$ <sup>6</sup>, as a source of the  $Cr(CO)_5$  unit, and a two fold excess of ( $\mu$ -4,4'-dimethyl-2,2'-bipyridine) ( $dmbpy$ ) in an attempt to isolate the  $Cr(CO)_5(dmbpy)$  complex (equation 2.1.1).  $Cr(CO)_5(cis\text{-cyclo-octene})$  is an excellent source of  $Cr(CO)_5$  units as the complex is labile in solutions above 243K with respect to the ligand. This reaction was executed at 273K under an argon atmosphere.



The result was surprising as the complex isolated was a ligand bridged metal carbonyl complex,  $(\text{Cr}(\text{CO})_5)_2(\text{dmbpy})$ . From equation 2.1.1, it is observed that when the complex is formed 3/2 moles of the ligand remains in solution. One would anticipate that with the initial stoichiometry, the reaction would yield a complex where the ligand is either coordinated in a monodentate or bidentate fashion. Previous workers have employed up to a one hundred fold excess of ligand and have observed the  $\text{M}(\text{CO})_4(\text{L})$   $\text{M} = \text{Cr}, \text{Mo}$  or  $\text{W}$ ,  $\text{L} = 4,4'$ -dialkyl-2,2'-bipyridine<sup>4</sup>, species while detecting the  $\text{M}(\text{CO})_5(\text{L})$  complex.

The isolation of this bridging 2,2'-bipyridine complex was confirmed by elemental analysis and subsequently by single crystal X-ray analysis. A second complex,  $(\text{PPN})_2[\text{Pt}(\text{C}_6\text{F}_5)_3(\mu\text{-}2,2'\text{-bpy})\text{Pt}(\text{C}_6\text{F}_5)_3]$  was also characterised and its molecular structure determined<sup>7</sup>, in which the bpy ligand acted as a bridge between two metal centres. The 4,4'-bipyridine ligand has been used to facilitate two metal centres but this is not a chelating ligand. However, investigators using 4,4'-bipyridine have also isolated the monodentately coordinated species  $\text{M}(\text{CO})_5(4,4'\text{-bipyridine})$ . Upon warming a solution of the  $(\text{Cr}(\text{CO})_5)_2(\text{dmbpy})$ <sup>5</sup> complex in toluene the chelate species,  $\text{Cr}(\text{CO})_4(\text{dmbpy})$ , was observed with regeneration of the parent hexacarbonyl. This was also surprising as many workers assumed that the ring closure of  $\text{M}(\text{CO})_5(\text{L})$  complexes occurred *via* an intramolecular CO extrusion process, although this was not detected<sup>3,4</sup>.

The  $(\text{PPN})_2[\text{Pt}(\text{C}_6\text{F}_5)_3(\mu\text{-}2,2'\text{-bpy})\text{Pt}(\text{C}_6\text{F}_5)_3]$ <sup>7</sup> complex was recrystallised by slow diffusion (*ca* two weeks at 243K) of *n*-hexane into a solution of the complex in  $\text{CH}_2\text{Cl}_2$ . The feasibility of isolating this complex, containing bridging *trans*-bpy, was attributed to the non-rigidity of the free ligand and its adoption of a *trans* configuration in the solid state. The  $(\text{Cr}(\text{CO})_5)_2(\text{dmbpy})$ <sup>5</sup> complex was recrystallised from a solution of toluene and pentane and initially it was thought that its

isolation was because of its insolubility in pentane. As the complex is insoluble in pentane but soluble in toluene we decided to repeat the synthesis using toluene. This synthesis of  $(\text{Cr}(\text{CO})_5)_2(\text{dmbpy})$  was repeated at 273K while monitoring by infrared spectroscopy. If the complex formed in toluene solution then it's possible that there is some other phenomenon responsible for the isolation of this complex. However, if the monodentately coordinated complex was formed then the isolation of the ligand bridged metal carbonyl complex could be attributed to the insolubility of this complex in solution.

The synthesis was monitored by infrared spectroscopy since use of this method of spectroscopy allows one to distinguish between the monodentate and bridging species. Complexes of the type,  $\text{M}(\text{CO})_5(\text{amine})$ , possess  $\text{C}_{4v}$  symmetry and exhibit three bands in the  $\nu\text{CO}$  stretching region of the infrared spectrum ( $2200\text{--}1700\text{cm}^{-1}$ ). If the ligand, coordinated to the metal centre in a monodentate fashion, is large then the symmetry of the complex is reduced to pseudo  $\text{C}_{4v}$  symmetry. When a ligand such as bpy or a substituted bpy acts as a bridge<sup>10</sup> between metal centres the overall symmetry of the complex is reduced from  $\text{C}_{4v}$  (or pseudo  $\text{C}_{4v}$ ) to  $\text{C}_s$ . Thus, the complex will exhibit four bands in the  $\nu\text{CO}$  stretching region of the infrared spectrum. On this basis, the reaction of  $\text{Cr}(\text{CO})_5(\text{cis-cyclo-octene})$  with dmbpy was monitored by infrared spectroscopy with the confidence of being able to distinguish between two possible complexes that may be formed.

## 2.2 Results and discussion

### 2.2.1 Monitoring the formation of $(\text{Cr}(\text{CO})_5)_2(\text{dmbpy})$ , at 273K, in toluene solution by infrared spectroscopy.

The addition of a five fold excess of dmbpy in toluene solution ( $0.1815 \text{ mol dm}^{-3}$ ), to a sample of  $\text{Cr}(\text{CO})_5(\text{cis-cyclo-octene})$  ( $0.0363 \text{ mol dm}^{-3}$ ), was monitored by infrared spectroscopy at 273K. The temperature was maintained at 273K by the use of a variable temperature (VTIR) solution cell.

There were a number of adjustments made to the standard Specac 21000 VTIR solution cell. A pictorial representation of the VTIR solution cell is presented in the Experimental section. An injection port at the top of the cell leads into the temperature chamber where it is connected to a metal sample container, by teflon tubing. The metal container, attached to the entry port of the solution cell by means of teflon tubing, with more tubing at the exit port, leading to a waste bottle. The adjustments were made to the VTIR cell in anticipation of monitoring reactions more accurately and possibly making their monitoring more feasible. In this study the  $\text{Cr}(\text{CO})_5(\text{cis-cyclo-octene})$  complex was held in the metal sample container while a five fold excess of the ligand, dmbpy dissolved in toluene solution ( $0.1815 \text{ mol dm}^{-3}$ ), was injected in at 273K. The VTIR system allows the ligand and the  $\text{Cr}(\text{CO})_5(\text{cis-cyclo-octene})$  complex to be pushed into the solution cell to react while filtering any undissolved particles by means of two small metal frits at the bottom of the sample container. Thus, we are able to monitor all reactions as they occur, using this method of spectroscopy.

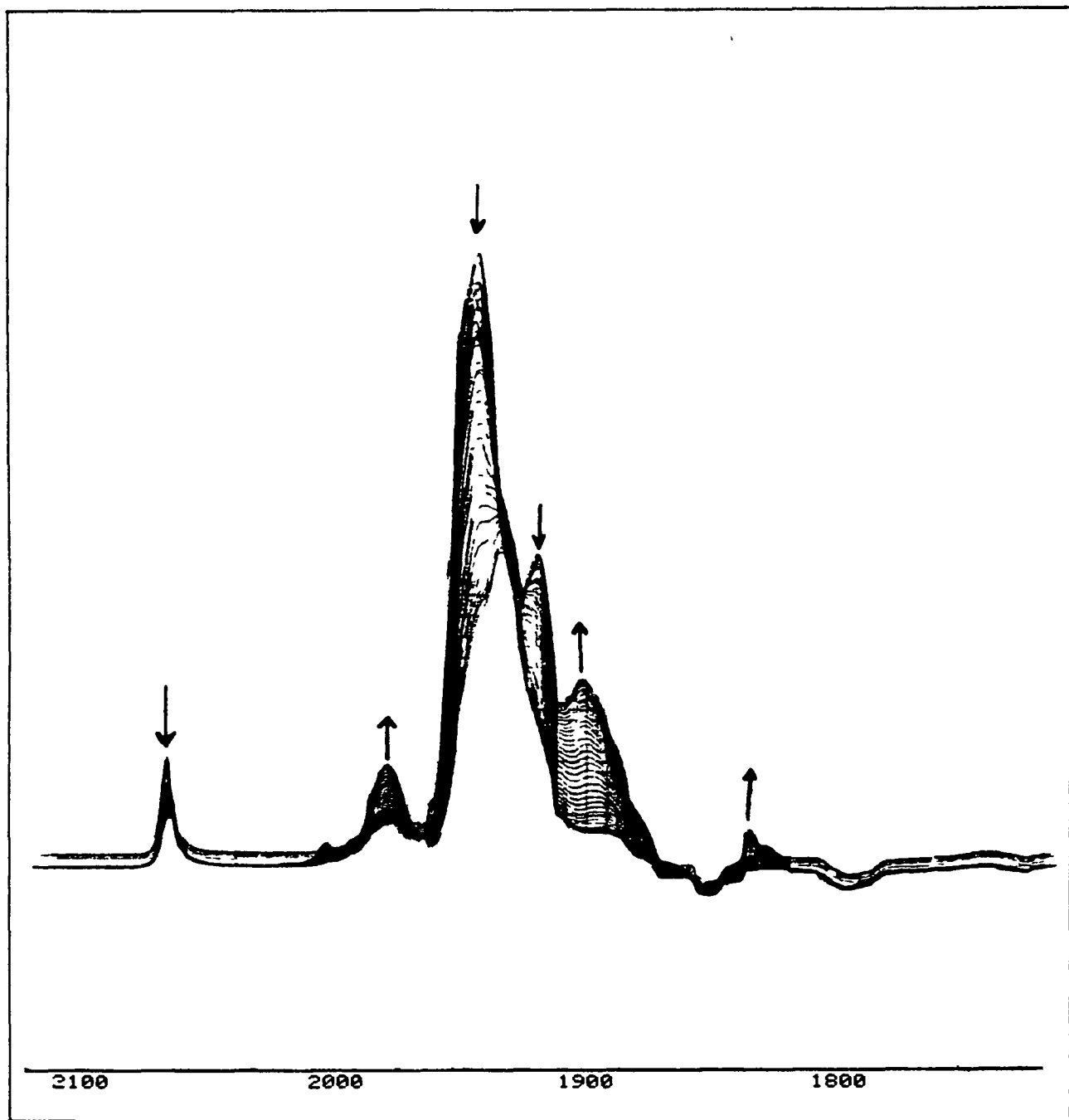
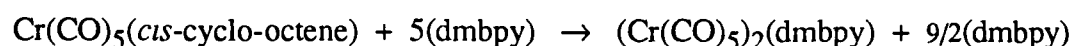


Figure 2.2 1 1 The spectral changes, monitored by infrared spectroscopy, upon the addition of a five fold molar excess of dmbpy, dissolved in toluene solution ( $0.1815 \text{ mol dm}^{-3}$ ), to a sample of  $\text{Cr(CO)}_5(\text{cis-cyclo-octene})$  ( $0.0383\text{m}$ ) at 273K, with 3 minute intervals between scans

The spectral changes occurring upon addition of a five fold excess of dmbpy, dissolved in toluene solution (0.1815 mol dm<sup>-3</sup>), to a sample of Cr(CO)<sub>5</sub>(*cis*-cyclo-octene) (0.0363m) at 273K as monitored by infrared spectroscopy, are presented in Figure 2.2 1 1. The reaction was scanned every three minutes while the temperature was maintained at 273K. Initial bands at 2066, 1979 and 1944cm<sup>-1</sup> correspond to the Cr(CO)<sub>5</sub>(*cis*-cyclo-octene) complex in toluene solution. The bands at 2068, 1980, 1936, 1920 and 1903cm<sup>-1</sup> are consistent with the spectrum of the (Cr(CO)<sub>5</sub>)<sub>2</sub>(dmbpy)<sup>5</sup> in toluene solution. The band at 1980cm<sup>-1</sup> corresponds to the formation of some Cr(CO)<sub>6</sub>. Thus, the remaining bands are consistent with the formation of (Cr(CO)<sub>5</sub>)<sub>2</sub>(dmbpy). As stated previously the formation of the bridging complex would be identified by the observation of four bands in the νCO stretching region of the infrared spectrum. The bands at 2068, 1936, 1920 and 1903cm<sup>-1</sup> correspond to the A<sub>1</sub>, E (which is split at 1944 and 1920cm<sup>-1</sup>) and A<sub>1</sub>(2) modes of a pseudo C<sub>4v</sub> species in which the overall symmetry is reduced to C<sub>s</sub>. Had the monodentately coordinated complex, Cr(CO)<sub>5</sub>(dmbpy) been formed then the split in the E mode would not be observed and there would be only one band observed stretching in the region between 1944 and 1920cm<sup>-1</sup>. The formation of some chelate product, Cr(CO)<sub>4</sub>(dmbpy), was observed by the growth of two bands at 2005 and 1837cm<sup>-1</sup>.



equation 2.2.1.1

With the use of a five fold molar excess of ligand (equation 2.2.1.1) one would anticipate the reaction to favour the formation of the chelate species, Cr(CO)<sub>4</sub>(dmbpy). However, 9/2 moles of unreacted ligand are left in the solution. The formation of this complex was confirmed by repeating the reaction on a large scale. A solution of the ligand, dissolved in toluene, was added to a sample of Cr(CO)<sub>5</sub>(*cis*-cyclo-octene), under an argon atmosphere, and left to recrystallise at 238K. Removal



of the solvent and comparison with an authentic sample of the complex confirmed its formation in toluene solution. The chelate species,  $\text{Cr(CO)}_4(\text{dmbpy})$ , was also prepared and characterised.

It seems apparent that the isolation of this ligand bridged complex is not attributable to its insolubility in the non-polar solvent used in the recrystallisation process. There must be some chemical phenomenon responsible for the isolation of such a complex. As a model to estimate the conformation of a monodentately coordinated 2,2'-bipyridine complex, the molecular structure of  $\text{Cr(CO)}_5(2\text{-phpy})^{10}$  (Figure 2.2.1.2) was determined.

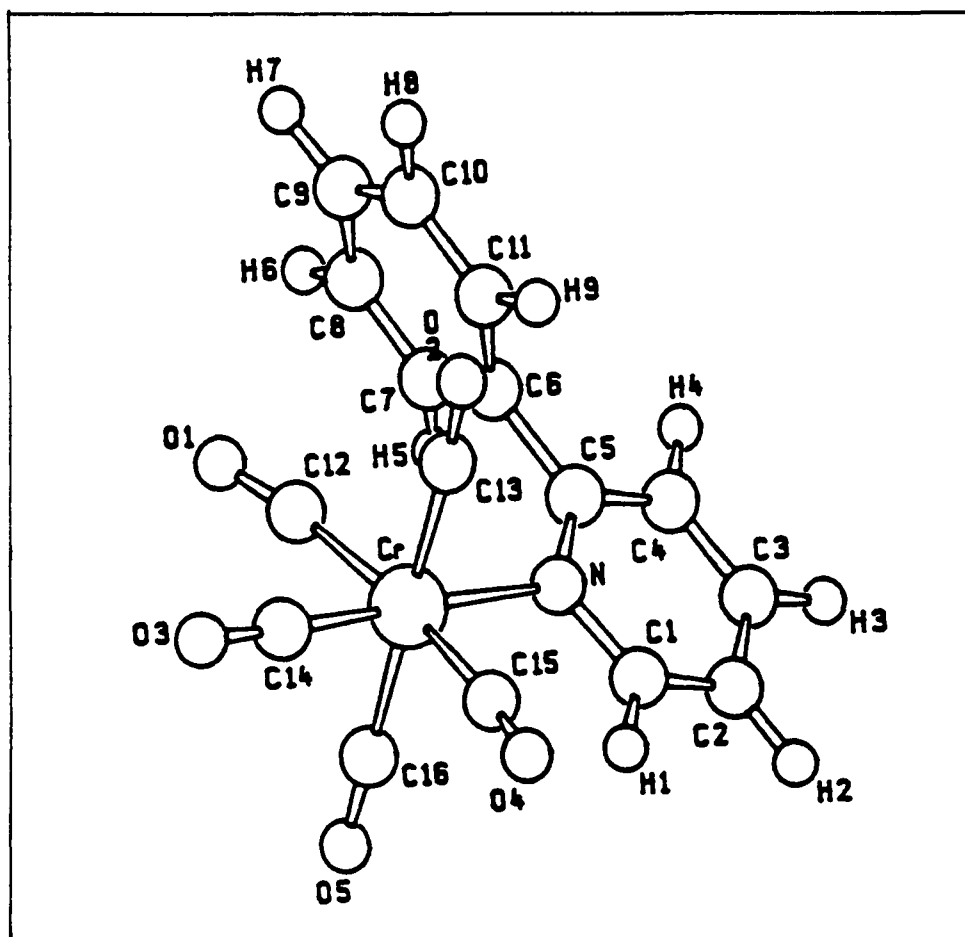


Figure 2.2.1.2 The molecular structure of  $\text{Cr(CO)}_5(2\text{-phpy})^{10}$

The angle between the pyridine and phenyl ring was determined to be  $112^\circ$ . This conformation is required for steric reasons, to minimise the possibility of steric interaction between the phenyl ring and the equatorial carbonyl ligands. It is possible that the conformational change induced on the ligand upon coordination of a potentially chelating ligand has some effect in determining the complex formed. One possibility is that the conformational change induced upon coordination of one pyridyl nitrogen in dmbpy affects the basicity of the uncoordinated nitrogen.

A substituent has a base strengthening effect if its insertion into a molecule, in place of a hydrogen atom, increases the electron density at other points in the molecule. The factors that affect the  $pK_a$  value of a ligand are those which also affect ring closure e.g. steric hindrance, conformation, mesomeric, electrostatic and inductive effects<sup>11</sup>. The replacement of a CO ligand in a metal hexacarbonyl complex by another ligand, A, gives a complex  $M(CO)_5(A)$  in which the CO ligands are either more or less labile than they were in the original complex. Angelici<sup>12</sup> divided ligands into two categories of labilising and non-labilising ligands, based on their effect on M-CO (M = Cr, Mo, or W) bonding, compared to that of the parent hexacarbonyl. The labilising ligands have donor atoms which are H, N, O, or the halogens, while donor atoms of non-labilising ligands are P, As, Sb, or S. The labilising ligands were categorised as "hard" bases and the non-labilising ligands as "soft" bases, based on Pearson's<sup>13</sup> categorisation.

### 2.2.2 CNDO calculations for 2,2'-bipyridine and 2,2'-bipyridinium<sup>2+</sup>

The conformational change induced upon the ligand in  $Cr(CO)_5(2\text{-phpy})$ <sup>10</sup> raised many questions and since previous workers had related the basicity of the ligand to reaction rates we decided to investigate further. To estimate the effect of

conformational changes on the  $pK_a$  of the conjugate acid of bpy, the energy difference between bpy and its conjugate acid, 2,2'-bipyridinium<sup>2+</sup> (bpy<sup>2+</sup>), was calculated for a range of angles( $\theta$ ) These calculations were performed by Dr D. A Morton-Blake at the University of Dublin<sup>14</sup>, using the solvaton model of the CNDO method.

The results, shown in Table A 1 (Appendix A), represent the stabilisation of the biprotonated species compared to the parent bpy, and are in electron volts (eV) The larger the numbers the more stable the conformation The various rows are for conformations between *cis* ( $\theta = 0^\circ$ ) and *trans* ( $\theta = 180^\circ$ ) The columns, for varying D values, represent different solvent polarities, from D= 1 (vacuum) to D= 10 (dielectric constant= 100, close to that of water)

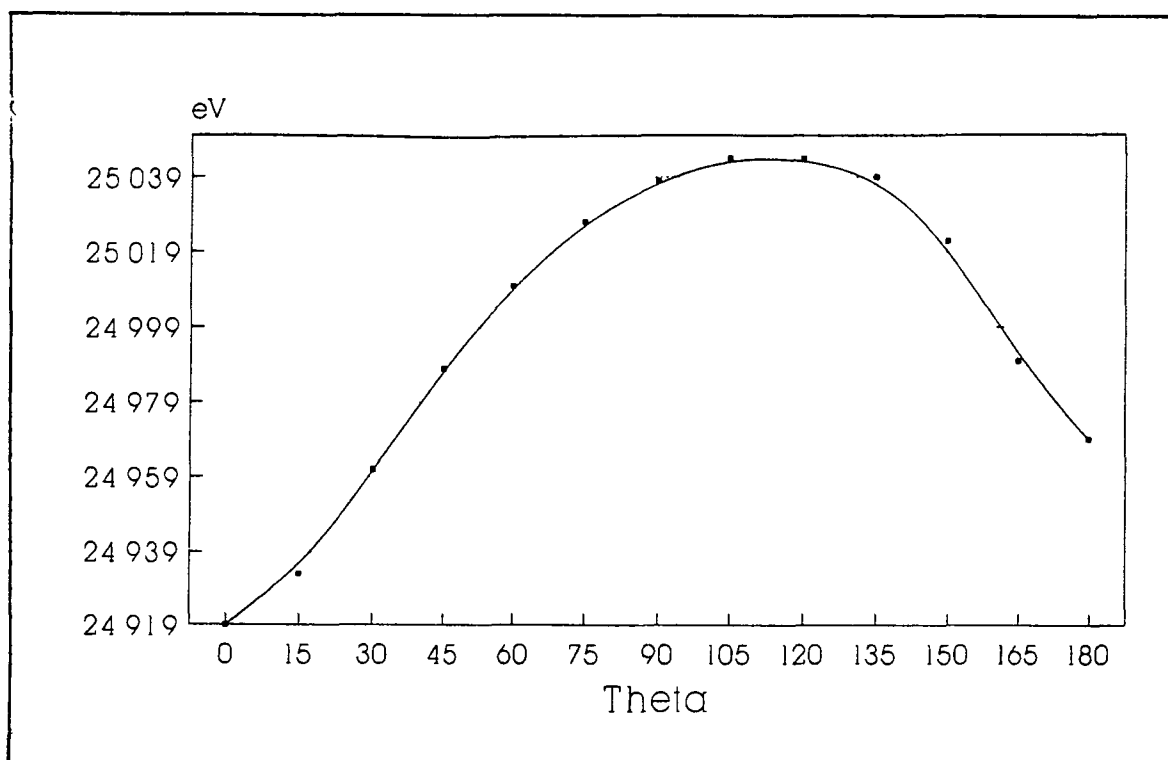


Figure 2.2 2 1 The plot of the values obtained for the stabilisation of the biprotonated bpy species compared to the parent bpy in non-polar media (D= 1), over a range of angles from 0 to 180°

The plots for  $D=1$  and  $D=10$  are presented in Figures 2.2.2.1 and 2.2.2.2, respectively

In non-polar media, Figure 2.2.2.1, the  $pK_a$  is at a maximum when the rings make a twist of  $105-120^\circ$ . The implication is that the conformational change, induced on the ligand upon coordination of one pyridyl nitrogen, required for steric reasons plays a role in the determination of the complex formed. This implies that coordination of one pyridyl nitrogen, in bpy, will increase the basicity of the uncoordinated pyridyl nitrogen, by virtue of the conformational change necessary to achieve this mode of coordination. It is possible that the uncoordinated pyridyl nitrogen, in a monodentately coordinated bpy, will compete more effectively for  $M(CO)_5$  units than the free ligand. This would then favour the formation of ligand bridged metal carbonyl species, and perhaps explain the formation of  $(Cr(CO)_5)_2(dmbpy)$ , in equation 2.1.1, as the principal product

An early investigation of the reaction kinetics of substitution reactions of bipyridyl complexes of  $M(CO)_4(bpy)$  with a series of phosphites<sup>15</sup> observed a dependence of the ligand basicity on the rate of reaction. The second order rate constant  $k_2$  was found to increase with increasing basicity of the ligands. Angelici and Ingemanson<sup>16</sup> investigated the rates and mechanisms of amine displacement from  $W(CO)_5(amine)$  as a function of the basicity of the primary, secondary, and tertiary amines and also of the nucleophilicity of the phosphine or phosphite, L. The first order rate constant  $k_1$ , assumed to correspond to the breaking of the W-N bond, was found to decrease in the order of increasing basicity of the amine. The substitution reactions with a series of phosphines and phosphites were found to decrease in the order of decreasing nucleophilicity of the incoming ligands. The basicity of the ligand has been implicated in affecting the rate of reaction whether it is coordinated in a bidentate manner or as an incoming ligand. There has not been any study on the basicity of the

ligand when coordinated in a monodentate manner. A list of  $pK_a$  values for a series of ligands is presented in Table 2.2.1.1. The effect of the basicity of the ligand on the rate of the chelation reaction has been disputed by some workers because there are a number of phosphorus ligands of both higher and lower basicity than pyridine which possess similar labilising abilities<sup>15</sup>.

Table 2.2.1.1 The  $pK_a$  values of a series of ligands

Ligand	$pK_a$
pyridine	5.23
aniline	4.61
2-phenylpyridine	4.64
2,2'-bipyridine	4.51
4,4'-dimethyl-2,2'-bipyridine	5.45
2,2'-bipyridylamine	7.14
1,10-phenanthroline	4.86

The substitution reactions of  $M(CO)_5(A)$  by a ligand L were studied and when A is a labilising ligand such as pyridine the M-CO bonds *trans* to pyridine are strengthened with a subsequent weakening of the M-CO bonds *cis* to pyridine<sup>12</sup>. This results in a greater ease of replacement of CO by an incoming ligand, L, and the formation of *cis*- $M(CO)_5(A)(L)$ . When the A of  $M(CO)_5(A)$  is a non-labilising ligand, such as  $P(OR)_3$ , substitution by L usually occurs at a position *trans* to the bound ligand<sup>12</sup>.

The molecular structure of  $(Cr(CO)_5)_2(dmbpy)^5$ , shown in Figure 2.2.2.3, shows the two pyridine rings to be twisted at an angle of *ca* 90° relative to each other. The molecular structure of  $(PPN)_2[Pt(C_6F_5)_3(\mu-2,2'-bpy)Pt(C_6F_5)_3]^7$  is

not presented here but it should be noted that the two pyridine rings of the bpy ligand are an angle of  $41.89^\circ$ . The bpy ligand is not as sterically hindered in the latter complex thus resulting in a smaller angle between the rings. Creaven also isolated the  $(\text{Cr}(\text{CO})_5)_2(\text{bpy})$  complex<sup>10</sup>, confirmed by elemental analysis, where the bpy ligand facilitated two metal centres

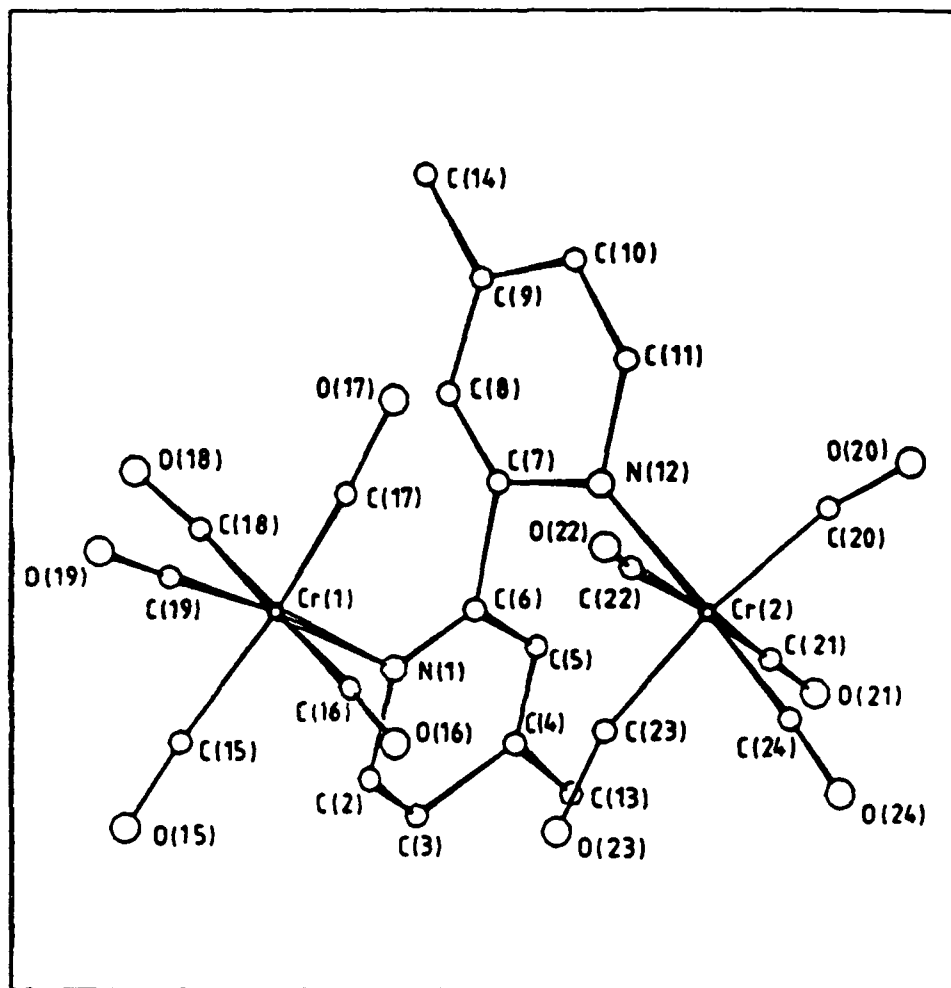


Figure 2.2.2 The molecular structure of  $(\text{Cr}(\text{CO})_5)_2(\text{dmbpy})$ <sup>10</sup>

In polar media, however, Figure 2.2.3 shows that the  $\text{pK}_a$  of the conjugate acid of bpy is at a maximum when the torsional angle between the two pyridine rings is  $0^\circ$  (*cis*). This corresponds to a maximum value in the energy curve. This would infer that, in polar media, bpy is ideal as a chelating ligand, but would not

act as a bridge between two metal centres. Until the isolation and characterisation of the ligand bridged metal carbonyl complexes discussed here, bpy and substituted and bpy ligands had been isolated and characterised in complexes where the ligand was coordinated in a bidentate fashion<sup>3,4</sup>. The reaction of these ligands with  $M(CO)_6$  to form the  $M(CO)_4(L)$  species,  $L = \text{bpy}$ , substituted bpy, was reported to occur so rapidly that the intermediates in the reaction could only be detected

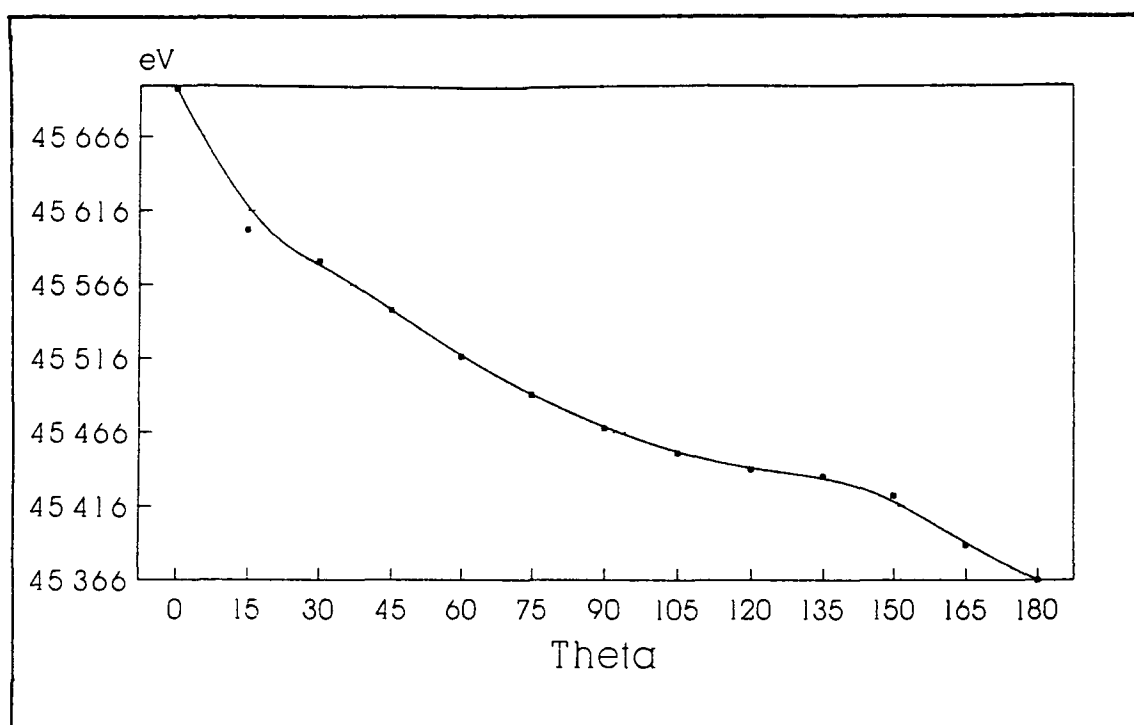


Figure 2.2.2.3 The plot of the values obtained for the stabilisation of the biprotonated bpy species compared to the parent bpy, in polar media ( $D = 10$ ), over a range of angles from 0 to 180°

In inert and basic solvents it has been shown<sup>17</sup> that bpy exists in an *s-trans* (Figure 2.2.2.4) conformation. Increasing the acidity of the solvents resulted in one or two protons being completely transferred from the solvent to the pyridine nitrogens. The angle between the two pyridine rings was estimated<sup>17</sup> to change from 0

to between 108-125°. This angle was confirmed by other workers<sup>18</sup> Recent work<sup>19</sup> showed that the angle of twist between two phenyl rings in 4-cyanobiphenyl to be 37.4°, while that of biphenyl is 37°. Admittedly the difference is small but serves to illustrate the effect of the addition of a base weakening substituent on the conformation, adopted by a ligand

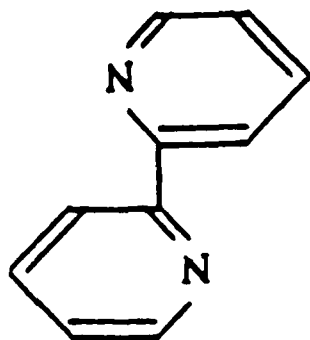


Figure 2.2.2.4 The *s-trans* conformation of bpy<sup>17</sup>

The isolation of the stable  $M(CO)_5(L)$  species,  $L =$  di-2-pyridylmethane (dpym), 1,2-di-2-pyridylethane (dppe), with the potentially chelating bidentate ligands coordinated in a monodentate fashion was reported by Marx and Lees<sup>20</sup> These complexes, excluding the  $Mo(CO)_5(dpym)$  complex, exhibited no tendency to form the chelate species at room temperature Irradiation of the  $M(CO)_5(dpym)$ ,  $M = Cr, W$ , resulted in the formation of the  $M(CO)_4(dpym)$  species but further irradiation of the  $M(CO)_5(dppe)$  species did not yield the chelated species The absence of chelation was attributed to poor  $\sigma$ -overlap between the  $\sigma$ -orbital of the uncoordinated nitrogen atom and the metal d orbital Also the addition of bridging carbon atoms in bpy was thought to result in a substantial reduction in M-N overlap<sup>20</sup> We are interested in the isolation of these complexes and from the results presented above believe that the isolation of these complexes is resultant from the lack of steric interaction between the ligand and either the metal centre or one of the carbonyl groups The coordination of one of the



pyridyl nitrogens does not result in a conformational change in the ligand with no subsequent increase in the basicity of the uncoordinated nitrogen. Thus, only the monodentately coordinated intermediate was isolated.

### 2.2.3 CNDO calculations using dimethyldiimine and dimethyldiiminium.

The results were obtained using the solvation model<sup>14</sup> and they are presented in Table A.2 (Appendix A). An environment of infinite dielectric constant is included. The structure of the dimethyldiimine ligand is presented in Figure 2.2.3.1. The plot for  $D=1$  is presented in Figure 2.2.3.2 and Figure 2.2.3.3 represents the plot for  $D=10$ .

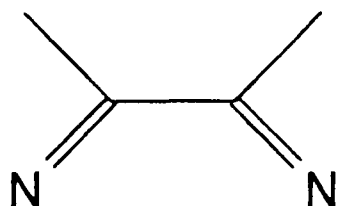


Figure 2.2.3.1 The structure of the dimethyldiimine ligand

In the case of non-polar media the  $pK_a$  of the conjugate acid of dimethyldiimine is at a maximum when the torsional angle is  $105^\circ$ . From Table 2.2.3.1 it may be observed that the  $pK_a$  is at a maximum when the torsional angle is  $90^\circ$  for all remaining values of  $D$ . This may be observed from figure 2.2.3.2 also. The most obvious difference between this study and the bpy/bpy<sup>2+</sup> system is that the  $pK_a$  of the uncoordinated nitrogen atom is at a maximum, which favours the formation of ligand bridged metal carbonyl complexes, in all media polarities.

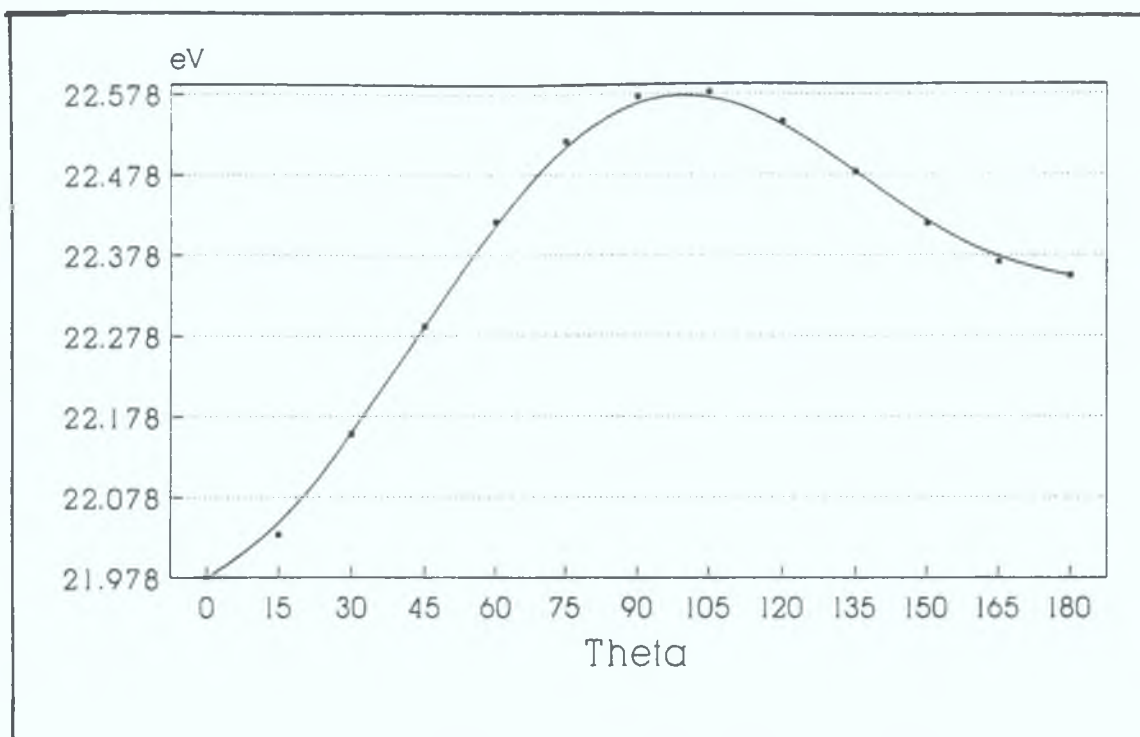


Figure 2.2.3.2: The plot of the values obtained for the stabilisation of the biprotonated dimethyldiiminium species compared to the parent, in non-polar media ( $D=1$ ), over a range of angles from 0 to 180°.

However, it seems unlikely that the coordination of one nitrogen of the dimethyldiimine ligand would result in steric interactions with either the metal or one of the carbonyl groups. Thus, there will be no conformational change induced upon coordination of the ligand and the monodentately coordinated complex will be isolated.

N,N'-dimethyldiimine is one of the simplest ligands in the diimine class. Similar ligands include 1,4-diazabutadiene (1,4-dab), glyoxal-N,N'-dimethyldiimine and glyoxaldiimine. An early report<sup>21</sup> claimed that these ligands adopted an *s-trans* conformation in solution. A rotational barrier of *ca.* 20kJ mol<sup>-1</sup> was reported as necessary to achieve the *cis* planar conformation, which is present in the chelate form.

When dimethyldimine is coordinated in a monodentate fashion to an  $M(CO)_5$  fragment, there is no steric interaction between the ligand and either the metal centre or one of the carbonyl groups. Thus, no conformational change is induced on the ligand upon coordination and there will be no subsequent increase in the basicity of the uncoordinated nitrogen.

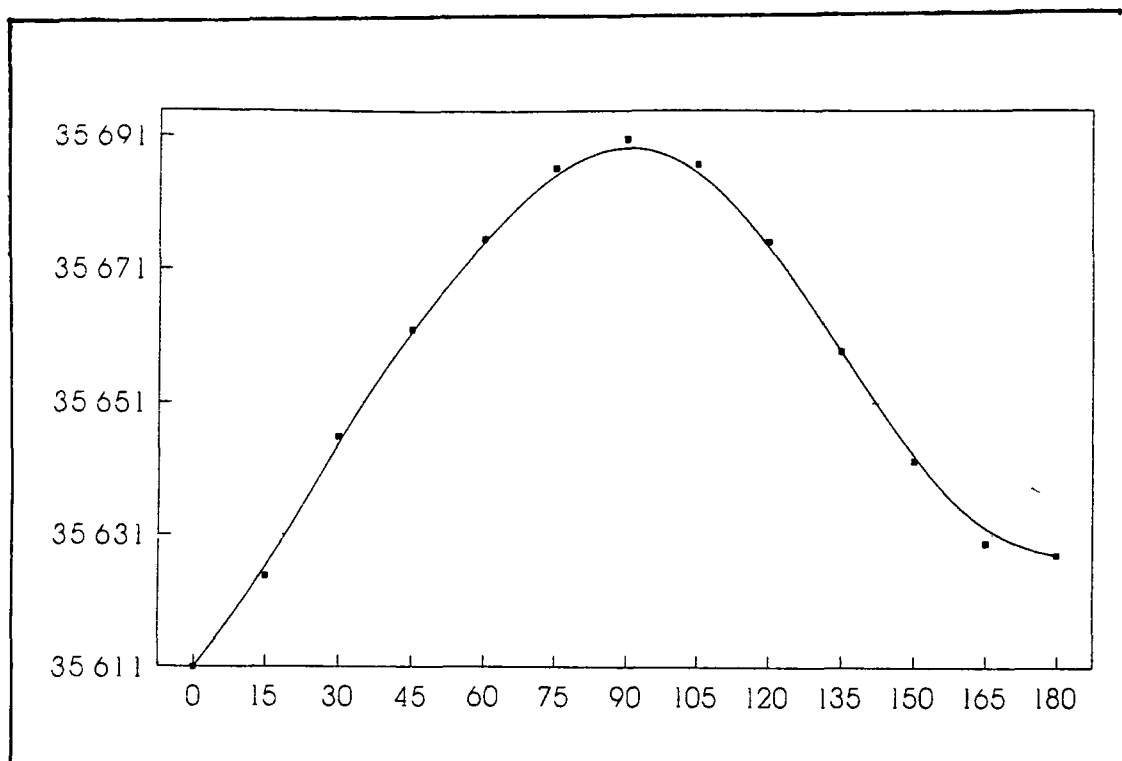


Figure 2.2.3.3 The plot of the values obtained for the comparison of the energy difference between dimethyldimine and its conjugate base, in polar media ( $D=10$ ), over a range of angles from 0 to 180°

Investigations<sup>3</sup> into the mechanism of chelate formation using 1,4-dab as the ligand resulted in  $M(CO)_5(L)$  complex formation ( $M = Cr, Mo, \text{ or } W$ ). The stability of these monodentate complexes was attributed to H-bonding between the  $\beta H$  and one of the carbonyl groups or metal centre. The isolation of  $M(CO)_5(en)^1$  complexes and their apparent stability was surprising in view of the fact that some

workers indicated the en ring closure mechanism to be rapid. The stability of these complexes was attributed to a reduction of the ligand orbital overlap that is necessary to bring about chelation and to the diminished affinity of the ligand electrons for the metal centre. The en ligand is similar to the dimethyldiamine ligand and its coordination to a metal centre would result in no steric interaction with either the metal centre or one of the carbonyl groups thus, resulting in the formation of the monodentately coordinated  $M(CO)_5(en)$  complex.

## 2.3 Summary

The isolation and characterisation of  $(\text{Cr}(\text{CO})_5)_2(\text{dmbpy})^5$ , the first ligand bridged metal carbonyl complex, using a 2,2'-bipyridine ligand, was surprising. The isolation of this complex was attributed to its insolubility in the solvent used. However, repeating the reaction, while monitoring by infrared spectroscopy, in another solvent, yielded the complex. Since solubility did not play a role, there had to be another phenomenon responsible for the isolation of such a complex. The isolation of another complex with bpy acting as a bridge in the  $(\text{PPN})_2[(\text{C}_6\text{F}_5)_3\text{Pt}(\mu\text{-bpy})\text{Pt}(\text{C}_6\text{F}_5)]^7$  was also reported.

The molecular structure of  $\text{Cr}(\text{CO})_5(2\text{-phpy})^{10}$  was determined as a model to estimate the conformation of a monodentately coordinated bpy complex. The phenyl ring was twisted  $112^\circ$  relative to the pyridine ring to minimise any steric interactions between the ligand and either the metal centre or one of the carbonyl groups. Thus, the conformational change, induced upon coordination of one pyridine nitrogen, may have an effect on the uncoordinated nitrogen such that it may compete more effectively for the  $\text{M}(\text{CO})_5$  units than the free ligand.

To estimate the effect of conformational changes on the  $\text{pK}_a$  of the conjugate acid of bpy the energy difference between bpy and its conjugate acid,  $\text{bpy}^{2+}$ , was calculated for a range of angles ( $\theta$ ), between the two pyridine rings<sup>14</sup>. From the results, it was observed that in polar media the  $\text{pK}_a$  of the conjugate acid is at a maximum when the angle between the two pyridine rings lies in the range  $105\text{-}120^\circ$ . In non-polar media the  $\text{pK}_a$  of the conjugate acid was found to be at a maximum when the angle between the two rings was  $0^\circ$ . The molecular structure of the  $(\text{Cr}(\text{CO})_5)_2(\text{dmbpy})^5$  complex was determined and the angle between the two rings

was 90°. In the case of the  $(PPN)_2[(C_6F_5)_3Pt(\mu\text{-bpy})Pt(C_6F_5)_3]^7$  complex the pyridine rings made a twist of 41.89° relative to each other to minimise any steric interactions.

We propose that coordination of one pyridine nitrogen in bpy results in a conformational change of the ligand to minimise steric interactions between the ligand and either the metal centre or one of the carbonyl groups. This conformational change induced on the ligand causes an increase in the  $pK_a$  of the uncoordinated nitrogen such that it competes more effectively than the free ligand for coordination of another  $M(CO)_5$  unit. Thus, the formation of a ligand bridged metal carbonyl complex will be observed. In polar media the  $pK_a$  of the uncoordinated nitrogen of the conjugate acid is at a maximum when the complex has adopted the *cis* conformation, indicating that there will be no formation of a ligand bridged metal carbonyl complex. In polar media the preferred complex will be when bpy is coordinated in a bidentate fashion as in the chelated complex.

For the dimethyldimine ligand, the  $pK_a$  of the uncoordinated nitrogen of the conjugate acid was estimated to be at a maximum when the two halves of the molecule were twisted 90-105° relative to each other in all media polarities. However, coordination of one nitrogen in the dimethyldimine ligand would not result in a conformational change of the ligand to minimise any steric interactions between the ligand and either the metal centre or the carbonyl groups. Thus, there will be no formation of a ligand bridged metal carbonyl complex utilising this ligand. Only the monodentately coordinated complex will be formed.

We have attempted the synthesis of a number of  $M(CO)_5(L)$  complexes ( $M = Cr$  or  $W$ ) ( $L = \mu\text{-4,4'-diphenyl-2,2'-bipyridine}$ , *bis*-picolylamine, 2-aminomethylpyridine, 2,2'-bipyridylamine and 1,10-phenanthroline) in an effort to elucidate the mechanism of chelate formation at group 6 metal carbonyl centres. The

molecular structure of the  $\text{W(CO)}_5(2,2\text{-bipyridylamine})$  complex was determined as a model for the monodentately coordinated diimine complexes

## 2.4 References

- 1 Marx, D E., Lees, A J *Inorg Chem* 1987, **26** 2254
- 2 (a) Carter, M J., Beattie, J K *Inorg Chem* 1970, **9** 1233.  
(b) Louw, W J., Robb, W *Inorg Chim Acta* 1969, **3** 303
- 3 (a) Schadt, M J , Gresalfi, N J , Lees, A J. *J Chem Soc , Chem Commun.* 1984, 506  
(b) Schadt, M J , Gresalfi, N J., Lees, A J *Inorg Chem* 1985, **24** 2942.  
(c) Schadt, M J., Lees, A J *J Am Chem Soc* 1986, **25** 672
- 4 Kazlauskas, R J , Wrighton, M S *J Am Chem Soc* 1982, **104** 5784.
- 5 (a) Creaven, B S , Grevels, F-W , Long, C *Inorg Chem* 1989, **28** 2231.  
(b) Creaven, B S., Long, C , Howie, R. A , McQuillan, G P., Low, J. *Inorg Chim Acta* 1989, **157** 151
- 6 Grevels, F-W , Skibbe, V *J Chem Soc , Chem Commun* 1984, 681.
- 7 Uson, R., Fornies, J , Tomas, M., Casas, J M., Fortuno, C *Polyhedron* 1989, **8** 2209
- 8 Zulu, M M , Lees, A J *Inorg Chem* 1988, **27** 1139
- 9 (a) Cotton, F A , Kraihanzel, C S *J Am Chem Soc* 1962, **84**. 4432  
(b) Cotton, F A , Kraihanzel, C S *Inorg Chem* 1963, **2** 533
- 10 *Photochemical, thermal and spectroscopic studies of metal carbonyl complexes* Creaven, B S Ph D Thesis, Dublin City University, 1989.
- 11 *pKa prediction for organic acids and bases* Perrin, D D., Dempsey, B., Serjent, E P Chapman and Hall, London, 1981
- 12 Angelici, R J *Organomet Chem Rev* 1968, **3** 173
- 13 Pearson, R *J Am Chem Soc* 1963, **22** 3533
- 14 Dr D A Morton-Blake, University of Dublin, Trinity College, Dublin 2, Ireland



- 15 (a) Angelici, R J., Graham, J R *J Am Chem Soc* 1965, **24** 5586  
(b) Angelici, R J., Graham, J R *J Am Chem Soc* 1965, **24**:5590
- 16 Ingemanson, C H , Angelici, R J *Inorg Chem* 1968, **7** 2646
- 17 Castellano, S., Gunther, H., Ebersole, S *J Phys. Chem* 1965, **69**. 4166.
- 18 Nakamoto, K *J Phys Chem* 1960, **64** 1420.
- 19 Emsley, J W., Horne, T J , Celebre, G , De Luca, G., Longeri, M. *J. Chem Soc , Faraday Trans* 1992, **88** 1679.
- 20 Marx, D E., Lees, A J *Inorg Chem* 1987, **26** 620
- 21 Benedix, R , Birner, P., Birnstock, F., Hennig, H., Hofmann, H-J. *J Mol Struct* 1979, **51** 99

### **Chapter 3**

**The isolation, characterisation and reactions of a series of  $M(CO)_5(L)$  complexes in the solid and solution state.**

### 3.1 Introduction

There has been a considerable effort directed towards understanding the electronic structure of carbonyl complexes of Cr, Mo, and W. In the UV-visible spectrum the band position and intensity have been determined for a series of complexes and the information obtained has been valuable in the understanding of a number of photochemical systems. The  $M(CO)_6$  complexes exhibit a number of intense transitions in the UV-visible region which are associated with Ligand Field (LF),  $M \rightarrow L$ , and  $L \rightarrow M$  Charge-Transfer (CT) absorptions.

The UV-visible spectra of  $M(CO)_6$  ( $M = Cr, Mo, \text{ or } W$ ) complexes are dominated by two intense Metal to Ligand Charge Transfer bands (MLCT) at 280 and 230 nm. The LF transitions at 320 and 260 nm are seen as shoulders on these bands. These bands are assigned the  $^1A_{1g} \rightarrow ^1T_{1g}$  and  $^1A_{1g} \rightarrow ^1T_{2g}$  LF transitions, respectively. Matrix isolation techniques have allowed the study of the photogenerated coordinately unsaturated  $M(CO)_5$  species by UV-visible and also infrared spectroscopy. Vibrational spectra of photogenerated  $M(CO)_5$  in low temperature matrices show it to have a square pyramidal<sup>1,2</sup> ( $C_{4v}$ ) structure. One reported metal atom-ligand co-condensation investigation proposes a  $D_{3h}$  structure for  $Cr(CO)_5$ <sup>3</sup>, which has been disputed by others<sup>1,2</sup>. The removal of a CO group from  $M(CO)_6$  to generate the  $C_{4v}$  species should affect the d-orbital diagram as shown in Figure 3.1.1.

The lowest energy spectral feature<sup>4</sup> of  $M(CO)_5$  has been assigned as the  $^1A(e_4b_2^2) \rightarrow ^1E(e_3b_2^2a_1^1)$  ligand field (LF) absorption. The lowest energy absorption band for  $M(CO)_5$  is significantly red-shifted when compared to  $M(CO)_6$ . Absorption spectra for  $M(CO)_5(L)$  ( $L \ll CO$  in LF strength) have been assigned in the low energy region<sup>5-8</sup>. If  $L$  is lower in the spectrochemical series than CO the d orbitals will split in a similar way to  $M(CO)_5$ . If  $L$  has low lying  $\pi^*$  orbitals an MLCT

transition may be the lowest energy transition in  $M(CO)_5(L)$  complexes. Varying the ligand, L, results in a variation of the CT band position. The more electron-releasing substituents give a higher energy CT absorption. The MLCT bands are very solvent sensitive, more polar solvents give blue shifted CT band maxima, while LF bands are little affected. Consequently, when LF and MLCT bands are overlapping, it is possible to resolve them by varying the solvent polarity<sup>9</sup>.

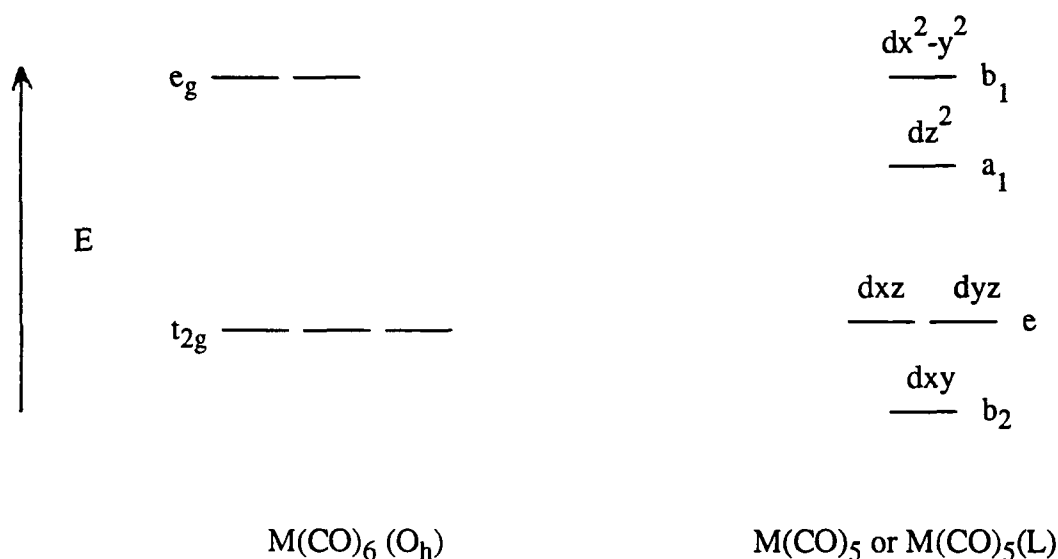


Figure 3 1.1. The one-electron diagram for  $O_h$  and  $C_{4v}$  complexes

Infrared spectroscopy has proved to be a valuable source of information with respect to the structure and bonding of metal carbonyl complexes<sup>10</sup>. It has already been mentioned in Chapter 2 that with the information derived from infrared spectroscopy it is possible to distinguish between monodentatively coordinated ligands and those which act as a bridge between two metal centres. Infrared spectroscopy can provide information on the symmetry of a complex from the number of carbonyl stretching bands.

In this Chapter the characterisation of the  $M(CO)_x(L)$  complexes ( $M = Cr$  or  $W$ ,  $x = 3, 4$ , or  $5$ ) will be outlined, and their reactions in both solution and solid

state discussed. The chemical kinetics of the reactions have been determined, where possible, in an effort to elucidate the mechanism for their subsequent reactions. It was necessary to attempt the synthesis of a number of  $M(CO)_5(L)$  complexes to see whether the conformational change induced on the ligand upon coordination of one  $M(CO)_5$  unit played a role in determining the complex formed, as proposed in Chapter

2

### 3.2.1. The synthesis and characterisation of $(\text{Cr}(\text{CO})_5)_2(\text{dphbpy})$ ( $\text{dphbpy} = \mu\text{-4,4'-biphenyl-2,2'-bipyridine}$ ) and its reactions in solution and solid state.

#### 3.2.1.1. The preparation of $(\text{Cr}(\text{CO})_5)_2(\text{dphbpy})$

A sample of  $\text{Cr}(\text{CO})_5(\text{cis-cyclo-octene})$  was reacted with a solution of  $\text{dphbpy}$ , dissolved in toluene, in a 2 : 1 molar ratio at 273K under an argon atmosphere in the hope of forming the  $(\text{Cr}(\text{CO})_5)_2(\text{dphbpy})$  species. The ligand exists, in its free form in solution, in the *s-trans* conformation<sup>11</sup>. Based on previous structural analysis of  $\text{Cr}(\text{CO})_5(2\text{-phpy})$ , it was anticipated that the coordination of one pyridyl nitrogen to a  $\text{Cr}(\text{CO})_5$  unit would induce a conformational change on the ligand, with a subsequent increase in the  $\text{pK}_a$  of the uncoordinated nitrogen of the conjugate acid. This uncoordinated nitrogen would then compete more effectively for the remaining  $\text{Cr}(\text{CO})_5$  units than the free ligand, which would result in the formation of the ligand bridged metal carbonyl complex. The isolation of this complex was predicted from Chapter 2 and its subsequent reaction to form the  $\text{Cr}(\text{CO})_4(\text{dphbpy})$  chelate product, in the solid and solution state was studied.

Two other such complexes have been successfully isolated and characterised<sup>12,13</sup>. The molecular formula of the complex was confirmed by elemental analysis.

### 3.2.1.2. The characterisation of $(\text{Cr}(\text{CO})_5)_2(\text{dphbpy})$ by infrared and UV-visible spectroscopy.

The vibrational spectra of metal carbonyl complexes are generally obtained between 2200 and 1700 wavenumbers. This region provides a wealth of information relating to structure and bonding.  $\text{M}(\text{CO})_5(\text{amine})$  ( $\text{M} = \text{Cr}, \text{Mo}, \text{W}$ ) complexes are ideally of  $\text{C}_{4v}$  symmetry, resulting in three infrared allowed CO stretching vibrations, two of symmetry  $\text{A}_1$  and one of E symmetry<sup>10</sup>

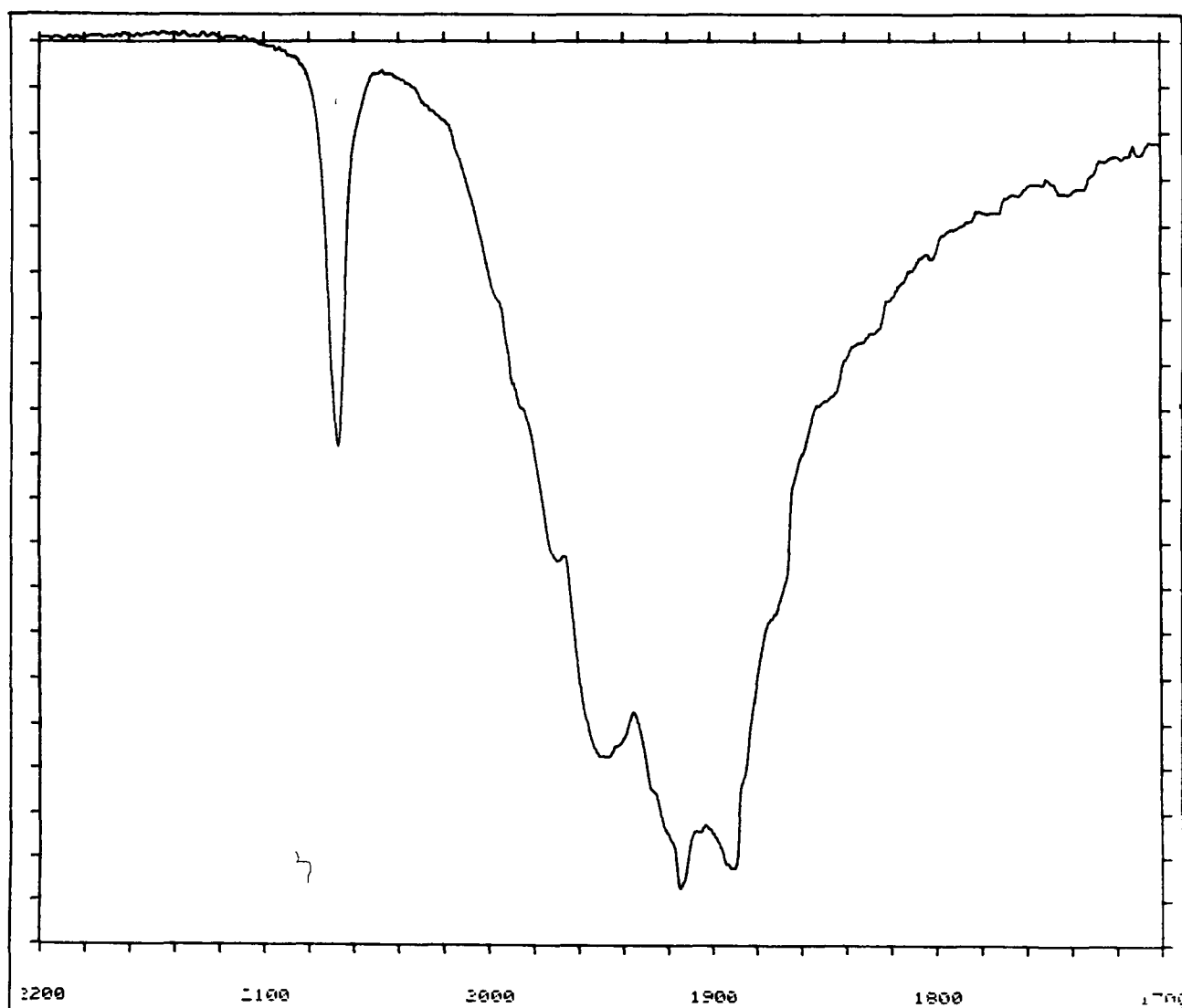


Figure 3 2.1.2 1 The infrared spectrum of a sample of  $(\text{Cr}(\text{CO})_5)_2(\text{dphbpy})$ , pressed in a KBr pellet

The infrared spectrum of a sample of  $(\text{Cr}(\text{CO})_5)_2(\text{dphbpy})$ , pressed in a KBr pellet, is presented in Figure 3.2.1.2.1. The complex exhibits bands at 2066, 1947, 1915 and  $1891\text{cm}^{-1}$ , which is consistent with a pseudo  $\text{C}_{4v}$  species where the ligand is coordinated in a monodentate fashion. These bands are assigned to the  $\text{A}_1$ ,  $\text{E}_1$  (the 'E' mode is split in the spectrum at 1947 and  $1915\text{cm}^{-1}$ ) and the  $\text{A}_1(2)$  modes of a  $\text{C}_{4v}$  complex, respectively. The presence of a shoulder at *ca*  $1972\text{cm}^{-1}$  is attributed to the normally forbidden  $\text{B}_1$  mode. This band is Raman active only in complexes of  $\text{C}_{4v}$  symmetry, but gains some intensity because the structure of the ligand makes it impossible for the molecule to have perfect  $\text{C}_{4v}$  symmetry<sup>10</sup>. This perturbation of the symmetry of the molecule about the metal carbonyl centre is effective in reducing the overall symmetry from pseudo  $\text{C}_{4v}$  to  $\text{C}_s$ . The removal of the degeneracy of the E mode is also indicative of a perturbation of the local symmetry.

This splitting of the E mode has been noted previously<sup>12,14</sup>, where ligands have facilitated two metal centres. Had the  $\text{Cr}(\text{CO})_5(\text{dphbpy})$  complex formed, the infrared spectrum would have exhibited three bands for a complex possessing pseudo  $\text{C}_{4v}$  symmetry. The E mode would have been represented by one band occurring in the region between 1947 and  $1915\text{cm}^{-1}$ . An infrared spectrum of the  $(\text{Cr}(\text{CO})_5)_2(\text{dphbpy})$  complex in toluene solution ( $4.753 \times 10^{-3}\text{mol dm}^{-3}$ ) is presented in Figure 3.2.1.2.2. This affords a clearer view of this splitting, resulting in two bands at 1937 and  $1924\text{cm}^{-1}$ . However, the  $\text{B}_1$  mode is masked by the presence of the  $\text{T}_{1u}$  band of  $\text{Cr}(\text{CO})_6$  at *ca*  $1980\text{cm}^{-1}$ , which is formed rapidly when the pure  $(\text{Cr}(\text{CO})_5)_2(\text{dphbpy})$  is dissolved in toluene. The  $\text{A}_1(2)$  mode manifests itself as a shoulder on the E mode at  $1906\text{cm}^{-1}$ .



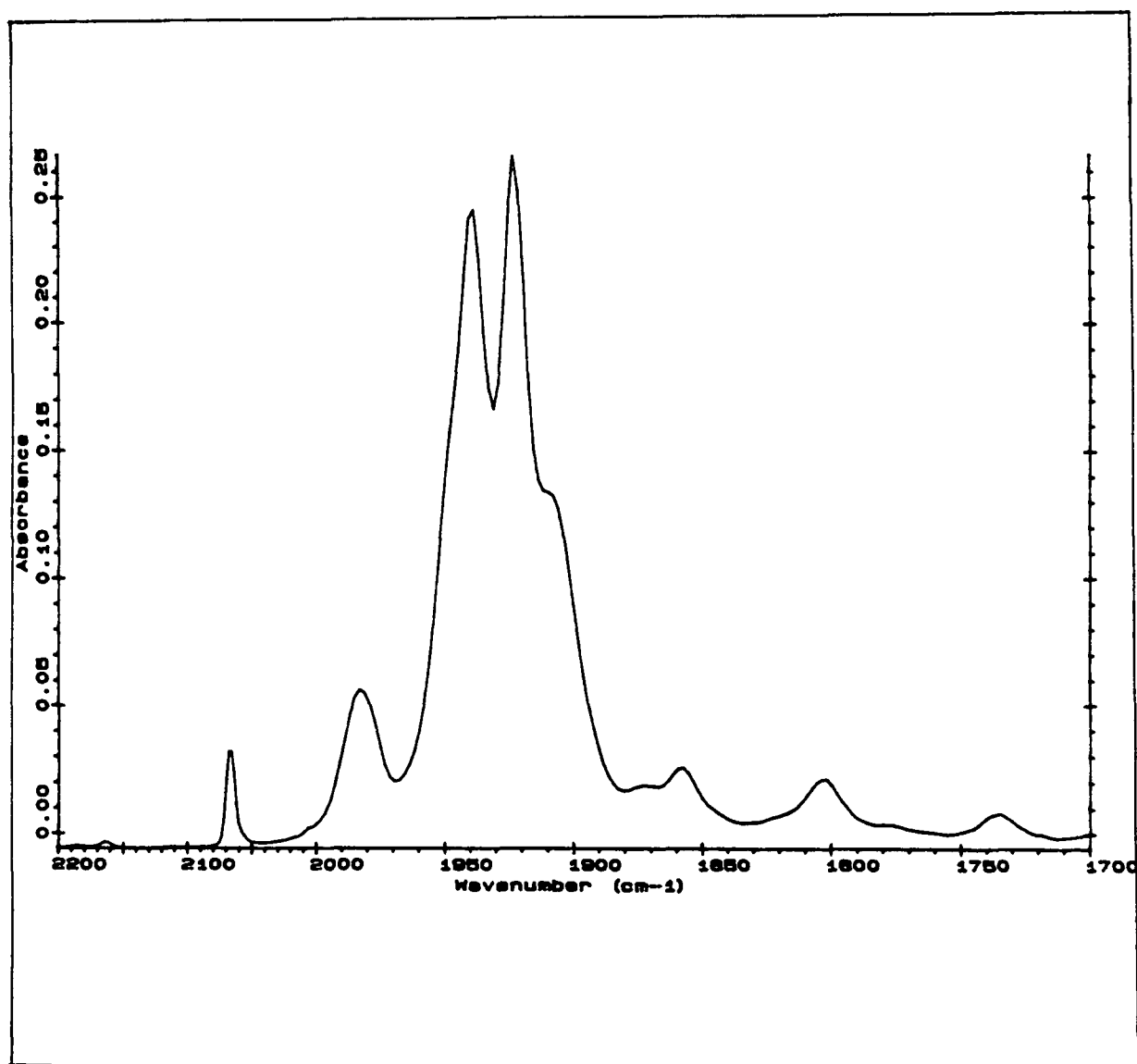


Figure 3.2 1.2 1 The infrared spectrum of a sample of  $(\text{Cr}(\text{CO})_5)_2(\text{dphbpy})$  in toluene solution ( $4.753 \times 10^{-3} \text{ mol dm}^{-3}$ )

The UV/visible absorption of a solution of  $(\text{Cr}(\text{CO})_5)_2(\text{dphbpy})$  ( $4.215 \times 10^{-4} \text{ mol dm}^{-3}$ ) in degassed toluene is presented in Figure 3 2 1.2.3 The spectrum exhibits a low energy absorption band centred at 404nm

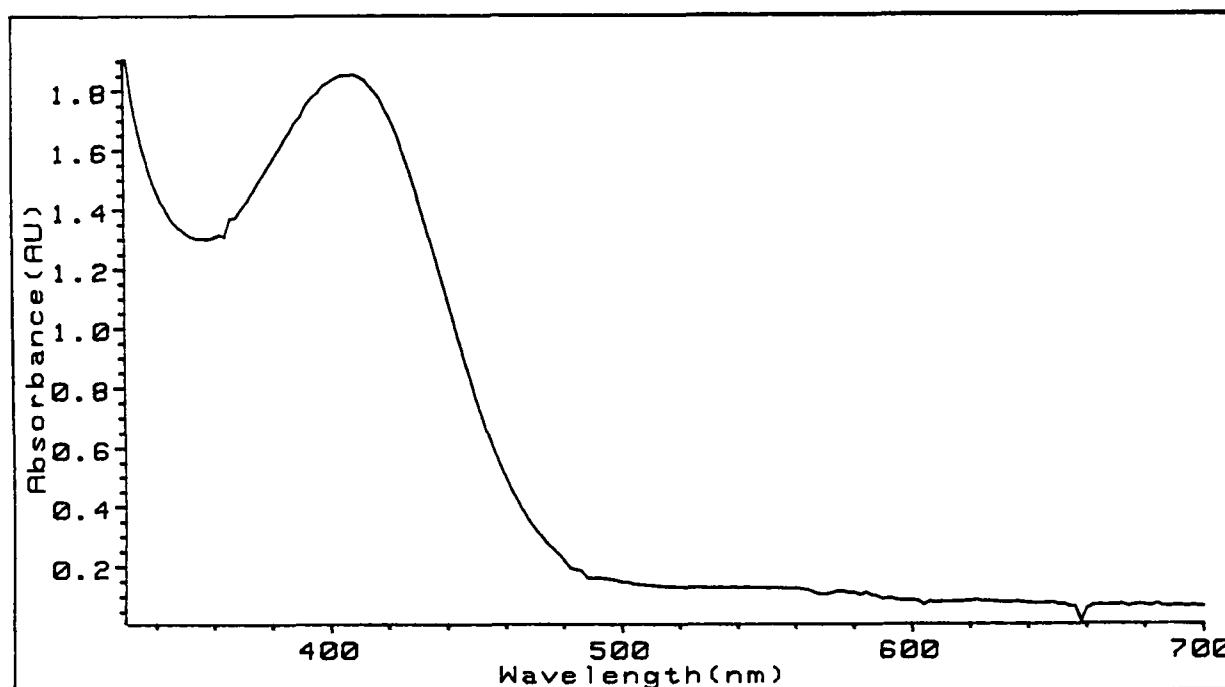


Figure 3 2 1.2.3 The absorption spectrum of a sample of  $(\text{Cr}(\text{CO})_5)_2(\text{dphbpy})$  in toluene solution ( $4.215 \times 10^{-4} \text{ mol dm}^{-3}$ )

Perutz and Turner<sup>4</sup> proposed that the lowest absorption band for  $\text{M}(\text{CO})_5$  in a variety of matrices, is attributed to a  $^1\text{A}(\text{e}^4\text{b}_2^2) \rightarrow ^1\text{E}(\text{e}^3\text{b}_2^2\text{a}_1^1)$  LF transition. Upon comparison with other spectra (Table 3 2.1 2 1) the absorption band at 404nm may be assigned the LF transition. There is no MLCT band exhibited by the complex so it is assumed that it overlaps with the LF band and is thus masked.

The mononuclear and binuclear complexes of 4,4'-bpy and bpe<sup>14</sup> have similar absorption bands. The energy of the  $\pi^*$  orbitals may be assessed by the position of the MLCT bands. The MLCT bands of the  $(\text{W}(\text{CO})_5)_2(\text{L})$  and  $\text{W}(\text{CO})_5(\text{L})$  ( $\text{L} = 4,4'$ -

bpy and bpe) complexes are slightly lower in energy than the LF bands, indicative of stabilisation, to a small extent, of the ligand  $\pi^*$  orbitals<sup>14</sup> In contrast, the MLCT bands of the  $(\text{Cr}(\text{CO})_5)_2(\text{L})$  ( $\text{L} = \text{dphbpy}$ ,  $\text{bpy}$ ,  $\text{dmbpy}$ ) and  $\text{Cr}(\text{CO})_5(4\text{-phpy})$  complexes overlap with their LF transition band The energy of the ligand  $\pi^*$  orbital is dependant upon the degree of conjugation present in the complex The absence of an MLCT band above 404nm in the  $(\text{Cr}(\text{CO})_5)_2(\text{dphbpy})$  complex suggests little  $\pi^*$  conjugation in the complex The crystal structure of a similar complex<sup>15</sup> presented in Figure 2.2.2.3 shows a twist of  $ca\ 90^\circ$  of the pyridine rings relative to each other The absence of coplanarity in the solid form is suggested in solution also, by the absence of any MLCT band above 410nm<sup>12</sup> A disturbance of coplanarity of the dphbpy ligand in the  $(\text{Cr}(\text{CO})_5)_2(\text{dphbpy})$  complex is thus implied

Table 3.2.1.2.1. A comparison of the absorption bands exhibited by some mononuclear and binuclear complexes of diimine ligands

Complex	Lambda Max	MLCT	Reference
$(\text{Cr}(\text{CO})_5)_2(\text{dphbpy})$	404	overlaps with LF	this work
$(\text{Cr}(\text{CO})_5)_2(\text{bpy})$	410	overlaps with LF	13
$(\text{Cr}(\text{CO})_5)_2(\text{dmbpy})$	410	overlaps with LF	12
$(\text{W}(\text{CO})_5)_2(4,4'\text{-bpy})$	404	438	14
$\text{W}(\text{CO})_5(4,4'\text{-bpy})$	400	overlaps with LF	14
$\text{W}(\text{CO})_5(\text{bpe})$	402	440 (sh)	14
$(\text{W}(\text{CO})_5)_2(\text{bpe})$	404	450	14
$\text{Cr}(\text{CO})_5(4\text{-phpy})$	396	overlaps with LF	16

bpe= *trans*-1,2-bis-(4-pyridylethylene)

Previously in Chapter 2, it was proposed that the formation of a ligand bridged metal carbonyl complex was preceded by a disturbance of the coplanarity of

the ligand. This disturbance of coplanarity was proposed as a prerequisite for the formation of such species. Thus, the absence of  $\pi^*$  conjugation is not surprising when studying the absorption spectra of such species. Bipyridine<sup>11</sup> ligands exhibit absorption bands at 290nm attributable to a  $\pi$ - $\pi^*$  transition. The absence of this band in the  $(\text{Cr}(\text{CO})_5)_2(\text{dphbpy})$  species is suggestive of a higher bpy based  $\pi^*$  energy level in the complex than in the free ligand or chelate  $\text{Cr}(\text{CO})_4(\text{dphbpy})$ . Again the implication of an absence of coplanarity between the two pyridine rings arises, preventing efficient overlap of the  $\pi$  systems on the rings.

### **3.2.1.3. The reactions of $(\text{Cr}(\text{CO})_5)_2(\text{dphbpy})$ in the solid state, as monitored by infrared spectroscopy.**

The infrared spectral changes observed upon heating a sample of  $(\text{Cr}(\text{CO})_5)_2(\text{dphbpy})$ , pressed in a KBr pellet, are shown in Figure 3.2.1.3.1. The bands assigned to this complex are seen to diminish with a simultaneous growth of bands at 2006, 1887, 1870 and 1806 $\text{cm}^{-1}$ , following warming to 393K and scanning at five minute intervals. These four new bands may be assigned to the  $A_1$ ,  $B_1$ ,  $A_1^2$  and  $B_2$  modes of a  $C_{2v}$  *cis*- $\text{Cr}(\text{CO})_4(\text{dphbpy})$  complex. The assignments for the CO stretching modes are based on those of Cotton and Kraihanzel<sup>10</sup> for the corresponding 2,2'-bipyridyl complexes. The assignments were justified by the virtual identity of the  $\text{Cr}(\text{CO})_4(\text{bpy})$  and  $\text{Cr}(\text{CO})_4(\text{dphbpy})$  solution spectra. The formation of  $\text{Cr}(\text{CO})_6$  was observed in the solution state but as it is a volatile compound it sublimes and its formation is not detected while warming the  $(\text{Cr}(\text{CO})_5)_2(\text{dphbpy})$  complex in the solid state.

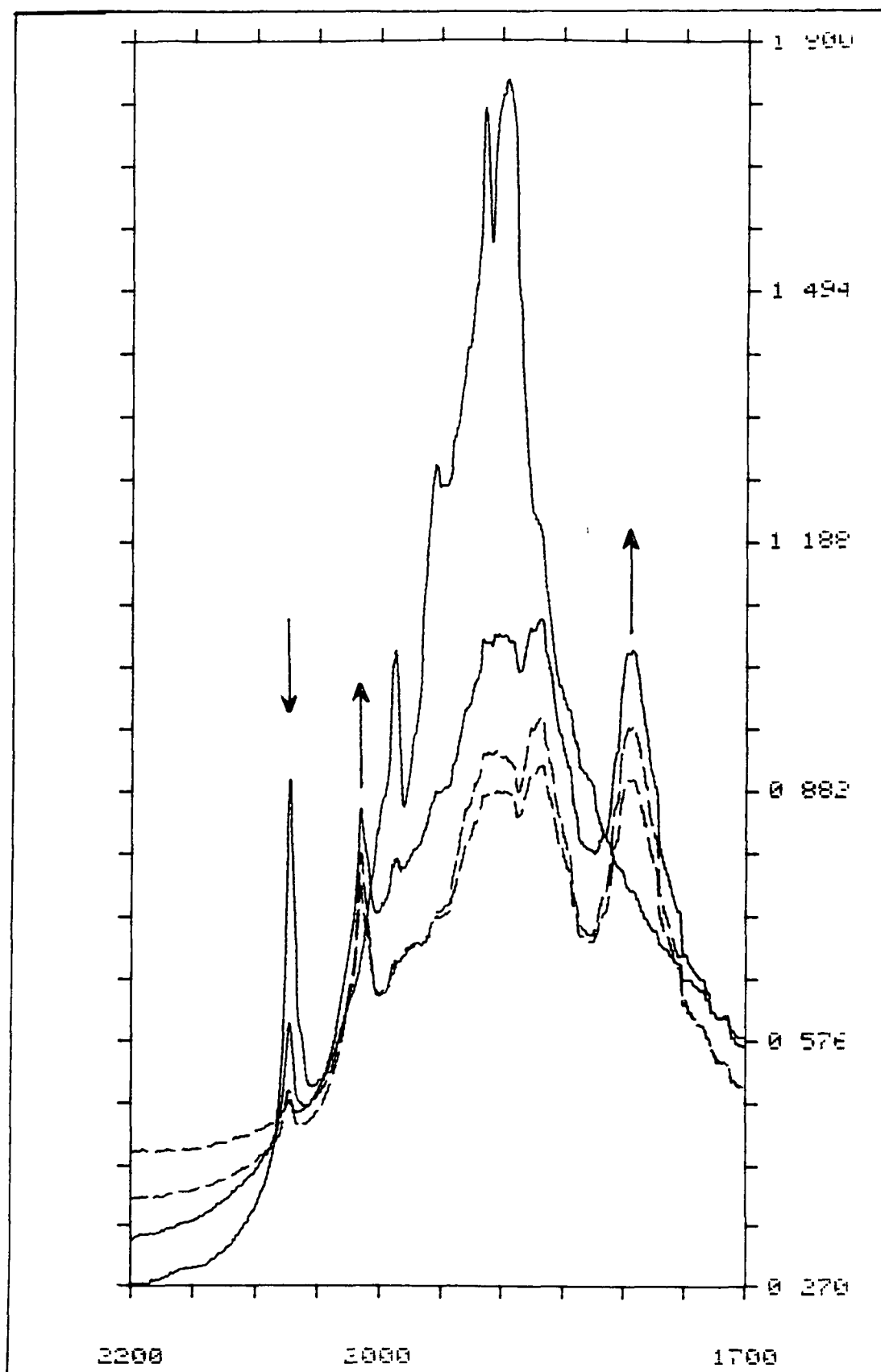


Figure 3 2 1 3 1 The infrared spectrum of a sample of  $(\text{Cr}(\text{CO})_5)_2(\text{dphbpy})$ , pressed in a KBr pellet, following warming to 393K and scanning at five minute intervals.

### 3.2.1.4. The reactions of $(\text{Cr}(\text{CO})_5)_2(\text{dphbpy})$ in toluene solution, in the absence and presence of excess ligand, as monitored by infrared spectroscopy.

The reaction of the  $(\text{Cr}(\text{CO})_5)_2(\text{dphbpy})$  complex in solution was monitored by infrared spectroscopy in the hope of obtaining the stoichiometry of the reaction by determining the molar extinction coefficients. The infrared spectral changes occurring upon standing a sample of  $(\text{Cr}(\text{CO})_5)_2(\text{dphbpy})$ , dissolved in toluene solution ( $4.753 \times 10^{-3} \text{ mol dm}^{-3}$ ), at ambient temperature are presented in Figure 3.2.1 4.1, using a 0.1 mm pathlength.

The bands at 2066, 1937, 1924, and 1906 which were assigned to the  $(\text{Cr}(\text{CO})_5)_2(\text{dphbpy})$  species, are seen to diminish in intensity with a concomitant growth of new bands at 2005, 1980, 1898, 1843 and  $1794 \text{ cm}^{-1}$ . The band at  $1980 \text{ cm}^{-1}$  may be attributed to the formation of  $\text{Cr}(\text{CO})_6$ . The bands at 2005, 1898, 1843 and  $1796 \text{ cm}^{-1}$  may be assigned the  $A_1$ ,  $B_1$ ,  $A_1(2)$  and  $B_2$  modes of a *cis*- $\text{Cr}(\text{CO})_4(\text{dphbpy})$  complex possessing  $C_{2v}$  symmetry<sup>10</sup>. The  $B_1$  band at  $1898 \text{ cm}^{-1}$  was observed as a shoulder only. The regeneration of the parent hexacarbonyl was surprising in light of the fact that many workers assumed the mechanism of chelate formation from  $\text{Cr}(\text{CO})_5(\text{bpy})$  occurred via an intramolecular CO extrusion process<sup>17</sup>. If this were so the regeneration of the parent hexacarbonyl should not be observed. A 50% regeneration of the parent hexacarbonyl has been observed by other investigators with the reaction of the  $(\text{Cr}(\text{CO})_5)_2(\text{dmbpy})$ <sup>12</sup> and  $(\text{Cr}(\text{CO})_5)_2(\text{bpy})$ <sup>13</sup> complexes, in toluene solution at ambient temperature. The formation of the  $\text{Cr}(\text{CO})_4(\text{dpe})$  and  $\text{Cr}(\text{CO})_6$  from  $(\text{Cr}(\text{CO})_5)_2(\text{dpe})$  ( $\text{dpe} = \text{Ph}_2\text{PCH}_2\text{CH}_2\text{PPh}_2$ ) in a 1:1 molar ratio has also been observed upon heating a sample of the complex, dissolved in *n*-octane solution<sup>18</sup>.

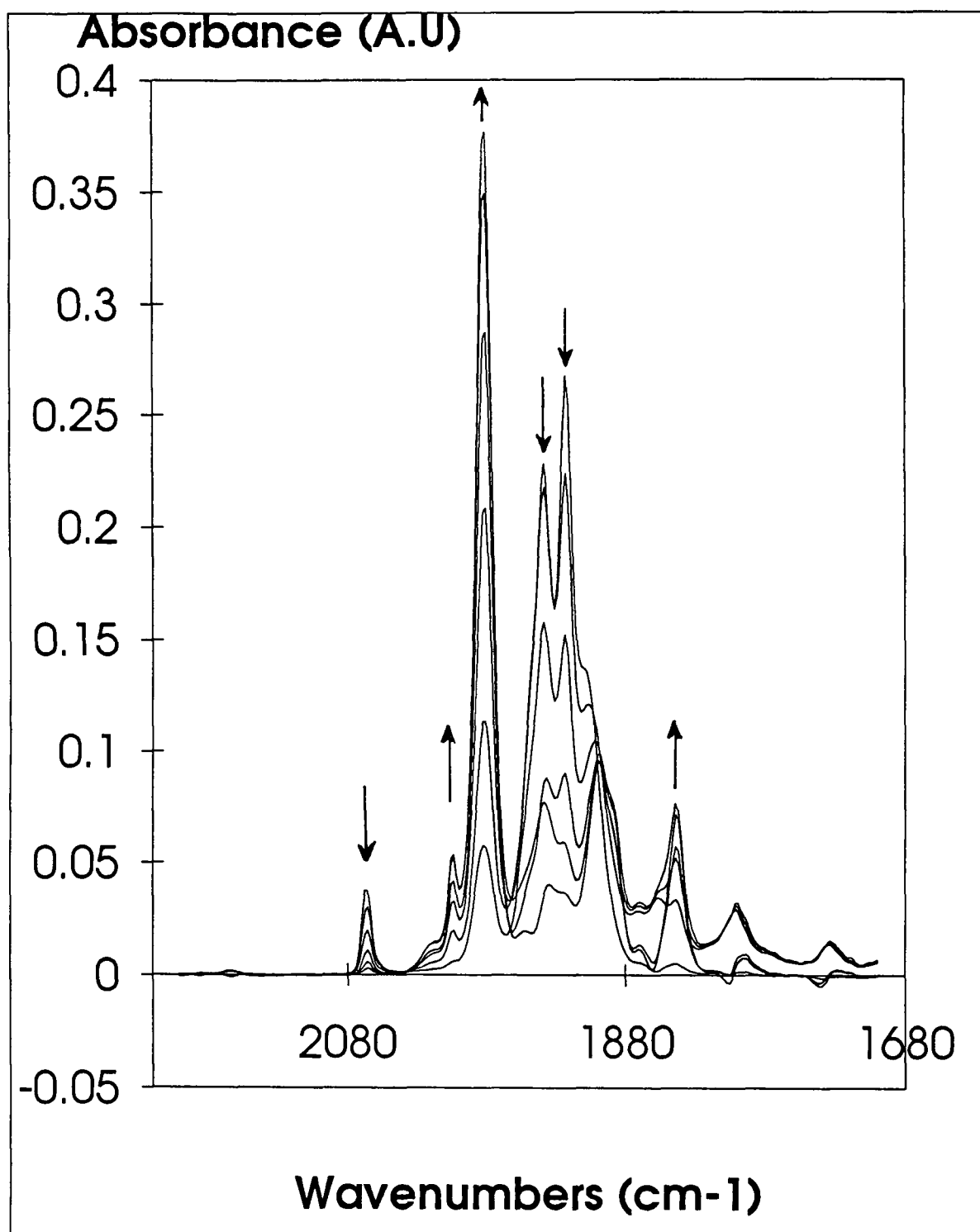


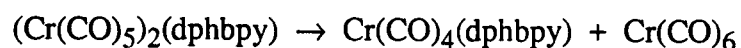
Figure 3.2 1 4 1 The infrared spectral changes occurring upon standing a sample of  $(\text{Cr}(\text{CO})_5)_2(\text{dphbpy})$ , dissolved in toluene solution ( $4.753 \times 10^{-3} \text{ mol dm}^{-3}$ ), at ambient temperature for 0, 5, 10, 15, 20 and 24 minutes, using a 0.1 mm pathlength

By determining the molar extinction coefficients of the various complexes it was possible to determine the stoichiometry of the reaction, by monitoring the changes in the absorbance over time. The data for the determination of the molar extinction coefficients is presented in Table 3.2.1 4 1

Table 3 2.1 4 1.. The experimental data for the determination of the molar extinction coefficients of the  $(\text{Cr}(\text{CO})_5)_2(\text{dphbpy})$  and  $\text{Cr}(\text{CO})_4(\text{dphbpy})$  complexes, by infrared spectroscopy using a 0.2mm pathlength

Complex	Concentration ( $\text{mol dm}^{-3}$ )	Absorbance (A. U.)	$\epsilon$ ( $\text{dm}^3 \text{mol}^{-1} \text{cm}^{-1}$ )
$(\text{Cr}(\text{CO})_5)_2(\text{dphbpy})$ 2066 $\text{cm}^{-1}$	$2.032 \times 10^{-3}$	0.0358	880
	$1.482 \times 10^{-3}$	0.0256	863.7
	$2.252 \times 10^{-4}$	0.0091	866.3
			$\epsilon = 873$
$\text{Cr}(\text{CO})_4(\text{dphbpy})$ 1843 $\text{cm}^{-1}$	$2.4138 \times 10^{-3}$	0.0908	1880.8
	$1.832 \times 10^{-3}$	0.0739	2016.9
	$1.397 \times 10^{-3}$	0.0545	1950.6
			$\epsilon = 1949$
$\text{Cr}(\text{CO})_6^{13}$			14,505

From the results obtained the stoichiometry of the reaction is presented in equation 3.2.1 4.1



equation 3 2.1 4.1



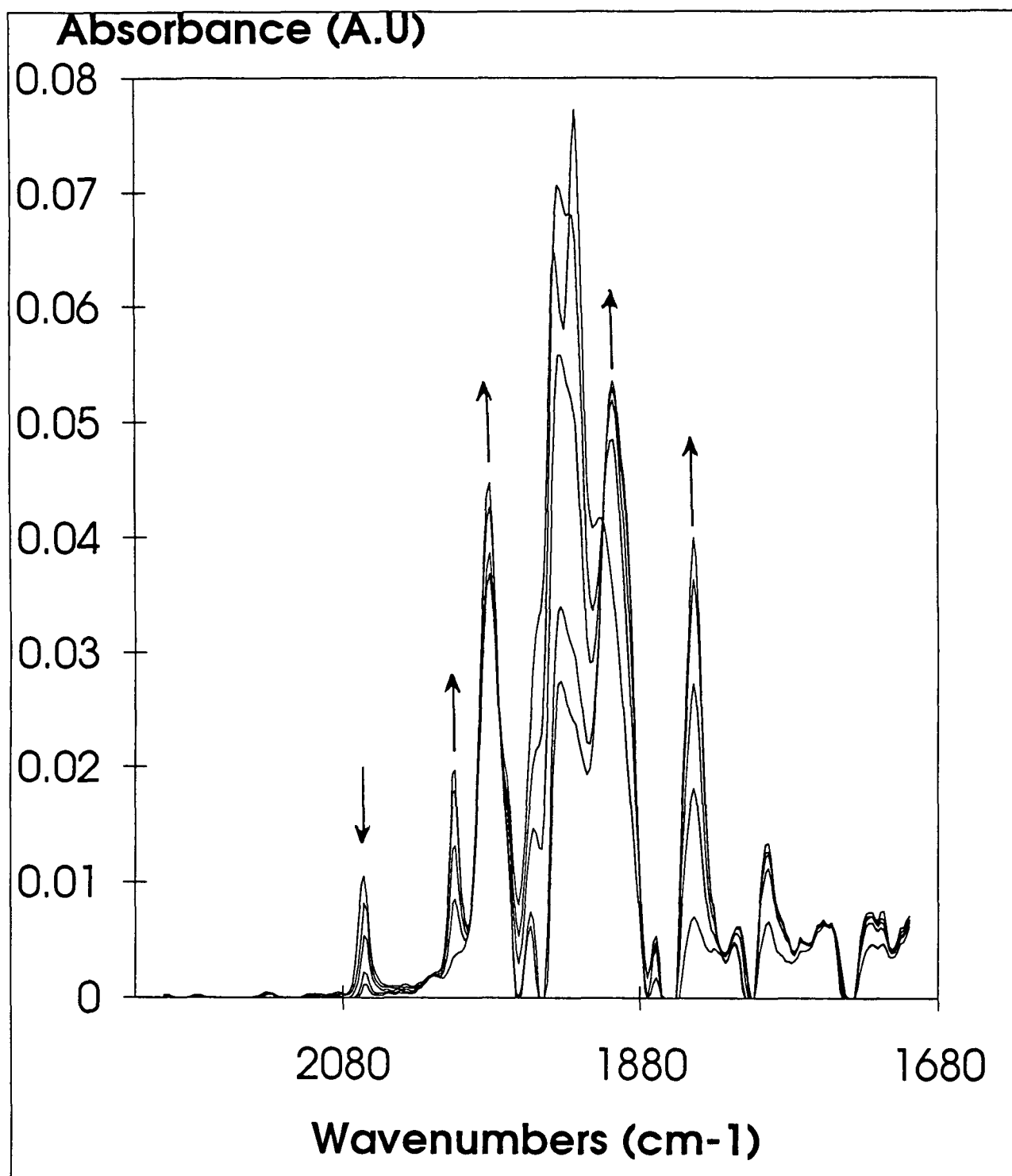
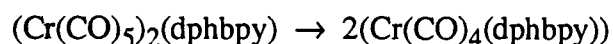


Figure 3 2 1 4.2 The infrared spectral changes occurring upon standing a sample of  $(\text{Cr}(\text{CO})_5)_2(\text{dphbpy})$ , dissolved in toluene solution ( $5.22 \times 10^{-4} \text{ mol dm}^{-3}$ ) containing excess ligand ( $3.24 \times 10^{-2} \text{ mol dm}^{-3}$ ), at ambient temperature for 0, 4, 8, 16 and 22 minutes, using a 0.2 mm pathlength

It appears that an intramolecular CO extrusion process plays no role here. This stoichiometry was observed by Creaven<sup>12,13</sup> during the study of the  $(\text{Cr}(\text{CO})_5)_2(\text{dmbpy})$  and  $(\text{Cr}(\text{CO})_5)_2(\text{bpy})$  complexes.

The infrared spectral changes, using a 0.2mm pathlength, occurring upon standing a sample of  $(\text{Cr}(\text{CO})_5)_2(\text{dphbpy})$ , dissolved in toluene solution ( $5.22 \times 10^{-4} \text{ mol dm}^{-3}$ ) containing excess ligand ( $3.24 \times 10^{-2} \text{ mol dm}^{-3}$ ), at ambient temperature are presented in Figure 3.2.1.4.2. The most striking difference between this study and that conducted in the absence of any excess ligand is the suppression of the formation of the parent hexacarbonyl. In the absence of any excess ligand there is a 50% regeneration of the  $\text{Cr}(\text{CO})_6$  compound which is reduced to *ca* 3% in the presence of excess ligand. The intensity of the bands corresponding to the  $\text{Cr}(\text{CO})_4(\text{dphbpy})$  complex have also appeared to increase. By monitoring the changes in the absorbance over time it was possible to determine the stoichiometry of the reaction, which is presented in equation 3.2.1.4.2.



equation 3.2.1.4.2

This stoichiometry is consistent with a CO extrusion process. It appears that the presence of excess ligand the  $(\text{Cr}(\text{CO})_5)_2(\text{dphbpy})$  complex forms two moles of  $\text{Cr}(\text{CO})_5(\text{dphbpy})$  which results in the formation of two moles of  $\text{Cr}(\text{CO})_4(\text{dphbpy})$ . To further propose a mechanism for the reaction of this complex, the activation parameters must be determined.

### 3.2.1.5. The reaction of $(\text{Cr}(\text{CO})_5)_2(\text{dphbpy})$ in toluene solution, in the absence and presence of excess ligand, as monitored by UV-visible spectroscopy

The reaction of a solution of  $(\text{Cr}(\text{CO})_5)_2(\text{dphbpy})$  ( $5.048 \times 10^{-4} \text{ mol dm}^{-3}$ ) (Figure 3 2 1 5.1 a) in degassed toluene, upon standing at room temperature, was monitored by UV-visible spectroscopy. The band centred at 404nm, corresponding to the  $^1\text{A} \rightarrow ^1\text{E}$  LF transition of  $(\text{Cr}(\text{CO})_5)_2(\text{dphbpy})$  depletes with the concomitant growth of a band at 556nm. Two isosbestic points, maintained at 366 and 450nm are indicative of a reaction uncomplicated by side or subsequent reactions. The final spectrum (presented in Figure 3 2 1 5 1.b), recorded at 4000 seconds exhibits two bands at *ca* 400 and 556nm, which correspond to the *cis*- $\text{Cr}(\text{CO})_4(\text{dphbpy})$  complex. The band at 556nm has been assigned the MLCT band, while the band at 400nm is the  $^1\text{A} \rightarrow ^1\text{A}$  LF transition. The position of the MLCT band is substantially lowered by the formation of the chelate product, indicative of a restoration of coplanarity in a highly conjugated complex.

The rate constant for the formation of  $\text{Cr}(\text{CO})_4(\text{dphbpy})$  was determined by monitoring the growth of the MLCT band at 556nm. The rate constant was calculated using Hewlett-Packard kinetics software, which employs a curve fitting method for first order kinetics. The slope of the plotted line is taken as the rate constant for the reaction,  $k_{\text{obs}}$ , which was calculated as  $2.5 \times 10^{-4} \text{ s}^{-1}$  at 299K for this complex. The plot of the absorbance at 556nm against time for the formation of  $\text{Cr}(\text{CO})_4(\text{dphbpy})$  is presented in Figure 3 2 1 5 2, and a single exponential function is fitted to this curve.

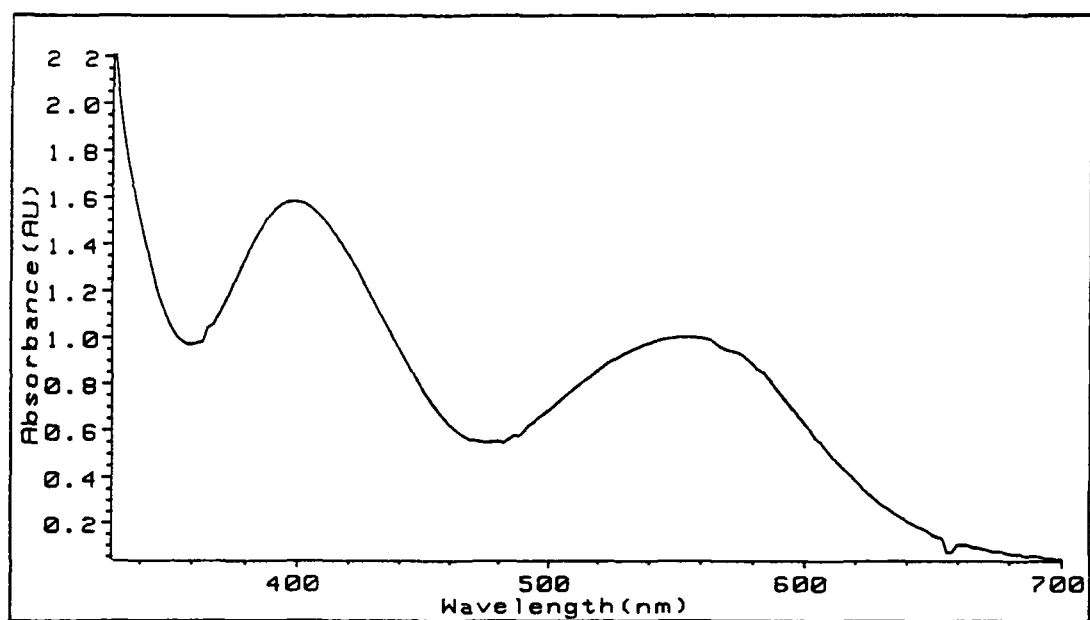
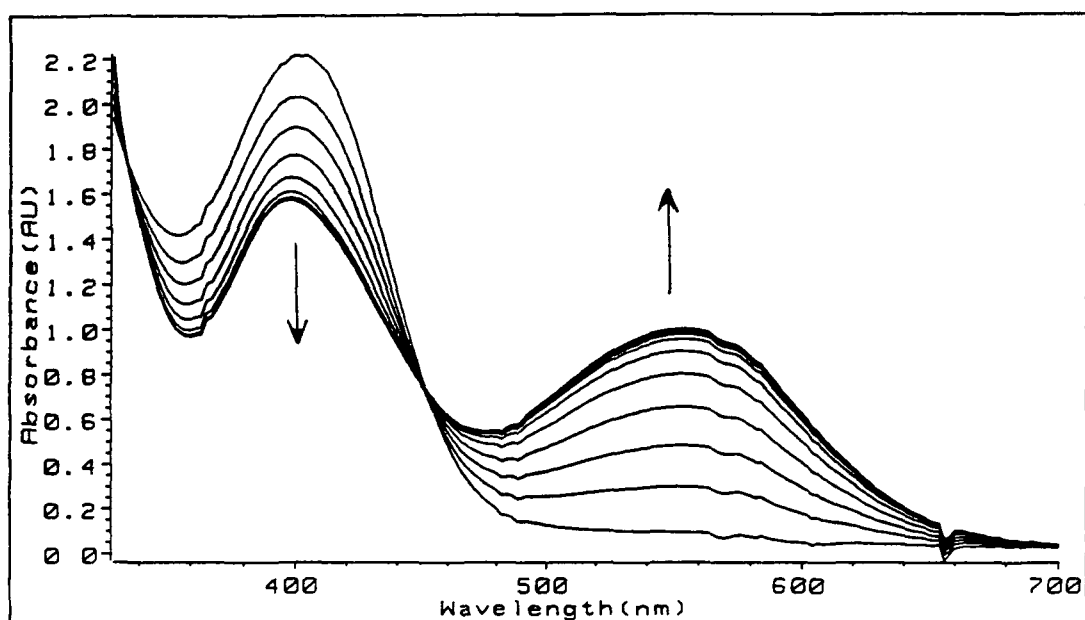


Figure 3 2 1 5 1 The spectral changes occurring upon standing a sample of  $(\text{Cr}(\text{CO})_5)_2(\text{dphbpy})$  ( $5.048 \times 10^{-4} \text{ mol dm}^{-3}$ ) in toluene solution at 299K and (b) the spectrum recorded after standing for 4000 seconds

Similar studies have been performed using  $(\text{Cr}(\text{CO})_5)_2(\text{bpy})^{13}$  and  $(\text{Cr}(\text{CO})_5)_2(\text{dmbpy})^{12}$ . The rate constant for the formation of  $\text{Cr}(\text{CO})_4\text{bpy}^{13}$  was found to be  $8.33 \times 10^{-3} \text{ s}^{-1}$  at 293K while  $k_{\text{obs}}$  for the formation of  $\text{Cr}(\text{CO})_4(\text{dmbpy})^{12}$  was  $3.33 \times 10^{-4} \text{ s}^{-1}$  at 293K. The formation of  $\text{Cr}(\text{CO})_4(\text{dphbpy})$  appears slower than that for the bpy and dmbpy ligands and this may be attributed to an increase in steric hindrance. The rate constant for the formation of the chelate complex using photoinitiated  $\text{W}(\text{CO})_5$  and the bpy, dmbpy and dphbpy ligands resulted in an ordering of the ligands based on the  $k_{\text{obs}}$ , which was  $\text{bpy} > \text{dmbpy} > \text{dphbpy}$ , which is the order of increasing steric hindrance<sup>19</sup>.

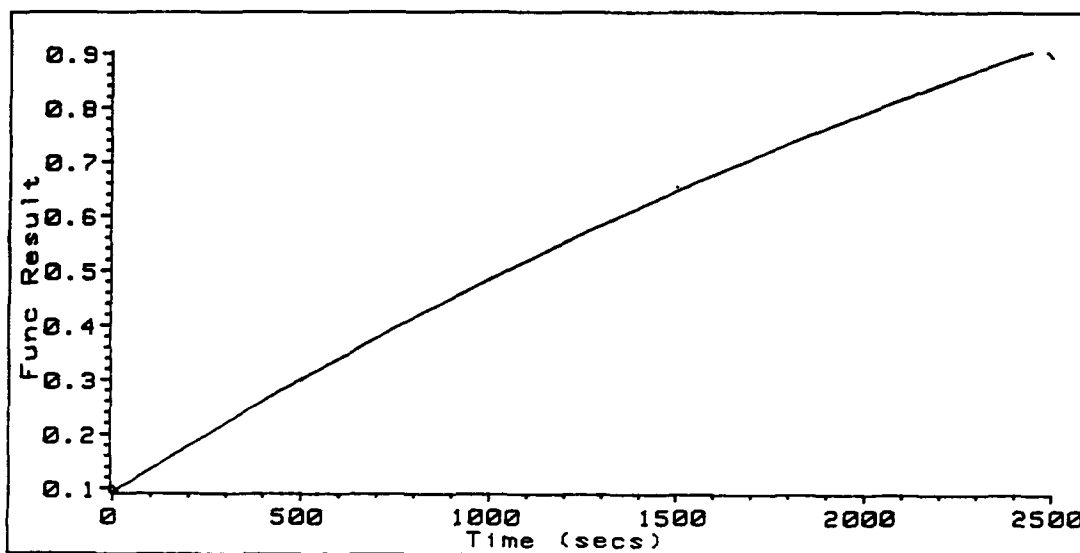


Figure 3.2.1.5.2 The plot of absorbance at 556nm against time for the formation of  $\text{Cr}(\text{CO})_4(\text{dphbpy})$ , as monitored by UV-visible spectroscopy at 556nm

The introduction of an excess of ligand into the reaction of  $(\text{Cr}(\text{CO})_5)_2(\text{dphbpy})$  in toluene solution had a substantial effect on the amount of  $\text{Cr}(\text{CO})_4(\text{dphbpy})$  formed, as verified by infrared spectroscopy. It may be possible that

the introduction of excess ligand will have an effect on the rate of formation of the chelate species. Previous workers<sup>20,21,22</sup> have employed up to a 100 fold excess of ligand while measuring the rate of chelate formation. We have measured the kinetics for the formation of  $\text{Cr(CO)}_4(\text{dphbpy})$  in toluene solution containing a range of ligand concentrations, while monitoring the reactions by UV-visible spectroscopy.

The spectral changes occurring upon standing a sample of  $(\text{Cr(CO)}_5)_2(\text{dphbpy})$  in toluene solution ( $4.215 \times 10^{-4} \text{ mol dm}^{-3}$ ) containing excess ligand ( $3.24 \times 10^{-3} \text{ mol dm}^{-3}$ ) at 299K, are shown in Figure 3.2.1.5.3. The band at 556nm, corresponding to the MLCT band of  $\text{Cr(CO)}_4(\text{dphbpy})$ , appears to have intensified with the addition of excess ligand, relative to the LF transition at 404nm of the  $(\text{Cr(CO)}_5)_2(\text{dphbpy})$  complex.

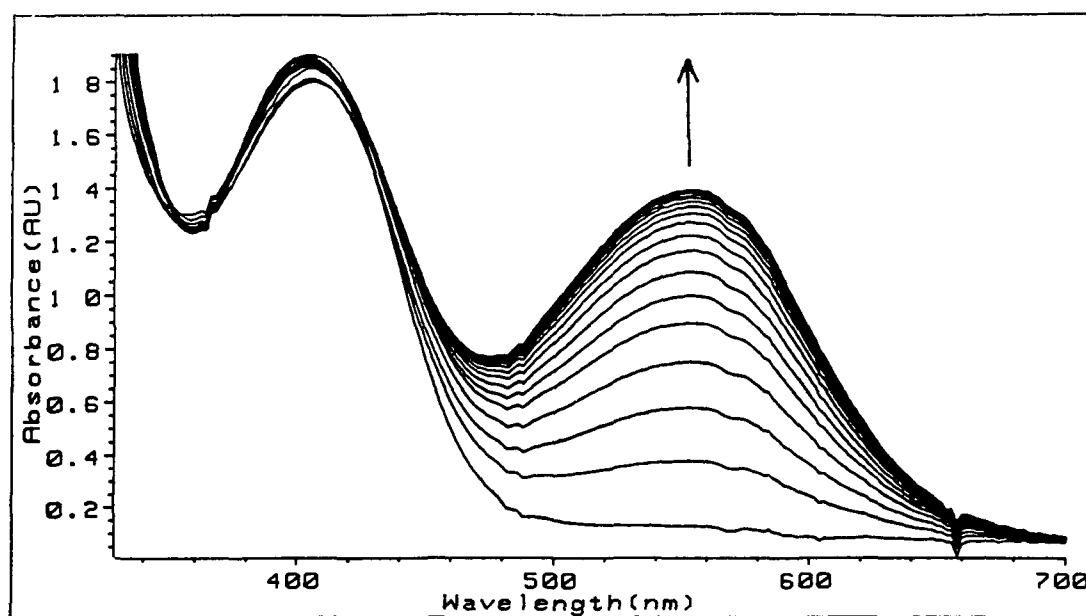


Figure 3.2.1.5.3 The spectral changes occurring upon standing a sample of  $(\text{Cr(CO)}_5)_2(\text{dphbpy})$  in toluene solution ( $4.215 \times 10^{-4} \text{ mol dm}^{-3}$ ) containing excess ligand ( $3.24 \times 10^{-3} \text{ mol dm}^{-3}$ ) at 299K.

The maintenance of isosbestic points at *ca* 340 and 436nm is indicative of a reaction uncomplicated by side or subsequent reactions. The addition of varying concentrations of excess ligand appears to have had a substantial effect on the  $k_{\text{obs}}$  for the formation of  $\text{Cr}(\text{CO})_4(\text{dphbpy})$ . Table 3.2.1.5.1 lists the  $k_{\text{obs}}$  for the various concentrations of excess dphbpy used, while the plot of these values is presented in Figure 3.2.1.5.4.

Table 3.2.1.5.1 The variation of  $k_{\text{obs}}$ , for the formation of  $\text{Cr}(\text{CO})_4(\text{dphbpy})$ , with increasing ligand concentrations of dphbpy

Conc. of dphbpy (mol dm <sup>-3</sup> )	$k_{\text{obs}}$ @ 556nm (s <sup>-1</sup> )
0	$2.498 \times 10^{-4}$
$3.85 \times 10^{-3}$	$9.424 \times 10^{-4}$
$1.549 \times 10^{-2}$	$1.106 \times 10^{-3}$
$1.97 \times 10^{-2}$	$1.157 \times 10^{-3}$
$3.3 \times 10^{-2}$	$1.202 \times 10^{-3}$

The curve in Figure 3.2.1.5.4 exhibits a plateau, which is suggestive of an equilibrium process. However, it may also be indicative of an alteration in the reaction course resultant from the addition of excess ligand. It was not possible to determine the stoichiometry of the reaction here because of the overlap of the LF band of  $\text{Cr}(\text{CO})_4(\text{dphbpy})$  at 400nm with the LF/MLCT band of  $(\text{Cr}(\text{CO})_5)_2(\text{dphbpy})$ . Previous work of this type<sup>12</sup> involved a study of the effect of varying ligand concentration on  $k_{\text{obs}}$  for the formation of  $\text{Cr}(\text{CO})_4(\text{dmbpy})$ . The plateau effect was also observed and attributed to an alteration in the reaction pathway, resulting from the addition of excess ligand.

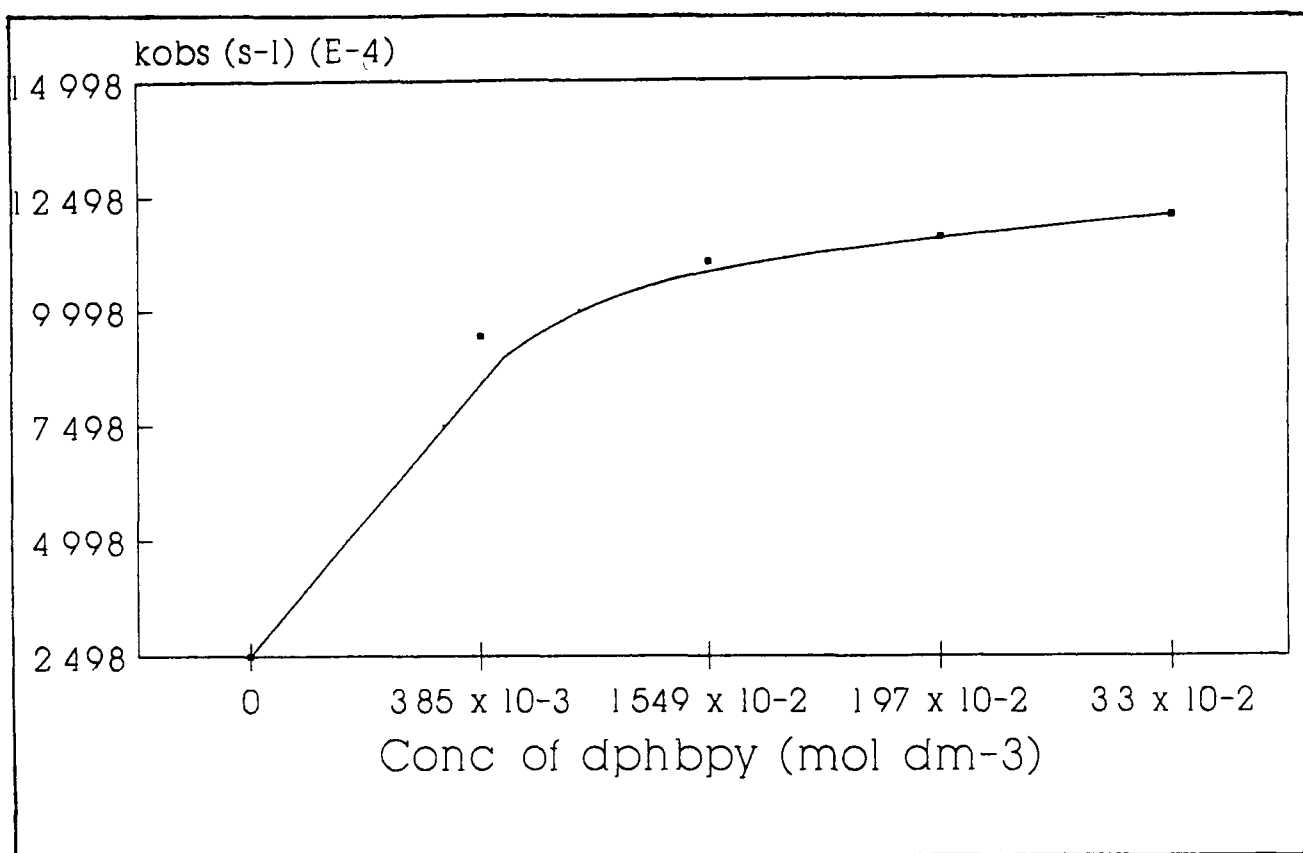


Figure 3 2 1.5 4 The dependence of  $k_{\text{obs}}$  ( $\text{s}^{-1}$ ), for the formation of  $\text{Cr}(\text{CO})_4(\text{dphbpy})$ , on the concentration of dphbpy added ( $\text{mol dm}^{-3}$ )

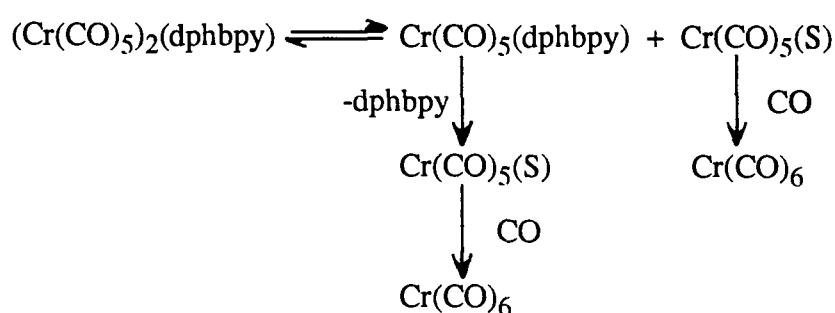
Addition of free ligand caused an increase of  $k_{\text{obs}}$  to a maximum value of  $1.2 \times 10^{-3} \text{ s}^{-1}$ , for the formation of  $\text{Cr}(\text{CO})_4(\text{dphbpy})$  Lees<sup>19,21,22</sup> *et al* have performed much work on the mechanism of ring closure using both photoinitiated and isolated  $\text{M}(\text{CO})_5\text{L}$  intermediates. The rate of chelate formation was found to be dependant on the nature of the ligand. This dependence was frequently interpreted as an implication of an associative mechanism. This may be attributed to the fact that these workers monitored chelation reactions in the presence of a 100 fold excess of ligand i.e. in the plateau region of free ligand concentration. In this work and previous investigations<sup>12,13</sup>, the rate of ring closure showed no dependence on ligand concentration.



### 3.2.1.6. The reaction of $(\text{Cr}(\text{CO})_5)_2(\text{dphbpy})$ in CO saturated toluene, as monitored by UV-visible spectroscopy

The spectral changes occurring upon dissolution of a sample of  $(\text{Cr}(\text{CO})_5)_2(\text{dphbpy})$  in CO saturated toluene ( $1.418 \times 10^{-4} \text{ mol dm}^{-3}$ ) are presented in Figure 3.2.1.6.1, as monitored by UV-visible spectroscopy. The LF band at 404nm, corresponding to  $(\text{Cr}(\text{CO})_5)_2(\text{dphbpy})$  is observed to diminish in intensity with no growth of new bands, i.e. the MLCT band at 556nm, corresponding to the  $\text{Cr}(\text{CO})_4(\text{dphbpy})$  species is not observed. However, the maintenance of an isosbestic point at ca 320nm indicates that a 'clean' reaction is taking place, possibly to form  $\text{Cr}(\text{CO})_6$ . The final spectrum, recorded after 360s, is presented in Figure 3.2.1.6.1 b.

Under these conditions the observed rate constant was found to be  $1.12 \times 10^{-2} \text{ s}^{-1}$ , which is almost 45 times faster than the reaction observed in the absence of CO or excess ligand. This implies that the dissociation of  $(\text{Cr}(\text{CO})_5)_2(\text{dphbpy})$  into  $\text{Cr}(\text{CO})_5$  and dphbpy is competing with the formation of  $\text{Cr}(\text{CO})_4(\text{dphbpy})$  from  $\text{Cr}(\text{CO})_5(\text{dphbpy})$ . However, the former reaction appears to be dominant as CO reacts with  $\text{Cr}(\text{CO})_5(\text{dphbpy})$  to regenerate  $\text{Cr}(\text{CO})_6$ . The presence of CO in solution suppresses the regeneration of  $(\text{Cr}(\text{CO})_5)_2(\text{dphbpy})$  from  $\text{Cr}(\text{CO})_5(\text{S})$  and  $\text{Cr}(\text{CO})_5(\text{dphbpy})$ . The reaction is summarised in the following Scheme



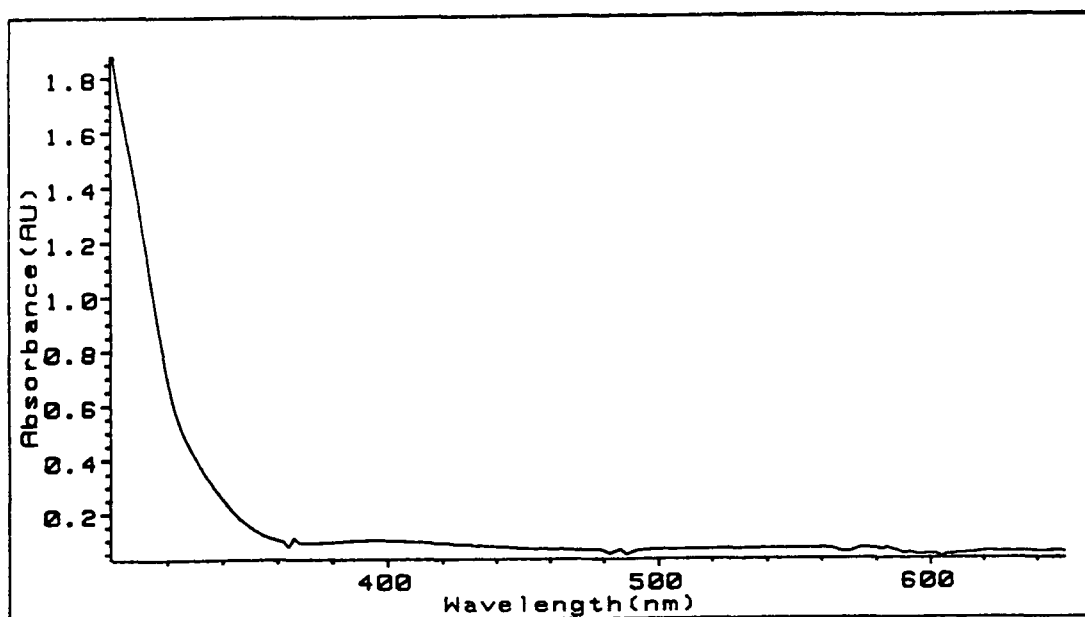
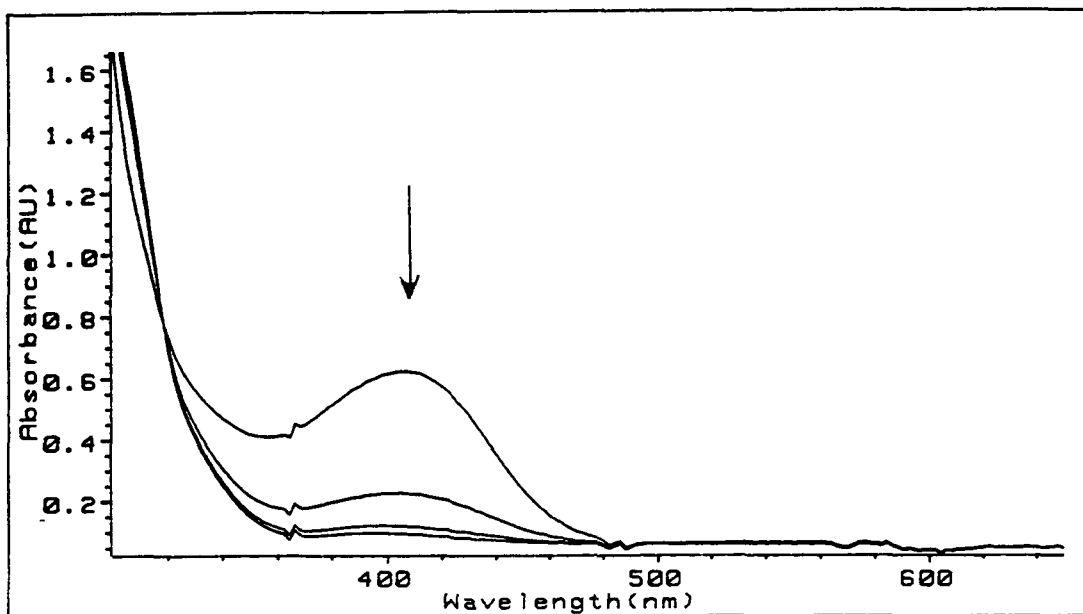
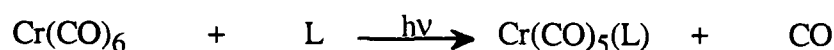


Figure 3.2.1.6.1 (a) The spectral changes occurring upon standing a sample of  $(\text{Cr}(\text{CO})_5)_2(\text{dphbpy})$  ( $1.418 \times 10^{-4} \text{ mol dm}^{-3}$ ) in CO saturated toluene and (b) the final spectrum, recorded after 360s

The  $k_{\text{obs}}$  for the formation of  $\text{Cr}(\text{CO})_6$  from the reaction of  $(\text{Cr}(\text{CO})_5)_2(\text{dmbpy})^{12}$  with CO in toluene, at ambient temperature, was found to be  $1.7 \times 10^{-1} \text{ s}^{-1}$ . This is approximately 1.5 times faster than the  $k_{\text{obs}}$  obtained in this study. This is in good agreement with previous work<sup>21</sup>. Wrighton's<sup>17</sup> irradiation work using the 4,4'-dialkyl-2,2'-bipyridine ligands and  $\text{M}(\text{CO})_6$  with  $\sim 1 \text{ mM}$  CO showed no regeneration of the parent carbonyl, however, this work was carried out in the presence of excess ligand. However, the  $\text{M}(\text{CO})_5(2\text{-phpy})$  photoinitiated intermediate regenerated  $\text{M}(\text{CO})_6$  with a rate constant of  $2.4 \times 10^{-4} \text{ s}^{-1}$ , for  $\text{M} = \text{Cr}$ , and  $3.3 \times 10^{-4} \text{ s}^{-1}$ , for  $\text{M} = \text{Mo}$ , in the presence of  $\sim 1 \text{ mM}$  CO. The regeneration of *ca* 50%  $\text{Mo}(\text{CO})_6$  from  $\text{Mo}(\text{CO})_5\text{L}$  ( $\text{L} = \text{piperidine (pip), py}$ )<sup>22</sup> has been observed to occur at room temperature. Unfortunately, this study was not performed in the presence of any CO. However, in CO saturated solution, the complex  $\text{Cr}(\text{CO})_5(\text{cis-cyclo-octene})$  has been observed to undergo a rapid and complete conversion to  $\text{Cr}(\text{CO})_6$ <sup>24</sup>. This reaction is significantly retarded if executed in the presence of an excess of *cis-cyclo-octene*. The reaction may be summarised in the following equations



$\text{L} = \text{cis-cyclo-octene}$

### 3.2.1.7. The activation parameters for the formation of $\text{Cr}(\text{CO})_4(\text{dphbpy})$ in the absence and presence of excess ligand.

The activation parameters for the formation of  $\text{Cr}(\text{CO})_4(\text{dphbpy})$  in the absence and presence of excess dphbpy are presented in Tables 3.2.1.7.1 and 3.2.1.7.2, respectively. The plots of the data are given in Figures 3.2.1.7.1 and 3.2.1.7.2.

Table 3.2.1.7.1. Experimental data for the determination of the activation parameters for the formation of  $\text{Cr}(\text{CO})_4(\text{dphbpy})$  in the absence of any excess ligand

Temperature (K)	$\text{Ln}(k_{\text{obs}})$	$\text{Ln}(k_{\text{obs}}/T)$
299	-7.857	-13.557
304	-7.287	-13.004
308	-6.741	-12.47
313	-6.146	-11.89
318	-5.856	-11.618

Arrhenius plot

$$\text{Slope} = -10,400 \pm 700$$

$$\text{Int} = 26.9 \pm 0.1$$

$$\text{Corr} = 0.994$$

Eyring plot

$$\text{Slope} = -10,000 \pm 700$$

$$\text{Int} = 20.2 \pm 0.1$$

$$\text{Corr} = 0.993$$

$$E_a = 86 \pm 7 \text{ kJ mol}^{-1}$$

$$\Delta H^\ddagger = 84 \pm 7 \text{ kJ mol}^{-1}$$

$$\Delta S^\ddagger = -29 \pm 5 \text{ J K}^{-1} \text{ mol}^{-1}$$

Table 3.2 1 7.2 Experimental data for the determination of the activation parameters for the formation of  $\text{Cr}(\text{CO})_4(\text{dphbpy})$  in the presence of excess ligand.

Temperature (K)	$\text{Ln}(k_{\text{obs}})$	$\text{Ln}(k_{\text{obs}}/T)$
299	-6 957	-12 657
304	-6 519	-12.236
308	-6 098	-11 83
313	-5.658	-11 4
318	-5.3	-11.06

Arrhenius Plot

$$\text{Slope} = -8,400 \pm 200$$

$$\text{Int} = 21.2 \pm 3 \times 10^{-2}$$

$$\text{Corr} = 0.998$$

Eyring Plot

$$\text{Slope} = -8,100 \pm 200$$

$$\text{Int.} = 14.6 \pm 3 \times 10^{-2}$$

$$\text{Corr} = 0.998$$

$$E_a = 70 \pm 2 \text{ kJ mol}^{-1}$$

$$\Delta H^\ddagger = 68 \pm 3 \text{ kJ mol}^{-1}$$

$$\Delta S^\ddagger = -76 \pm 5 \text{ J K}^{-1} \text{ mol}^{-1}$$

The apparent difference in activation parameter values for both cases is suggestive of different rate determining steps for the two processes. From the Arrhenius plots the activation energy, calculated from the slopes, gave values of  $86 \text{ kJ mol}^{-1}$  in the absence of any excess ligand, and  $70 \text{ kJ mol}^{-1}$  in the presence of excess ligand. The bond dissociation energy for the  $\text{Cr-N}^{25}$  bond in  $\text{Cr}(\text{CO})_5(\text{py})$  is  $106 \text{ kJ mol}^{-1}$  while the activation enthalpy for CO dissociation from  $\text{Cr}(\text{CO})_6^{20}$  is *ca*  $168 \text{ kJ mol}^{-1}$ . It is apparent from the differences in activation enthalpies that CO dissociation is not the sole process in the rate determining step. A comparison of activation

enthalpies between this and other studies is tabulated in Table 3 2.1.7.3, where the formation of the chelate was determined in the presence of excess ligand

Table 3 2.1 7 3 A comparison of the activation enthalpies between this study and previous studies

Metal	Ligand	$\Delta H^\ddagger(\text{kJ mol}^{-1})$	$\Delta S^\ddagger(\text{J K}^{-1}\text{mol}^{-1})$	Reference
Cr	$\text{Cr}(\text{CO})_5(\text{dphbpy})$	68	-76.	this work
Cr	$\text{Cr}(\text{CO})_5(\text{bpy})$	73	-52	13
Cr	$\text{Cr}(\text{CO})_5(\text{dmbpy})$	92	5	12
Cr	$1,4'-(\text{C}_3\text{H}_7)(\text{dab})$	80	-47	21
Cr	$1,4'-(\text{C}_4\text{H}_9)(\text{dab})$	68	-60	21
Cr	$1,4'-(\text{C}_6\text{H}_{11})(\text{dab})$	73	-70	21

In the presence of excess ligand, the activation enthalpies for the 1,4'-dab and bpy complexes closely resemble that obtained in this study Lees<sup>21</sup> *et al* have assumed that the main energy barrier to chelate formation from  $\text{M}(\text{CO})_5(\text{L})$  was M-CO bond breaking and this was taken as the rate determining step An early study by Angelici and Ingemanson<sup>26</sup> on the rate of amine dissociation in  $\text{W}(\text{CO})_5(\text{amine})$  complexes showed the strength of the W-N bond to be dependant on the basicity of the free ligand They proposed that as the basicity of the ligand decreased the bond strength also decreased For the ligands dphbpy, bpy, dmbpy, the  $\text{pK}_a$  of the conjugate acid of the free ligand varies in the order  $\text{dphbpy} < \text{bpy} < \text{dmbpy}$  This order of basicity is reflected in the activation enthalpies for the formation of the chelate complexes  $\text{Cr}(\text{CO})_5(\text{L})$  It is possible that the breaking of a Cr-N bond, is involved in the rate determining step, since the enthalpies of activation for the formation of  $\text{Cr}(\text{CO})_4(\text{L})$  ( $\text{L} = \text{bpy}, \text{dmbpy}, \text{dphbpy}$ ) reflect the strength of the Cr-N bonds

The negative entropy of activation values for the formation of  $\text{Cr}(\text{CO})_4(\text{dphbpy})$  in both the absence and presence of excess ligand are in good agreement with the assumption of Lees<sup>21</sup> *et al* of an associative process for the 1,4'-dab complexes. A negative entropy of activation value was determined for the formation of  $\text{Cr}(\text{CO})_4(\text{dphbpy})$  in the absence of excess ligand, becoming even more negative in the presence of excess ligand. This is indicative of a greater ordering of the transition state for reactions in the presence of an excess of ligand.

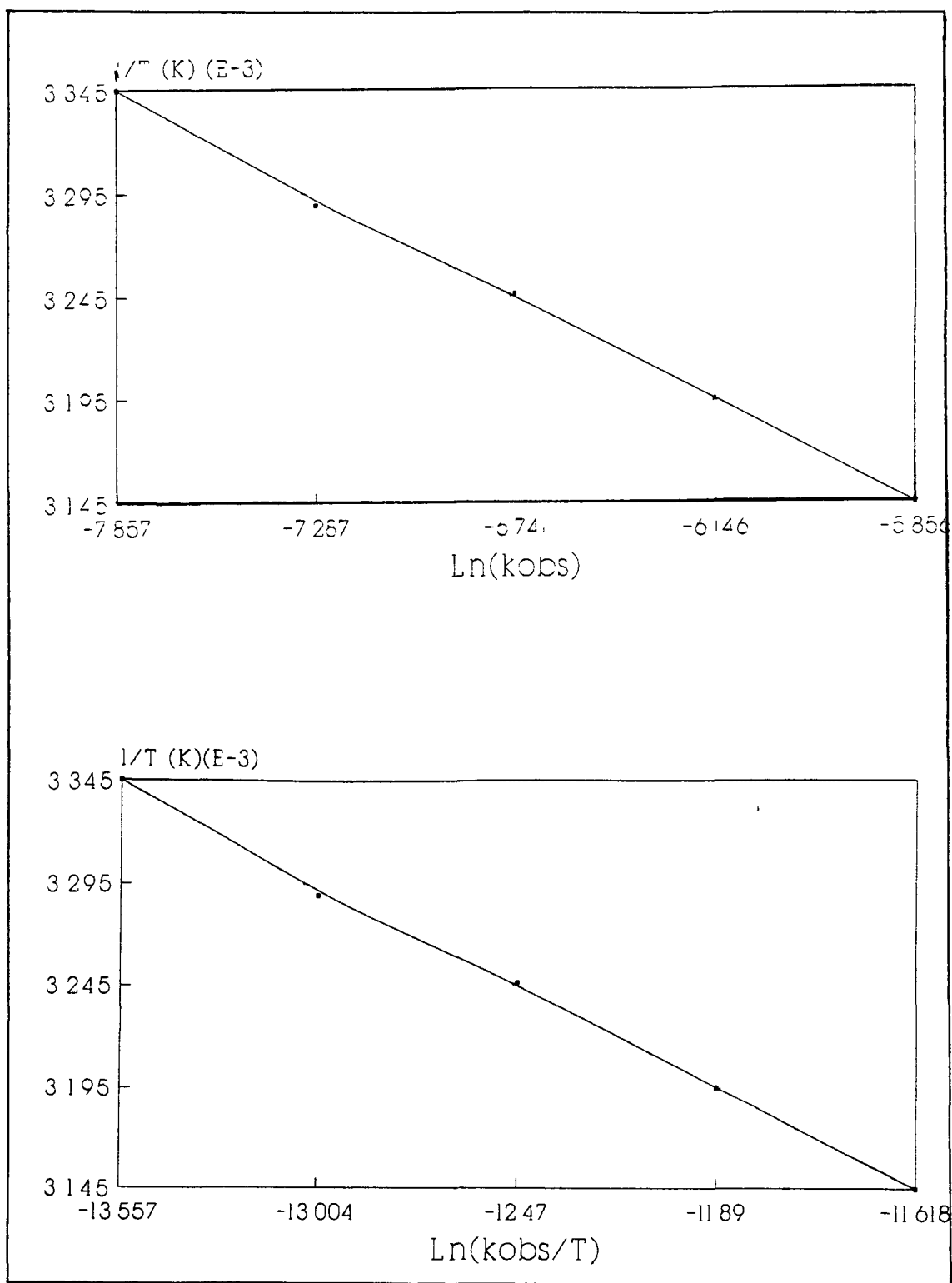


Figure 3 2 1 7 1 The (a) Arrhenius and (b) Eyring plots of the values obtained for the activation parameters for the formation of  $\text{Cr}(\text{CO})_4(\text{dphbpy})$  in the absence of any excess ligand



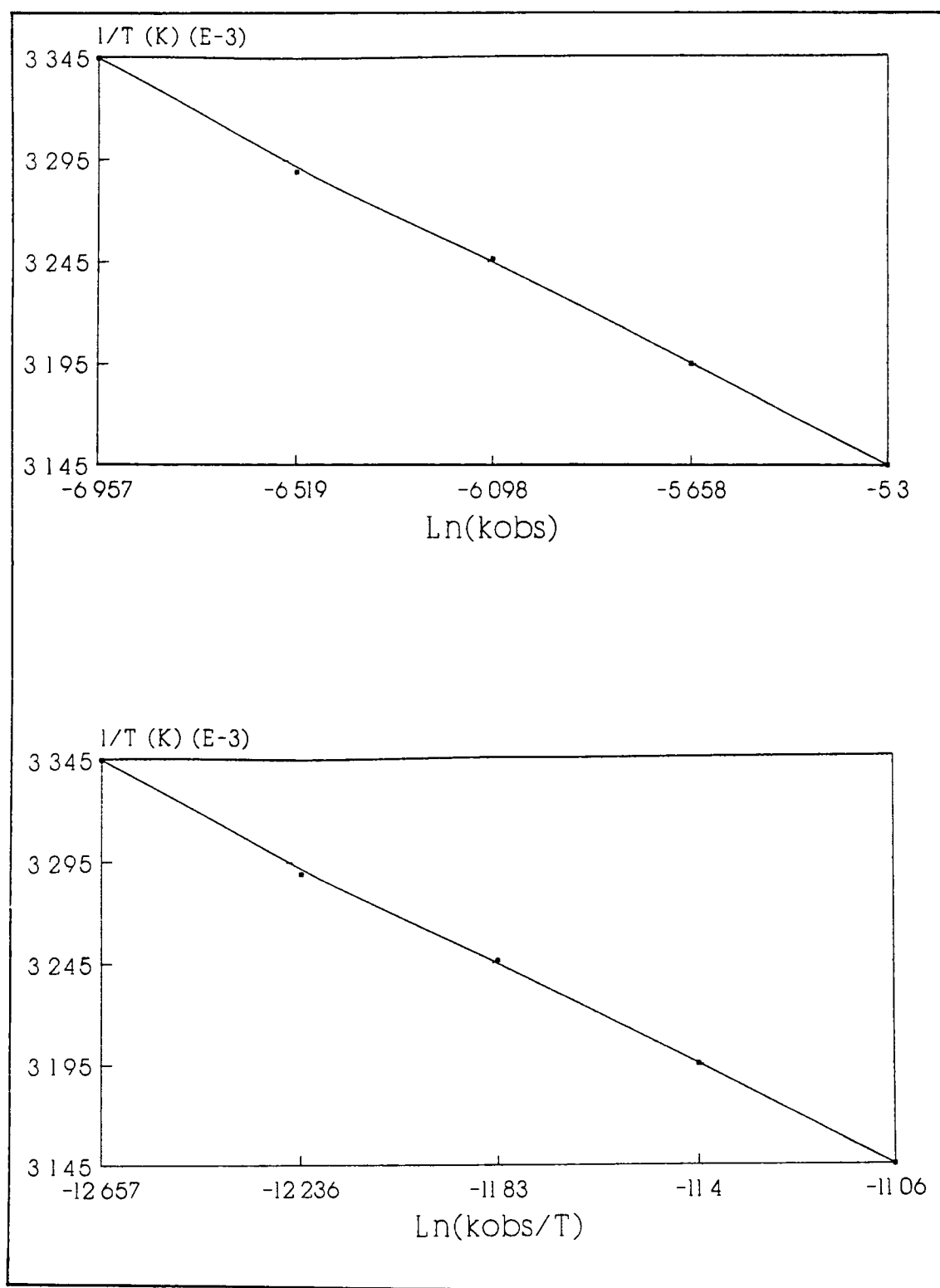


Figure 3.2.17.2 The (a) Arrhenius and (b) Eyring plots of the values obtained for the activation parameters for the formation of  $\text{Cr}(\text{CO})_4(\text{dphbpy})$  in the presence of excess ligand

### 3.2.1.8. Summary

The reaction of  $\text{Cr(CO)}_5(\text{cis-cyclo-octene})$  with the dphbpy ligand, dissolved in toluene solution, was performed at 273K under an argon atmosphere. The isolation of the  $(\text{Cr(CO)}_5)_2(\text{dphbpy})$  complex was predicted on the basis of the results presented in Chapter 2. It was anticipated that coordination of one  $\text{Cr(CO)}_5$  unit to the ligand would result in a conformational change on the ligand to minimise any steric interactions between the ligand and either the metal or one of the carbonyl groups. The conformational change induced upon the ligand was predicted to result in an increase in the  $\text{pK}_a$  of the uncoordinated nitrogen of the conjugate acid, resulting in a competition between the coordinated complex and the free ligand for the  $\text{Cr(CO)}_5$  units. However, because of the increase in the  $\text{pK}_a$  of the uncoordinated nitrogen it was anticipated that the coordinated complex would compete more effectively for the coordination of the  $\text{Cr(CO)}_5$  units than the free ligand, resulting in the formation of the ligand bridged metal carbonyl complex. The isolation of the  $(\text{Cr(CO)}_5)_2(\text{dphbpy})$  complex was confirmed by elemental analysis.

The complex was characterised by infrared and UV-visible spectroscopy. The infrared spectrum of the complex exhibited four bands in the  $\nu\text{CO}$  region. The E mode was split at 1937 and 1924 $\text{cm}^{-1}$ , which is indicative of a ligand acting as a bridge between two metal centres. The UV-visible spectrum of the complex exhibited one low energy band centred at 404nm. Upon comparison with other spectra this band was assigned the  $^1\text{A} \rightarrow ^1\text{E}$  LF transition band with the MLCT band overlapping. The absence of any MLCT band above 404nm is an indication of a disturbance of the conjugation of the ligand. The absence of a band at 290nm, which corresponds to the  $\pi\text{-}\pi^*$  transition of the ligand supports a disturbance of coplanarity.



(Cr(CO)<sub>5</sub>)<sub>2</sub>(dphbpy) in the absence of excess ligand would indicate an associative pathway involving the transition state. In the absence of excess ligand the rate determining step was proposed involve the breaking of the Cr-N bond. In the presence of excess ligand the rate determining step was proposed to be a concerted process involving the breaking of the Cr-N bond and the association of a CO group.

### 3.2.2 The synthesis and characterisation of the $M(CO)_5(bpa)$ ( $M = Cr$ or $W$ ; $bpa = bis\text{-}picolylamine$ ) complexes and their reactions in solution.

#### 3.2.2.1 The preparation of the $M(CO)_5(bpa)$ complexes

The reaction of  $Cr(CO)_5(cis\text{-}cyclo\text{-}octene)$  and photogenerated  $W(CO)_5(THF)$  with a solution of *bis*-picolylamine (*bpa*, Figure 3.2.2.1.1) in toluene resulted in the formation of  $Cr(CO)_5(bpa)$  and  $W(CO)_5(bpa)$ , respectively (This was confirmed by elemental analysis) The isolation of  $M(CO)_5(bpa)$  complex with the ligand coordinated in a monodentate manner was predicted from the results outlined in Chapter 2 The coordination of one  $M(CO)_5$  unit by the ligand should not result in a conformational change to minimise the possibility of any steric interactions The ligand has three nitrogens available for coordination and was the only tridentate ligand employed in this work The two terminal coordination sites of the ligand are identical but differ from the central site

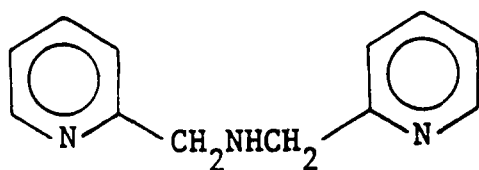


Figure 3.2.2.1.1 *bis*-picolylamine

These complexes were characterised using infrared and UV-visible spectroscopy, and where applicable NMR spectroscopy Subsequent reactions of  $M(CO)_5(bpa)$  resulted in the formation of the  $M(CO)_4(bpa)$  and  $M(CO)_3(bpa)$  species Where possible, these intermediates were also fully characterised, with a view to determining the mode of

coordination of the ligand. Unfortunately, the  $\text{Cr(CO)}_4(\text{bpa})$  species could not be isolated and characterised although its formation from a sample of  $\text{Cr(CO)}_5(\text{bpa})$  had been observed. The  $\text{M(CO)}_3(\text{bpa})$  species were also isolated and characterised.

**3.2.2.2 The characterisation of  $M(CO)_5(bpa)$  by infrared, UV-visible and  $^1H$  n.m.r. spectroscopy.**

The infrared spectrum of  $Cr(CO)_5(bpa)$ , pressed in a KBr pellet, is presented in Figure 3.2.2 2 1

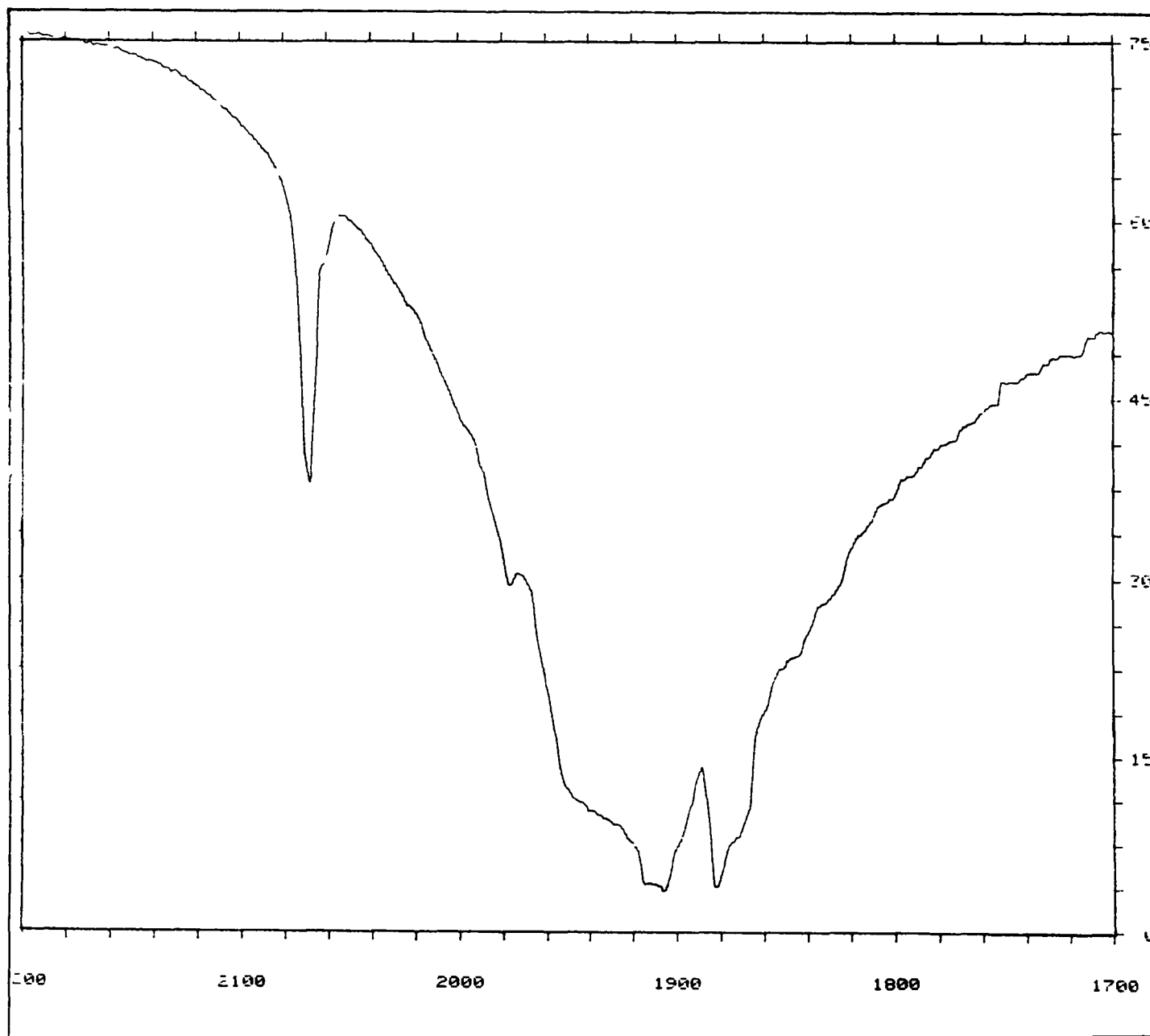


Figure 3.2.2 2 1 The infrared spectrum of a sample of  $Cr(CO)_5(bpa)$ , pressed in a KBr pellet.

Complexes of the type  $M(CO)_5(\text{amine})$  possess perfect  $C_{4v}$  symmetry and exhibit three bands in the  $\nu CO$  region of the infrared spectrum, two of  $A_1$  symmetry and one of E symmetry<sup>10</sup> This  $M(CO)_5(\text{bpa})$  complex exhibits four bands in the  $\nu CO$  region at 2068, 1976, 1906 and  $1882\text{cm}^{-1}$  These bands may be assigned the  $A_1$ ,  $B_1$ , E and  $A_1(2)$  bands of a complex possessing pseudo  $C_{4v}$  symmetry<sup>10</sup> The increased intensity of the  $B_1$  mode is indicative of a reduction of the local symmetry of the molecule Table 3 2 2 2 1 outlines the  $\nu CO$  stretching frequencies for both complexes in the solid state (KBr) and in solution (toluene)

Table 3 2.2 2.1 A comparison of the  $\nu CO$  stretching frequencies of  $M(CO)_5(\text{bpa})$  in solid (KBr) and in solution (toluene)

$Cr(CO)_5(\text{bpa})$ $\nu CO$ (KBr) $\text{cm}^{-1}$	$W(CO)_5(\text{bpa})$ $\nu CO$ (KBr) $\text{cm}^{-1}$	$Cr(CO)_5(\text{bpa})$ $\nu CO$ (toluene) $\text{cm}^{-1}$	$W(CO)_5(\text{bpa})$ $\nu CO$ (toluene) $\text{cm}^{-1}$
2068	2073	2066	2070
1976	1985	1978	1970
1906	1906	1928	1925
1882	1866	1900	1896

The  $B_1$  mode at  $1985\text{cm}^{-1}$  has also increased in intensity for the  $W(CO)_5(\text{bpa})$  complex implying a reduction of symmetry in this complex The  $B_1$  mode occurring at  $1976\text{cm}^{-1}$  for  $Cr(CO)_5(\text{bpa})$  and at  $1978\text{cm}^{-1}$  for  $W(CO)_5(\text{bpa})$  is masked in toluene solution by the  $T_{1u}$  band of the parent carbonyls which occur at *ca*  $1980\text{cm}^{-1}$  and *ca*  $1977\text{cm}^{-1}$ , respectively This may be seen from a solution spectrum of a sample of the  $W(CO)_5(\text{bpa})$  complex ( $1.912 \times 10^{-3}\text{mol dm}^{-3}$ ) dissolved in toluene



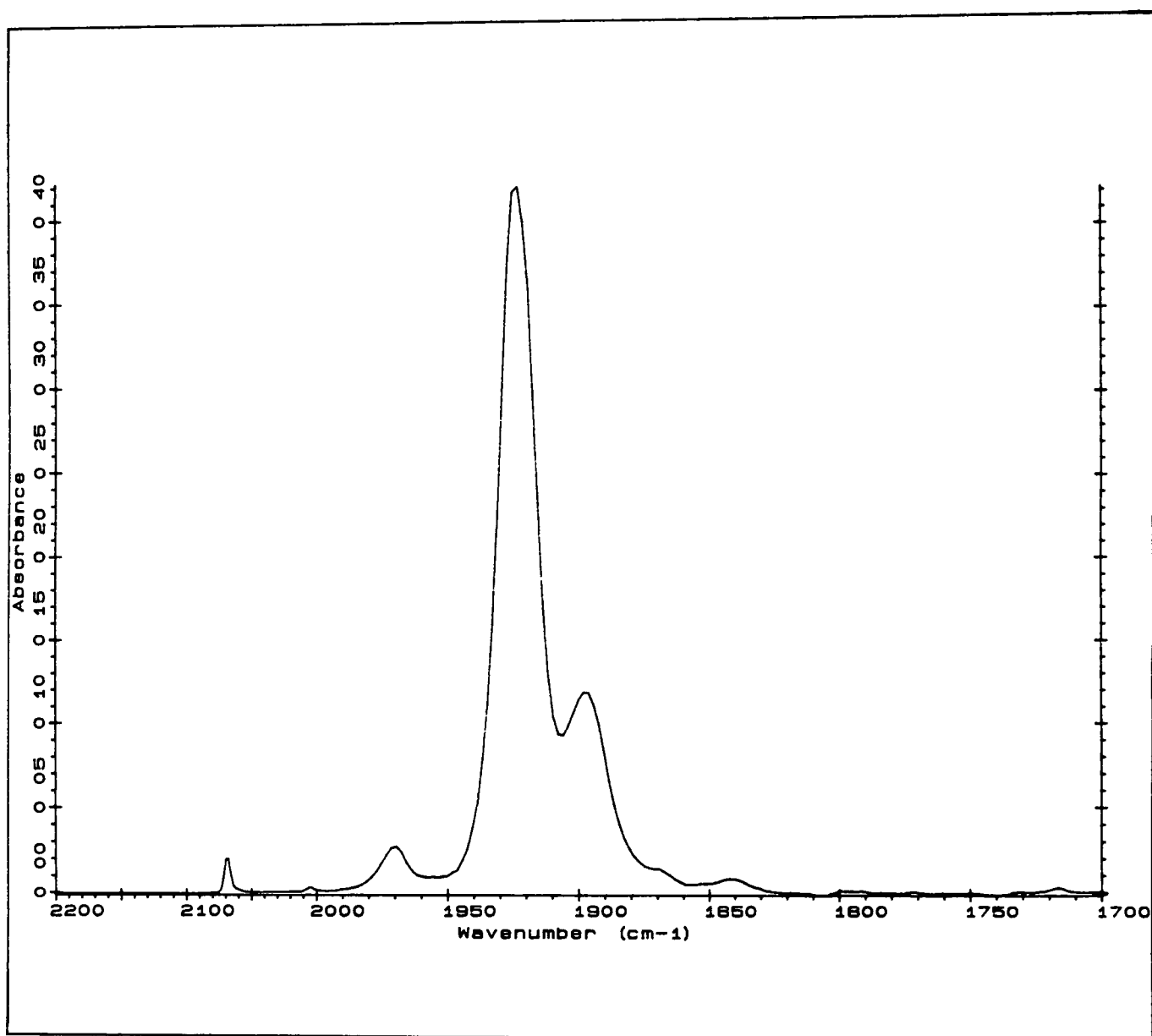


Figure 3.2.2.2.2 The infrared spectrum of a sample of  $\text{W}(\text{CO})_5(\text{bpa})$  dissolved in toluene solution ( $1.912 \times 10^{-3} \text{ mol dm}^{-3}$ )

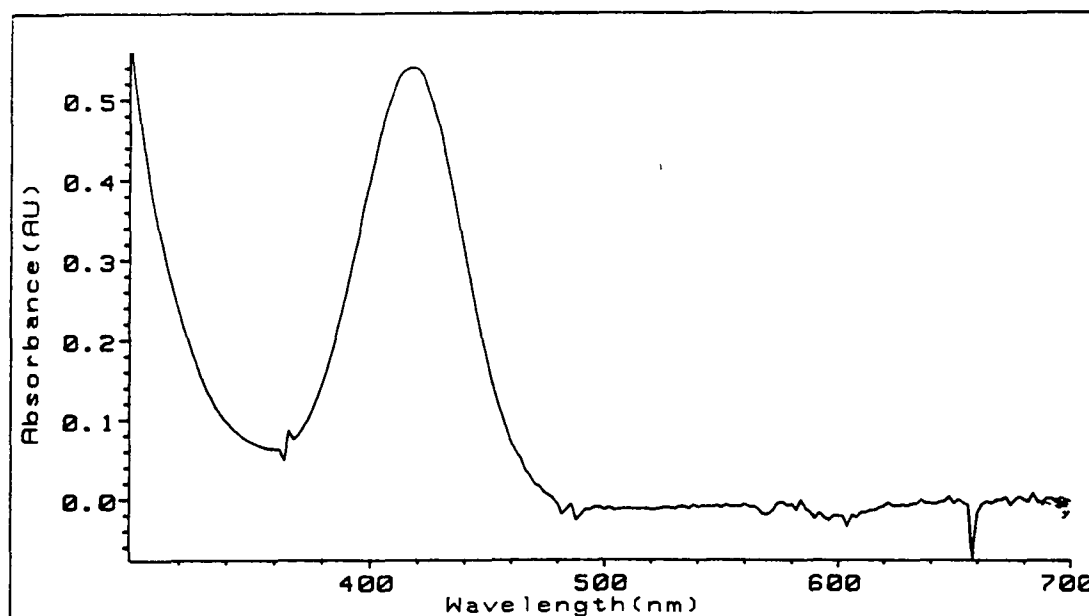


Figure 3.2.2.3 The UV-visible spectra of  $\text{Cr}(\text{CO})_5(\text{bpa})$  ( $1.285 \times 10^{-4} \text{ mol dm}^{-3}$ ) in toluene solution

The UV-visible spectra for the  $\text{Cr}(\text{CO})_5(\text{bpa})$  complex, dissolved in toluene solution ( $1.285 \times 10^{-4} \text{ mol dm}^{-3}$ ), is presented in Figure 3.2.2.3. The  $\text{Cr}(\text{CO})_5(\text{bpa})$  complex has one band, centred in the visible region at 416 nm, while the  $\text{W}(\text{CO})_5(\text{bpa})$  complex exhibits two bands at 304 and 400 nm. The band at 416 nm for the  $\text{Cr}(\text{CO})_5(\text{bpa})$  complex may be assigned the LF ( $^1\text{A} \rightarrow ^1\text{E}$ ) transition overlapping the MLCT band. Upon comparison with a spectrum of the free ligand, in toluene solution, the band at 304 nm, for the  $\text{W}(\text{CO})_5(\text{bpa})$  complex, may be assigned a  $\pi\text{-}\pi^*$  IL band, which occurs at 288 nm in the spectrum of the free ligand. The band at 400 nm may be assigned the  $^1\text{A} \rightarrow ^1\text{E}$  LF transition of the  $\text{W}(\text{CO})_5(\text{bpa})$  complex. The spectrum of the  $\text{W}(\text{CO})_5(\text{bpa})$  complex exhibits a shoulder on the LF band at 440 nm. This band may be assigned the  $^1\text{A} \rightarrow ^3\text{E}$  transition, a spin forbidden transition, which gains intensity because of the spin-orbit coupling. The absence of an MLCT band

above 416 and 400nm for the  $\text{Cr}(\text{CO})_5(\text{bpa})$  and  $\text{W}(\text{CO})_5(\text{bpa})$  complexes has been observed previously with the  $(\text{Cr}(\text{C})_5)_2(\text{dphbpy})$  complex

The  $\text{W}(\text{CO})_5(\text{pyridine})^{27}$  complex exhibits two bands at 385 and 440nm which are assigned the  $^1\text{A} \rightarrow ^1\text{E}$  LF transition and the  $^1\text{A} \rightarrow ^3\text{E}$  spin forbidden transitions. The  $\text{Cr}(\text{CO})_5(\text{pyridine})^{27}$  complex exhibits a low energy band centred at *ca* 400nm corresponding to the  $^1\text{A} \rightarrow ^1\text{E}$  LF transition. The bands exhibited by these pyridine complexes are very similar to those studied in this work

The mode of coordination, adopted by the ligand, was determined by the use of  $^1\text{H}$  nmr spectroscopy. The spectrum of a sample of  $\text{Cr}(\text{CO})_5(\text{bpa})$ , dissolved in  $\text{CDCl}_3$ , exhibited resonances at 8.7(s), 7.65(s), 7.25(s), 4.84(s) and 4.0(s)ppm (s= singlet). The spectrum of the  $\text{W}(\text{CO})_5(\text{bpa})$  complex, dissolved in  $\text{CDCl}_3$ , exhibited resonances at 8.7(d), 7.74(t), 7.28(t), 5.65(s), and 4.3(m)ppm (d= doublet, m= multiplet). The aromatic resonances represent the protons on the pyridine rings while the singlets at 4.84ppm, for the  $\text{Cr}(\text{CO})_5(\text{bpa})$  complex, and 5.65ppm, for the  $\text{W}(\text{CO})_5(\text{bpa})$  complex, represent the central nitrogen proton. The symmetry of the spectra is suggestive of coordination of the ligand *via* the central nitrogen. The bands at 4.0ppm for the  $\text{Cr}(\text{CO})_5(\text{bpa})$  complex and at 4.3ppm for the  $\text{W}(\text{CO})_5(\text{bpa})$  complex represent the resonances for the  $\text{CH}_2$  protons. Had the ligand coordinated *via* either of the pyridine nitrogens then two separate sets of resonances should have been observed for the pyridine protons.

### 3.2.2.3 The reactions of the $\text{M}(\text{CO})_5(\text{bpa})$ complexes in the solid state

The infrared spectral changes occurring upon heating a sample of  $\text{Cr}(\text{CO})_5(\text{bpa})$ , pressed in a KBr disc, and warmed to 333K for thirty minutes are

presented in Figure 3.2.2.3.1. The bands at 2068, 1976, 1906 and 1882 cm<sup>-1</sup>, previously assigned to the Cr(CO)<sub>5</sub>(bpa) species, are seen to diminish with the growth of new bands at 2010, 1980, 1862 and 1778 cm<sup>-1</sup>. These bands correspond to the A<sub>1</sub>, B<sub>1</sub>, A<sub>1</sub>(2) and B<sub>2</sub> modes of a *cis*-Cr(CO)<sub>4</sub>(bpa) complex possessing C<sub>2v</sub> symmetry. A sample of the W(CO)<sub>5</sub>(bpa), pressed in a KBr disc, was heated to 353 K for twenty minutes and the bands previously assigned to this complex were observed to diminish with a concomitant growth of new bands. The new bands at 2002, 1974, 1808 and 1763 cm<sup>-1</sup> were assigned to the A<sub>1</sub>, B<sub>1</sub>, A<sub>1</sub>(2) and B<sub>2</sub> modes of the *cis*-W(CO)<sub>4</sub>(bpa) complex possessing C<sub>2v</sub> symmetry. The formation of this complex was confirmed by comparison with the spectra of an authentic sample, whose formation was confirmed by elemental analysis.

Heating a sample of the W(CO)<sub>4</sub>(bpa) complex, pressed in a KBr pellet, to 353 K for 90 minutes resulted in a depletion of the bands associated with this complex and a growth of two new bands at 1886 and 1763 cm<sup>-1</sup> (Figure 3.2.2.3.2). These bands may be assigned the A<sub>1</sub> and E modes of a *fac*-W(CO)<sub>3</sub>(bpa) complex possessing C<sub>3v</sub> symmetry<sup>10</sup>. Unfortunately, the Cr(CO)<sub>4</sub>(bpa) complex could not be isolated so this procedure was not repeated for this complex. This assignment of the W(CO)<sub>3</sub>(bpa) complex as a *fac* isomer is in agreement with the molecular structure determination of the (Mn(bpa)<sub>2</sub>)(ClO<sub>4</sub>)<sub>2</sub><sup>28</sup> complex in which the ligand was coordinated in a tridentate fashion.

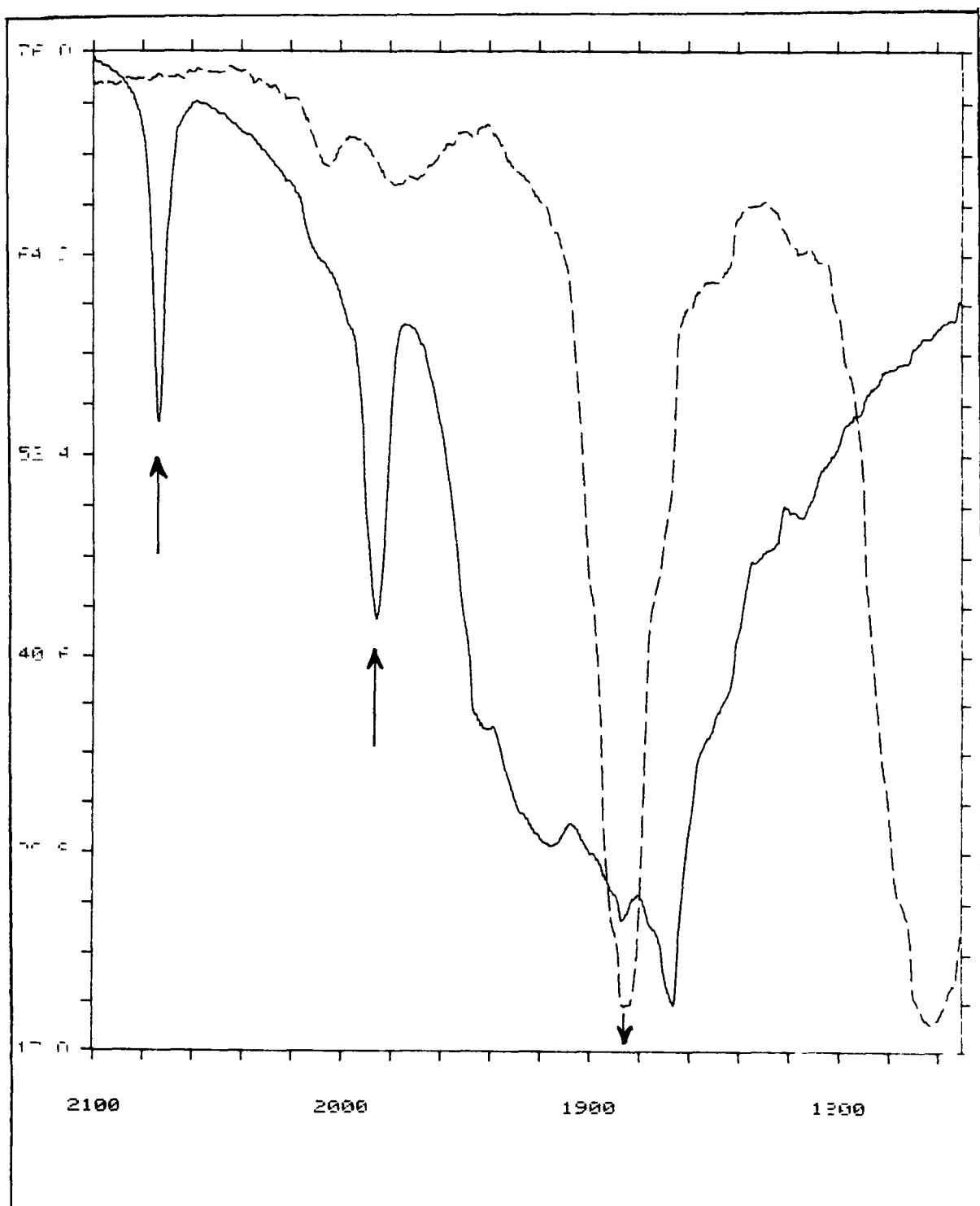


Figure 3.2 2.3.1 The infrared spectral changes occurring upon warming a sample of  $\text{Cr}(\text{CO})_5(\text{bpa})$ , pressed in a KBr pellet, to 333K for 20 minutes

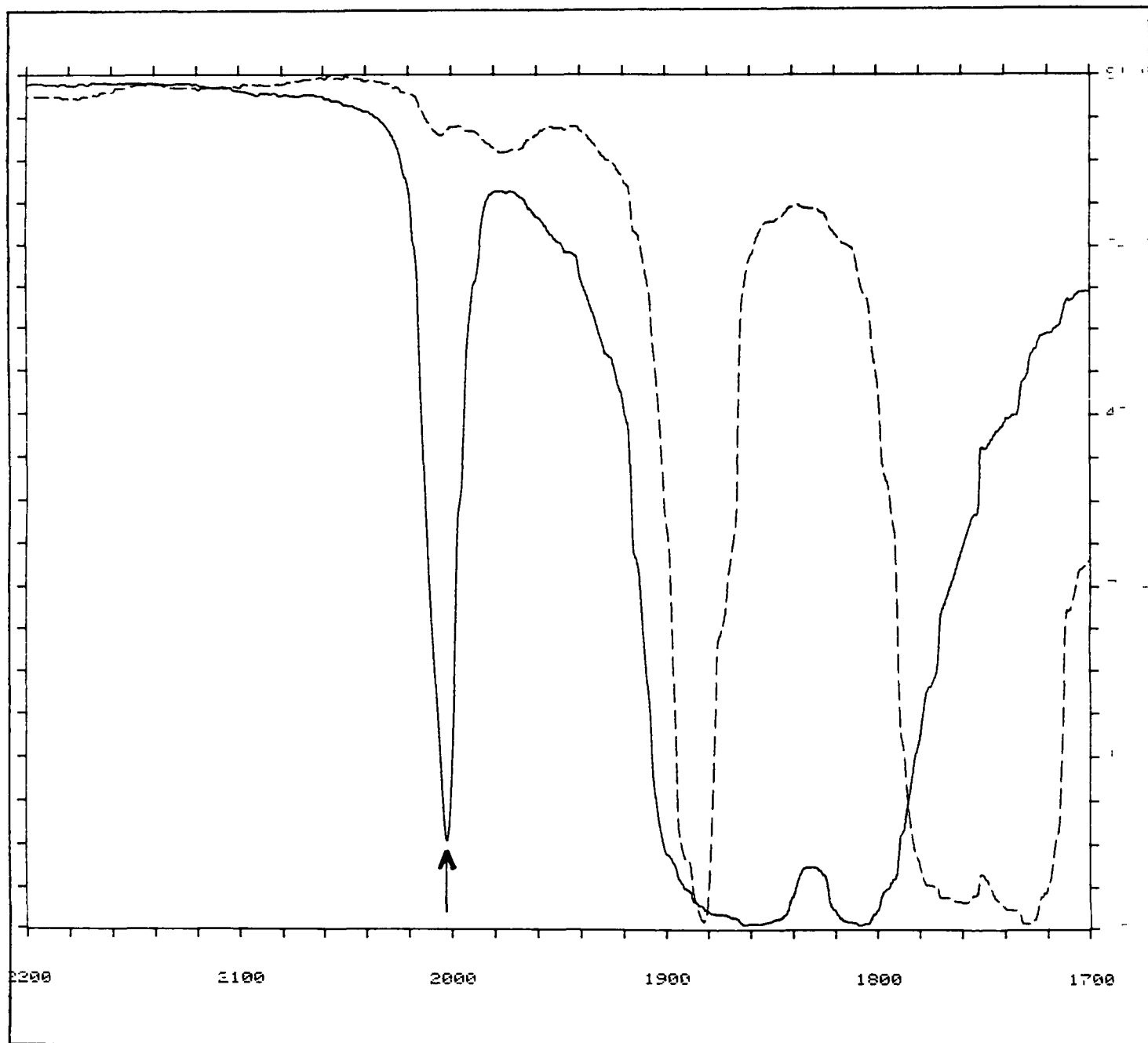
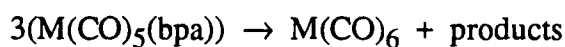


Figure 3.2.2.3 2: The infrared spectral changes occurring upon warming a sample of  $\text{W}(\text{CO})_4(\text{bpa})$ , pressed in a KBr disc, to 353K for 90 minutes

Thermogravimetric analysis of a sample of  $\text{W}(\text{CO})_5(\text{bpa})$  revealed a weight loss of 21% in the range 363 to 413K. Previously it was assumed that the mechanism of chelate formation occurred *via* an intramolecular CO extrusion process<sup>17</sup>. If this were so, then the weight loss should have been 5.35%. Calculations show that if the weight loss is attributed to the sublimation of  $\text{W}(\text{CO})_6$ , then for every three moles of  $\text{W}(\text{CO})_5(\text{bpa})$  present one mole of  $\text{W}(\text{CO})_6$  is produced. In the case of the  $\text{Cr}(\text{CO})_5(\text{bpa})$  complex the weight loss observed upon thermogravimetric analysis, in the range 363 to 413K was 17%. Had the weight loss been as a consequence of intramolecular CO extrusion then the figure should have been 7.16%. If this weight loss is attributed to the sublimation of  $\text{Cr}(\text{CO})_6$ , then for every three moles of  $\text{Cr}(\text{CO})_5(\text{bpa})$  present one mole of  $\text{Cr}(\text{CO})_6$  is produced. This is represented in equation 3.2.2.3.1



equation 3.2.2.3.1

The regeneration of  $\text{M}(\text{CO})_6$  has been observed by Darensbourg *et al*<sup>23</sup> with the  $\text{Mo}(\text{CO})_5(\text{amine})$  complex but was suppressed by the introduction of excess ligand. In order to confirm the regeneration of the  $\text{M}(\text{CO})_6$  compounds it was necessary to determine the infrared spectral changes occurring upon heating a sample of the  $\text{M}(\text{CO})_5(\text{bpa})$  complex, dissolved in toluene solution.

#### 3.2.2.4 The reactions of the $\text{M}(\text{CO})_5(\text{bpa})$ complexes in toluene solution, in the absence and presence of excess ligand, as monitored by infrared spectroscopy.

The infrared spectral changes occurring upon heating a sample of  $\text{W}(\text{CO})_5(\text{bpa})$ , dissolved in toluene ( $1.912 \times 10^{-2} \text{ mol dm}^{-3}$ ), from 298 to 333K over a 35 minute period are presented in Figure 3.2.2.4.1. Each spectrum represents a five

minute interval. The bands at 2070, 1970, 1925 and 1896 $\text{cm}^{-1}$  were seen to diminish in intensity with the production of bands at 2005, 1866, 1837 and 1796 $\text{cm}^{-1}$ . The band at 1977 $\text{cm}^{-1}$  was seen to decrease initially but increase in intensity after 5 minutes, indicating the generation of the parent hexacarbonyl. The new bands may be assigned the  $A_1$ ,  $B_1$ ,  $A_1(2)$  and  $B_2$  modes of the *cis*- $\text{W}(\text{CO})_4(\text{bpa})$  complex. After 35 minutes the bands corresponding to the  $\text{W}(\text{CO})_4(\text{bpa})$  complex were observed to diminish with no new bands being produced. An infrared spectrum of the precipitate produced revealed it to be the  $\text{W}(\text{CO})_3(\text{bpa})$  complex. The molar extinction coefficients for the  $\text{W}(\text{CO})_5(\text{bpa})$ ,  $\text{W}(\text{CO})_4(\text{bpa})$  and  $\text{W}(\text{CO})_6$  species were determined and the stoichiometry of the reaction calculated, based on the spectral changes above. The data for the determination of the molar extinction coefficients of these complexes are presented in Table 3.2.2.4.1.

The infrared spectral changes occurring upon heating a sample of  $\text{Cr}(\text{CO})_5(\text{bpa})$ , dissolved in toluene solution from 298 to 323K over a forty minute period while scanning every five minutes, was also monitored. The bands at 2066, 1928 and 1900 $\text{cm}^{-1}$  were observed to diminish in intensity with a growth of new bands at 2007, 1874, 1840 and 1782 $\text{cm}^{-1}$ . The band at 1978 $\text{cm}^{-1}$  was seen to decrease initially but increase again after five minutes. The bands at 2007, 1874 (as a shoulder), 1840 and 1782 are assigned the  $A_1$ ,  $B_1$ ,  $A_1(2)$  and  $B_2$  modes of the *cis*- $\text{Cr}(\text{CO})_4(\text{bpa})$  complex, possessing  $C_{2v}$  symmetry. Isolation of the  $\text{Cr}(\text{CO})_4(\text{bpa})$  complex proved impossible and thus the determination of the molar extinction coefficients for this species and consequently the complete stoichiometry for the reaction. However, the ratio of  $\text{Cr}(\text{CO})_6$  formed was determined by determining the molar extinction coefficients for the  $\text{Cr}(\text{CO})_5(\text{bpa})$  and  $\text{Cr}(\text{CO})_6$  species (Table 3.2.2.4.1).



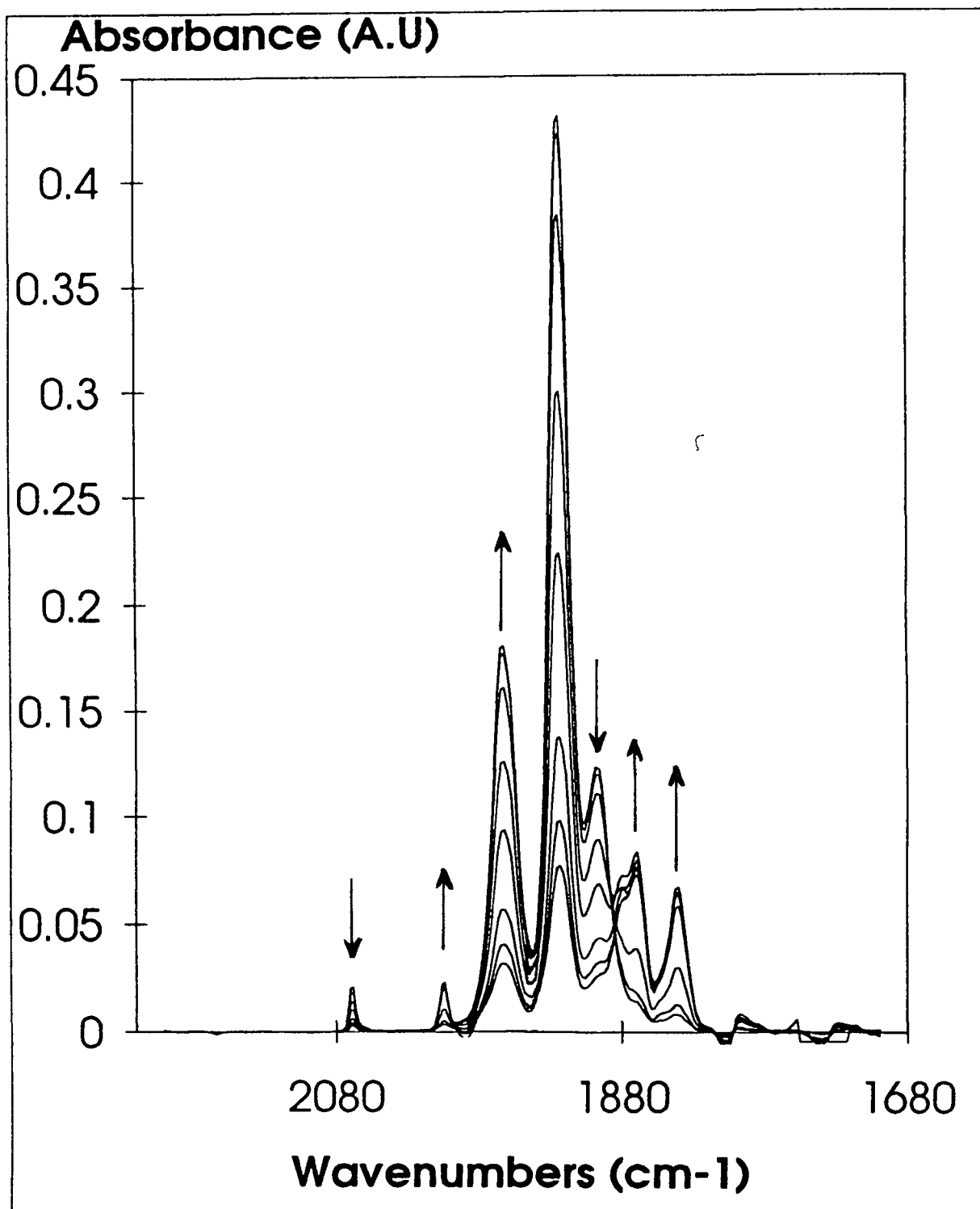


Figure 3 2 2 4 1 The infrared spectral changes occurring upon heating a sample of  $\text{W(CO)}_5(\text{bpa})$ , dissolved in toluene solution ( $1.912 \times 10^{-3} \text{ mol dm}^{-3}$ ), from 298 to 333K over a 35 minute period while scanning every 5 minutes

Table 3 2 2 4 1 The data used in the determination of the molar extinction coefficients of the  $\text{M}(\text{CO})_5(\text{bpa})$ ,  $\text{W}(\text{CO})_4(\text{bpa})$  and  $\text{M}(\text{CO})_6$  species

Complex	Concentration ( $\text{mol dm}^{-3}$ )	Absorbance (A. U.)	$\epsilon$ ( $\text{dm}^3 \text{mol}^{-1} \text{cm}^{-1}$ )
$\text{Cr}(\text{CO})_5(\text{bpa})$ $1897\text{cm}^{-1}$ *	$1.5987 \times 10^{-3}$	0.0312	1951.5
	$1.0658 \times 10^{-3}$	0.0217	2026.5
	$7.994 \times 10^{-4}$	0.0162	2036
			$\epsilon = 2005$
$\text{Cr}(\text{CO})_6$			14,505 <sup>12</sup>
$\text{W}(\text{CO})_5(\text{bpa})^{**}$ $2068\text{cm}^{-1}$	$2.248 \times 10^{-2}$	0.241	536
	$7.824 \times 10^{-3}$	0.0843	538
	$1.912 \times 10^{-3}$	0.0212	554
			$\epsilon = 543$
$\text{W}(\text{CO})_4(\text{bpa})^{**}$ $1837\text{cm}^{-1}$	$6.0613 \times 10^{-3}$	0.4846	3998.3
	$3.3674 \times 10^{-3}$	0.2811	4173.8
	$2.3786 \times 10^{-3}$	0.1976	4153.7
			$\epsilon = 4109$
$\text{W}(\text{CO})_6^*$ $1977\text{cm}^{-1}$	$1.364 \times 10^{-2}$	2.0622	15518
	$7.275 \times 10^{-3}$	1.1441	15726
			$\epsilon = 15,622$

\* using 0.1 mm pathlength

\*\* using 0.2 mm pathlength

From the calculations the stoichiometry of the reaction of  $\text{M}(\text{CO})_5(\text{bpa})$  is presented as that in equation 3 2 2 4 1



equation 3.2.2 4 1

The ratio of parent hexacarbonyl regenerated from the  $\text{Cr}(\text{CO})_5(\text{bpa})$  complex is identical to that for the  $\text{W}(\text{CO})_5(\text{bpa})$  complex, so the stoichiometry of the reaction presented in equation 3.2.2 4.1 is assumed to be the same as that of the  $\text{Cr}(\text{CO})_5(\text{bpa})$  complex.

Since the  $\text{W}(\text{CO})_3(\text{bpa})$  complex was produced upon heating the  $\text{W}(\text{CO})_4(\text{bpa})$  species it was necessary to try and elucidate the complete stoichiometry of this reaction. Owing to the insolubility of the  $\text{W}(\text{CO})_3(\text{bpa})$  complex in most organic solvents gravimetric analysis was used in an attempt to determine the stoichiometry of the reaction. Experiments confirmed a 97% production of the  $\text{W}(\text{CO})_3(\text{bpa})$  from the  $\text{W}(\text{CO})_4(\text{bpa})$  complex. In this case it appears that the mechanism of ring closure occurs *via* an intramolecular CO extrusion process. As it was not possible to repeat this procedure with the  $\text{Cr}(\text{CO})_4(\text{bpa})$  species it is assumed that this stoichiometry holds for the formation of the  $\text{Cr}(\text{CO})_3(\text{bpa})$  species.

As seen in the previous section, the introduction of excess ligand effectively doubled the amount of chelate formed. Infrared spectra were obtained on freshly prepared solutions of the  $\text{M}(\text{CO})_5(\text{bpa})$  complexes, containing excess ligand, and compared to the spectra obtained on the same solution after 24 hours at 298K. The spectra are presented in Figure 3.2 2 4 2 for the  $\text{Cr}(\text{CO})_5(\text{bpa})$  complex.

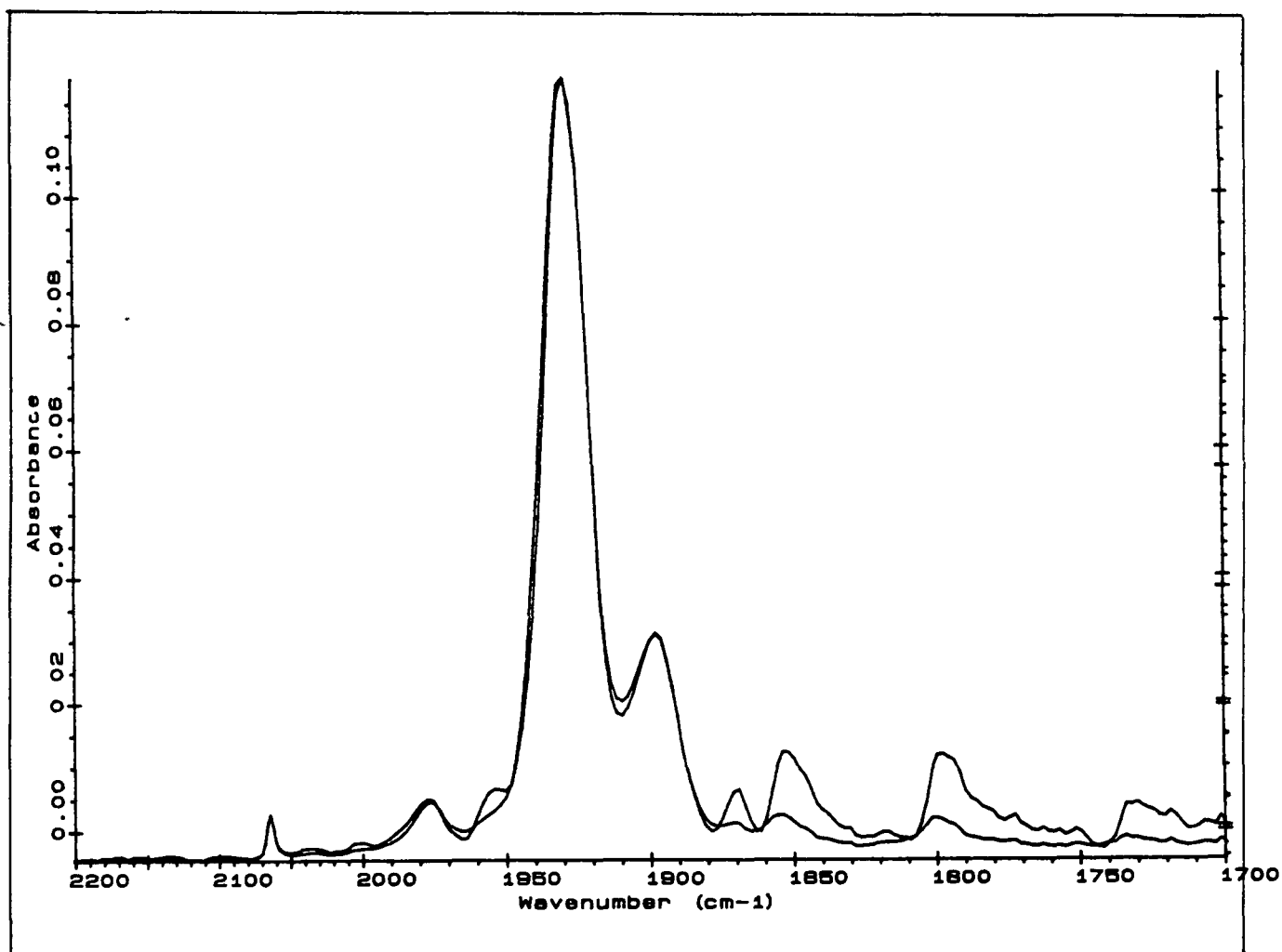


Figure 3.2 2 4.2 The infrared spectra of a sample of  $\text{Cr}(\text{CO})_5(\text{bpa})$ , dissolved in toluene ( $1.557 \times 10^{-3} \text{ mol dm}^{-3}$ ) containing excess ligand ( $5.56 \times 10^{-3} \text{ mol dm}^{-3}$ ), at 298K for twenty four hours before scanning

The bands assigned to this complex showed no change after 24 hours. The suppression of the formation of both  $M(CO)_4(bpa)$  and  $M(CO)_6$  species does not support the proposal that the formation of  $M(CO)_4(bpa)$  is achieved *via* a simple CO extrusion process.

When a series of  $Mo(CO)_5(L)$  ( $L = RSCH_2CH_2SR$ ,  $R = p-XC_6H_4$ ,  $X = NO_2$ ,  $H$ ,  $Me$ ,  $OME$ ,  $NME_2$ , or  $CMe_3$ ) were heated in hydrocarbon solution the formation of the  $Mo(CO)_4(L)$  and  $Mo(CO)_6$  complexes were observed in a 1:1 molar ratio<sup>29</sup>. Introduction of excess ligand into the reaction resulted in the suppression of the  $Mo(CO)_6$  compound, while forming the  $Mo(CO)_4(L)$  species. Darensbourg<sup>23</sup> noted that the introduction of excess amine into the reaction of  $Mo(CO)_5(amine)$  ( $amine = py$ ,  $pip$ ) at high temperatures, resulted in the suppression of the formation of the parent hexacarbonyl. In the case of the complexes studied here the addition of excess ligand resulted in the suppression of not only the parent hexacarbonyls but also of the formation of the  $M(CO)_4(bpa)$  complexes.

This procedure was repeated for the  $W(CO)_4(bpa)$  complex. A sample of the complex, dissolved in toluene containing excess ligand, was brought to reflux temperatures for thirty minutes at 385K. Product analysis showed a 94% generation of  $W(CO)_3(bpa)$ . It appears likely that mechanism of ring closure for the  $W(CO)_4(bpa)$  complex occurs *via* an intramolecular CO extrusion process, in which the introduction of excess ligand has little or no effect on the amount of  $W(CO)_3(bpa)$  produced.

The mode of coordination adopted by the ligand, in the  $W(CO)_4(bpa)$  complex, was determined by the use of  $^1H$  nmr spectroscopy. The spectrum of a sample of the complex, dissolved in  $CDCl_3$ , exhibits bands at 8.9(d), 8.6(d), 7.75(m), 7.3(m), 5.3(s), 4.4(m), and 4.1(m)ppm. The spectrum is suggestive of coordination of the ligand *via* the central and one pyridine nitrogen. Had the ligand coordinated *via* the

two pyridine nitrogens then the spectrum would have displayed one set of resonances corresponding to the protons on the pyridine rings. There are two sets of multiplets for the aliphatic protons at 4.4 and 4.1 ppm. The spectrum for the  $\text{W(CO)}_5(\text{bpa})$  complex exhibits one set of resonances for the aliphatic protons, which is also seen in the spectrum of the  $\text{W(CO)}_3(\text{bpa})$  complex.

### **3.2.2.5 The reactions of the $\text{M(CO)}_5(\text{bpa})$ complexes in toluene solution, in the absence and presence of excess ligand, as monitored by UV-visible spectroscopy**

The UV-visible spectral changes occurring upon standing a sample of  $\text{Cr(CO)}_5(\text{bpa})$ , dissolved in toluene solution ( $1.285 \times 10^{-4} \text{ mol dm}^{-3}$ ), at 298K are presented in Figure 3.2.2.5.1. The band at 416nm, corresponding to the LF band of the complex, is seen to deplete with a concomitant growth of new bands at 358 and 496nm. The maintenance of an isosbestic point at 312nm is an indication of a reaction uncomplicated by side or subsequent reactions. The final spectrum recorded after 870 minutes is presented in Figure 3.2.2.5.1(b). The bands at 358 and 496nm may be assigned the LF and MLCT bands of the  $\text{Cr(CO)}_4(\text{bpa})$  species.

Throughout this section the spectra of the complexes have alternated, owing to the similarity of the complexes. However, the differences in the UV-visible spectral changes of both complexes, upon standing at 298K for a specific time, merits a separate viewing. The spectral changes upon standing a sample of  $\text{W(CO)}_5(\text{bpa})$  in toluene solution ( $1.388 \times 10^{-4} \text{ mol dm}^{-3}$ ), at 298K are presented in Figure 3.2.2.5.2 and the final spectrum, recorded after 690 minutes, is presented in Figure 3.2.2.5.2(b).

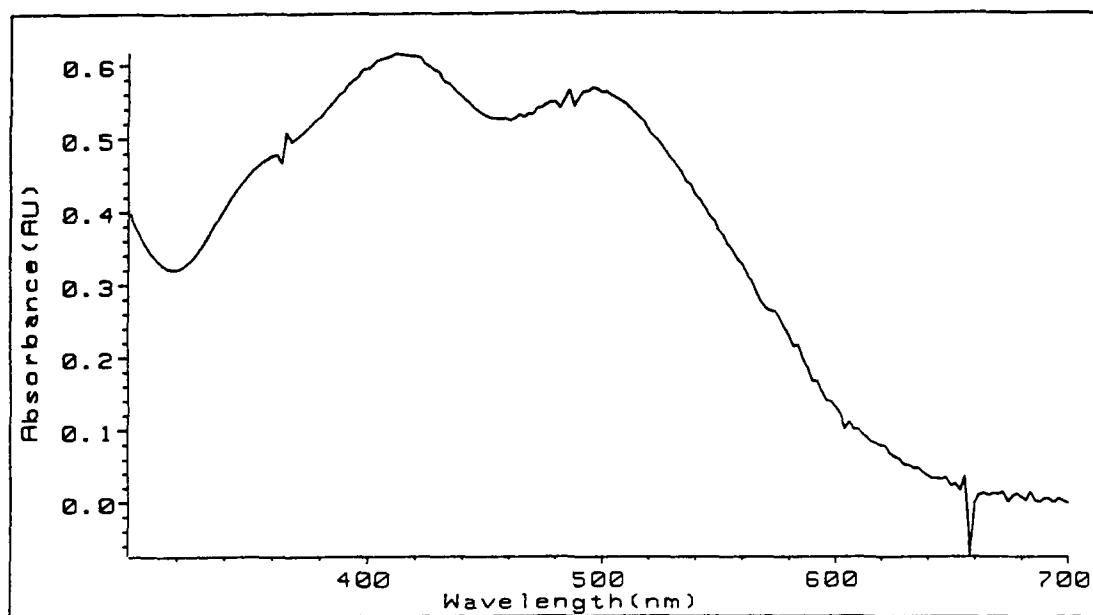
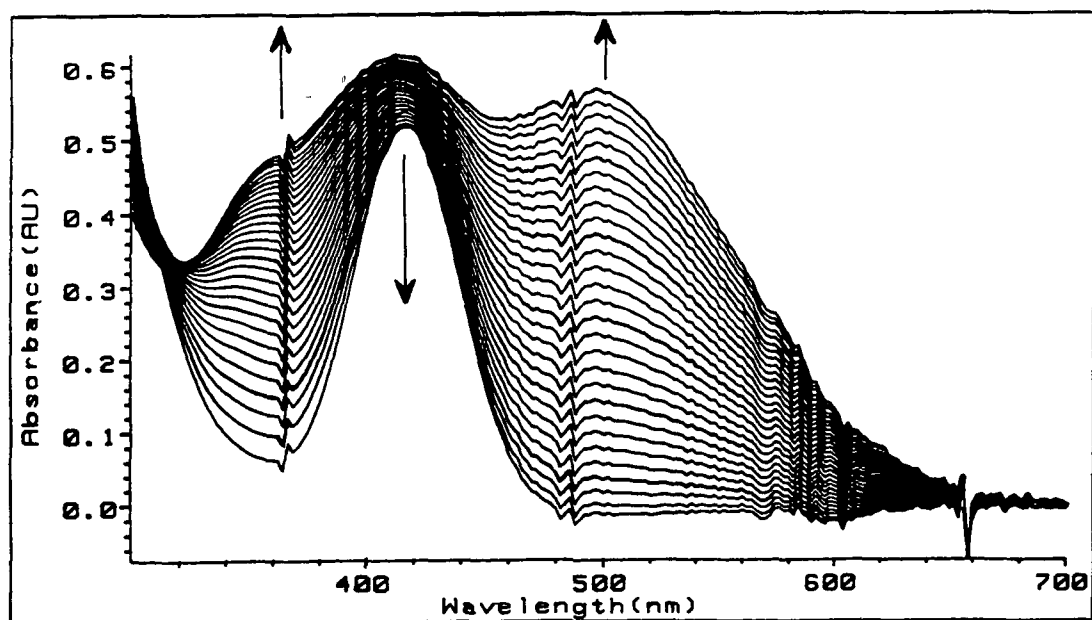


Figure 3.2.2.5.1 The (a) UV-visible spectral changes occurring upon standing a sample of  $\text{Cr}(\text{CO})_5(\text{bpa})$ , dissolved in toluene ( $1.285 \times 10^{-4} \text{ mol dm}^{-3}$ ), at 298K and (b) the final spectrum recorded after 870 minutes

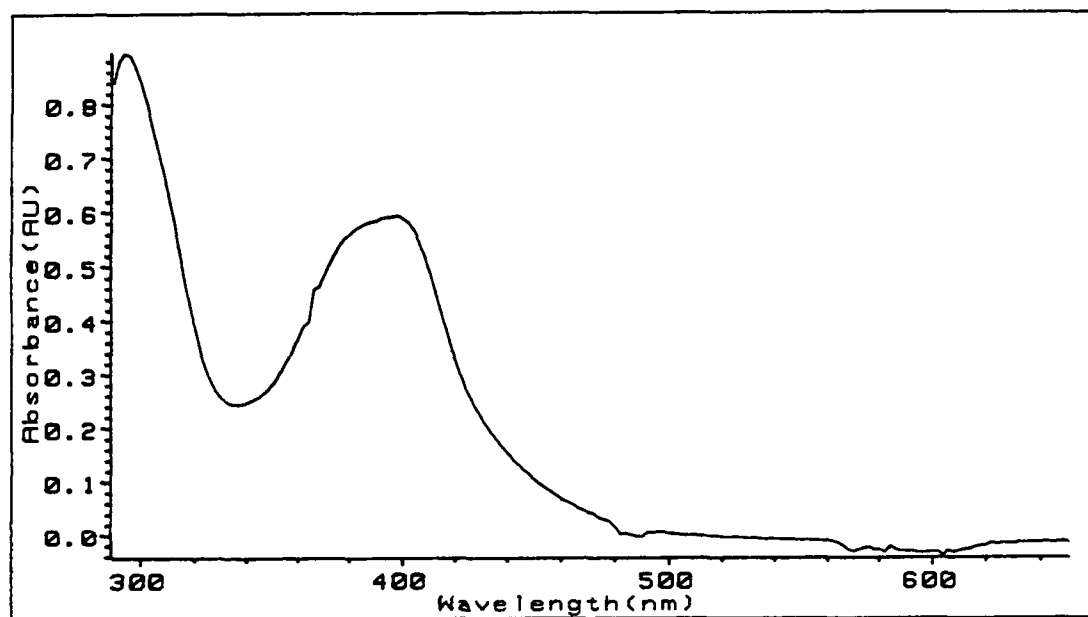
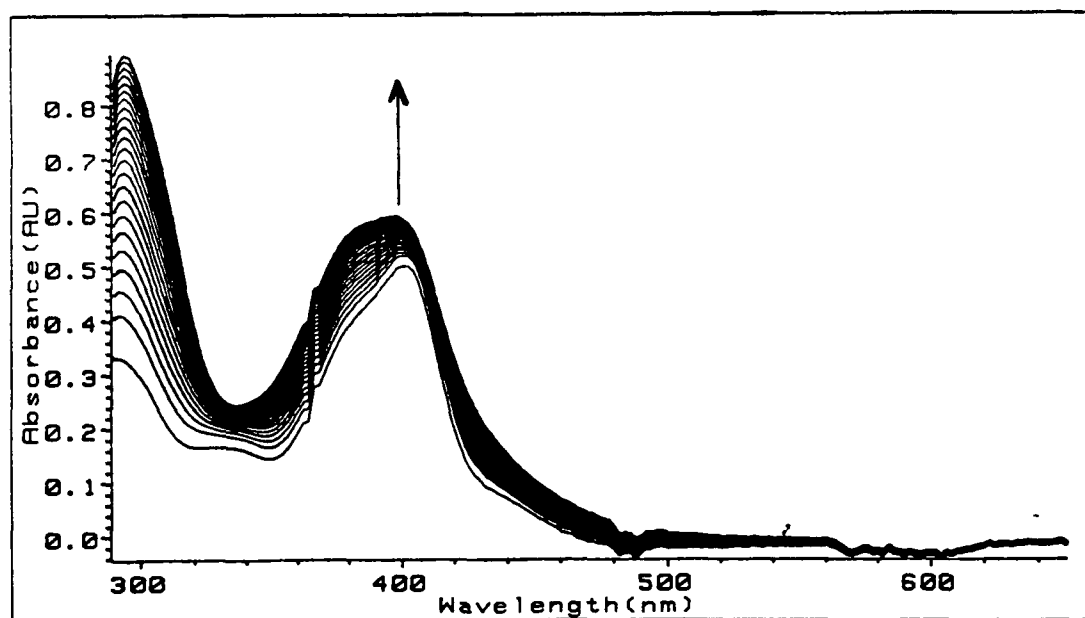


Figure 3.2.2.2 (a) The spectral changes occurring upon standing a sample of  $\text{W(CO)}_5(\text{bpa})$ , dissolved in toluene ( $1.388 \times 10^{-4} \text{ mol dm}^{-3}$ ), at 298K and (b) the final spectrum, recorded after 690 minutes.



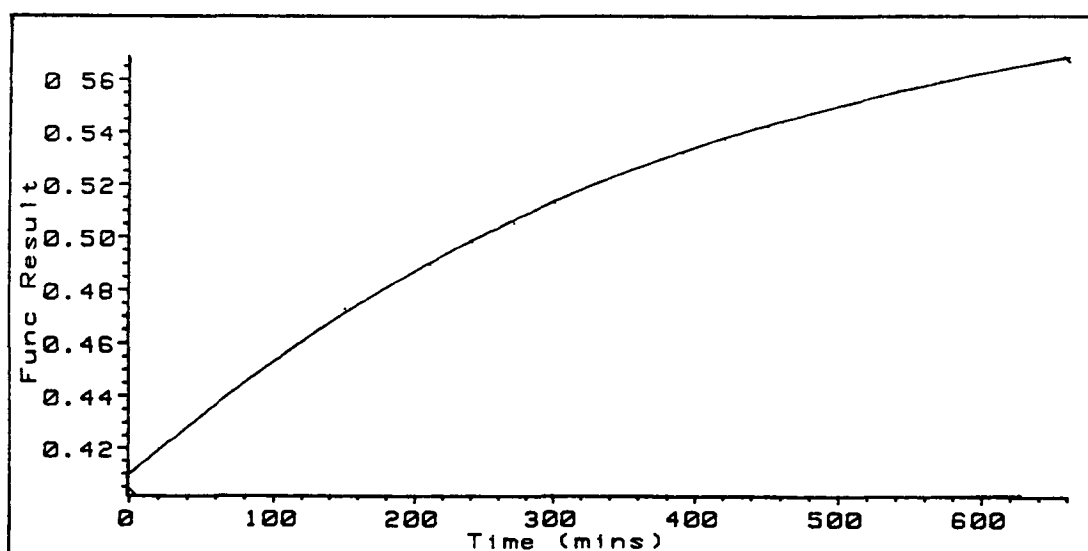
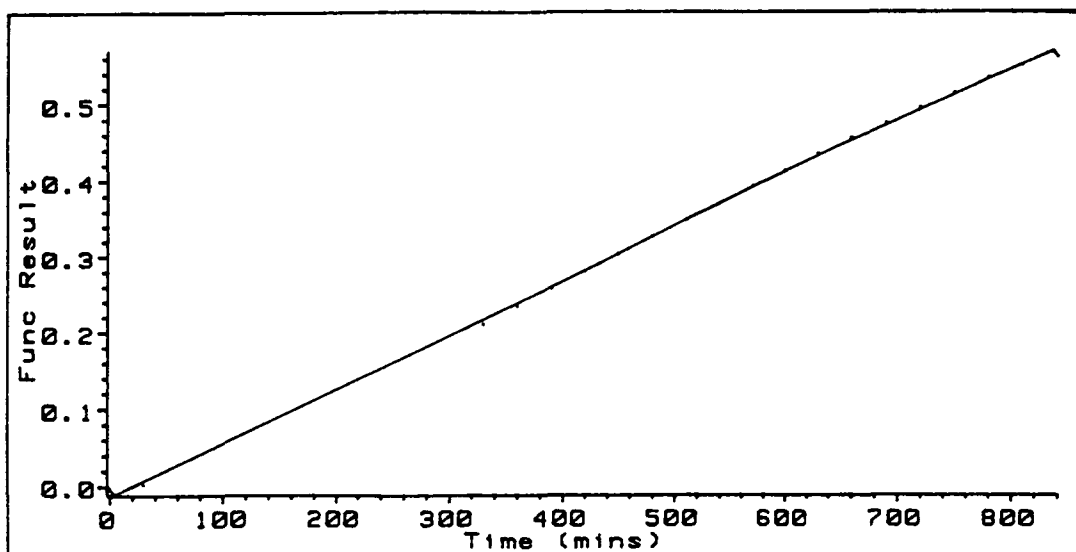


Figure 3.2 2.5 3 The variation of the absorbance with time for the formation of the (a)  $\text{Cr}(\text{CO})_4(\text{bpa})$  and (b)  $\text{W}(\text{CO})_4(\text{bpa})$  complexes, as monitored at 496 and 382nm, respectively.

The bands at 304 and 400nm corresponding to the complex are seen to increase, but shift slightly to 288 and 382nm, respectively. These bands correspond to the bands of the  $\text{W(CO)}_4(\text{bpa})$  complex, by comparison with an authentic sample. The band at 288nm corresponds to the  $\pi\text{-}\pi^*$  IL band while the band at 382nm corresponds to the LF transition which is overlapping the MLCT band. A plot of the variation of absorbance with time for the formation of the  $\text{Cr(CO)}_4(\text{bpa})$  complex is presented in Figure 3.2.2.5.3(a) and for the formation of the  $\text{W(CO)}_4(\text{bpa})$  complex in Figure 3.2.2.5.3(b), as monitored at 496 and 382nm, respectively.

As the  $\text{Cr(CO)}_4(\text{bpa})$  complex could not be isolated the mode of coordination was determined for the  $\text{W(CO)}_4(\text{bpa})$  complex only. It was determined, by  $^1\text{H}$  n.m.r. spectroscopy, that the W atom was coordinated to one of the pyridine nitrogens and the central nitrogen. A UV-visible spectrum of the  $\text{W(CO)}_3(\text{bpa})$  complex, dissolved in dimethylsulfoxide, exhibits a low energy band at 428nm which may be assigned the MLCT band of the  $\text{W(CO)}_3(\text{bpa})$  species. In the case of the  $\text{Cr(CO)}_3(\text{bpa})$  complex the lowest energy band is at 486nm, in THF solution, which is not shifted greatly from that of the  $\text{Cr(CO)}_4(\text{bpa})$  species.

The observed rate constant for the formation of the  $\text{Cr(CO)}_4(\text{bpa})$  complex, determined by the growth of the band at 496nm was found to be  $1.537 \times 10^{-6} \text{ s}^{-1}$ . The rate constant for the formation of the  $\text{W(CO)}_4(\text{bpa})$  complex, determined by the growth of the band at 382nm was found to be  $41.57 \times 10^{-6} \text{ s}^{-1}$ . The formation of the  $\text{W(CO)}_4(\text{bpa})$  complex occurs approximately 27 times faster than that for the Cr analogue.

The  $\text{M(CO)}_5(\text{L})$ <sup>30</sup> (M= Cr, Mo, or W, L= di-2-pyridylmethane (dpym), 1,2-di-2-pyridylethane (dppe)) complexes were found to be thermally stable at room temperature, with the exception of the  $\text{Mo(CO)}_5(\text{dpym})$ , showing no tendency to form

the chelated complexes. Further irradiation of the  $\text{Cr}(\text{CO})_5(\text{dpym})$  and  $\text{W}(\text{CO})_5(\text{dpym})$  complexes resulted in the formation of the chelated complexes but the  $\text{M}(\text{CO})_5(\text{dpve})$  did not form the chelated complexes when irradiated. These ligands are very similar to the bpa ligand employed in this study and the absence of chelation was attributed to poor  $\sigma$ -overlap between the  $\sigma$ -orbital of the uncoordinated nitrogen atom and the metal d orbitals. It was proposed that the addition of bridging carbon atoms in bpy, to yield the dpym and dpve ligands, results in a substantial reduction in M-N overlap.

The introduction of excess ligand into the reaction of the  $\text{M}(\text{CO})_5(\text{bpa})$  complexes at ambient temperature, as monitored by infrared spectroscopy, had the effect of suppressing the formation of the  $\text{M}(\text{CO})_4(\text{bpa})$  and  $\text{M}(\text{CO})_6$  complexes. It may be suggested that the introduction of excess ligand into the reaction will have an effect on the rate of formation of the chelate product, as observed with the  $(\text{Cr}(\text{CO})_5)_2(\text{dphbpy})$  complex. The rate constant for the formation of the  $\text{M}(\text{CO})_4(\text{bpa})$  complex with varying concentrations of ligand has been monitored by UV-visible spectroscopy.

The spectral changes occurring upon standing a sample of  $\text{Cr}(\text{CO})_5(\text{bpa})$ , dissolved in toluene solution ( $1.316 \times 10^{-4} \text{ mol dm}^{-3}$ ) containing excess ligand ( $4.145 \times 10^{-2} \text{ mol dm}^{-3}$ ), at 298K are presented in Figure 3.2.2.5.4, as monitored by UV-visible spectroscopy.

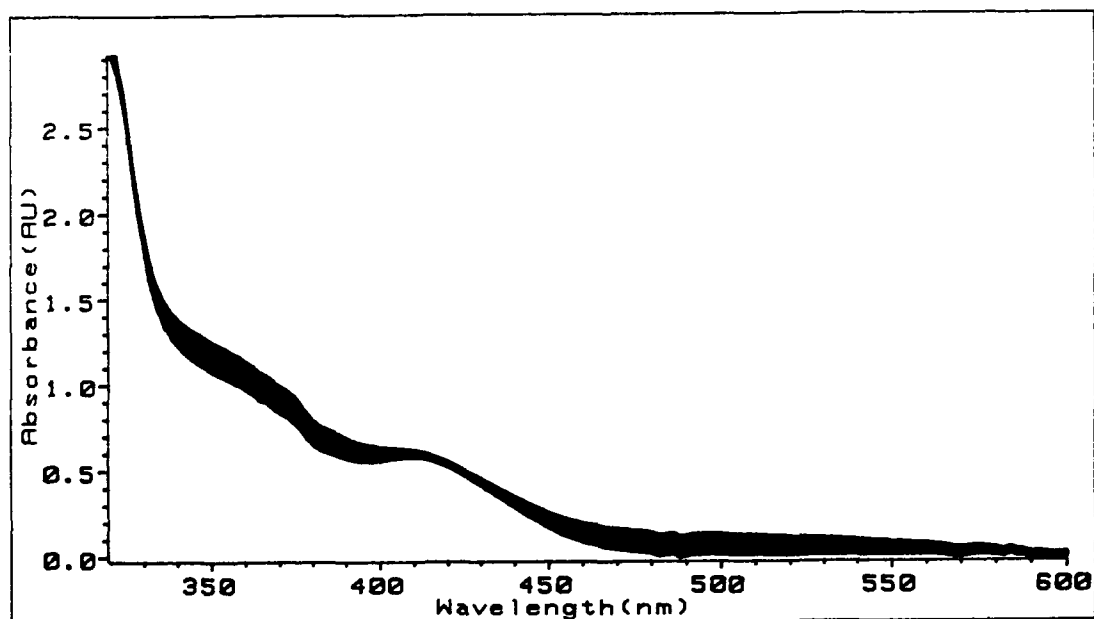


Figure 3.2.2.5.4 The spectral changes occurring upon standing a sample of  $\text{Cr}(\text{CO})_5(\text{bpa})$ , dissolved in toluene solution ( $1.316 \times 10^{-4} \text{ mol dm}^{-3}$ ) containing excess ligand ( $4.145 \times 10^{-2} \text{ mol dm}^{-3}$ ), at 298K

Table 3.2.2.5.1 The dependence of  $k_{\text{obs}}$  ( $\text{s}^{-1}$ ) for the formation of  $\text{Cr}(\text{CO})_4(\text{bpa})$  on the concentration of ligand added.

Concentration ( $\text{mol dm}^{-3}$ )	$k_{\text{obs}}$ ( $\text{s}^{-1}$ )
0	$15.37 \times 10^{-7}$
$1.24 \times 10^{-2}$	$6.287 \times 10^{-7}$
$1.467 \times 10^{-2}$	$4.158 \times 10^{-7}$
$4.145 \times 10^{-2}$	$3.701 \times 10^{-7}$
$5.576 \times 10^{-2}$	$3.465 \times 10^{-7}$

It appears that the growth of the bands at 358 and 496nm, corresponding to the formation of the  $\text{Cr(CO)}_4(\text{bpa})$  complex, has been suppressed along with the depletion of the band at 416nm, corresponding to the  $\text{Cr(CO)}_5(\text{bpa})$  complex

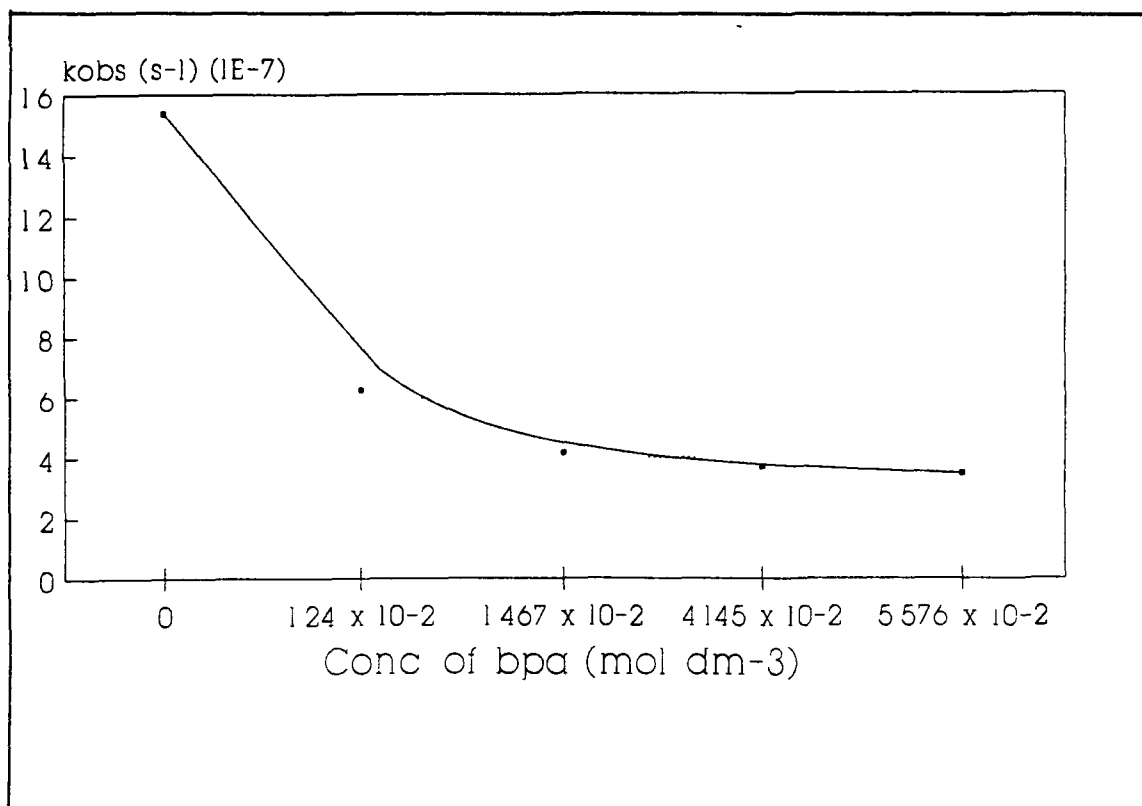


Figure 3 2 2.5 5 The dependence of  $k_{\text{obs}}$  for the formation of  $\text{Cr(CO)}_4(\text{bpa})$  on the concentration of added ligand

The addition of varying concentrations of excess ligand into the reaction results in the complete suppression of the growth of the bands at 358 and 496nm. The variation of the  $k_{\text{obs}}$  for these reactions is presented in Figure 3.2 2.5 5 and tabulated in Table 3 2 2 5 1. The addition of excess ligand had the effect of reducing the  $k_{\text{obs}}$  to a minimum of  $3.465 \times 10^{-7} \text{ s}^{-1}$  for the formation of the  $\text{Cr(CO)}_4(\text{bpa})$  complex.

The results for the dependence of the  $k_{\text{obs}}$  for the formation of the  $\text{W(CO)}_4(\text{bpa})$  complex on the addition of varying concentrations of excess ligand are

tabulated in Table 3.2.2.5.2. The rate constant was reduced to a minimum value of  $1.68 \times 10^{-6} \text{ s}^{-1}$  for the formation of the  $\text{W(CO)}_4(\text{bpa})$  species. This is still greater than that obtained for the  $\text{Cr(CO)}_5(\text{bpa})$  reactions in the presence of excess ligand.

Table 3.2.2.5.2 The dependence of  $k_{\text{obs}}$  for the formation of the  $\text{W(CO)}_4(\text{bpa})$  complex on the addition of varying concentrations of excess ligand

Concentration ( $\text{mol dm}^{-3}$ )	$k_{\text{obs}}$ ( $\text{s}^{-1}$ )
0	$41.57 \times 10^{-6}$
$1.005 \times 10^{-2}$	$16.54 \times 10^{-6}$
$2.26 \times 10^{-2}$	$13.62 \times 10^{-6}$
$4.92 \times 10^{-2}$	$10.32 \times 10^{-6}$
$6.68 \times 10^{-2}$	$1.175 \times 10^{-6}$
$7.86 \times 10^{-2}$	$1.68 \times 10^{-6}$

The addition of excess ligand appears to have had a reverse effect on the formation of the formation of the  $\text{M(CO)}_5(\text{bpa})$  complexes compared to that for the formation of the  $\text{Cr(CO)}_4(\text{dphbpy})$  species. The reduction of the  $k_{\text{obs}}$  to a constant minimum value may be an indication of an equilibrium process or an alteration in the reaction pathways.

### 3.2.2.6 The reactions of the $\text{M(CO)}_5(\text{bpa})$ complexes in CO saturated toluene as monitored by UV-visible spectroscopy.

The spectral changes occurring upon standing a sample of  $\text{Cr(CO)}_5(\text{bpa})$  in CO saturated toluene ( $1.898 \times 10^{-4} \text{ mol dm}^{-3}$ ), at 298K are presented in Figure 3.2.2.6.1, and the final spectrum, recorded after 870 minutes is presented in

Figure 3.2.2.6 1(b) The band at 416nm is seen to diminish but there is no new growth of bands (i.e. the band at 496nm corresponding to the formation of the  $\text{Cr(CO)}_4(\text{bpa})$  complex is not observed). The maintenance of isosbestic points at 364 and 470nm is an indication of a reaction uncomplicated by side or subsequent reactions. It appears that the introduction of CO into the reaction results in the suppression of the  $\text{Cr(CO)}_4(\text{bpa})$  species with a subsequent regeneration of the parent hexacarbonyl (this was confirmed by monitoring the reaction by infrared spectroscopy). The observed rate constant for the depletion of the  $\text{Cr(CO)}_5(\text{bpa})$  complex at 416nm was determined to be  $4.81 \times 10^{-5} \text{ s}^{-1}$ . This is approximately 31 times faster than the reaction of the complex in the absence of any excess ligand. This implies that the complex is labile with respect to the ligand in solution. This is represented in equation 3.2.2.7 1. This phenomenon was observed with the  $(\text{Cr(CO)}_5)_2(\text{dphbpy})$  complex and also at a faster rate than that observed for the reaction in the absence of any excess ligand.



equation 3.2.2.7 1

A sample of the  $\text{W(CO)}_5(\text{bpa})$  complex, dissolved in CO saturated toluene ( $2.497 \times 10^{-4} \text{ mol dm}^{-3}$ ), was monitored by UV-visible spectroscopy, at 298K and the spectral changes are very different from that of the  $\text{Cr(CO)}_5(\text{bpa})$  complex.

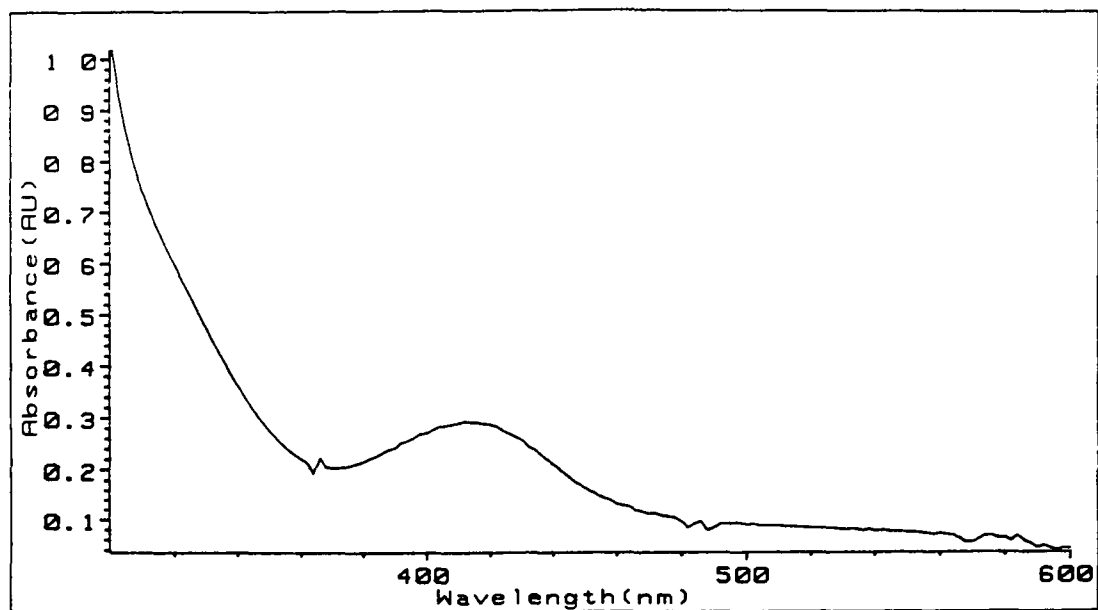
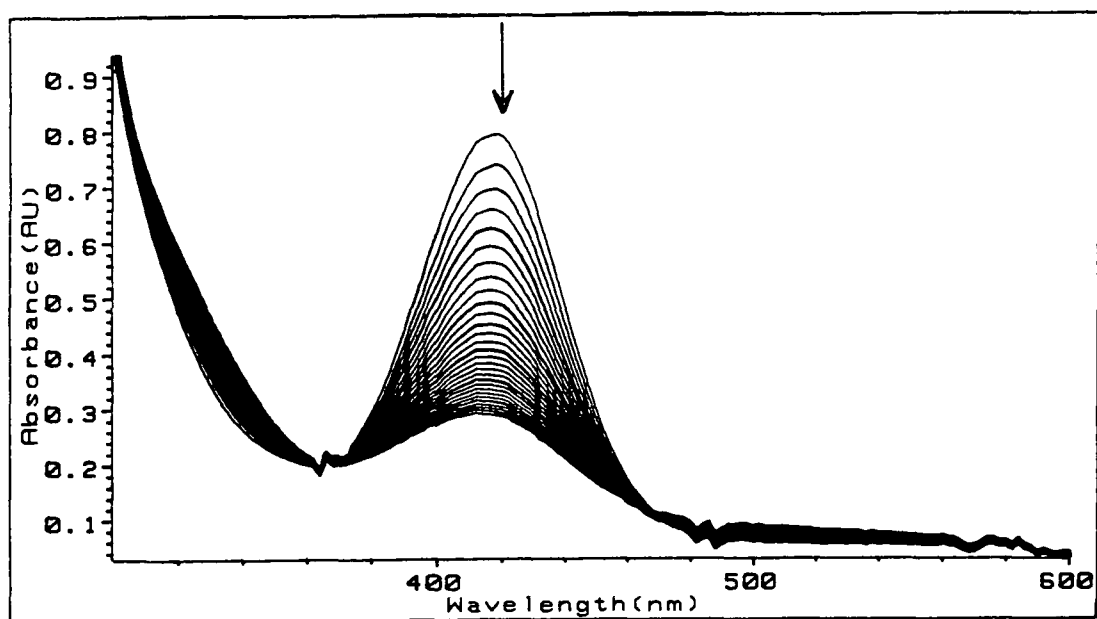


Figure 3.2.2.6 1 (a) The spectral changes occurring upon standing a sample of  $\text{Cr}(\text{CO})_5(\text{bpa})$  in CO saturated toluene ( $1.898 \times 10^{-4} \text{ mol dm}^{-3}$ ) at 298K and (b) the final spectrum recorded after 870 minutes



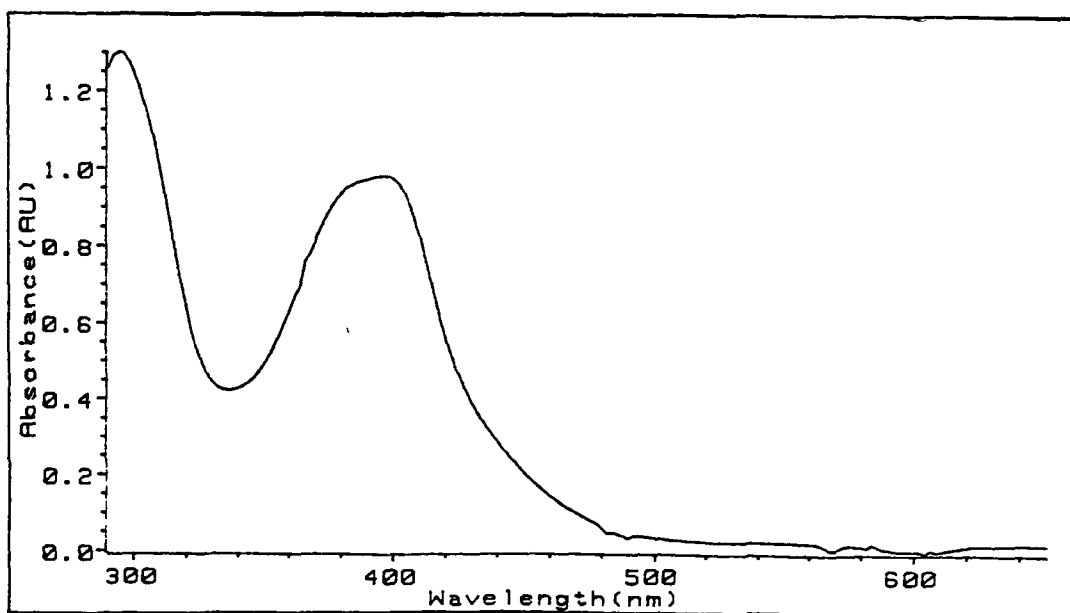
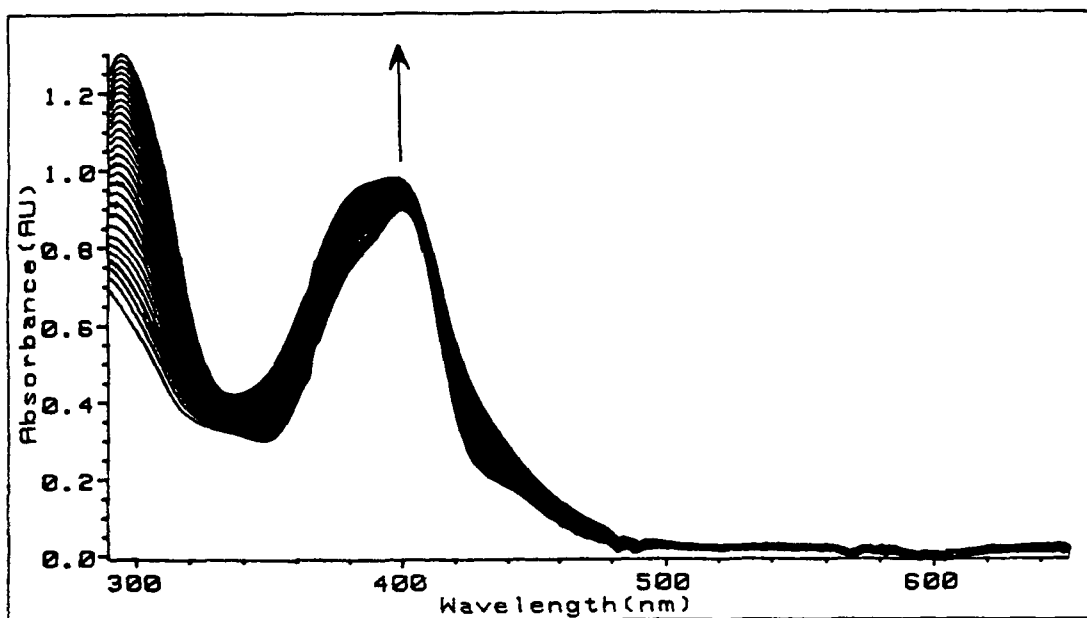


Figure 3 2 2 6 2 (a) The spectral changes occurring upon standing a sample of  $\text{W(CO)}_5(\text{bpa})$ , dissolved in CO saturated toluene ( $2.497 \times 10^{-4} \text{ mol dm}^{-3}$ ), at 298K and (b) the final spectrum recorded after 870 minutes

Instead of observing a suppression of the bands associated with the  $\text{W(CO)}_4(\text{bpa})$  species, these bands were observed to grow. Despite the presence of the CO, the  $\text{W(CO)}_5(\text{bpa})$  complex, which does not appear to be labile with respect to loss of the ligand, forms the  $\text{W(CO)}_4(\text{bpa})$  species. The observed rate constant for this reaction was determined to be  $2.023 \times 10^{-5} \text{ s}^{-1}$ , by monitoring the growth of the band at 382 nm. The reaction, for the formation of the  $\text{W(CO)}_4(\text{bpa})$  complex, in the absence of any excess ligand is twice as fast as this reaction. Thus, the presence of CO in solution seems to have had some effect on the  $k_{\text{obs}}$ . The spectral changes occurring upon standing a sample of  $\text{W(CO)}_5(\text{bpa})$ , dissolved in CO saturated toluene ( $2.497 \times 10^{-4} \text{ mol dm}^{-3}$ ), at 298 K, and the final spectrum recorded after 870 minutes, are presented in Figure 3.2.2.6.2(a) and (b) respectively.

The monitoring of this reaction by infrared spectroscopy revealed a slight formation of the  $\text{W(CO)}_4(\text{bpa})$  and generation of the parent hexacarbonyl. The  $\text{W(CO)}_5(\text{bpa})$  complex remained in solution and did not react with the CO in solution. It appears that this complex is not labile with respect to loss of the ligand in the presence of CO.

**3.2.2.7 The activation parameters for the formation of the  $M(CO)_4(bpa)$  species from  $M(CO)_5(bpa)$  in the absence and presence of excess ligand.**

The experimental data for the determination of the activation parameters for the formation of the  $M(CO)_4(bpa)$  complexes from  $M(CO)_5(bpa)$  in the absence and presence of excess ligand is presented in Tables 3.2.2.7.1 and 3.2.2.7.2

Table 3.2.2.7.1 Experimental data for the determination of the activation parameters for the formation of  $M(CO)_4(bpa)$  in the absence of any excess ligand

Complex formed	Temperature (K)	Ln ( $k_{obs}$ )	Ln( $k_{obs}/T$ )
<b>Cr (CO)<sub>4</sub>(bpa)</b>	298	-13.38	-19.08
	303	-12.1	-17.815
	313	-10.83	-16.58
	323	-9.64	-15.42
	333	-7.86	-13.667
<b>W(CO)<sub>4</sub>(bpa)</b>	298	-11.3	-16.99
	303	-10.72	-16.43
	313	-9.22	-14.96
	323	-8.02	-13.79
	333	-7.21	-13.019

Table 3.2.2.7.2 The experimental data for the determination of the activation parameters for the formation of  $M(CO)_4(bpa)$  in the presence of excess ligand

Complex formed	Temperature (K)	$\ln(k_{obs})$	$\ln(k_{obs}/T)$
<b>Cr(CO)<sub>4</sub>(bpa)</b>	298	-14.22	-19.92
	303	-13.74	-19.45
	313	-12.78	-18.53
	323	-11.81	-17.59
	333	-10.83	-16.63
<b>W(CO)<sub>4</sub>(bpa)</b>	298	-12.17	-17.87
	303	-11.9	-16.9
	313	-9.925	-15.67
	323	-9.048	-14.82
	333	-8.05	-13.86

The plots for the experimental data are given in Figures 3.2.2.7.1 to 3.2.2.7.4. The data from the Arrhenius and Eyring plots is presented in Table 3.2.2.7.3.

Table 3.2.2.7.3 The results obtained from the Arrhenius and Eyring plots for the formation of  $M(CO)_4(bpa)$  in the absence and presence of ligand

Complex	Arrhenius Plot	Eyring Plot
<b>Cr(CO)<sub>4</sub>(bpa)</b>	Slope -14700 ± 900 Intercept 36.25 ± 0.3 Corr 0.994	-14400 ± 900 29.5 ± 0.3 0.994
<b>Cr(CO)<sub>4</sub>(bpa) + bpa</b>	Slope -9600 ± 200 Intercept 17.9 ± 0.5 Corr 0.9994	-9300 ± 200 11.2 ± 0.5 0.9993
<b>W(CO)<sub>4</sub>(bpa)</b>	Slope -12000 ± 500 Intercept 28.8 ± 0.2 Corr 0.997	-11600 ± 600 22.1 ± 0.2 0.997
<b>W(CO)<sub>4</sub>(bpa) + bpa</b>	Slope -11300 ± 700 Intercept 26.0 ± 0.2 Corr 0.995	-11000 ± 700 19.3 ± 0.2 0.994

The results from the calculations, using the data from the Arrhenius and Eyring plots, are presented in Table 3.2.2.7.4

Table 3 2 2 7 4 The activation parameters for the formation of the  $M(CO)_4(bpa)$  species in the absence and presence of excess ligand

Complex formed	Excess L	Ea (kJ mol <sup>-1</sup> )	$\Delta H^\ddagger$ (kJ mol <sup>-1</sup> )	$\Delta S^\ddagger$ (J K <sup>-1</sup> mol <sup>-1</sup> )
Cr(CO) <sub>4</sub> (bpa)	no	123 ± 6	120 ± 6	48 ± 5
Cr(CO) <sub>4</sub> (bpa)	yes	80 ± 2	77 ± 2	-104 ± 5
W(CO) <sub>4</sub> (bpa)	no	100 ± 4	97 ± 5	-14 ± 5
W(CO) <sub>4</sub> (bpa)	yes	94 ± 6	92 ± 6	-37 ± 5

The most striking feature of the results is the large difference in the activation energy for the formation of the  $Cr(CO)_4(bpa)$  species in the absence and presence of excess ligand. This is indicative of two different rate determining steps for the formation of this complex. As stated previously, the activation enthalpy for the breaking of a Cr-N bond in  $Cr(CO)_5(py)^{25}$  is 106 kJ mol<sup>-1</sup>. The result obtained for the activation enthalpy for the formation of  $Cr(CO)_4(bpa)$ , in the absence of any excess ligand, is 123 kJ mol<sup>-1</sup>. In the presence of excess ligand the activation enthalpy is reduced to 80 kJ mol<sup>-1</sup>. The activation enthalpy for the breaking of a Cr-CO bond in  $Cr(CO)_6^{20}$  is 168 kJ mol<sup>-1</sup> which appears to be too high a value to play a role here. The activation enthalpy for the formation of  $Cr(CO)_4(bpa)$  in the absence of any excess ligand is almost identical to that obtained for the breaking of a Cr-N bond and thus the rate determining step for this process may involve the breaking of a Cr-N bond. This is in agreement with the regeneration of the parent hexacarbonyl in the presence of CO. The entropy value calculated supports the assumption of a dissociative pathway.

In the presence of excess ligand the activation enthalpy is reduced to 80 kJ mol<sup>-1</sup> which is in good agreement with previous studies for the formation of Cr(CO)<sub>4</sub>(bpy)<sup>13</sup> in the presence of excess ligand. The entropy values for the formation of Cr(CO)<sub>4</sub>(bpa) in the absence and presence of excess ligand are 48 and -104 J K<sup>-1</sup> mol<sup>-1</sup>, respectively, indicative of a dissociative pathway becoming highly associative in nature with the introduction of excess ligand.

The activation enthalpies for the formation of the W(CO)<sub>4</sub>(bpa) complex, in the absence and presence of excess ligand, are similar, in contrast to that for the formation of the Cr(CO)<sub>4</sub>(bpa) species. This implies that the pathways for the formation of the complex in the absence and presence of excess ligand are similar. A comparison of the activation parameters between this study and others is presented in Table 3.2.2.7.5.

The activation enthalpy for the breaking of a W-CO bond in W(CO)<sub>6</sub><sup>25</sup> was calculated to be 167 kJ mol<sup>-1</sup>. The activation enthalpies for the formation of W(CO)<sub>4</sub>(bpa) in the absence and presence of excess ligand are much less than this value, which would indicate that the breaking of a W-CO bond is not involved in the transition state. From Table 3.2.2.7.5 the activation enthalpy for the breaking of a W-N bond in W(CO)<sub>5</sub>(morpholine)<sup>26</sup>, in the absence of excess ligand, is very similar to that obtained in this investigation. It would appear from this comparison that the activation enthalpies correspond to the breaking of a W-N bond, but the negative entropy values indicate the associative nature of the transition state.

Table 3.2 2 7 5 A comparison of the activation parameters between this study and other similar investigations

Ligand	Metal	$\Delta H^\ddagger$ (kJ mol <sup>-1</sup> )	$\Delta S^\ddagger$ (J K <sup>-1</sup> mol <sup>-1</sup> )	Reference
bpa	W	97	-14	this work
bpa	W	92	-37	this work
morpholine	W	94	-53.3	26
2-C <sub>5</sub> H <sub>4</sub> CHNR (R= <sup>i</sup> Pr)	W	57.5	-98.2	22
2-C <sub>5</sub> H <sub>4</sub> CHNR (R= nBu)	W	26.8	-179	22
2-C <sub>5</sub> H <sub>4</sub> CHNR (R= <sup>t</sup> Bu)	W	82	-56.9	22
2-C <sub>5</sub> H <sub>4</sub> CHNR (R= Ph)	W	45.6	-140.2	22

The breaking of a W-N bond may be the rate determining step but in the presence of CO there is some driving force which alters the equilibrium of the reaction and the regeneration of the parent hexacarbonyl is not observed. The entropy values for the formation of the W(CO)<sub>4</sub>(bpa) complex in the presence and absence of excess ligand are small and it may be possible that the reaction pathway may involve an interchange process.



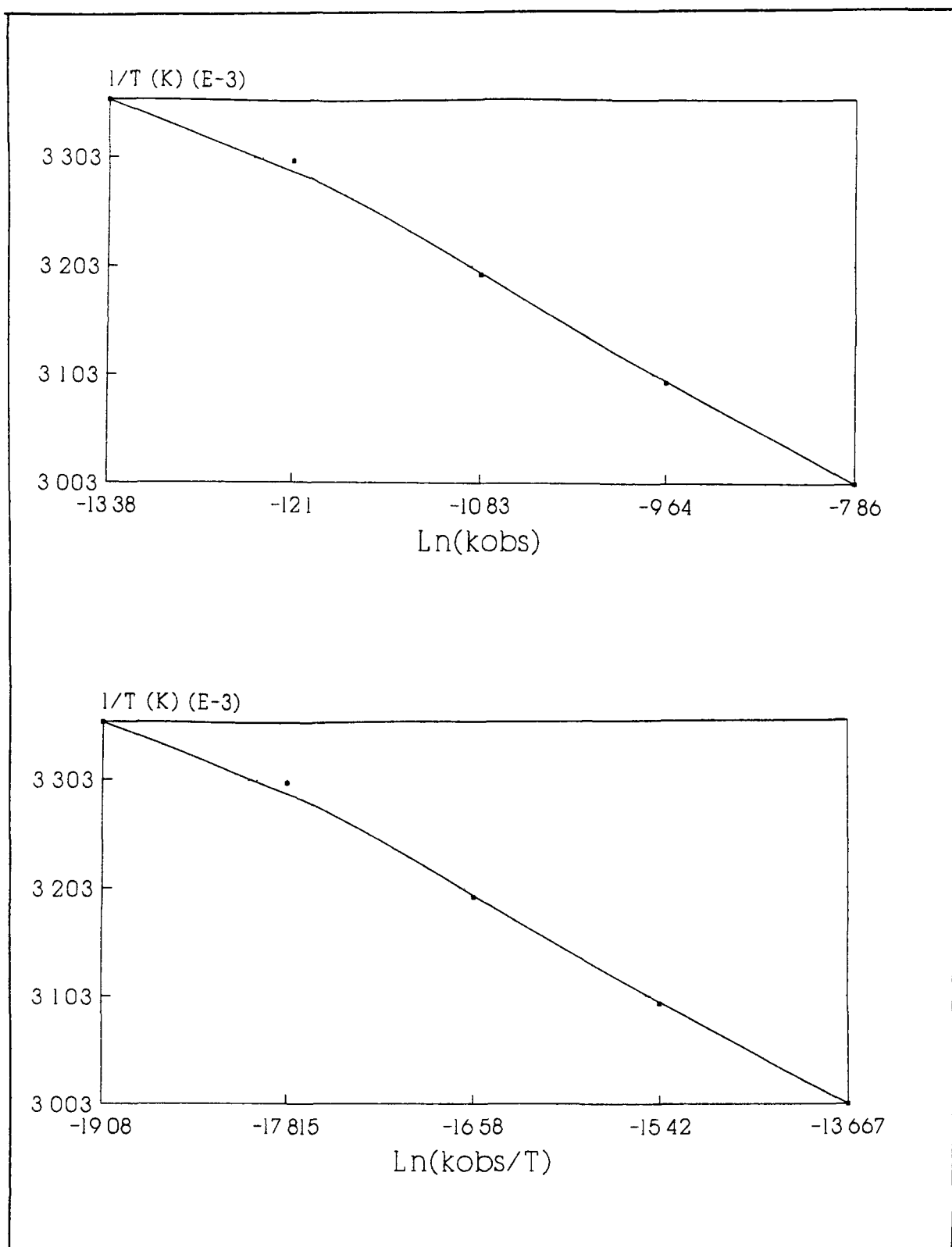


Figure 3.2.2.7.1 The (a) Arrhenius and (b) Eyring plots for the formation of the  $\text{Cr}(\text{CO})_4(\text{bpa})$  complex in the absence of any excess ligand

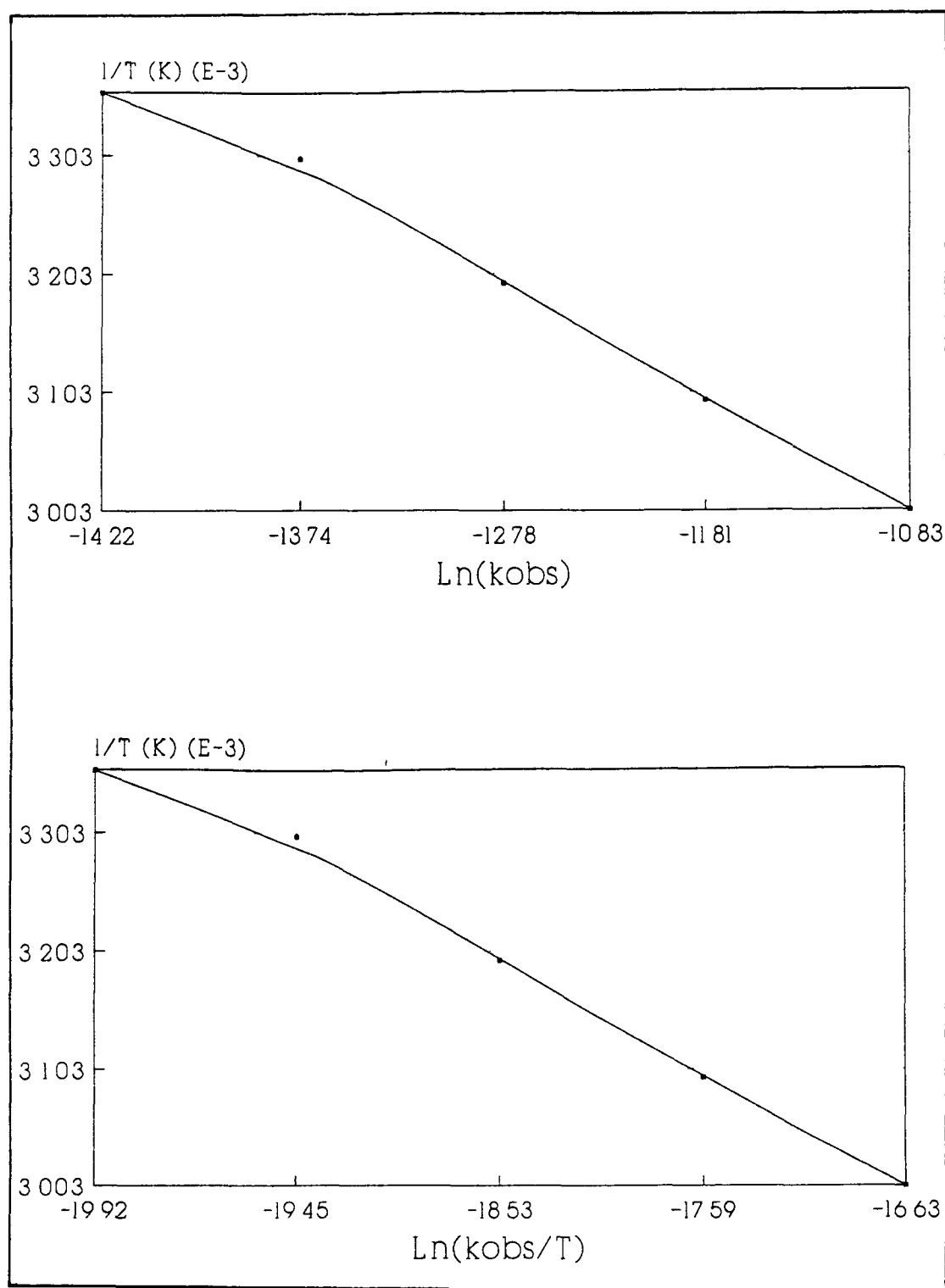


Figure 3 2.2 7.2. The (a) Arrhenius and (b) Eyring plots for the formation of the  $\text{Cr}(\text{CO})_4(\text{bpa})$  complex in the presence of excess ligand.

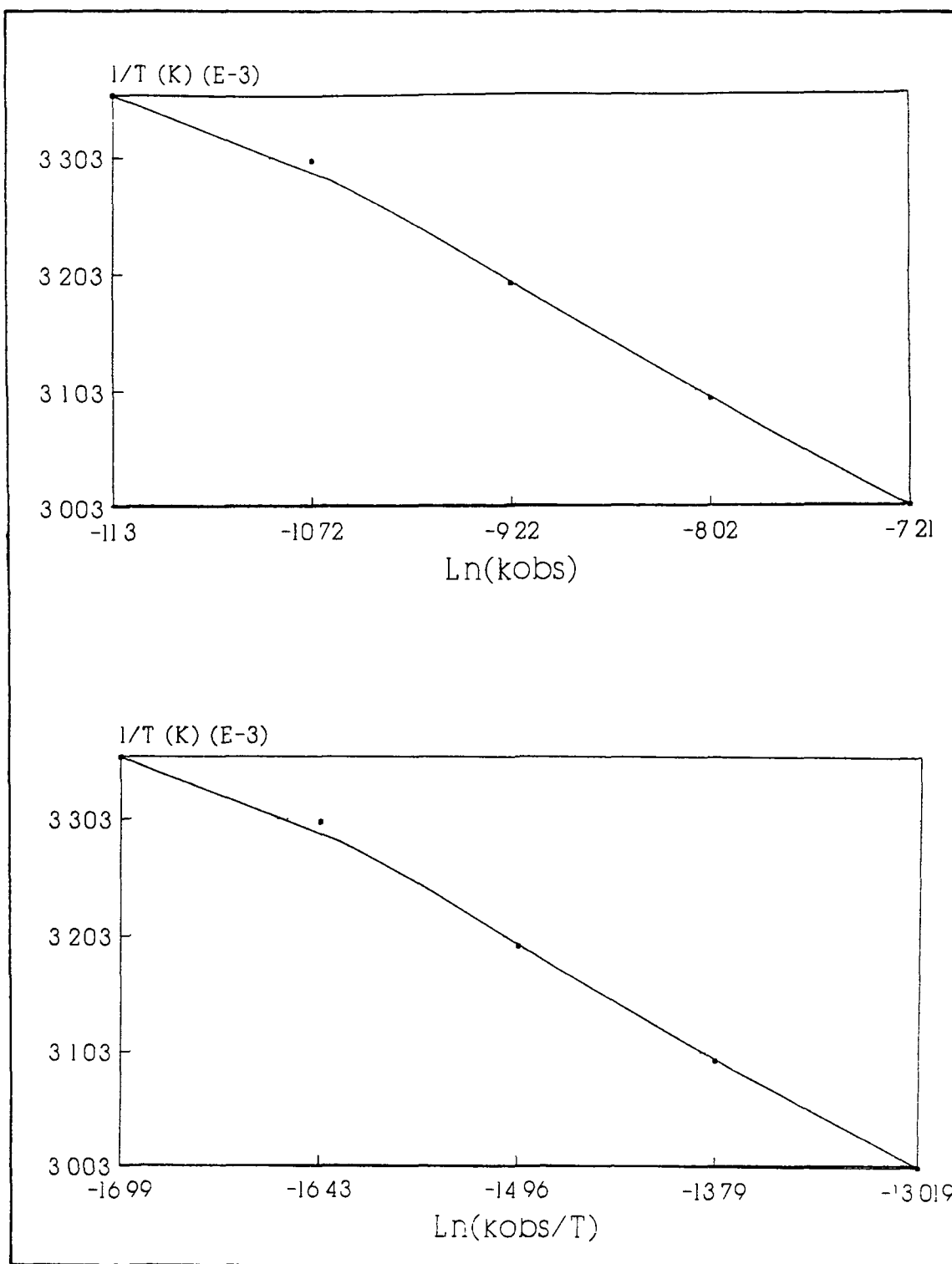


Figure 3 2 2.7 3 The (a) Arrhenius and (b) Eyring plots for the formation of the  $W(CO)_4(bpa)$  complex in the absence of any excess ligand

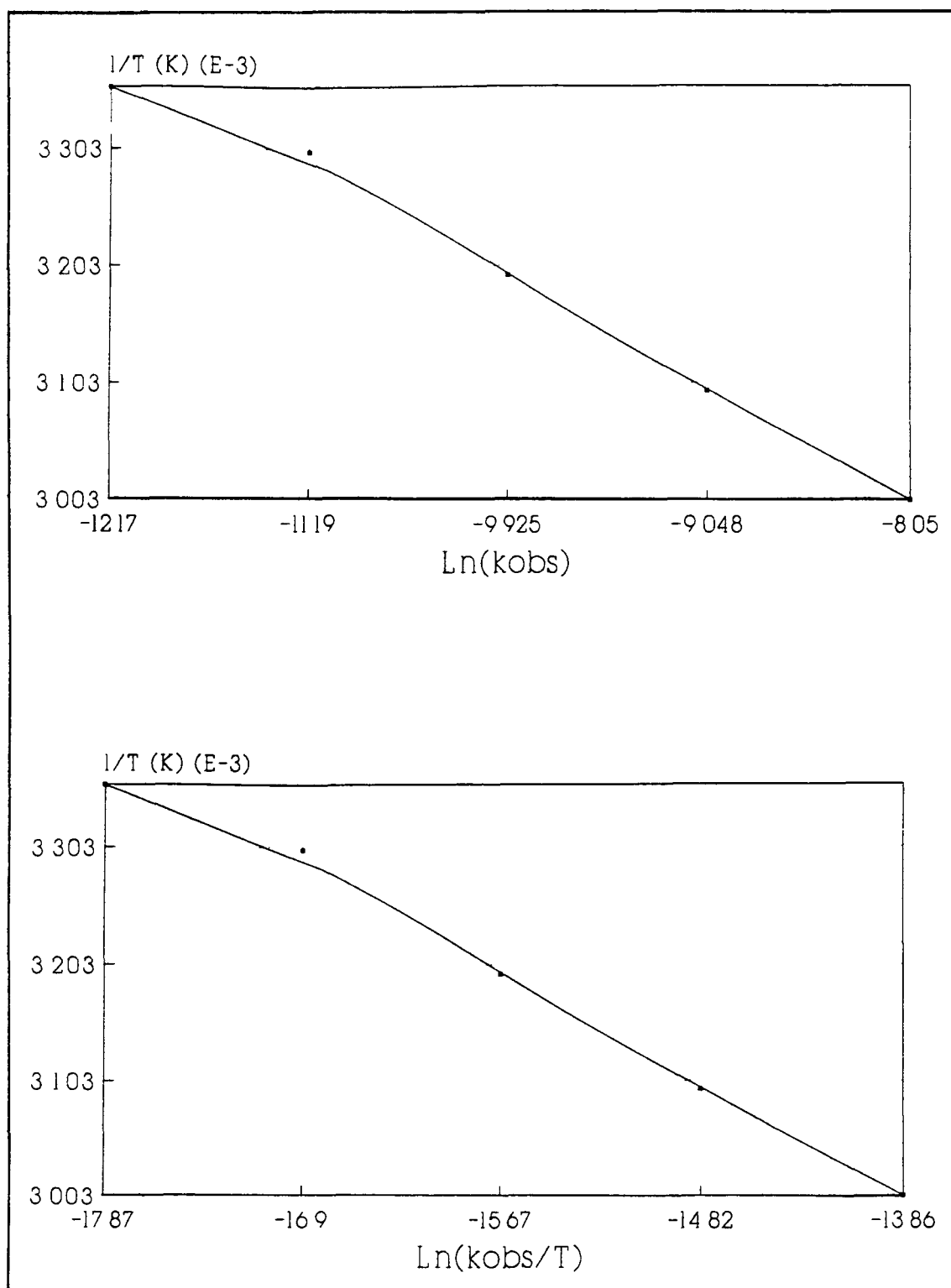


Figure 3.2.2.7.4 The (a) Arrhenius and (b) Eyring plots for the formation of the  $\text{W(CO)}_4(\text{bpa})$  complex in the presence of excess ligand

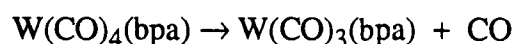
### 3.2.2.8 Summary

The  $M(CO)_5(bpa)$  complexes were isolated and characterised by infrared, UV-visible spectroscopy and elemental analysis. The reactions of these complexes were monitored by infrared and UV-visible spectroscopy in the absence and presence of excess ligand. From the reactions of the  $M(CO)_5(bpa)$  at elevated temperatures, as monitored by infrared spectroscopy, the stoichiometry of the reaction was determined to be that presented in equation 3.2.2.8.1



equation 3.2.2.8.1

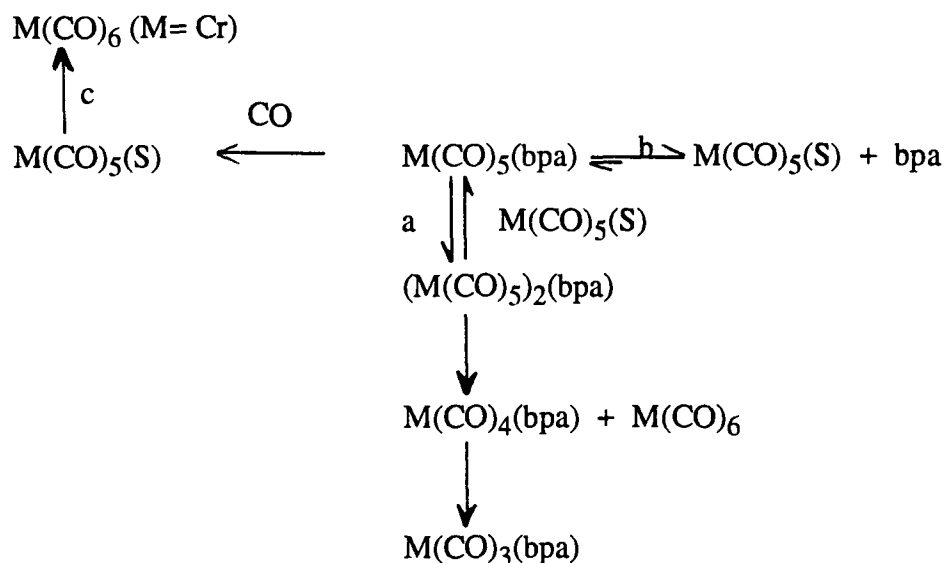
The  $W(CO)_4(bpa)$  complex was isolated and its thermal reaction to form the appropriate  $W(CO)_3(bpa)$  complex was determined to be in a 1:1 molar ratio (equation 3.2.2.8.2)



equation 3.2.2.8.2

In the presence of excess ligand the formation of both the  $M(CO)_4(bpa)$  and  $M(CO)_6$  complexes was suppressed. In the presence of CO saturated toluene the  $Cr(CO)_5(bpa)$  complex was observed to regenerate the parent hexacarbonyl, while the  $W(CO)_5(bpa)$  complex remained unchanged, apart from a minor reaction to form  $W(CO)_4(bpa)$  and  $W(CO)_6$ . A reaction mechanism is proposed in Scheme 3.2.2.8.1 to account for these observations.

**Scheme 3 2 2 8 1** The proposed reaction scheme for the  $M(CO)_5(bpa)$  complexes



S= toluene

In the absence of excess ligand (step a) the solvated species,  $M(CO)_5(S)$ , is produced which reacts with the  $M(CO)_5(bpa)$  complex to produce the ligand bridged metal carbonyl species,  $(M(CO)_5)_2(bpa)$ . This forms the chelated complex and the parent hexacarbonyl. In the presence of excess ligand (step b) the equilibrium involved in the production of the  $M(CO)_5(S)$  species is displaced. Thus the formation of the ligand bridged metal carbonyl complex is suppressed, and consequently the formation of the chelated complex and the parent hexacarbonyl. In the presence of CO in solution the  $Cr(CO)_5(bpa)$  complex produces the  $Cr(CO)_5(S)$  species which reacts with the CO to produce the  $Cr(CO)_6$  (step c) compound and suppresses the formation of the  $Cr(CO)_4(bpa)$  complex. In the presence of CO, the  $W(CO)_5(bpa)$  complex is not labile to loss of the ligand and the formation of the  $W(CO)_4(bpa)$  and  $W(CO)_6$  complexes is not observed.

The activation parameters for the formation of the  $\text{Cr}(\text{CO})_4(\text{bpa})$  complex in the absence of excess ligand indicate that the rate determining step may

involve the breaking of a Cr-N bond, while in the presence of excess ligand the pathway becomes highly associative in nature. The activation parameters for the formation of the  $\text{W(CO)}_4(\text{bpa})$  complex, in the absence (step a) and presence (step d) of excess ligand, indicate that the two pathways are similar. The activation enthalpies are very similar to that obtained for the breaking of a W-N bond in  $\text{W(CO)}_5(\text{morpholine})^{26}$ , in the absence of any excess ligand. However, the breaking of a W-N bond as the rate determining step does not explain the formation of the  $\text{W(CO)}_4(\text{bpa})$  in CO saturated solution.

### 3.2.3 The synthesis and characterisation of $\text{Cr}(\text{CO})_5(\text{ampy})$ (ampy= 2-aminomethylpyridine) and its reactions in solution and the solid state.

#### 3.2.3.1 The preparation of $\text{Cr}(\text{CO})_5(\text{ampy})$

The reaction of a solution of 2-aminomethylpyridine (ampy) in toluene with a sample of  $\text{Cr}(\text{CO})_5(\text{cis-cyclo-octene})$ , in a 1:1 molar ratio, resulted in the formation of  $\text{Cr}(\text{CO})_5(\text{ampy})$ . The molecular formula of the complex was confirmed by elemental analysis. The isolation of this complex with the ligand coordinated in a monodentate fashion was not surprising despite the ligand having two sites available for coordination. It was predicted from Chapter 2 that coordination of one pyridine nitrogen would not result in a conformational change being induced on the ligand. Thus, only the monodentately coordinated complex would be formed. The structure of this ligand is similar to the *bis*-picolylamine ligand in that it resembles half of the ligand (Figure 3.2.3.1.1). It closely resembles the pyridinal-2-imine ligand employed by Lees<sup>22</sup> *et al* for many investigations.

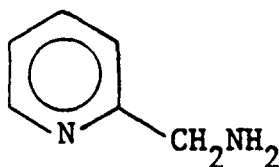


Figure 3.2.3.1.1 2-aminomethylpyridine

However, the reactivity of this ligand is very different in its reactivity than the two ligands mentioned above. This was the only non-symmetric bidentate ligand used in the study.



### 3.2.3.2 The characterisation of $\text{Cr}(\text{CO})_5(\text{ampy})$ using infrared and UV-visible spectroscopy.

The infrared spectrum of a sample of  $\text{Cr}(\text{CO})_5(\text{ampy})$ , pressed in a KBr pellet, at 293K, is presented in Figure 3.2 3.2.1

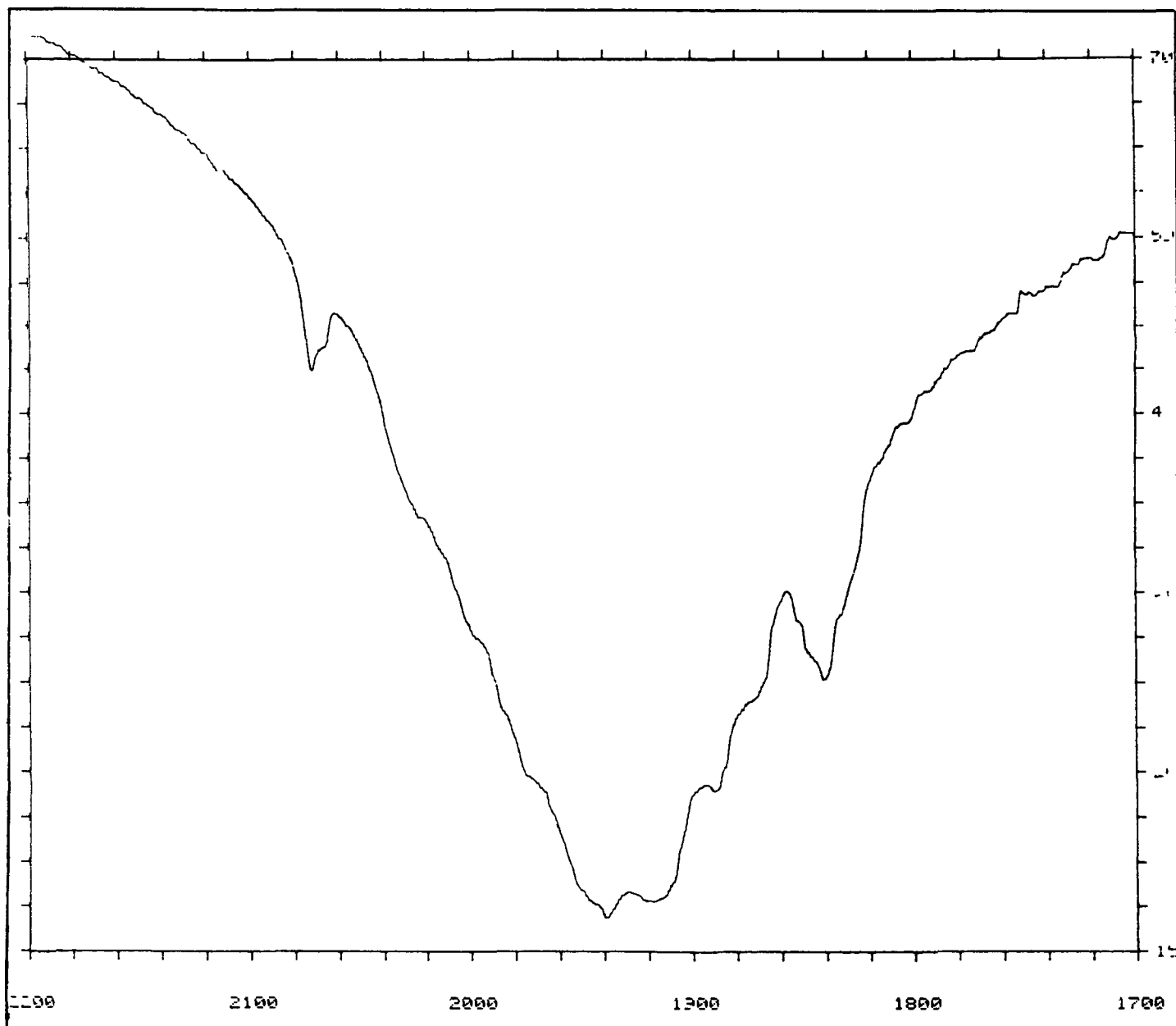


Figure 3 2.3 2.1 The infrared spectrum of a sample of  $\text{Cr}(\text{CO})_5(\text{ampy})$ , pressed in a KBr pellet, at 293K

The spectrum exhibits four bands in the CO stretching region at 2072, 1983, 1931 and 1903 $\text{cm}^{-1}$ , which correspond to the  $A_1$ ,  $B_1$ , E and  $A_1(2)$  modes, respectively, of a pseudo  $C_{4v}$  species<sup>10</sup>. The intensity of the normally forbidden  $B_1$  band is indicative of a reduction of the symmetry of the molecule about the metal carbonyl centre. This is attributed to the asymmetry of the ampy ligand, which distorts the complex so that it does not possess perfect  $C_{4v}$  symmetry.

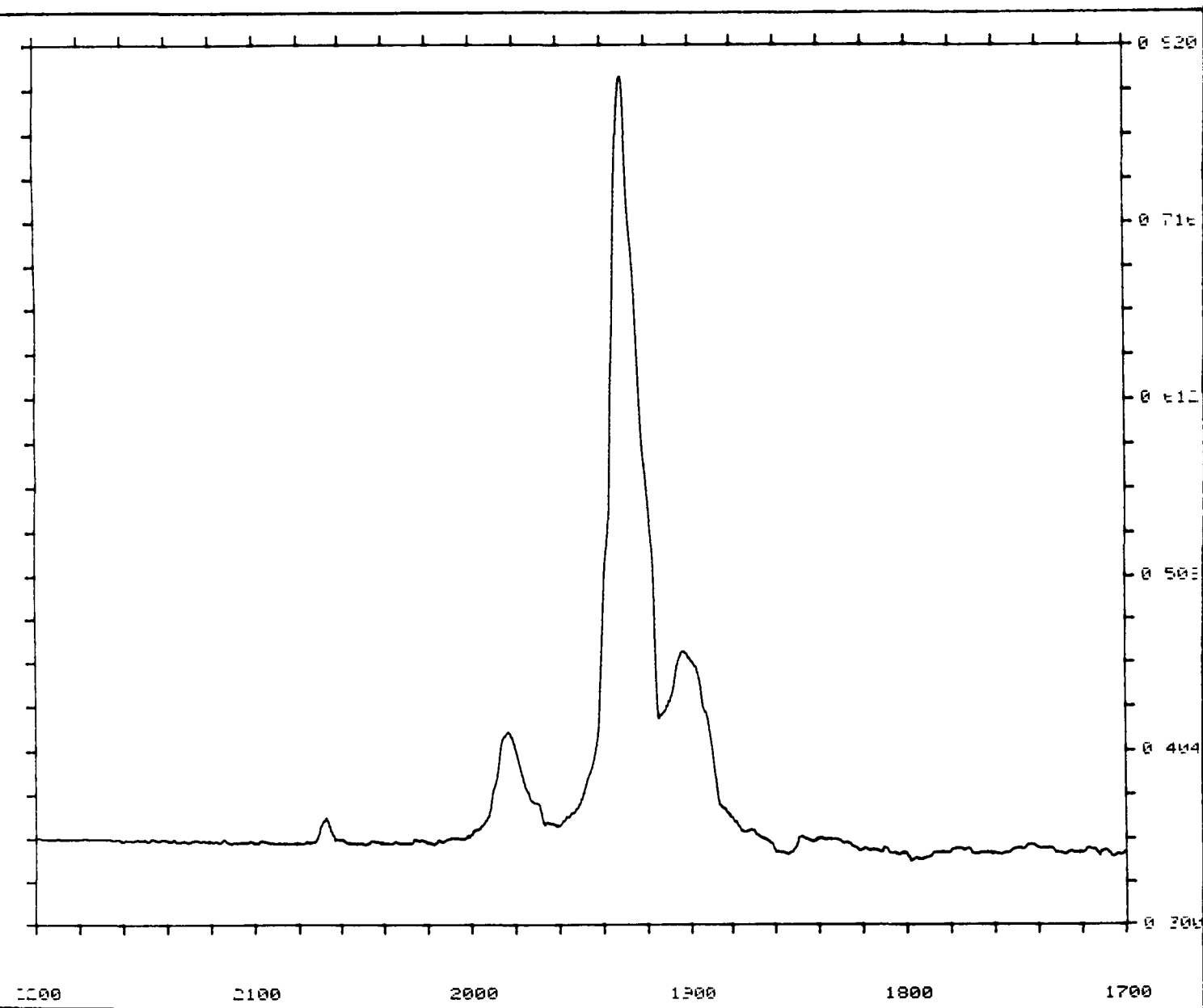


Figure 3.2 3.2.2 The infrared spectrum of a sample of  $\text{Cr}(\text{CO})_5(\text{ampy})$  dissolved in toluene ( $5.397 \times 10^{-3} \text{ mol dm}^{-3}$ ), at 298K

Upon comparison with the spectrum of a solution of the complex in toluene ( $5.397 \times 10^{-3} \text{ mol dm}^{-3}$ ) it is observed that the  $B_1$  mode is masked by the  $T_{1u}$  mode of the parent carbonyl (Figure 3.2 3.2.2 ) but a clearer view of the bands is portrayed.

The UV-visible spectrum of a solution of  $\text{Cr(CO)}_5(\text{ampy})$  in toluene ( $4.46 \times 10^{-4} \text{ mol dm}^{-3}$ ) is shown in Figure 3.2.3.2 3 The spectrum exhibits a low energy band in the visible region centred at 418nm. This band may be attributed to a  $^1A(e^4b_2^2) \rightarrow ^1E(e^3b_2^2a_1^1)$  LF transition. As observed previously with the other complexes used in this investigation, the MLCT band overlaps the LF band

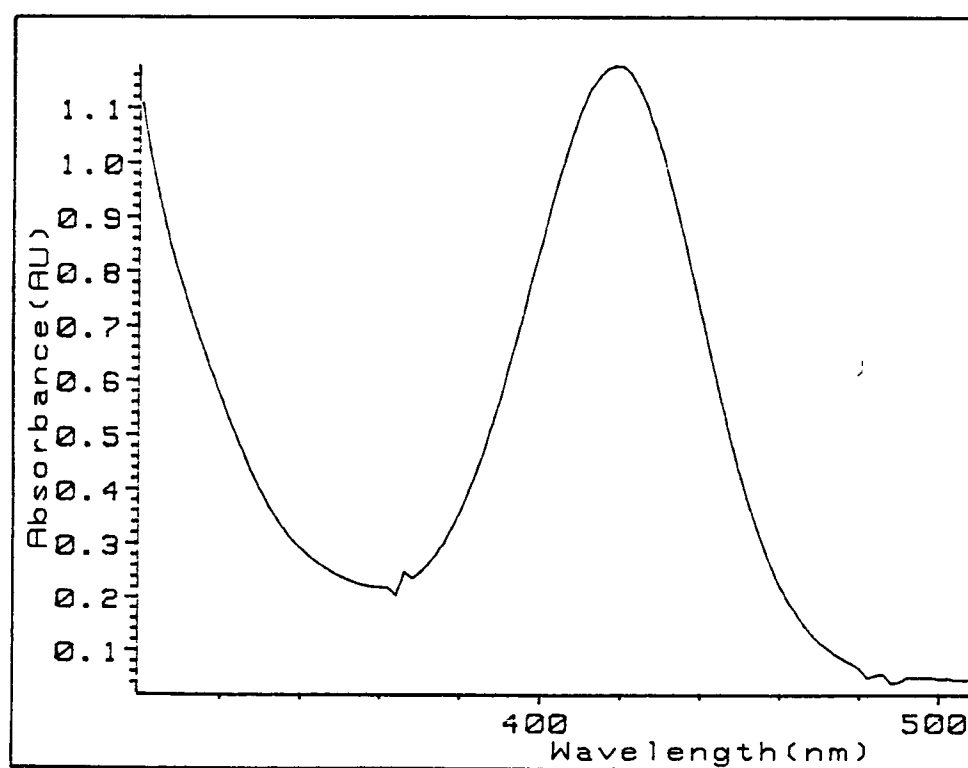


Figure 3 2 3 2 3 The UV-visible spectrum of a sample of  $\text{Cr(CO)}_5(\text{ampy})$  in toluene solution ( $4.46 \times 10^{-4} \text{ mol dm}^{-3}$ ) at 298K

The infrared spectrum, of a sample of  $\text{Cr}(\text{CO})_5(\text{ampy})$  pressed in a KBr pellet, presented in Figure 3.2.3.2.4, in which all the modes that were previously assigned to the  $\text{Cr}(\text{CO})_5(\text{ampy})$  complex appear to be split. This particular preparation involved the immediate precipitation of the complex from pentane, a relatively non-polar solvent, resulting in, what we assume to be, both the thermodynamic and kinetic products being isolated. The thermodynamic product, being the most stable, is that which is most commonly formed. The structure of the kinetic product is assumed to be that shown in Figure 3.2.3.2.5.

One possibility for the formation of this complex is the immediate recrystallisation. This complex was only observed in the solid state and rapidly converted to the stable thermodynamic product upon dissolution at ambient temperature. Unfortunately, preferential recrystallisation of this unique complex in a pure form was unsuccessful as was the attempted separation of the isomers. This complex also formed the chelate species,  $\text{Cr}(\text{CO})_4(\text{ampy})$ , when heated to a higher temperature.

An investigation into the mechanism of chelate formation at group 6 metal carbonyl centres employing pyridinal-2-imine<sup>22</sup> resulted in the formation of a pentacarbonyl intermediate in which the metal was coordinated to the imine nitrogen. However, this phenomenon was attributed to steric hindrance by the presence of a methyl group  $\alpha$  to the pyridine nitrogen.

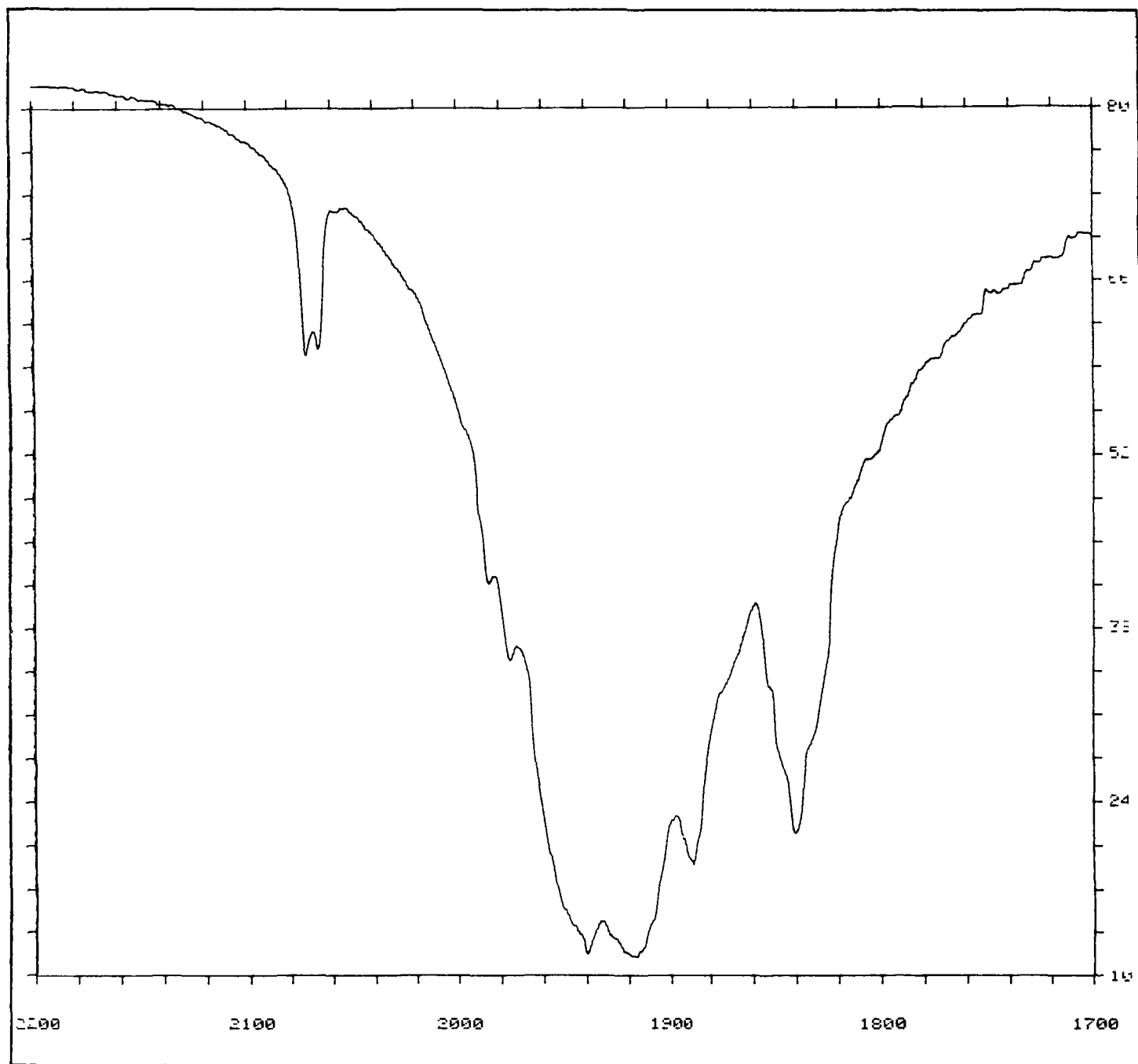


Figure 3.2.3 2 4 The infrared spectrum of a sample of  $\text{Cr}(\text{CO})_5(\text{ampy})$ , pressed in a KBr pellet, which exhibits a split in the bands previously assigned to the pseudo  $\text{C}_{4v}$  complex,  $\text{Cr}(\text{CO})_5(\text{ampy})$

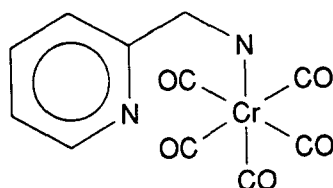


Figure 3 2 3 2 5 The structure of the kinetic product of  $\text{Cr(CO)}_5(\text{ampy})$

The characterisation of the  $\text{Cr(CO)}_5(\text{ampy})$  complex by  $^1\text{H}$  n.m.r spectroscopy was attempted to identify the mode of coordination. The  $^1\text{H}$  n.m.r. spectrum of the  $\text{Cr(CO)}_5(\text{ampy})$  complex, in  $\text{CDCl}_3$  at 298K, exhibited bands at 8.58(s), 7.69(s), 7.25(d), 5.11(s), 3.82(s), 2.57(s), 2.03(s), 1.67(s), 1.25(s), and 0.87(s)ppm, (s= singlet, d= doublet). The spectrum of the free ligand, in  $\text{CDCl}_3$  at 298K, exhibited bands at 7.75(s), 6.8(t), 6.48(d), 6.3(d), 3.14(d), 1.76(s), (t= triplet). It was not possible to assign a structure of the  $\text{Cr(CO)}_5(\text{ampy})$  complex on the basis of these spectra, as there was no clear indication of the mode of coordination.

### 3.2.3.3 The reactions of $\text{Cr(CO)}_5(\text{ampy})$ in the solid state

The infrared spectral changes observed upon heating a sample of  $\text{Cr(CO)}_5(\text{ampy})$ , pressed in a KBr pellet, to 353K for thirty minutes, are shown in Figure 3 2 3.3 1. The bands at 2072, 1983, 1931 and 1903 $\text{cm}^{-1}$  are seen to diminish with the concomitant growth of bands at 2006, 1983, 1866 and 1784 $\text{cm}^{-1}$ . It was expected that these bands were a result of the formation of the chelate product, *cis*- $\text{Cr(CO)}_4(\text{ampy})$ . Comparison of these bands with an authentic sample of  $\text{Cr(CO)}_4(\text{ampy})$  confirmed this assumption.

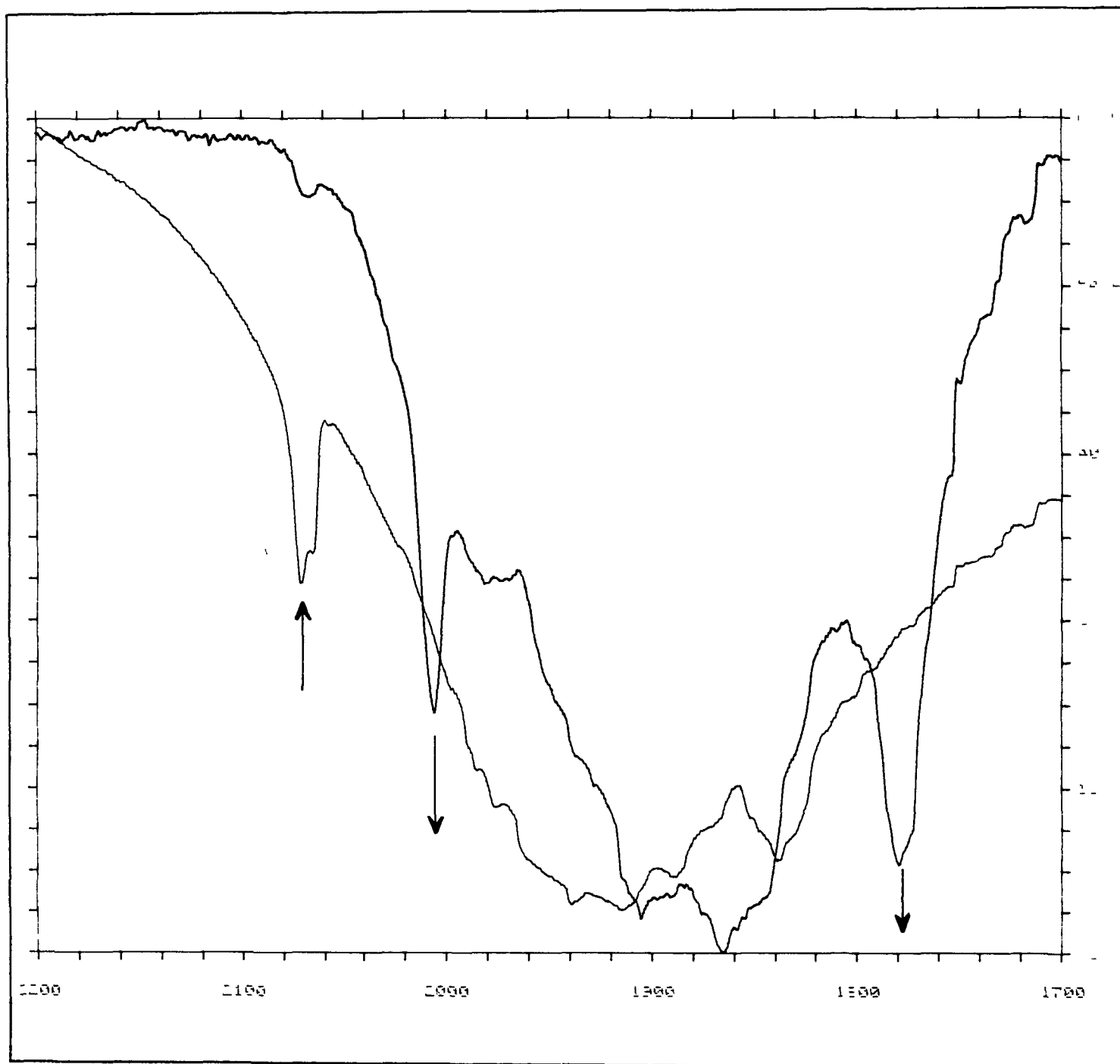
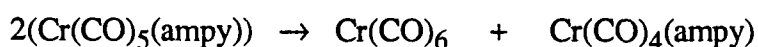


Figure 3.2.3 3 1 The infrared spectral changes occurring upon heating a sample of  $\text{Cr}(\text{CO})_5(\text{ampy})$ , pressed in a KBr pellet, to 353K for thirty minutes

The spectral bands were assigned the  $A_1$ ,  $B_1$ ,  $A_1(2)$  and  $B_2$  modes of the  $C_{2v}$  *cis*- $Cr(CO)_4(ampy)$  species, respectively, by comparison with the work of Cotton and Kraihanzel<sup>10</sup>.

Thermogravimetric analysis determined the weight loss upon heating a pure sample of  $Cr(CO)_5(ampy)$ . In chapter 1 it was mentioned that previous workers<sup>17</sup> assumed that the formation of the chelate product occurred *via* an intramolecular extrusion of CO. Thus, a weight loss of 9.33% should have been observed for the loss of CO from this complex, based upon the assumption of other workers. However, the actual weight loss was observed to be 37% between the temperatures of 90-140°C. It appears that a simple thermal extrusion of CO plays no role here. However, calculations show that if this weight loss is attributed to the sublimation of  $Cr(CO)_6$  then for every two moles of  $Cr(CO)_5(ampy)$  present one mole of  $Cr(CO)_6$  is produced (equation 3.2.3.1)



equation 3.2.3.1

The formation of the chelate product,  $Cr(CO)_4(ampy)$ , has been observed to form upon heating of a KBr pellet of a sample of  $Cr(CO)_5(ampy)$ , but the regeneration of the parent carbonyl was not observed. To investigate the formation of both complexes the study was repeated in toluene solution and monitored using infrared spectroscopy.



**3.2.3.4 The reactions of  $\text{Cr}(\text{CO})_5(\text{ampy})$  in toluene solution, in the absence and presence of excess ligand, as monitored by infrared spectroscopy.**

The infrared spectral changes, observed upon dissolution of  $\text{Cr}(\text{CO})_5(\text{ampy})$  in a nitrogen purged toluene ( $5.397 \times 10^{-3} \text{ mol dm}^{-3}$ ) heated to 335K are presented in Figure 3.2.3.4.1

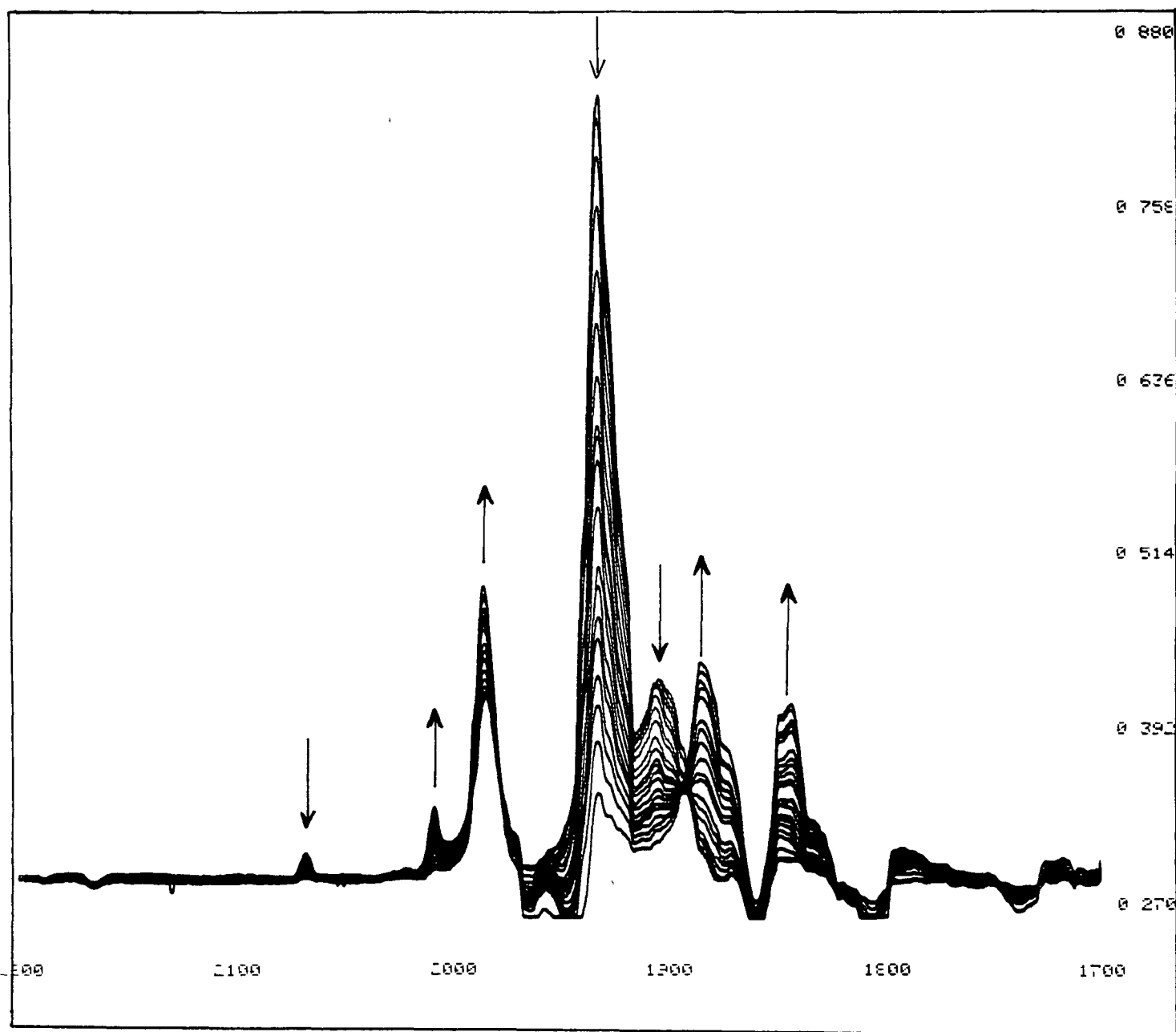


Figure 3.2.3.4.1 The infrared spectral changes occurring upon heating a solution of  $\text{Cr}(\text{CO})_5(\text{ampy})$  in toluene ( $5.397 \times 10^{-3} \text{ mol dm}^{-3}$ ) to 333K.

The bands at 2067, 1983, 1931 and 1903cm<sup>-1</sup>, which were assigned to the Cr(CO)<sub>5</sub>(ampy) complex, are seen to diminish with the concomitant growth of bands at 2006, 1983, 1866 and 1784cm<sup>-1</sup>. These bands were assigned to the A<sub>1</sub>, B<sub>1</sub>, A<sub>1</sub>(2) and B<sub>2</sub> modes previously.

The band at 1983cm<sup>-1</sup> was observed to decrease in intensity initially, but began to increase again after 4 minutes. This band is characteristic of the formation of Cr(CO)<sub>6</sub>. The maintenance of isosbestic points through the reaction is an indication of a reaction uncomplicated by side or subsequent reactions. It was possible, by knowing the molar extinction coefficients of Cr(CO)<sub>6</sub>, Cr(CO)<sub>5</sub>(ampy) and Cr(CO)<sub>4</sub>(ampy), to calculate the stoichiometry of the reaction from the changes in absorption. The data used in the determination of the various molar extinction coefficients is presented in Table 3.2.3.4.1.

Table 3.2.3.4.1 The experimental data for the determination of the molar extinction coefficients of Cr(CO)<sub>5</sub>(ampy) and Cr(CO)<sub>4</sub>(ampy)

Complex	Concentration (mol dm <sup>-3</sup> )	Absorbance (A. U.)	ε mol <sup>-1</sup> dm <sup>3</sup> cm <sup>-1</sup>
Cr(CO) <sub>5</sub> (ampy) 2067cm <sup>-1</sup>	5.397 x 10 <sup>-3</sup>	0.3675	6809
	3.998 x 10 <sup>-3</sup>	0.2712	6783
			ε = 6796
Cr(CO) <sub>4</sub> (ampy) 1877cm <sup>-1</sup>	10.01 x 10 <sup>-3</sup>	0.6372	6366
	5.745 x 10 <sup>-3</sup>	0.3798	6611
	5.236 x 10 <sup>-3</sup>	0.3582	6841
			ε = 6606
Cr(CO) <sub>6</sub>			14,505 <sup>12</sup>

The overall stoichiometry of the reaction may therefore be given by equation 3.2.3.4.1



equation 3.2.3.4.1

This stoichiometry was confirmed by repeating the procedure on a large scale. A solution of  $\text{Cr}(\text{CO})_5(\text{ampy})$  in toluene was brought to reflux temperature for thirty minutes and the chelate product was recovered and weighed (45% recovered). The result was in good agreement with equation 3.2.3.4.1

If the formation of the chelate product,  $\text{Cr}(\text{CO})_4(\text{ampy})$ , was preceded by an intramolecular extrusion of CO then the introduction of excess ligand into the reaction should have no effect on the yield of the reaction. The infrared spectrum, presented in Figure 3.2.3.4.2, is that of a sample of  $\text{Cr}(\text{CO})_5(\text{ampy})$  in toluene solution ( $2.07 \times 10^{-3} \text{ mol dm}^{-3}$ ) containing excess ligand ( $5.63 \times 10^{-3} \text{ mol dm}^{-3}$ ), which was scanned at 298K and left at 298K for 24 hours prior to subsequent scanning. The bands that were previously assigned to the formation of the  $\text{C}_{2v}$  *cis*- $\text{Cr}(\text{CO})_4(\text{ampy})$  species are not observed here. The regeneration of the parent carbonyl is also suppressed. The lack of spectral change is indicative of a mechanism of ring closure which does not involve a simple CO extrusion.

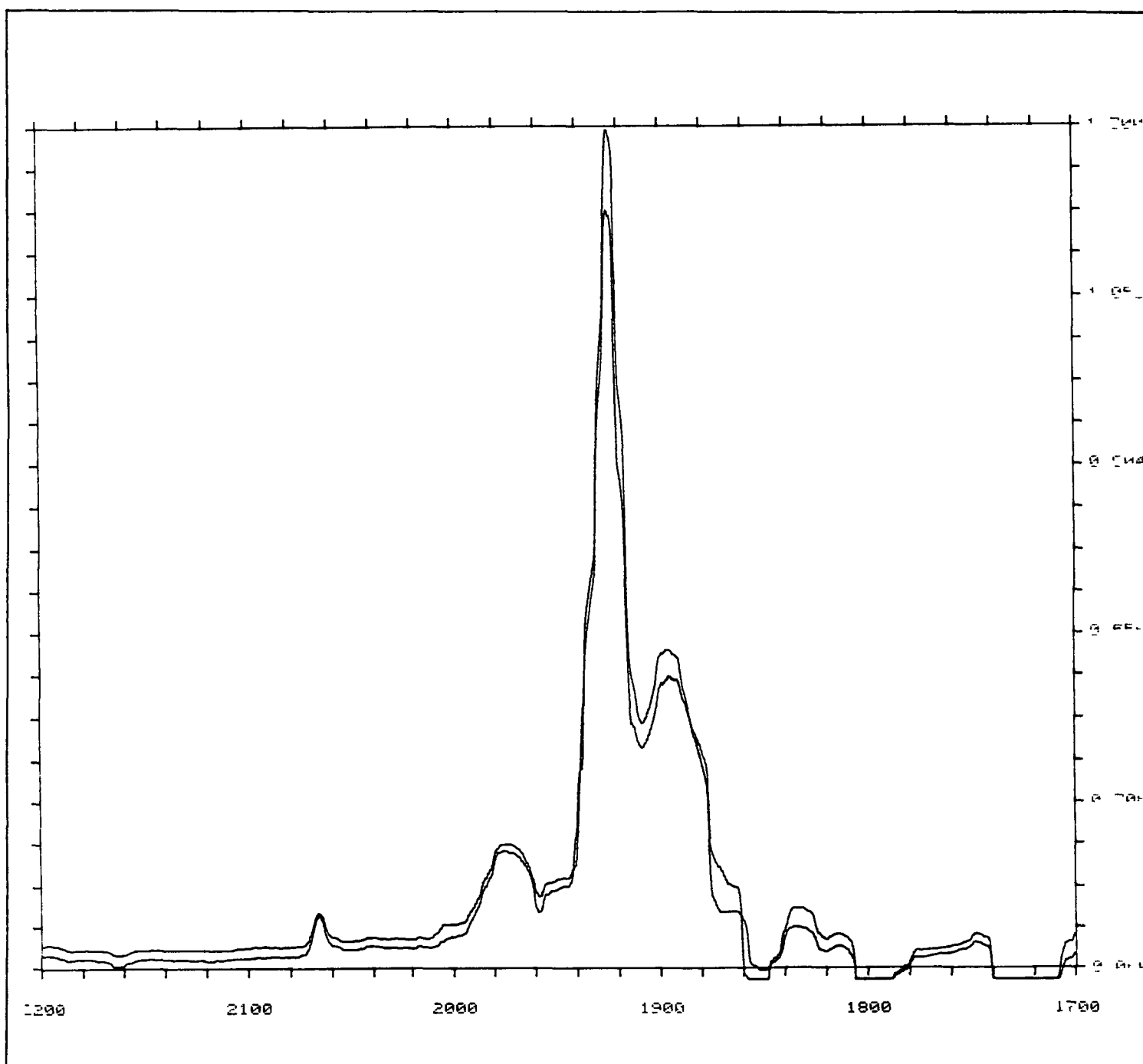


Figure 3.2 3 4 2 The infrared spectrum of a sample of  $\text{Cr}(\text{CO})_5(\text{ampy})$  in toluene solution ( $2.07 \times 10^{-3} \text{ mol dm}^{-3}$ ) containing excess ligand ( $5.63 \times 10^{-3} \text{ mol dm}^{-3}$ ), which was scanned at 298K and left for 24 hours at 298K prior to subsequent scanning.

### 3.2.3.5 The reactions of $\text{Cr}(\text{CO})_5(\text{ampy})$ in toluene solution, in the absence and presence of excess ligand, as monitored by UV-visible spectroscopy.

The spectral changes occurring upon standing a solution of  $\text{Cr}(\text{CO})_5(\text{ampy})$  in toluene ( $3.42 \times 10^{-4} \text{ mol dm}^{-3}$ ) at 298K are presented in Figure 3.2.3.5.1, as monitored by UV-visible spectroscopy. The maintenance of an isosbestic point at *ca* 444nm is an indication of a reaction uncomplicated by side or subsequent reactions. The LF band at 418nm is seen to decrease in intensity with a concomitant growth of a new band at 340nm. Upon comparison with other spectra this band may be assigned the LF band of  $\text{Cr}(\text{CO})_4(\text{ampy})$ . The MLCT band of a pure sample of  $\text{Cr}(\text{CO})_4(\text{ampy})$  occurs at 416nm which makes the determination of the stoichiometry of the reaction using this technique

The final spectrum, recorded after 840 minutes, is also shown in Figure 3.2.3.5.1(b). The plot of the variation of the absorbance with time for the formation of the  $\text{Cr}(\text{CO})_4(\text{ampy})$  complex, as monitored at 340nm, is presented in Figure 3.2.3.5.2 and a single exponential function is fitted to this curve. This complex differs from those analysed so far in that the MLCT band is slightly blue shifted from that of the  $\text{Cr}(\text{CO})_5(\text{ampy})$  species. However, the MLCT absorption is the lowest energy feature.

The rate constant for the formation of the  $\text{Cr}(\text{CO})_4(\text{ampy})$  species was determined to be  $6.349 \times 10^{-6} \text{ s}^{-1}$  from the growth of the LF band at 340nm. This is quite low when compared to the rate constant obtained for the  $(\text{Cr}(\text{CO})_5)_2(\text{dphbpy})$  species ( $2.5 \times 10^{-4} \text{ s}^{-1}$  at 299K). The monitoring, by UV-visible spectroscopy of the chelation reaction of  $\text{M}(\text{CO})_5(\text{en})^{31}$  to form  $\text{M}(\text{CO})_4(\text{en})$  and CO ( $\text{M} = \text{Cr}, \text{Mo}, \text{or W}$ ) determined the  $k_{\text{obs}}$  for the formation of the  $\text{Cr}(\text{CO})_4(\text{en})$  complex to be  $3 \times 10^{-4} \text{ s}^{-1}$ , in chloroform solution at 323K.

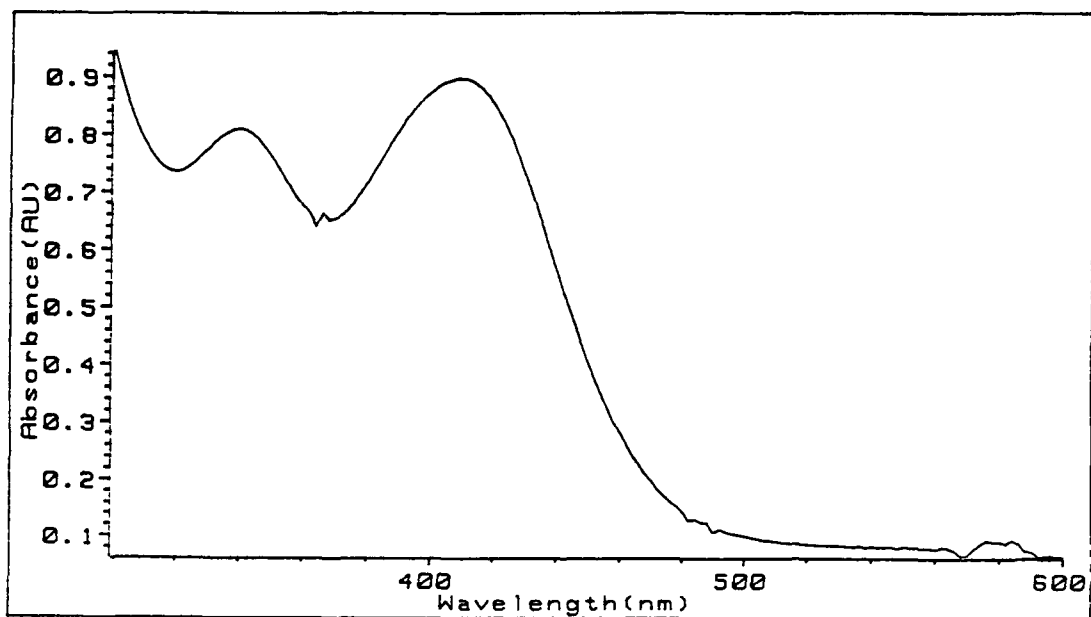
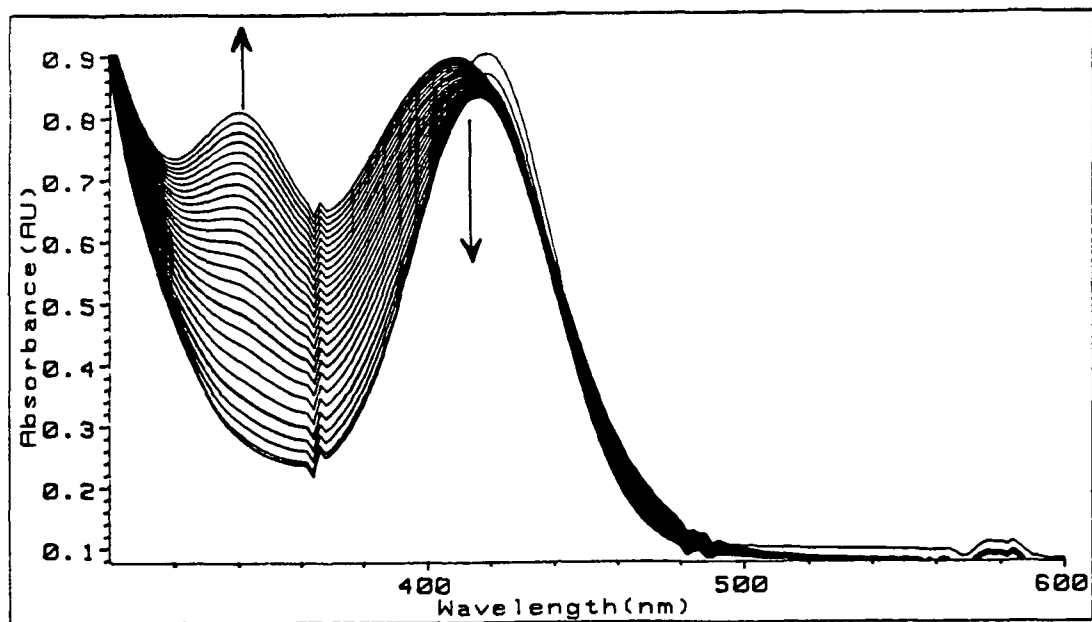


Figure 3 2.3.5.1 (a) The UV-visible spectral changes occurring upon standing a solution of  $\text{Cr}(\text{CO})_5(\text{ampy})$  in toluene ( $3.42 \times 10^{-4} \text{ mol dm}^{-3}$ ) at 298K and (b) the final spectrum recorded after 840 minutes.

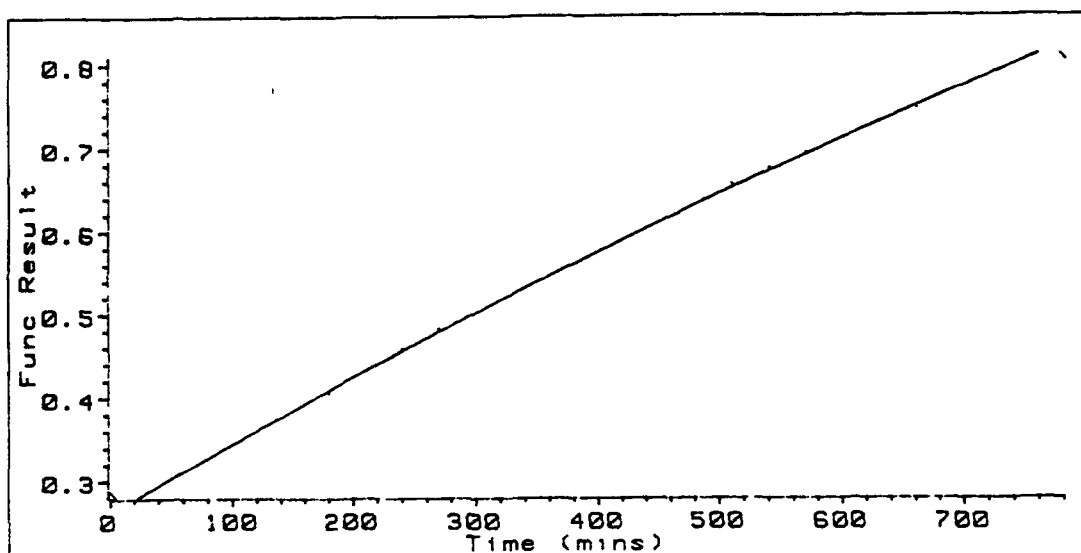


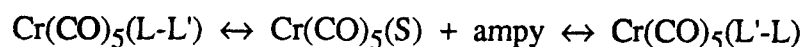
Figure 3 2.3.5 2 A plot of the variation of the absorbance with time for the formation of the  $\text{Cr(CO)}_4(\text{ampy})$  complex, as monitored at 340nm

The rate of formation of the  $\text{Cr(CO)}_4(\text{ampy})$  was determined to be  $3.616 \times 10^{-5} \text{ s}^{-1}$  at 323K which is slower than that determined for the formation of the  $\text{Cr(CO)}_4(\text{en})$  complex. A number of  $\text{M(CO)}_5(\text{L})$  complexes (L= phosphorus or arsenic ligand) have been observed to undergo a slow chelation reaction. The complex,  $\text{Cr(CO)}_5(\text{dpe})^{18}$ , ( $\text{dpe} = \text{Ph}_2\text{PCH}_2\text{CH}_2\text{PPh}_2$ ) undergoes ring closure with  $k_{\text{obs}} = 2.7 \times 10^{-6} \text{ s}^{-1}$  at 356K. The chelation of these complexes has been concluded to proceed *via* a largely dissociative mechanism. The rapid rates recorded for the chelation of the  $\text{M(CO)}_5(\text{dumme})$  complexes have been attributed to the substantial contribution of the associating ligand to the CO extrusion process<sup>22</sup>

The introduction of varying concentrations of excess ligand into the reaction was different to that observed with the  $\text{M(CO)}_5(\text{bpa})$  complexes. Using infrared spectroscopy, there were no spectral changes observed when excess ligand

was introduced. However, the introduction of excess ligand into the reaction while monitoring by UV-visible spectroscopy recorded the growth of a band at 340nm, concomitant with the formation of the chelate product,  $\text{Cr(CO)}_4(\text{ampy})$ . The intensity of this band relative to its growth in the absence of excess ligand appeared to have diminished. Initially, it was thought that the introduction of excess ligand into the reaction, monitored by UV-visible spectroscopy, resulted in the formation of some  $\text{Cr(CO)}_4(\text{ampy})$  but it was discovered that there was no formation of this complex. It should be noted that the concentrations of excess ligand employed in the UV-visible spectral studies were much greater than that used in the infrared studies where no formation of the  $\text{Cr(CO)}_4(\text{ampy})$  species was observed.

An initial increase of the excess ligand concentration resulted in an initial increase of the  $k_{\text{obs}}$ , measured at 340nm, with a concomitant depletion of the intensity of the growth of the band at 418nm. However, after a certain concentration of excess ligand the  $k_{\text{obs}}$  decreased to zero concomitant with no growth of the band at 340nm. The reaction of a sample of  $\text{Cr(CO)}_5(\text{ampy})$  dissolved in toluene solution ( $4.26 \times 10^{-4} \text{ mol dm}^{-3}$ ) with an excess of ligand ( $0.1239 \text{ mol dm}^{-3}$ ) is presented in Figure 3.2.3.5.2, as monitored by UV-visible spectroscopy, at 298K. The results of this study are tabulated in Table 3.2.3.5.1 and the plot of these values is presented in Figure 3.2.3.5.3. This had not been observed with any of the other complexes used in this study and proved quite puzzling. It may be possible that we are not observing the growth of the  $\text{Cr(CO)}_4(\text{ampy})$  species but an equilibrium of another type. It may be possible that we are observing an equilibrium of coordination of the metal between the two available nitrogens sites. This is represented in equation 3.2.3.5.1



equation 3.2.3.5.1



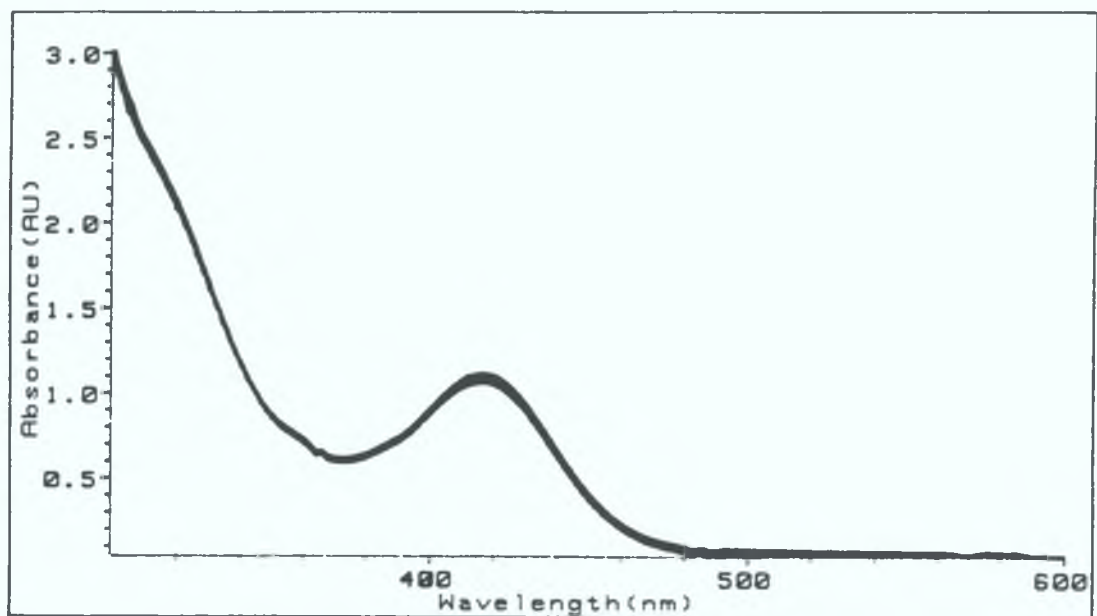


Figure 3.2.3.5.2: The reaction of a sample of  $\text{Cr(CO)}_5(\text{ampy})$  dissolved in toluene solution ( $4.26 \times 10^{-4} \text{ mol dm}^{-3}$ ) with an excess of ligand ( $0.1239 \text{ mol dm}^{-3}$ ), as monitored by UV-visible spectroscopy, at 298K.

Table 3.2.3.5.1: The variation of the  $k_{\text{obs}}$  for the formation of  $\text{Cr(CO)}_4(\text{ampy})$  at 340nm with varying concentrations of excess ligand.

Concentration of ampy ( $\text{mol dm}^{-3}$ )	$k_{\text{obs}}$ ( $\text{s}^{-1}$ )
0	$7.888 \times 10^{-6}$
$3.68 \times 10^{-2}$	$33.59 \times 10^{-6}$
$7.943 \times 10^{-2}$	$183.0 \times 10^{-6}$
$9.78 \times 10^{-2}$	0
$12.39 \times 10^{-2}$	0

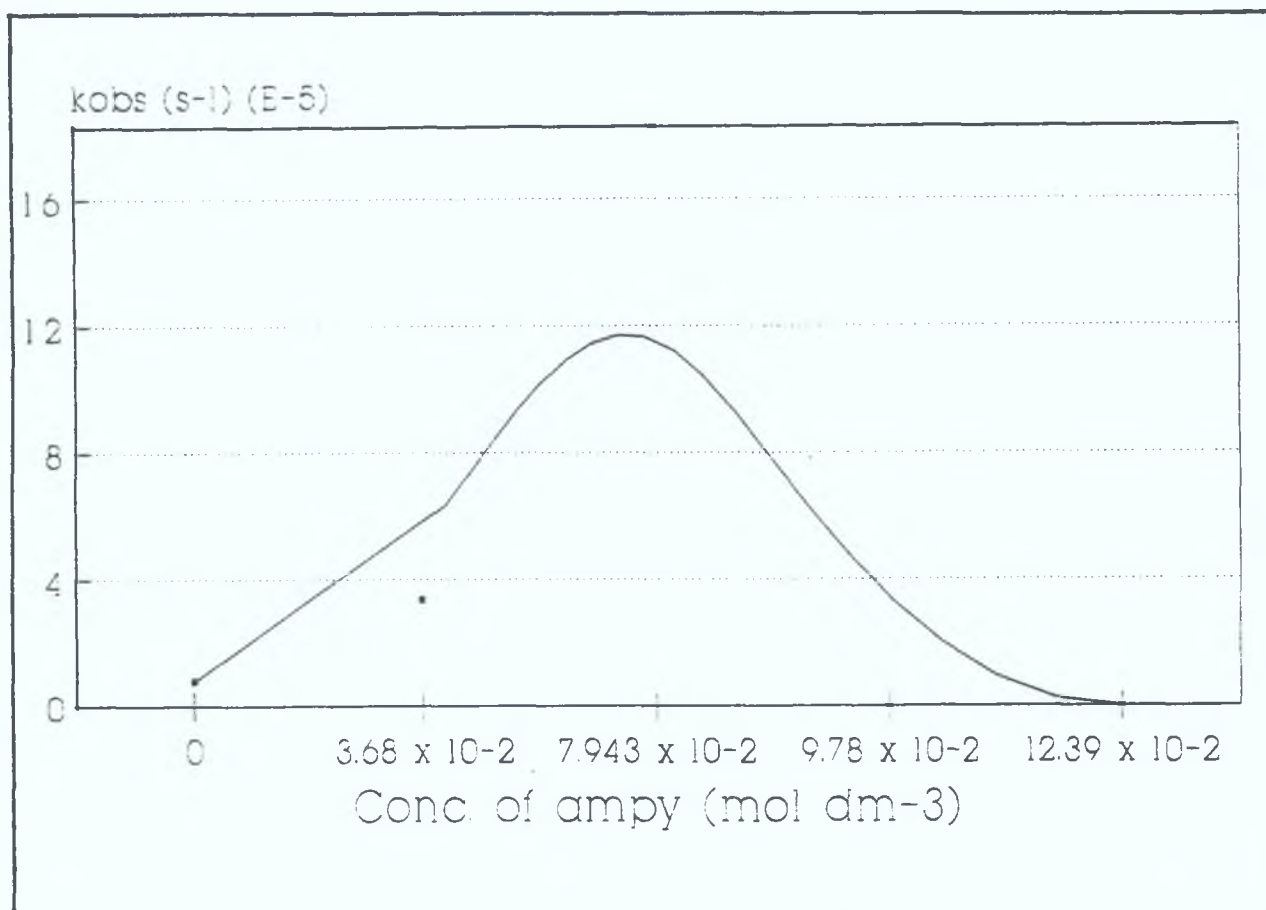


Figure 3.2.3.5.3: The variation of the  $k_{\text{obs}}$  for the formation of  $\text{Cr}(\text{CO})_4(\text{ampy})$  with varying concentrations of excess ligand.

The product precipitated from a toluene/pentane mixture exhibited a split in all the bands in the  $\nu_{\text{CO}}$  region of the infrared spectrum. This split was attributed to the formation of two products, a thermodynamic and kinetic product. At room temperature, in solution form, there was a rearrangement of the complex to form the stable thermodynamic product. It may be possible that there is a rapid exchange of coordination at low temperatures which manifests itself at ambient temperature in the presence of excess ligand. The initial increase of the band at 340nm in the presence of excess ligand may be resultant from the rapid exchange of coordination which occurs too quickly for the instrument to detect. There were a number of attempts made in an effort to substantiate this proposal, as discussed in the following section.

**3.2.3.6 The attempts at observing the proposed equilibrium process of the  $\text{Cr}(\text{CO})_5(\text{ampy})$  complex in the presence of excess ligand, as monitored by  $^1\text{H}$  n.m.r. spectroscopy.**

The  $^1\text{H}$  n.m.r spectrum of a sample of  $\text{Cr}(\text{CO})_5(\text{ampy})$  in  $\text{CDCl}_3$  containing a equimolar amount of ampy ligand, at 298K, exhibited bands at 8.55(s), 7.65(s), 7.24(d), 5.1(s), 3.89(d), 2.66(s), 2.02(d), 1.66(s), 1.23(s), and 0.86(s) ppm. It was anticipated that the addition of excess ligand would result in the appearance of separate bands for the free ligand. However, the spectrum of the complex in  $\text{CDCl}_3$  solution containing an equimolar amount of ampy does not appear to differ much from the spectrum of the complex itself.

It was anticipated that lowering of the temperature might slow the rate of exchange of the metal between the two available and result in a separation of the bands of the two complexes. The temperature was reduced in increments of 10K to 243K and a spectrum obtained at each temperature, but there was no change observed in the spectrum of the complex at 243K. Another sample of the complex containing an equimolar amount of ampy was scanned and left for twenty four hours at 293K prior to subsequent scanning. The resultant spectrum also showed no observable change from that of the  $\text{Cr}(\text{CO})_5(\text{ampy})$  complex.

The only option left was a titration of the complex with known amounts of excess ligand and monitoring this reaction by  $^1\text{H}$  n.m.r spectroscopy. Employing the formula

$$\frac{\delta_{\text{xs}} - \delta_{\text{l}}}{\delta_{\text{c}} - \delta_{\text{l}}}$$

where  $\delta_{\text{xs}}$  = the resonance of the  $\alpha\text{H}$  of the spectrum of the complex containing an equimolar amount of excess ligand;

$\delta_l$  = the resonance of the  $\alpha$ H of the spectrum of the free ligand,  
and  $\delta_c$  = the resonance of the  $\alpha$ H of the spectrum of the  $\text{Cr}(\text{CO})_5(\text{ampy})$  complex

By introducing various concentrations of excess ligand into the solution of the  $\text{Cr}(\text{CO})_5(\text{ampy})$  complex in  $\text{CDCl}_3$  ( $4.33 \times 10^{-2} \text{ mol dm}^{-3}$ ), it was hoped that by employing the formula, given above, and plotting the data, the resultant plot would exhibit a plateau, indicative of the presence of an equilibrium process between the available sites for coordination of the metal. The first spectrum of the complex contained no excess ligand and the resonance of the  $\alpha$ H was obtained. By introducing excess ligand it was hoped that there would be a change in the resonance of the  $\alpha$ H, resulting from the rapid exchange of coordination. It was anticipated that if the equilibrium process was to be observed using this method, then a plateau effect would be observed.

Table 3.2.3.6.1. The effect of varying the concentrations of excess ligand on the resonance of the  $\alpha$ H

Conc. of excess ligand ( $\text{mol dm}^{-3}$ )	$\frac{\delta_{xs} - \delta_l}{\delta_c - \delta_l}$ (ppm)
0	1
$6.39 \times 10^{-3}$	0.983
$4.483 \times 10^{-2}$	0.922
$8.317 \times 10^{-2}$	0.88
$10.23 \times 10^{-2}$	0.859
$12.79 \times 10^{-2}$	0.833
$22.375 \times 10^{-2}$	0.786
$28.765 \times 10^{-2}$	0.715

The attempts at observing the guest-host interaction were unsuccessful as the curve, presented in Figure 3.2.3.6.1, obtained for the data in Table 3.2.3.6.1, did not indicate the presence of an equilibrium process. It is proposed that the metal is rapidly exchanging coordination between the sites available on the coordinated ligand, and also with the free ligand in solution, and this process is occurring too rapidly to be detected.

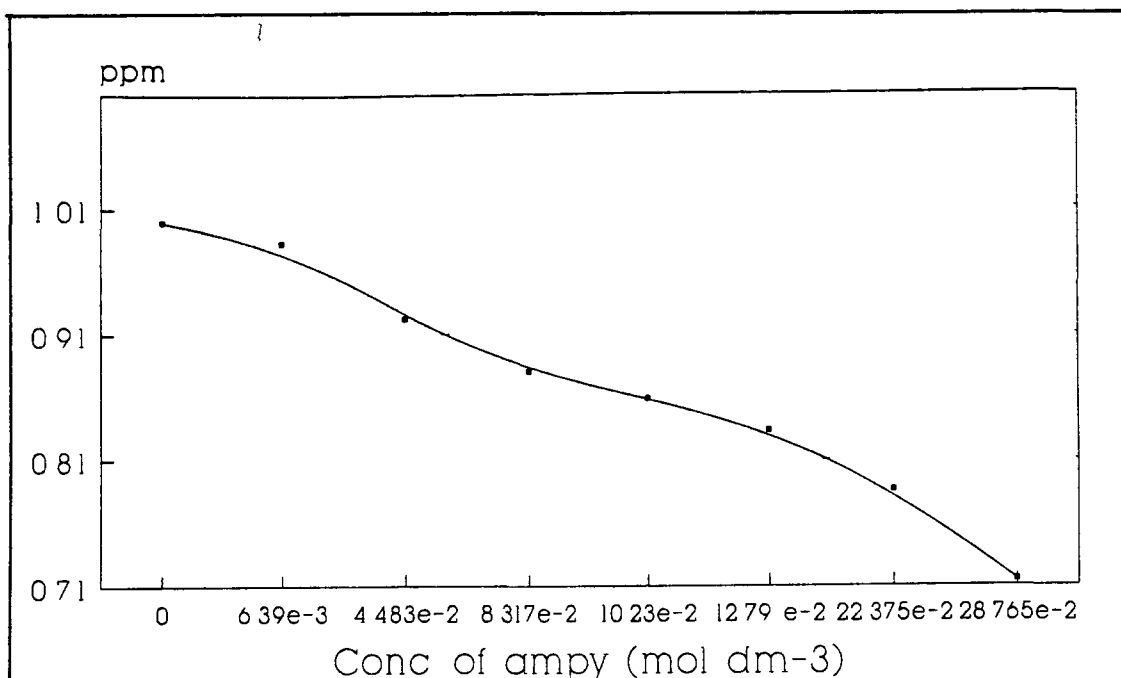


Figure 3.2.3.6.1 The effect of varying the concentration of excess ligand on the resonance of the  $\alpha\text{H}$

### 3.2.3.7 The reaction of $\text{Cr}(\text{CO})_5(\text{ampy})$ in CO saturated toluene, as monitored by UV-visible spectroscopy.

The spectral changes occurring upon standing a sample of  $\text{Cr}(\text{CO})_5(\text{ampy})$ , dissolved in CO saturated toluene ( $4.725 \times 10^{-4} \text{ mol dm}^{-3}$ ), at 298K for 840 minutes are presented in Figure 3.2.3.7.1, as monitored by UV-visible spectroscopy. There is a slight grow-in at 340nm but no depletion of the band at 418nm, corresponding to the  $\text{Cr}(\text{CO})_5(\text{ampy})$  complex. The saturation of the solution

with CO appears to have no effect on this reaction as opposed to the analogous reaction of  $(\text{Cr}(\text{CO})_5)_2(\text{dphbpy})$  complex

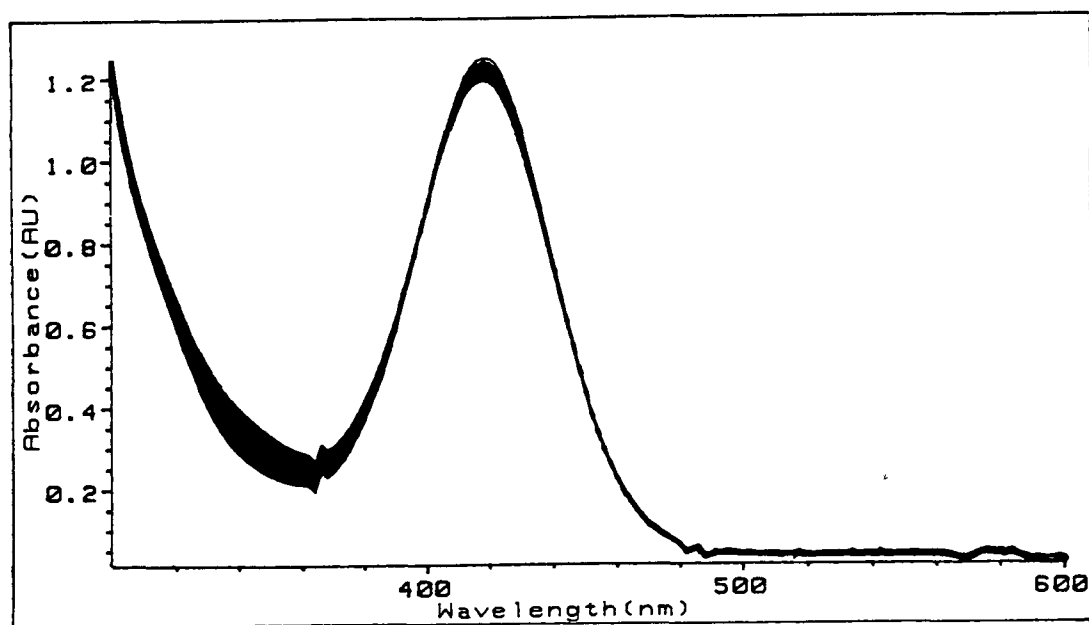


Figure 3.2 3 7 1 The UV-visible spectral changes occurring upon standing a sample of  $\text{Cr}(\text{CO})_5(\text{ampy})$ , dissolved in CO saturated toluene ( $4.725 \times 10^{-4} \text{ mol dm}^{-3}$ ) at 298K for 870 minutes

The UV-visible spectral changes observed upon standing a solution of  $(\text{Cr}(\text{CO})_5)_2(\text{dmbpy})$ <sup>12</sup> observed a depletion of the bands associated with this complex with no growth of new bands. This phenomenon was attributed to the regeneration of the parent hexacarbonyl resultant from the lability of the complex with respect to loss of the ligand. From this reaction it appears that the  $\text{Cr}(\text{CO})_5(\text{ampy})$  complex is not labile to loss of the ligand.

**3.2.3.8 The determination of the activation parameters for the formation of  $\text{Cr(CO)}_4(\text{ampy})$  in the absence of excess ligand.**

The data for the determination of the activation parameters for the formation of  $\text{Cr(CO)}_4(\text{ampy})$  in the absence of any excess ligand is presented in Table 3.2.3.8 1 The plots of these values are presented in Figure 3.2 3 8 1 It was not possible to determine the activation parameters for the formation of  $\text{Cr(CO)}_4(\text{ampy})$  in the presence of excess ligand.

Table 3.2 3.8 1 The data used in the determination of the activation parameters for the formation of the  $\text{Cr(CO)}_4(\text{ampy})$  complex in the absence of any excess ligand.

Temperature (K)	$\text{Ln}(k_{\text{obs}})$	$\text{Ln}(k_{\text{obs}}/T)$
298	-13 86	-19 56
305	-11 77	-17 49
313	-11 17	-16 92
323	-10 22	-16 00
333	-9 22	-15 03

Arrhenius Plot		Eyring Plot	
Slope	$-12100 \pm 1800$	Slope	$-11800 \pm 1800$
Int	$27 \pm 0.5$	Int	$21 \pm 0.5$
Corr	0.97	Corr	0.97

$$\begin{aligned} E_a &= 100 \pm 15 \text{ kJ mol}^{-1} \\ \Delta H^\ddagger &= 98 \pm 15 \text{ kJ mol}^{-1} \\ \Delta S^\ddagger &= -27 \pm 5 \text{ J K}^{-1} \text{ mol}^{-1} \end{aligned}$$

The activation energy for the formation of the  $\text{Cr(CO)}_4(\text{ampy})$  complex is similar to that obtained for the formation of the  $\text{Cr(CO)}_4(\text{bpy})^{13}$  species from  $(\text{Cr(CO)}_5)_2(\text{bpy})$ , in the absence of excess ligand. The activation enthalpy does not appear to involve the breaking of a  $\text{Cr-CO}^{25}$  bond ( $168 \text{ kJ mol}^{-1}$ ) in the transition state and the negative entropy of activation value indicates an associative pathway for the process. The rate determining step for the formation of  $\text{Cr(CO)}_4(\text{bpy})^{13}$  was assumed to contain a significant contribution from the breaking of a  $\text{Cr-N}$  bond. The activation enthalpy for the breaking of a  $\text{Cr-N}^{20}$  bond in  $\text{Cr(CO)}_5(\text{py})$  is  $106 \text{ kJ mol}^{-1}$  and the value obtained in this study is similar. The activation enthalpy for the breaking of a  $\text{Cr-N}$  bond in  $\text{Cr(CO)}_5(3\text{-picoline})^{32}$  is  $112.5 \text{ kJ mol}^{-1}$ . As stated previously, the difference in activation enthalpies may be attributed to the different  $\text{pK}_a$  values of the free ligands. The ampy ligand is a weaker base than pyridine and this is reflected in the strength of the  $\text{Cr-N}$  bond with a subsequent decrease in the activation enthalpy. Thus, the rate determining step is taken to be the breaking of the  $\text{Cr-N}$  bond. The negative entropy value is an indication of the associative nature of the transition state.

The determination of the activation parameters for the formation of  $\text{Cr(CO)}_4(\text{L})$  ( $\text{L} = \text{pyridine-2-carbaldehyde}$ )<sup>22</sup> yielded an activation enthalpy value of  $86.5 \text{ kJ mol}^{-1}$  and an activation entropy value of  $-31.7 \text{ J K}^{-1} \text{ mol}^{-1}$ . These results are also similar to those presented above but were executed in the presence of excess ligand. The mechanism of ring closure was attributed to the associative nature of the ligand when coordinated in a monodentate fashion and the substantial contribution of the associating ligand to CO extrusion. In the case of the  $\text{Cr(CO)}_5(\text{ampy})$  complex it seems unlikely that the mechanism of ring closure occurs *via* an intramolecular CO extrusion process. The regeneration of the parent hexacarbonyl precludes the assumption of a simple thermal extrusion of CO to form the chelate product  $\text{Cr(CO)}_4(\text{ampy})$ .



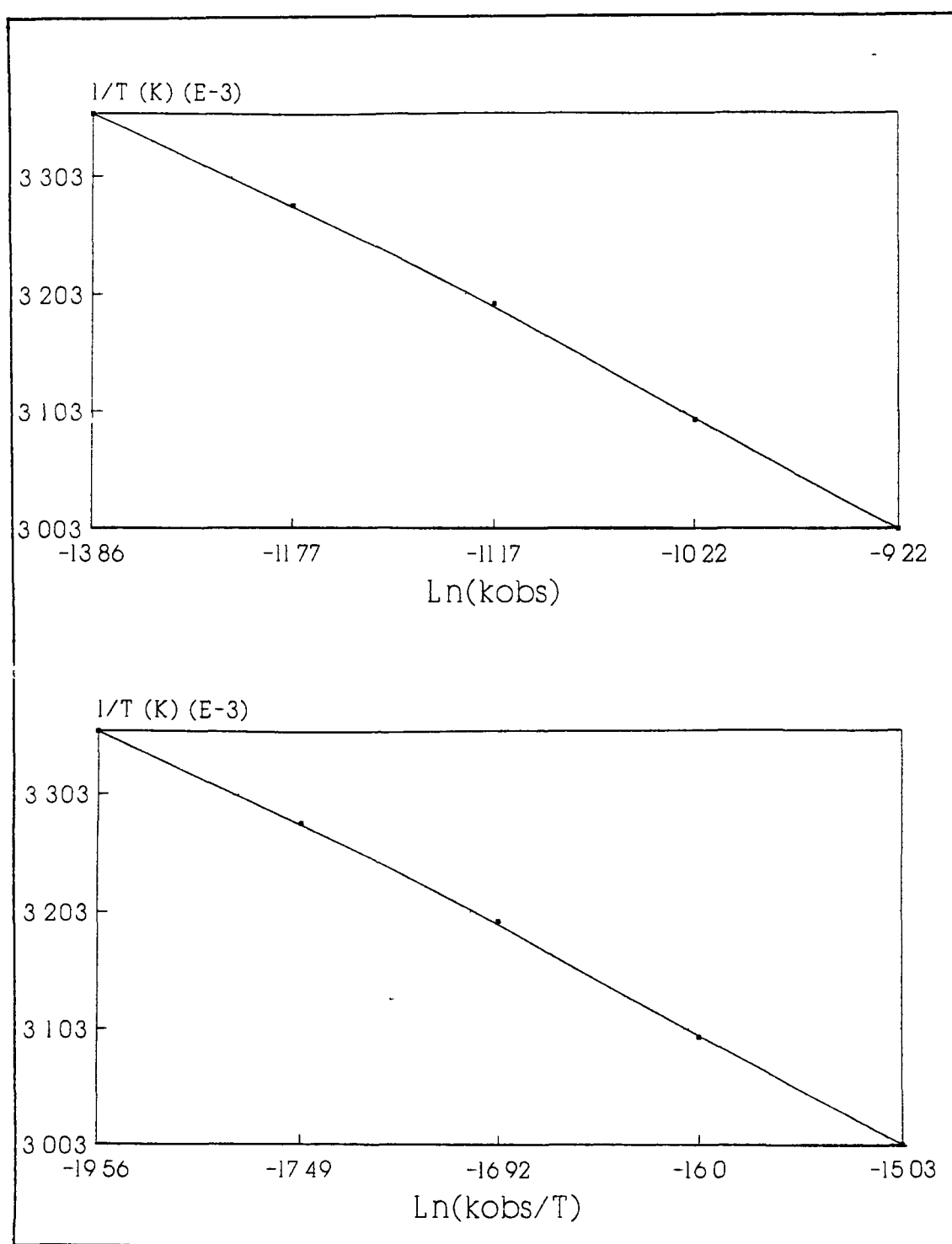
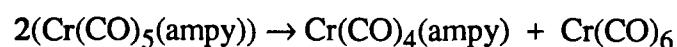


Figure 3.2 3 8.1 (a) The Arrhenius and (b) Eyring plots for the determination of the activation parameters for the formation of  $\text{Cr}(\text{CO})_4(\text{ampy})$  in the absence of excess ligand

### 3.2.3.9 Summary

The isolation of the  $\text{Cr}(\text{CO})_5(\text{ampy})$  complex was confirmed by elemental analysis and it was characterised by infrared and UV-visible spectroscopy. The isolation of this complex with the ligand coordinated in a monodentate fashion was predicted from Chapter 2. The infrared spectrum of the complex exhibited four bands in the  $\nu\text{CO}$  region, characteristic of a complex possessing pseudo  $\text{C}_{4v}$  symmetry, while the UV-visible spectrum exhibited a low energy band at 418nm which was assigned the  $^1\text{A} \rightarrow ^1\text{E}$  LF transition with the MLCT band overlapping. A unique infrared spectrum of the complex showed a doubling of the modes associated with the pseudo  $\text{C}_{4v}$  complex. This observation was attributed to the isolation of the two coordination isomers. The complex underwent rearrangement in solution at ambient temperature to form the stable thermodynamic product.

From the results presented a reaction mechanism is proposed in Scheme 3.2.3.8.1. The complex reacts to form the  $\text{Cr}(\text{CO})_6$  and  $\text{Cr}(\text{CO})_4(\text{ampy})$  complexes in a ratio presented in equation 3.2.3.8.1 (step a)

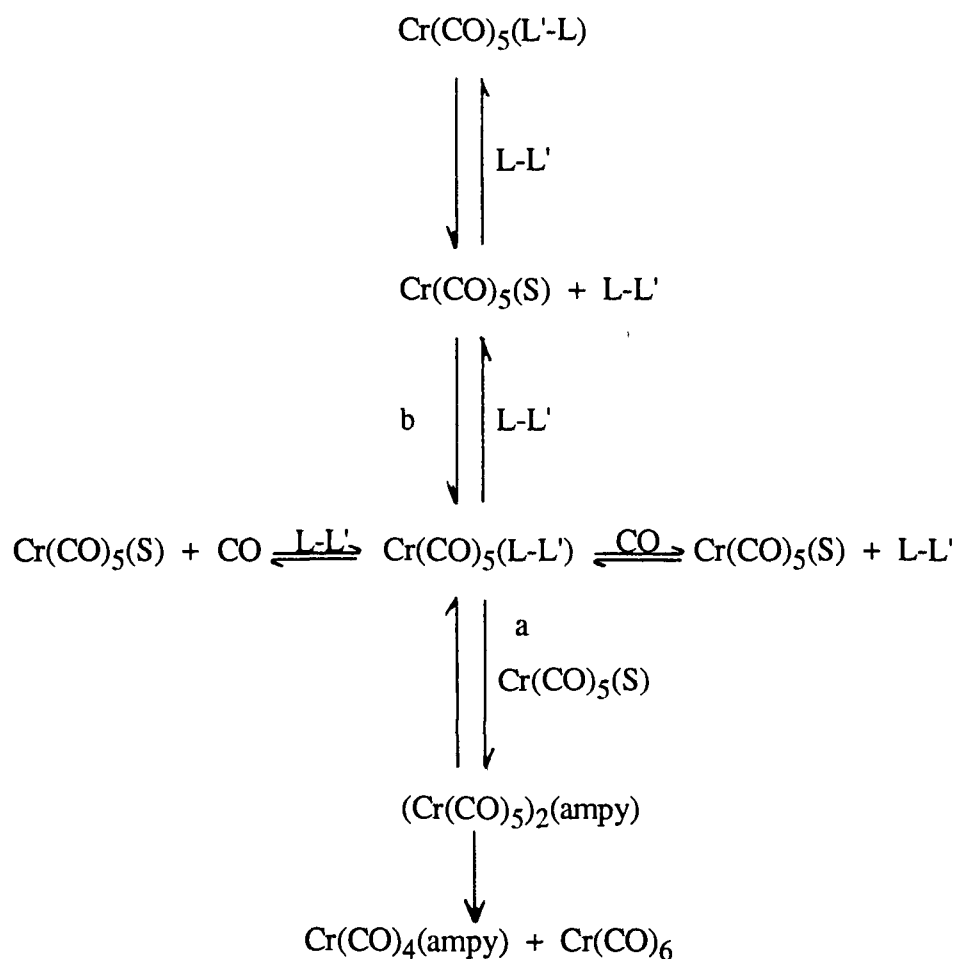


equation 3.2.3.8.1

The introduction of excess ligand results in the suppression of the formation of the  $\text{Cr}(\text{CO})_4(\text{ampy})$  and  $\text{Cr}(\text{CO})_6$  complexes as monitored by infrared spectroscopy. Monitoring this reaction by UV-visible spectroscopy resulted in the slight growth of a band at 340nm, initially thought to correspond to the formation of the  $\text{Cr}(\text{CO})_4(\text{ampy})$  complex. However, the growth of this band was attributed to an equilibrium process between coordination of the two nitrogens as the minimum concentration of excess

ligand employed was greater than that used in the infrared spectral studies (step b)  
 Attempts to elucidate this phenomenon were unsuccessful

Scheme 3.2 3.8.1 The proposed reaction mechanism for the  $\text{Cr}(\text{CO})_5(\text{ampy})$  complex



Upon standing a sample of  $\text{Cr}(\text{CO})_5(\text{ampy})$  in CO saturated toluene there was a slight growth of the band at 340nm, corresponding to the formation of the  $\text{Cr}(\text{CO})_4(\text{ampy})$  species but this growth was retarded significantly when compared to the reaction of the complex in the absence of any excess ligand or CO. Upon comparison with previous work it was concluded that the complex was not labile to loss of the ligand.

The activation parameters for the formation of the  $\text{Cr(CO)}_4(\text{ampy})$  complex, in the absence of any excess ligand, were determined. The rate determining step is proposed to involve the breaking of a Cr-N bond, despite the negative entropy of activation value

2

### 3.2.4 The synthesis and characterisation of $M(\text{CO})_5(\text{bipyam})$ complexes ( $M = \text{Cr}$ or $\text{W}$ ; $\text{bipyam} = 2,2'$ -dipyridylamine) and their reactions in the solid state and solution.

#### 3.2.4.1 The preparation of the $M(\text{CO})_5(\text{bipyam})$ complexes

The reaction of 2,2'-dipyridylamine ( $\text{bipyam}$ ) with  $\text{Cr}(\text{CO})_5(\text{cis-cyclo-octene})$  and photogenerated  $\text{W}(\text{CO})_5(\text{THF})$  yielded  $\text{Cr}(\text{CO})_5(\text{bipyam})$  and  $\text{W}(\text{CO})_5(\text{bipyam})$ , respectively. The formation of these complexes was confirmed by elemental analysis. Consideration of the structure of the  $\text{bipyam}$  ligand (Figure 3.2.4.1) indicated that the isolation of these complexes was possible and their monodentate coordination was not surprising.

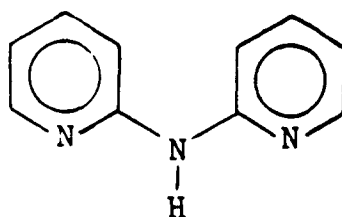


Figure 3.2.4.1: 2,2'-dipyridylamine

The  $\text{Cr}(\text{CO})_5(\text{bipyam})$  complex was not stable in solution and rapidly formed the chelate complex,  $\text{Cr}(\text{CO})_4(\text{bipyam})$ , in solution at room temperature. The  $\text{W}(\text{CO})_5(\text{bipyam})$  complex exhibited no tendency to form the chelate complex,  $\text{W}(\text{CO})_4(\text{bipyam})$ , at room temperature, either in solution or solid state. Studies on the reactions of these complexes were executed in solution and solid form, studies were performed in the solid state because of the insolubility of the  $M(\text{CO})_4(\text{bipyam})$  products in the organic solvents.<sup>33</sup> The molecular structure<sup>34</sup> of  $\text{W}(\text{CO})_5(\text{bipyam})$ , discussed in Chapter 4, was also determined.

### 3.2.4.2 The characterisation of the $M(CO)_5(bipyam)$ complexes by infrared and UV-visible spectroscopy.

The infrared spectral features of  $Cr(CO)_5(bipyam)$  and  $W(CO)_5(bipyam)$  are similar; the CO stretching frequencies differ only by a few wavenumbers. The infrared spectrum of a sample of  $W(CO)_5(bipyam)$ , pressed in a KBr pellet, is presented in Figure 3.2.4.2.1. A comparison of the  $\nu_{CO}$  stretching frequencies for both complexes, in solid (KBr) and solution (toluene) form, is presented in Table 3.2.4.2.1.

Table 3.2.4.2.1 A comparison of the infrared stretching vibrations for the  $Cr(CO)_5(bipyam)$  and  $W(CO)_5(bipyam)$  complexes in solid (KBr) and in toluene solution

$Cr(CO)_5(bipyam)$ $\nu_{CO}$ (KBr)	$W(CO)_5(bipyam)$ $\nu_{CO}$ (KBr)	$Cr(CO)_5(bipyam)$ $\nu_{CO}$ (toluene)	$W(CO)_5(bipyam)$ $\nu_{CO}$ (toluene)
2067	2072	2069	2071
1983	1974	1983	1976
1910	1931	1939	1925
1892	1914	1910	1915

The bands of each complex represent the  $A_1$ ,  $B_1$ , E and  $A_1(2)$  modes (going down the table) of a species possessing pseudo  $C_{4v}$  symmetry<sup>10</sup>. The presence of the  $B_1$  mode, which is normally forbidden, is an indication of a reduction of the symmetry of the complex. This may be attributed to the asymmetry of the dipyam ligand, which distorts the complex from perfect  $C_{4v}$  symmetry. The infrared spectrum of  $Cr(CO)_5(bipyam)$  in

toluene solution ( $2.69 \times 10^{-2} \text{ mol dm}^{-3}$ ), presented in Figure 3.2.4.2.2, provides a clearer view of the bands described

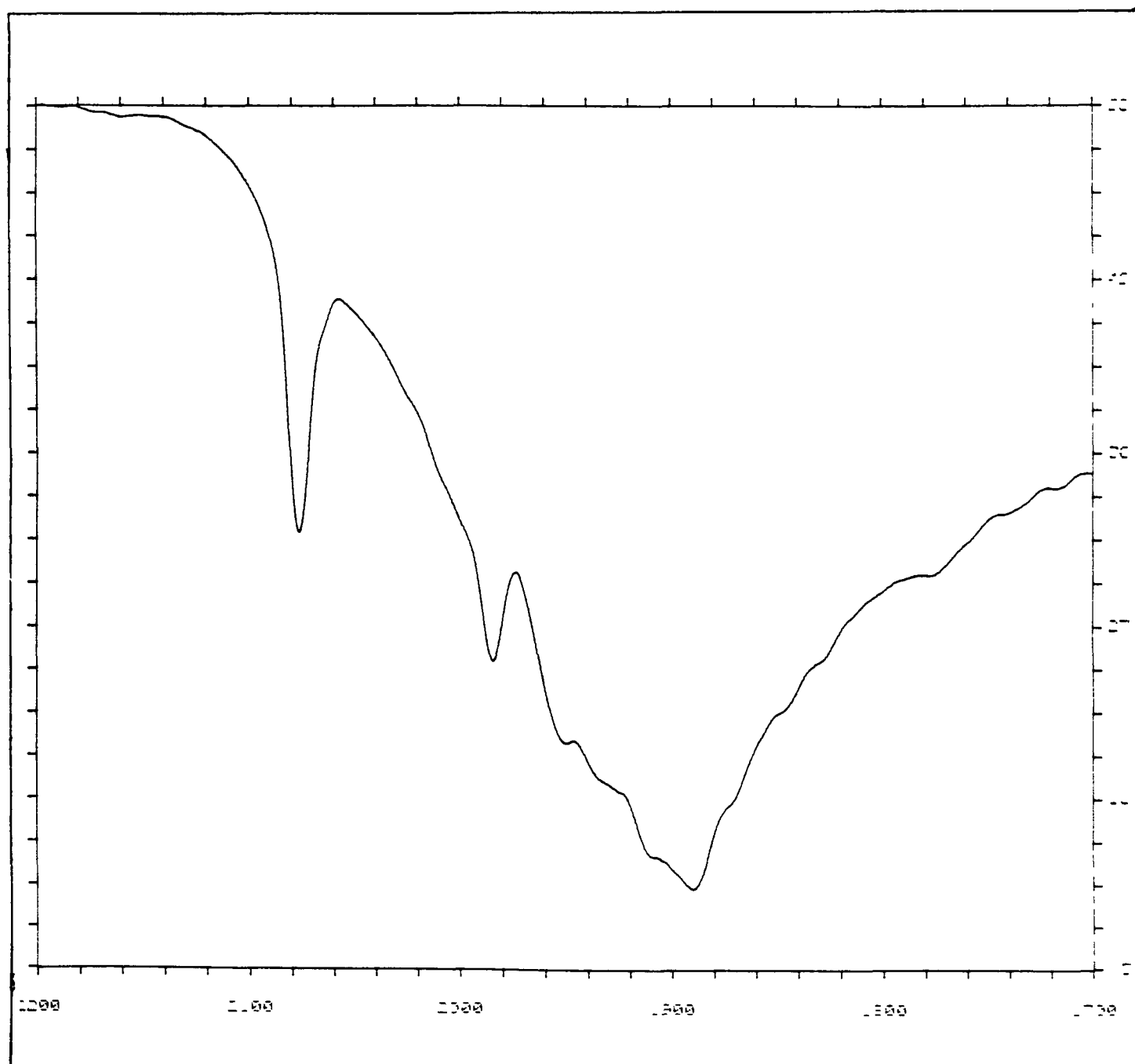


Figure 3.2.4.2.1. The infrared spectrum of a sample of  $\text{W}(\text{CO})_5(\text{bipyam})$ , pressed in a KBr pellet, at 298K

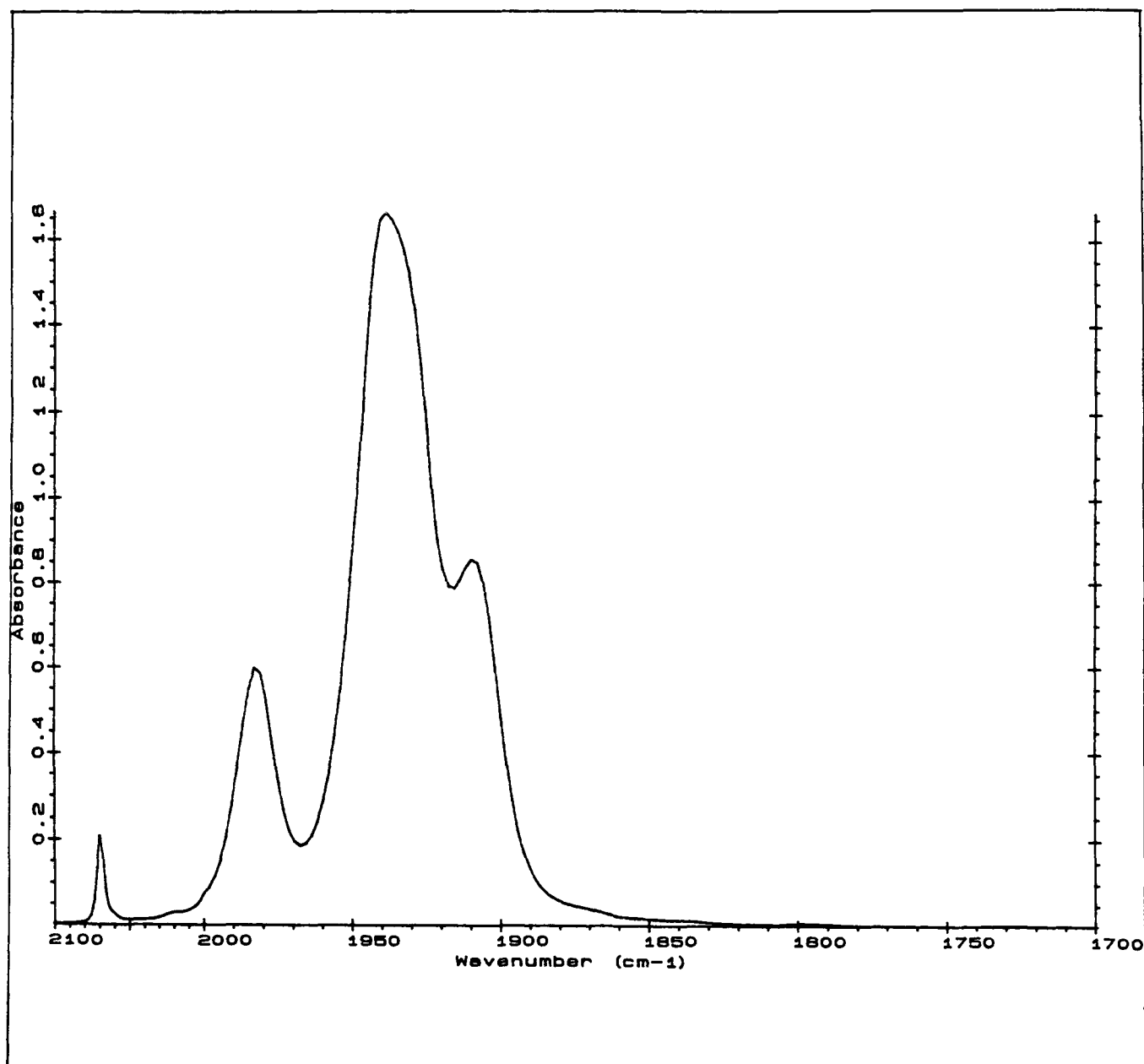


Figure 3.2 4.2 2: The infrared spectrum of a sample of  $\text{Cr}(\text{CO})_5(\text{bipyam})$  ( $2.69 \times 10^{-2} \text{ mol dm}^{-3}$ ) dissolved in toluene solution, at 298K.



However, the  $B_1$  mode is masked by the  $T_{1u}$  mode of the parent carbonyl. The  $B_1$  mode for the  $W(CO)_5(bipyam)$  complex is also masked in toluene solution by the  $T_{1u}$  band of the parent carbonyl which occurs at *ca*  $1977\text{cm}^{-1}$ .

The UV-visible spectrum of a sample of  $W(CO)_5(bipyam)$  in toluene solution ( $7.84 \times 10^{-5}\text{mol dm}^{-3}$ ), at 295K, is presented in Figure 3.2.4.2.3. This complex exhibits an absorption maxima band centred at 382nm which may be assigned the  $^1A \rightarrow ^1E$  LF band overlapping with the MLCT band. The band at 424nm which appears as a shoulder may be assigned the  $^1A \rightarrow ^3E$  transition, the spin-forbidden transition which is apparent because of spin-orbit coupling.

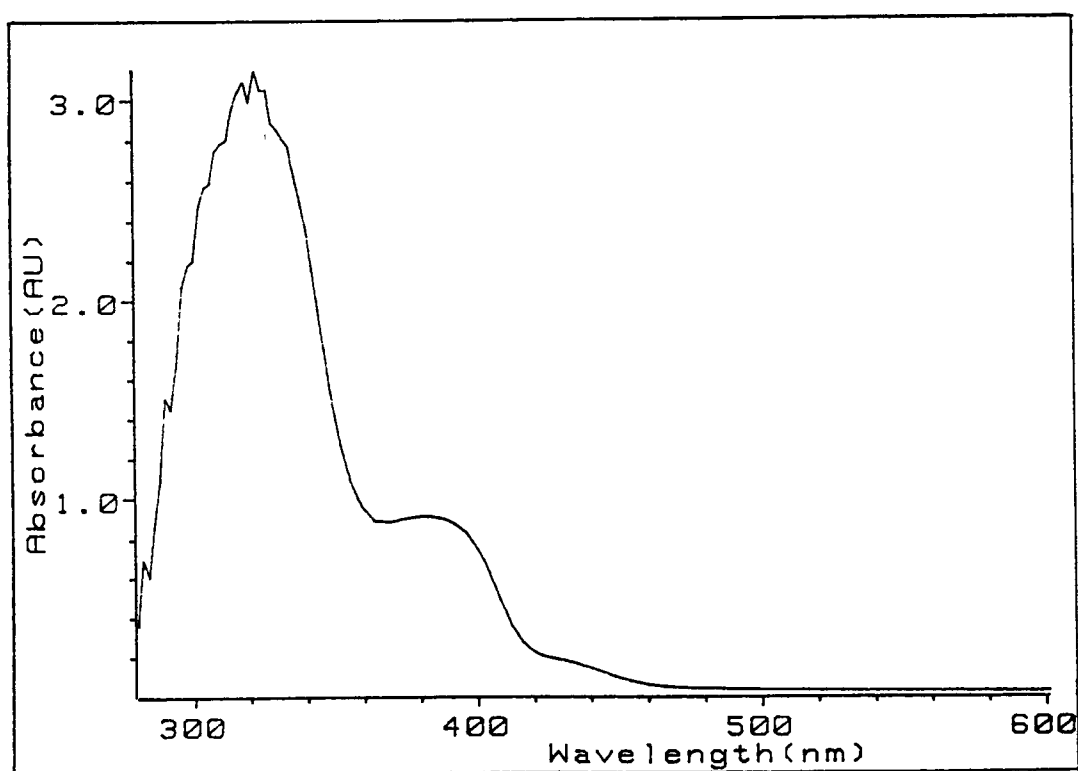


Figure 3.2.4.2.3 The UV-visible spectrum of a sample of  $W(CO)_5(bipyam)$ , dissolved in toluene ( $7.84 \times 10^{-5}\text{mol dm}^{-3}$ ), at 295K

The UV-visible spectrum of the  $\text{Cr(CO)}_5(\text{bipyam})$  species has a low energy band in the visible region centred at 408nm. This band may be assigned the  $^1\text{A} \rightarrow ^1\text{E}$  LF transition which overlaps the MLCT transition of the complex.

### 3.2.4.3 The reactions of $\text{M(CO)}_5(\text{bipyam})$ in the solid state

The infrared spectrum of a sample of  $\text{Cr(CO)}_5(\text{bipyam})$ , pressed in a KBr pellet and heated to 353K for sixty minutes, is presented in Figure 3.2.4.3.1. The bands at 2067, 1983, 1910 and  $1892\text{cm}^{-1}$  are observed to deplete with a growth of new bands at 2010, 1918, 1861 and  $1787\text{cm}^{-1}$ . Upon comparison with an infrared spectrum of  $\text{Cr(CO)}_4(\text{bipyam})$ <sup>33</sup> it was confirmed that this product had been formed. The four bands correspond to the  $\text{A}_1$ ,  $\text{B}_1$ ,  $\text{B}_2$  and  $\text{A}_1(2)$  modes of a *cis*- $\text{Cr(CO)}_4(\text{bipyam})$   $\text{C}_{2v}$  species<sup>33</sup>. Repeating this procedure, using the  $\text{W(CO)}_5(\text{bipyam})$  complex caused a depletion of the four infrared bands corresponding to the  $\text{C}_{4v}$  species, with a subsequent growth of new bands at 2004, 1900, 1859 and  $1776\text{cm}^{-1}$ . These bands were assigned the  $\text{A}_1$ ,  $\text{B}_1$ ,  $\text{B}_2$  and  $\text{A}_1(2)$  modes of a *cis*- $\text{W(CO)}_4(\text{bipyam})$  complex, possessing  $\text{C}_{2v}$  symmetry, upon comparison with the infrared spectrum of an authentic sample.

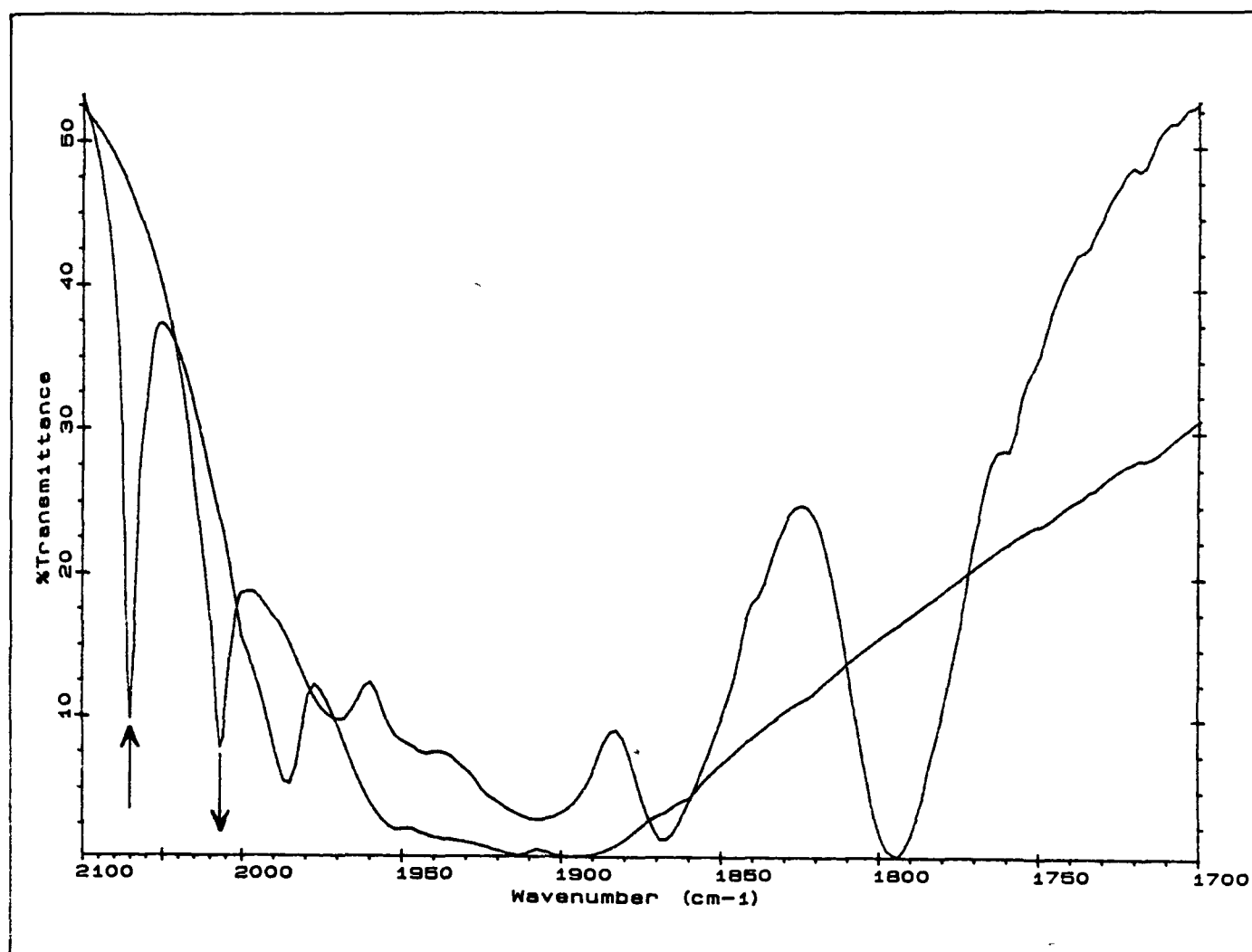
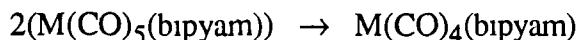


Figure 3.2 4 3 1. The infrared spectrum of a sample of  $\text{Cr}(\text{CO})_5(\text{bipyam})$ , pressed in a KBr pellet and heated to 353K for sixty minutes

Thermogravimetric analysis determined the weight loss upon heating a pure sample of  $\text{W(CO)}_5(\text{bipyam})$ . It had been assumed previously<sup>17</sup>, although not detected, that the mechanism of chelate formation occurred *via* an intramolecular thermal extrusion of CO. Assuming this, then a weight loss of 6% should have been observed. However, the actual weight loss was 35%, which occurred between the temperatures of 363-413K. Obviously, simple loss of CO cannot account for this but, calculations show that if this weight loss is attributed to the sublimation of  $\text{W(CO)}_6$  then one molecule of  $\text{W(CO)}_6$  is produced for every two molecules of  $\text{W(CO)}_5(\text{bipyam})$  present. Repeating this procedure, using a pure sample of  $\text{Cr(CO)}_5(\text{bipyam})$ , showed a weight loss of 31%. Assuming CO extrusion is effective then a weight loss of 7.71% should have been observed. Calculations show that if the weight loss is attributed to the sublimation of  $\text{Cr(CO)}_6$  then for every two moles of  $\text{Cr(CO)}_5(\text{bipyam})$  present one mole of  $\text{Cr(CO)}_6$  is produced (equation 3.2.4.3.1.)

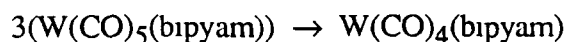


equation 3.2.4.3.1

#### 3.2.4.4 The reactions of $\text{M(CO)}_5(\text{bipyam})$ in solution

Owing to the insolubility of the  $\text{M(CO)}_4(\text{bipyam})$ <sup>33</sup> chelate complexes in organic solvents it was not possible to determine the stoichiometry of the reactions using infrared or UV-visible spectroscopy. To this end gravimetric analysis of the formation of the  $\text{M(CO)}_4(\text{bipyam})$  chelate complexes was employed.

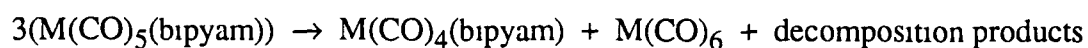
A solution of the  $\text{W(CO)}_5(\text{bipyam})$  complex in toluene ( $5.38 \times 10^{-3} \text{ mol dm}^{-3}$ ) was refluxed for thirty minutes and the precipitate formed was dried and analysed. Spectral characterisation revealed the formation of  $\text{W(CO)}_4(\text{bipyam})$  and the stoichiometry of the reaction as that presented in equation 3.2.4.4.1



equation 3.2.4.4.1

This gravimetric procedure was repeated for the  $Cr(CO)_5(bipyam)$  species and the stoichiometry for the formation of the  $Cr(CO)_4(bipyam)$  complex was identical to that presented in equation 3.2.4.4.1

The formation of the parent carbonyl was observed, by infrared spectroscopy, upon heating a solution of  $W(CO)_5(bipyam)$  ( $5.38 \times 10^{-3} \text{ mol dm}^{-3}$ ) in chlorobenzene (Figure 3.2.4.4.1) to 323K and maintaining that temperature for sixty minutes. From these results it was possible to determine the stoichiometry of the reaction, knowing the molar extinction coefficients of  $W(CO)_6$  and  $W(CO)_5(bipyam)$ . This procedure was repeated for a solution of  $Cr(CO)_5(bipyam)$  in toluene ( $3.47 \times 10^{-3} \text{ mol dm}^{-3}$ ) and the experimental data for the determination of the molar extinction coefficients is presented in Table 3.2.4.4.1. From these results the following stoichiometry is proposed (equation 3.2.4.4.2)



equation 3.2.4.4.2

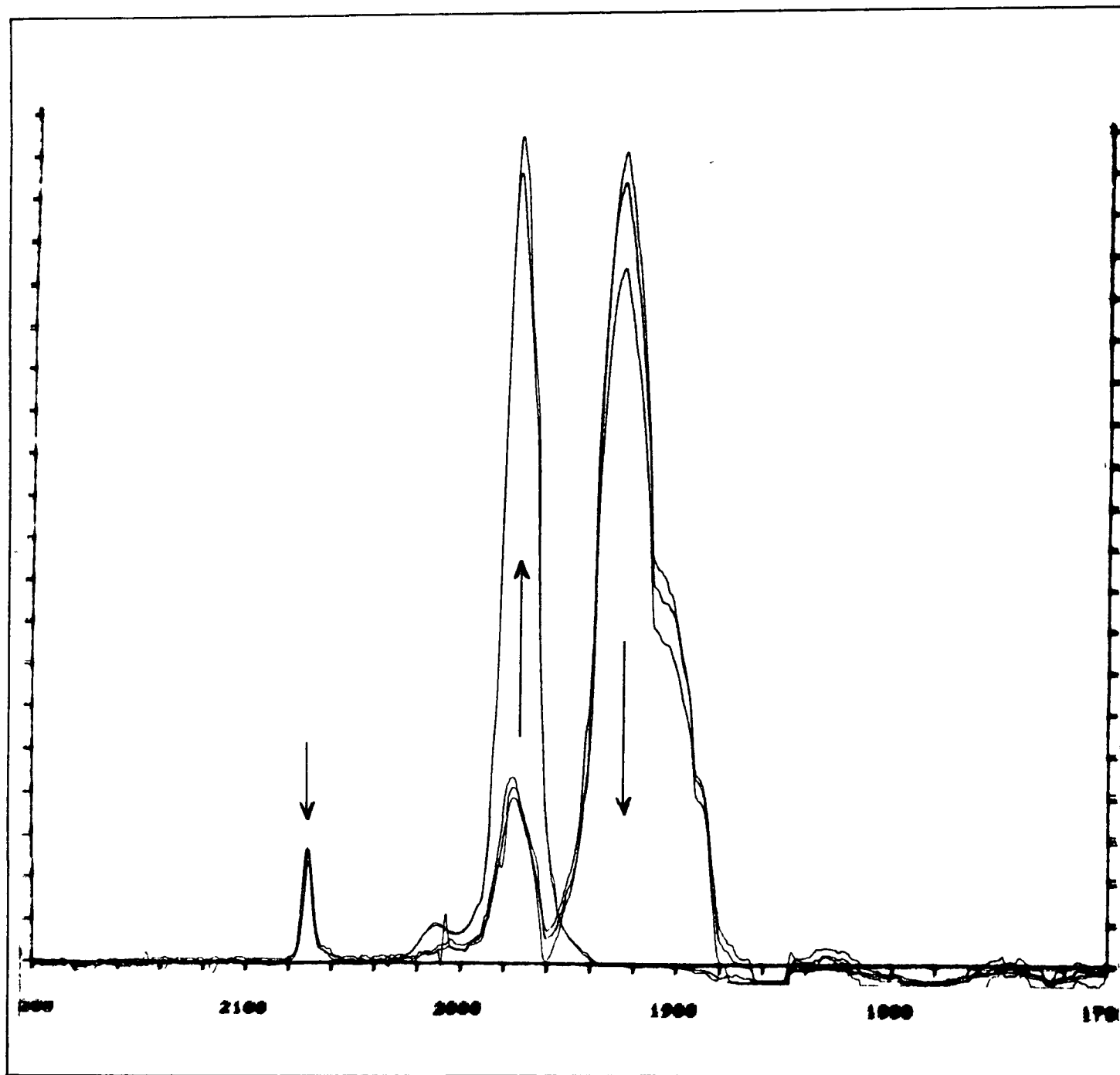


Figure 3 2 4 4.1 The infrared spectral changes occurring upon heating a solution of  $\text{W(CO)}_5(\text{bipyam})$  ( $5.38 \times 10^{-3} \text{ mol dm}^{-3}$ ), in chlorobenzene, to 323K and maintaining that temperature for sixty minutes

The maintenance of a solution of  $\text{W(CO)}_5(\text{bipyam})$  in chlorobenzene containing excess bipyam at 343K for sixty minutes resulted in no change in the infrared spectrum of the sample. Addition of excess ligand should not affect the formation of the chelate product,  $\text{M(CO)}_4(\text{bipyam})$ , if an intramolecular CO extrusion process is operative.

Table 3.2.4 4 1 Experimental data for the determination of the molar extinction coefficients of the  $\text{M(CO)}_5(\text{bipyam})$  complexes.

Complex	Concentration (mol dm <sup>-3</sup> )	Absorbance (A U)	$\epsilon$ mol <sup>-1</sup> dm <sup>3</sup> cm <sup>-1</sup>
$\text{W(CO)}_6$ 1974cm <sup>-1</sup>	9.47 x 10 <sup>-3</sup>	1.5024	15,861
	7.57 x 10 <sup>-3</sup>	1.2782	16,868
			$\epsilon = 16,364$
$\text{W(CO)}_5(\text{bipyam})$ 2071cm <sup>-1</sup>	6.73 x 10 <sup>-3</sup>	0.0594	882
	5.38 x 10 <sup>-3</sup>	0.051	946
	3.36 x 10 <sup>-3</sup>	0.0341	1012
			$\epsilon = 946$
$\text{Cr(CO)}_6$			$\epsilon = 14,505^{12}$
$\text{Cr(CO)}_5(\text{bipyam})$ 2069cm <sup>-1</sup>	2.69 x 10 <sup>-2</sup>	0.2105	782
	3.489 x 10 <sup>-3</sup>	0.0258	740
			$\epsilon = 761$

Repeating this procedure at ambient temperature for the  $\text{Cr(CO)}_5(\text{bipyam})$  complex also exhibited a suppression of parent carbonyl regeneration and formation of the chelate species,  $\text{Cr(CO)}_4(\text{bipyam})$ . These observations would indicate, and support the previous results, that CO extrusion plays no role in the mechanism of chelate formation, under these conditions. The absence of spectral change for a sample of

$\text{Cr}(\text{CO})_5(\text{bipyam})$ , dissolved in toluene solution ( $2.69 \times 10^{-3} \text{ mol dm}^{-3}$ ) containing excess ligand ( $3.25 \times 10^{-3} \text{ mol dm}^{-3}$ ) and left at ambient temperature for 24 hours are presented in Figure 3 2 4 4.2

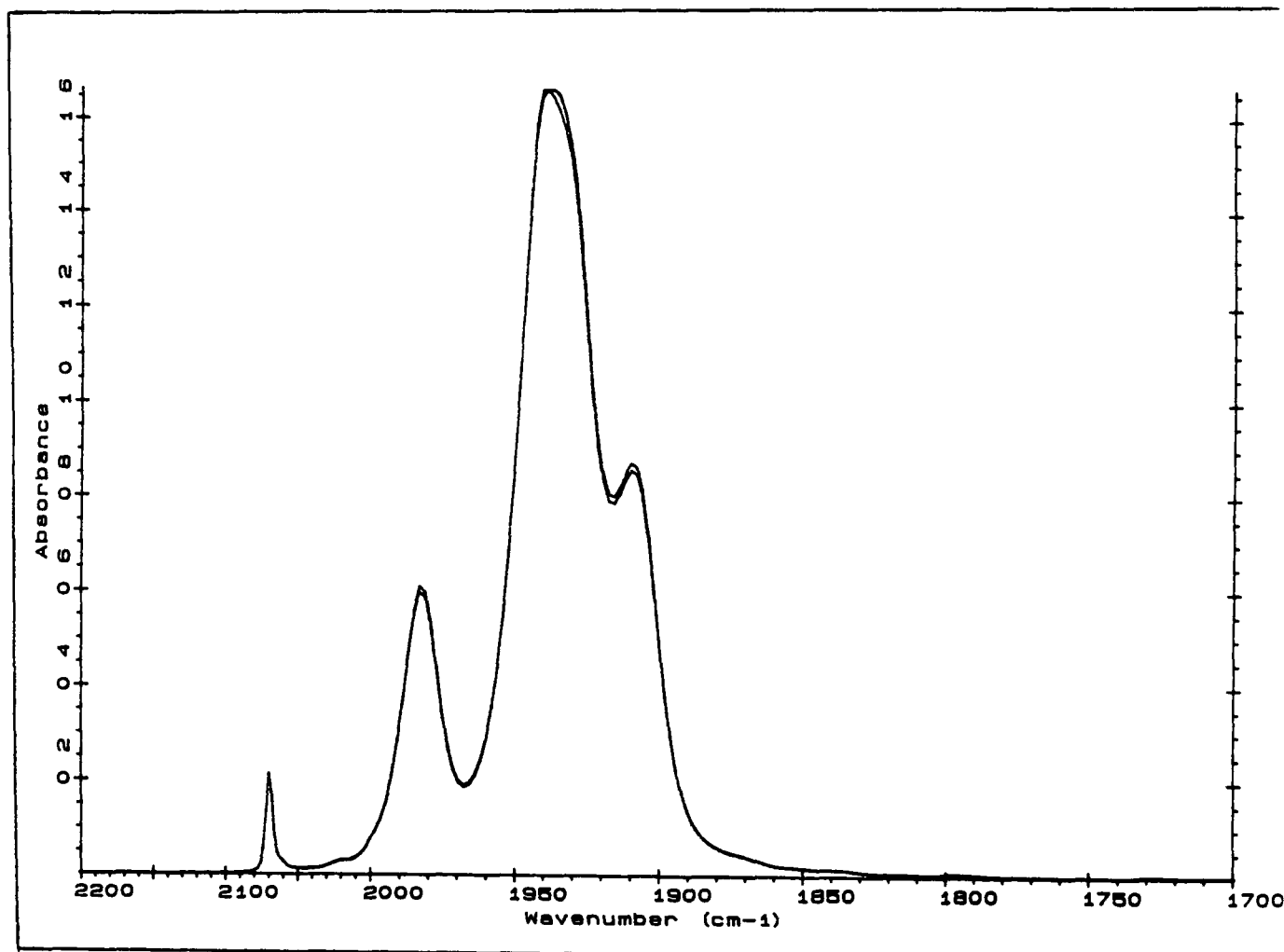
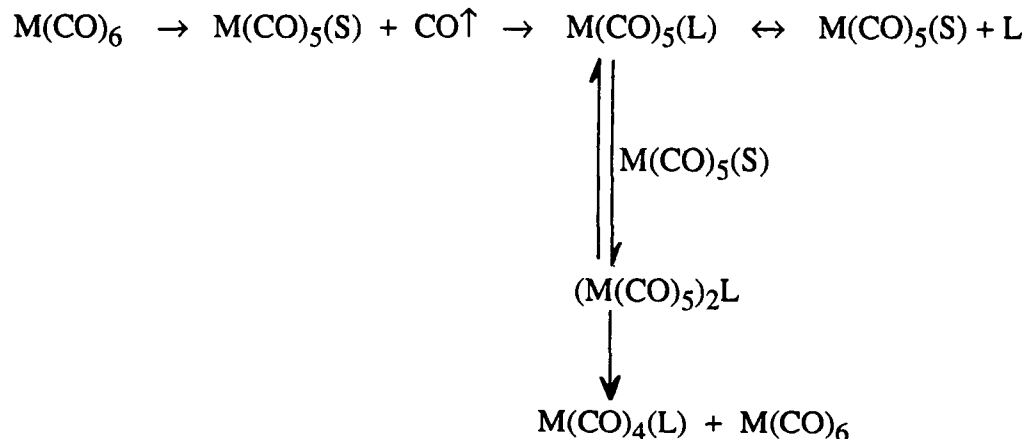


Figure 3 2 4 4 2 The infrared spectra obtained upon standing a sample of  $\text{Cr}(\text{CO})_5(\text{bipyam})$ , dissolved in toluene ( $2.69 \times 10^{-3} \text{ mol dm}^{-3}$ ) solution containing excess ligand ( $3.25 \times 10^{-3} \text{ mol dm}^{-3}$ ), at ambient temperature with subsequent scanning after 24 hours



The results thus far indicate that intramolecular CO extrusion does not play a significant role in the mechanism of chelate formation. To account for the reactions of the  $M(CO)_5(bipyam)$  complexes we propose that the chelate species,  $M(CO)_4(bipyam)$ , is formed *via* a ligand bridged metal carbonyl complex. Although no such intermediate was detected the results support the concept of the formation of such a complex. A reaction scheme, presented in Scheme 3.2.4.4.1, outlines the basis of the proposal. In the absence of excess ligand the complex produces two products,  $M(CO)_6$  and  $M(CO)_4(bipyam)$ . In the presence of excess ligand the equilibrium of the reaction is altered and the formation of the ligand bridged metal carbonyl species is suppressed, concomitant with the formation of the  $M(CO)_6$  and  $M(CO)_4(bipyam)$  species.

Scheme 3.2.4.4.1. A proposal of the reactions of the  $M(CO)_5(bipyam)$  complexes



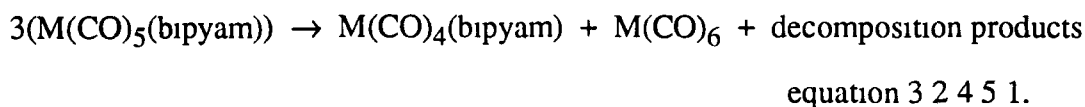
Unfortunately to elucidate the mechanism of chelate formation it is necessary to determine the activation parameters for the reactions in the presence and absence of excess ligand. This would present a problem because of the insolubility of the chelate products in organic solvents.

### 3.2.4.5 Summary

The  $M(CO)_5(bipyam)$  complexes were isolated and characterised by elemental analysis, infrared and UV-visible spectroscopy. The isolation of these complexes with the ligand coordinated in a monodentate fashion was not surprising. The investigation of the reactions of these complexes proved difficult because of the insolubility of the chelate products,  $M(CO)_4(bipyam)$ , in organic solvents.

The reaction of these complexes, as monitored by infrared spectroscopy, in the solid state revealed the formation of the chelate species,  $M(CO)_4(bipyam)$ . Thermogravimetric analysis of the complexes revealed a weight loss of 35% and 31% for the  $W(CO)_5(bipyam)$  and  $Cr(CO)_5(bipyam)$  complexes, respectively. One of the discrepancies associated with previous work was the assumption that chelate formation occurred via an intramolecular CO extrusion process even though this was never conclusively proven<sup>17</sup>. Had this been true then weight losses of 6% and 7.71% should have been observed for the  $W(CO)_5(bipyam)$  and  $Cr(CO)_5(bipyam)$  complexes, respectively. It is becoming increasingly apparent that a unimolecular CO extrusion does not play a significant role here. Calculations show that if the weight losses are attributed to the sublimation of the respective parent carbonyls then for every two moles of complex present one mole of parent is produced.

The stoichiometry for the reactions of the complexes was determined; gravimetrically for the formation of the chelate products. The regeneration of the parent carbonyls was monitored using infrared spectroscopy and the stoichiometry determined more accurately with the knowledge of the molar extinction coefficients. The stoichiometry of the reaction of the  $M(CO)_5(bipyam)$  complexes is presented in equation 3.2.4.5.1



To account for the reactions of these complexes we propose that a ligand bridged metal carbonyl intermediate is formed which subsequently produces the  $\text{M}(\text{CO})_4(\text{bipyam})$  and  $\text{M}(\text{CO})_6$  species. The suppression of the formation of these complexes by the incorporation of excess ligand into the reaction clearly indicates the non-participation of CO extrusion in this process. Although no such intermediate was detected the results indicate the concept of such an intermediate and the nature of the ligand indicates its ability to facilitate two metal centres. The reaction scheme presented in Scheme 3 2 4 4 1 is an attempt to explain the reactivity of the complexes but the insolubility of the chelate products presents difficulties in the elucidation of the exact mechanism. However, what is clear is that intramolecular CO extrusion appears to play no role in the mechanism of chelate formation for these complexes.

There are notable differences in the stoichiometry for the reactions of the  $\text{M}(\text{CO})_5(\text{bipyam})$  complexes in the solid and solution state. Despite the use of pure samples of the complexes the use of gravimetric analysis in the determination of the stoichiometry of the reaction frequently resulted in some product being left in the flask. While this gave an indication of the stoichiometry of the reaction it is not the most accurate of measurements.

### 3.2.5 The synthesis and characterisation of $\text{Cr(CO)}_4(\text{phen})$ (phen= 1,10-phenanthroline)

#### 3.2.5.1 The preparation of $\text{Cr(CO)}_4(\text{phen})$

The reaction of phen dissolved in toluene solution, with a sample of  $\text{Cr(CO)}_5(\text{cis-cyclo-octene})$  yielded the chelate product,  $\text{Cr(CO)}_4(\text{phen})$ . This was confirmed by elemental analysis and comparison with spectra of authentic samples. The isolation of this complex with the ligand bound in a bidentate manner was not surprising as the ligand is a rigid structure with the possibility of monodentate coordination not feasible. The ligand (Figure 3 2.5 1.1), unlike the 2,2'-bipyridine ligands, has the two nitrogens constrained to be geometrically suitable for bidentate ligation.

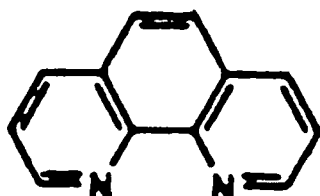


Figure 3 2.5 1.1 1,10-phenanthroline

The reaction of  $\text{Cr(CO)}_5(\text{cis-cyclo-octene})$  with a sample of phen, dissolved in toluene, was monitored by infrared spectroscopy at 273K, to see if the  $\text{Cr(CO)}_5(\text{phen})$  intermediate could be detected.

Many workers have attempted to detect the  $\text{Cr(CO)}_5(\text{phen})$  intermediate. The irradiation of a solution of methylcyclohexane. toluene (9 1)<sup>35</sup> at 100K containing 1

$\times 10^{-4}\text{M}$   $\text{M}(\text{CO})_6$  ( $\text{M} = \text{Cr}, \text{Mo}$  or  $\text{W}$ ) and  $10^{-2}\text{M}$  phen resulted in the formation of  $\text{M}(\text{CO})_4(\text{phen})$  with no detection of the monodentately coordinated intermediate. Oishi's<sup>36</sup> laser flash photolysis study of photochemical carbonyl substitution in  $\text{M}(\text{CO})_6$  with phen led to the detection of the  $\text{M}(\text{CO})_5(\text{phen})$  transient intermediate. He found that the rates of CO dissociation for the second carbonyl in  $\text{M}(\text{CO})_5(\text{phen})$  were  $10^3$  times greater than those reported by Lees *et al* for the formation of the  $\text{M}(\text{CO})_5(\text{bpy})$  complexes. However, much work has to be done before this mechanism may be elucidated.

### 3.2.5.2 The characterisation of $\text{Cr}(\text{CO})_4(\text{phen})$ by infrared and UV-visible spectroscopy.

The infrared spectrum of a sample of  $\text{Cr}(\text{CO})_4(\text{phen})$ , dissolved in toluene solution ( $2.26 \times 10^{-3} \text{ mol dm}^{-3}$ ) is presented in Figure 3 5 1 2 1, at 295K

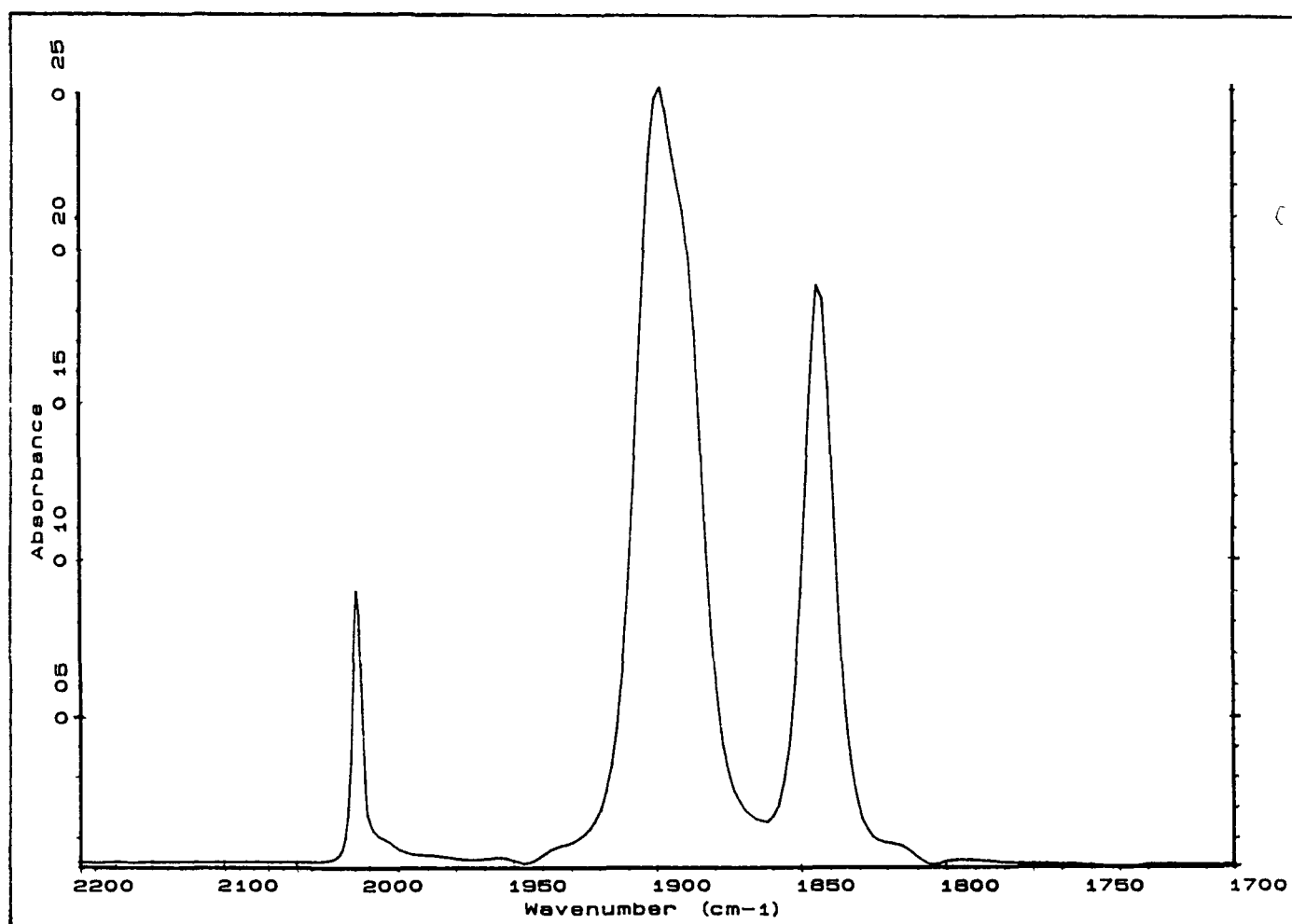


Figure 3.2.5.2.1. The infrared spectrum of a sample of  $\text{Cr}(\text{CO})_4(\text{phen})$ , dissolved in toluene solution ( $2.26 \times 10^{-3} \text{ mol dm}^{-3}$ ) at 295K

The bands at 2007.6, 1898.5 and 1843.5  $\text{cm}^{-1}$  were assigned the  $A_1$ ,  $B_1$ , and  $B_2$  modes of a complex possessing  $C_{2v}$  symmetry. The  $A_1(2)$  mode is present as a shoulder on the  $B_1$  mode. This assignment was confirmed by comparison with that reported in the literature.

The UV-visible spectrum of a sample of  $\text{Cr}(\text{CO})_4(\text{phen})$ , dissolved in toluene solution ( $3.08 \times 10^{-4} \text{ mol dm}^{-3}$ ) at 295K, is presented in Figure 3.2.5.2.2.

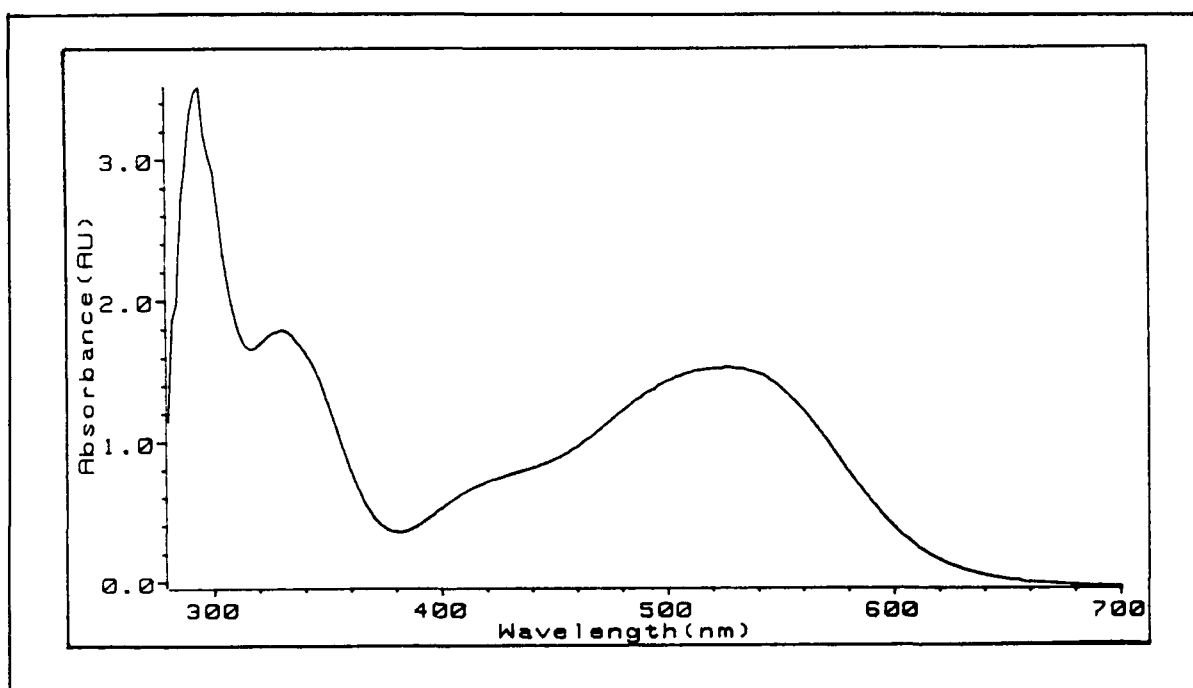


Figure 3.2.5.2.2 The UV-visible spectrum of a sample of  $\text{Cr}(\text{CO})_4(\text{phen})$ , dissolved in toluene solution ( $3.08 \times 10^{-4} \text{ mol dm}^{-3}$ ) at 295K.

The complex exhibits three bands at 294, 330(sh) and 528 nm. The band at 528 nm may be assigned the MLCT band of a highly conjugated molecule. The band at 330 nm may be assigned the  $^1A \rightarrow ^1E$  LF band with the band at 294 nm being assigned the  $\pi\text{-}\pi^*$  transition of the ligand, indicative of the coplanarity of a highly conjugated complex.

**3.2.5.3 The addition of a solution of phen in toluene to a sample of  $\text{Cr}(\text{CO})_5(\text{cis-cyclo-octene})$  at 273K, as monitored by infrared spectroscopy.**

The infrared spectral changes occurring upon addition of a solution of phen in toluene ( $6.6 \times 10^{-3} \text{ mol dm}^{-3}$ ) to a sample of  $\text{Cr}(\text{CO})_5(\text{cis-cyclo-octene})$  at 273K are presented in Figure 3 2 5.3 1

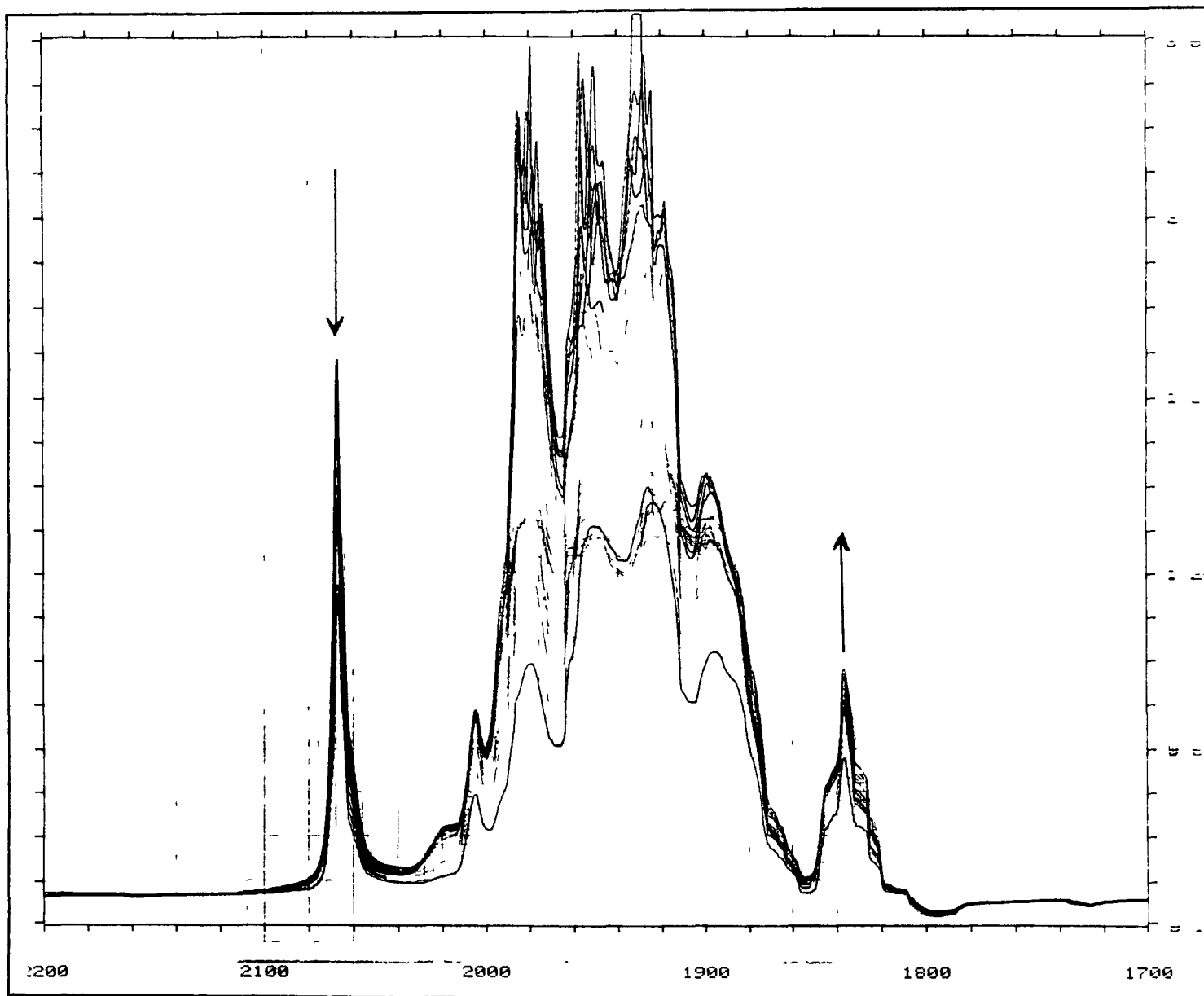


Figure 3 2.5 3 1.. The spectral changes occurring upon addition of a solution of phen in toluene ( $6.6 \times 10^{-3} \text{ mol dm}^{-3}$ ) to a sample of  $\text{Cr}(\text{CO})_5(\text{cis-cyclo-octene})$  as monitored by infrared spectroscopy at 273K



The initial bands at 2066, 1979 and 1944 $\text{cm}^{-1}$  correspond to  $\text{Cr}(\text{CO})_5(\text{cis-cyclo-octene})$  in toluene solution. These bands are observed to diminish with a concomitant growth of new bands at 2007, 1898 and 1843 $\text{cm}^{-1}$ . These bands were attributed to the formation of  $\text{Cr}(\text{CO})_4(\text{phen})$ , upon comparison with an infrared spectrum of an authentic sample. The band at 1980 $\text{cm}^{-1}$  corresponds to the formation of a small amount of  $\text{Cr}(\text{CO})_6$ . It may be possible that this regeneration of the parent carbonyl results from the decomposition of the  $\text{Cr}(\text{CO})_5(\text{cis-cyclo-octene})$  complex.

#### 3.2.5.4 Summary

The reaction of  $\text{Cr(CO)}_5(\text{ciscyclo-octene})$  with a solution of phen in toluene resulted in the formation of  $\text{Cr(CO)}_4(\text{phen})$ . This was not surprising as the ligand retains a rigid coplanar geometry with the two nitrogens constrained for bidentate ligation. This complex was characterised by infrared, UV-visible and elemental analysis.

As with other workers our attempts at the detection of the intermediate,  $\text{Cr(CO)}_5(\text{phen})$ , were unsuccessful. Elucidation of the mechanism of chelate formation for this ligand necessitates the use of rapid scanning spectroscopic and cryogenic techniques.

### 3.3 Summary

The isolation and characterisation of a series of  $(M(CO)_5)_x(L)$  ( $M = Cr$  or  $W$ ,  $x = 1$  or  $2$ ,  $L = dphbpy$ ,  $bpa$ ,  $ampy$  and  $bipyam$ ) and  $Cr(CO)_4(phen)$  have been discussed. Their reactions in the solid and solution state have been isolated and the reasons for their mode of coordination outlined in Chapter 2.

The infrared spectral features of the  $M(CO)_5(L)$  complexes exhibit the normally forbidden  $B_1$  mode which is indicative of a distortion of the ideal  $C_{4v}$  symmetry exhibited by these complexes<sup>10</sup>. In the case of the  $(Cr(CO)_5)_2(dphbpy)$  complex the E mode was split, indicating a reduction of the local symmetry from  $C_{4v}$  to  $C_s$ . The UV-visible spectra of the  $(M(CO)_5)_x(L)$  ( $L = dphbpy$ ,  $bpa$ ,  $bipyam$ ) complexes exhibited no MLCT bands above 418nm, which indicated little  $\pi^*$  conjugation.

The reactions of the  $(Cr(CO)_5)_2(dphbpy)$  complex are very similar to those described by Creaven<sup>12,13</sup> *et al* for the  $(Cr(CO)_5)_2(dmbpy)$  and  $(Cr(CO)_5)_2(bpy)$  complexes. A reaction scheme for the reactions of this complex is outlined in Scheme 3.2.1.8.1. The activation parameters for the formation of the  $Cr(CO)_4(dphbpy)$  in the absence and presence of excess ligand indicated two different pathways for the formation of the  $Cr(CO)_4(dphbpy)$  complex. In the absence of excess ligand the rate determining step was assumed to be the breaking of a Cr-N bond while in the presence of excess ligand the rate determining step, despite the negative entropy value, was also assumed to be the breaking of a Cr-N step. The reactions of the  $M(CO)_5(bpa)$  complex and  $Cr(CO)_5(ampy)$  were similar up to a point. The introduction of excess ligand into the reactions of the  $M(CO)_5(bpa)$  complexes resulted in a suppression of the formation of the  $M(CO)_4(bpa)$  and regeneration of the  $M(CO)_6$  complexes. The activation parameters for the formation of the  $Cr(CO)_4(bpa)$

complex in the presence and absence of excess ligand implied two different pathways existed. In the absence of excess ligand the rate determining step was assumed to be the breaking of a Cr-N bond while in the presence of excess ligand the negative entropy of activation indicated the associative character of the transition state. The activation parameters for the formation of the  $\text{W(CO)}_4(\text{bpa})$  complex in the absence and presence of excess ligand indicated the existence of similar pathways. In the case of the  $\text{Cr(CO)}_5(\text{ampy})$  complex the introduction of excess ligand resulted in an initial increase in the  $k_{\text{obs}}$  for the formation of the  $\text{Cr(CO)}_4(\text{ampy})$  complex, which was reduced to zero after a certain concentration of excess ligand. The minimum concentration of excess ligand, employed in the UV-visible studies, was greater than that used in the infrared studies, in which there was no formation of the  $\text{Cr(CO)}_4(\text{ampy})$  complex observed. The introduction of excess ligand was proposed to result in an equilibrium between coordination of the metal to the two available nitrogens. The activation parameters were determined in the absence of excess ligand and the activation enthalpy was similar to that for the breaking of a Cr-N bond in  $\text{Cr(CO)}_5(\text{pyridine})$ .

The variation in the  $k_{\text{obs}}$  for the formation of the  $\text{M(CO)}_4(\text{L})$  complexes varied greatly and this may be attributed to the strength of the M-N bonds, which is dependent on the  $\text{pK}_a$  of the conjugate acid of the ligand<sup>26</sup>. It was found that as the basicity of the ligand decreased the bond strength also decreased. The activation enthalpies should reflect this phenomenon.

The reactions of the  $\text{M(CO)}_5(\text{bipyam})$  complexes were also investigated but the activation parameters for the formation of the  $\text{M(CO)}_4(\text{bipyam})$  complexes were not determined owing to the insolubility of the chelate complexes<sup>33</sup>. However, the reactions of these complexes were similar to those discussed already. In the absence of any excess ligand the formation of the  $\text{M(CO)}_6$  compound was observed,

by infrared spectroscopy, and the formation of the  $\text{M}(\text{CO})_4(\text{bipyam})$  complexes was measured gravimetrically. In the presence of excess ligand the formation of the  $\text{M}(\text{CO})_6$  and  $\text{M}(\text{CO})_4(\text{bipyam})$  was suppressed. The  $\text{Cr}(\text{CO})_4(\text{phen})$  complex was also isolated and characterised by infrared and UV-visible spectroscopy. It was hoped that with the use of the transfer reagent,  $\text{Cr}(\text{CO})_5(\text{cis-cyclo-octene})$ , and the VTIR apparatus, the formation of an intermediate would be observed. Unfortunately, the formation of the  $\text{Cr}(\text{CO})_4(\text{phen})$  complex was observed with no detection of an intermediate.

### 3.4 Experimental

#### 3.4.1 Materials

All solvents used in the syntheses and spectroscopic studies were purified by standard techniques<sup>37</sup> Pentane, toluene (spectroscopic grade) 4,4'-biphenyl-2,2'-bipyridine, 2-aminomethylpyridine, and *cis*-cyclo-octene were obtained from Aldrich Chemical Co and were used without further purification. Hexacarbonyltungsten(0), 2,2'-bipyridylamine and 1,10-phenanthroline, obtained from Riedel-de-Haen were used as received, but toluene (analar grade) was distilled from LiAlH<sub>4</sub> and stored over CaH<sub>2</sub> Hexacarbonylchromium(0) from Strem Chemicals Inc was used as received Chlorobenzene was obtained from BDH Chemicals Ltd and was purified by the method in reference 37 prior to use and stored under an argon atmosphere. Cr(CO)<sub>5</sub>(*cis*-cyclo-octene) was prepared by the method outlined by Grevels and Skibbe<sup>24</sup> and stored at 253K, under an argon atmosphere, until needed. *Bis*-picolylamine was obtained as a gift from NEPRA and purified by vacuum distillation. Carbon monoxide, argon and nitrogen gases were used as supplied from IIG Ltd

#### 3.4.2 Equipment

##### 3.4.2.1 Infrared spectral studies

Infrared spectra were recorded on both a Perkin-Elmer 983G and Nicolet 205 FTIR spectrophotometer The wavenumber positions are accurate to  $\pm 2\text{cm}^{-1}$  All samples prepared in solution were deoxygenated prior to being introduced into the solution cells. The solution cells employed had NaCl windows, separated by

either lead or Teflon spacers ( $d = 0.1, 0.2\text{mm}$ ). Variable temperature spectra were obtained using a Specac 21000 VTIR cell (Figure 3.4.2.1).

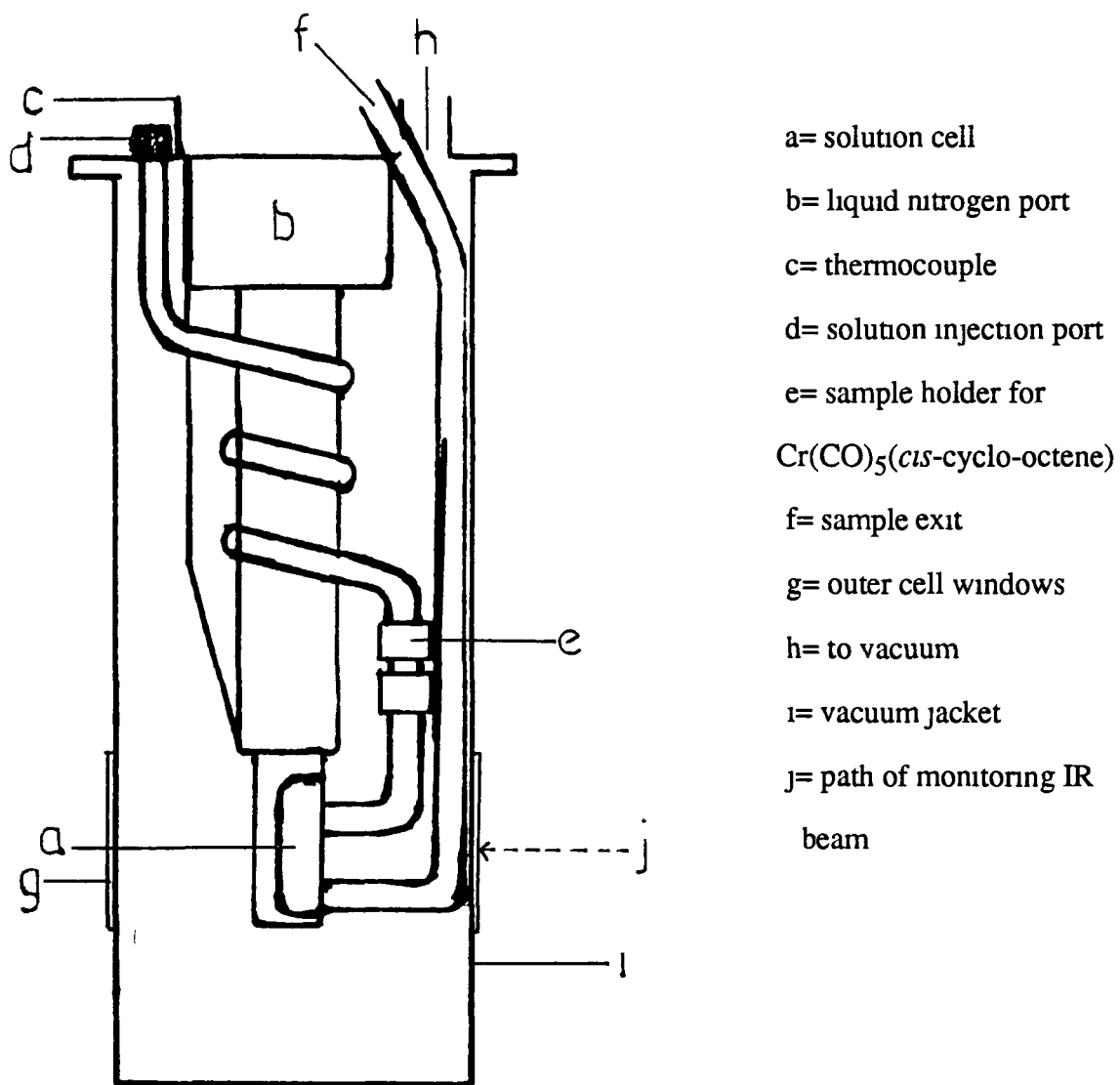


Figure 3.4.2.1. The variable temperature infrared cell

A sample of  $\text{Cr}(\text{CO})_5(\text{cis-cyclo-octene})$  was held in the sample holder (f) and a solution of the ligand dissolved in toluene injected into the system at the injection port (e) while the reaction is monitored by the infrared spectrophotometer

#### 3.4.2.2 UV-visible spectral studies

The UV-visible spectra were obtained using a Hewlett-Packard 8452A diode-array spectrophotometer fitted with a Chemstation data station. Peak positions were accurate to  $\pm 2\text{nm}$ . In determining the kinetic parameters the complex was placed in a sample cuvette (10mm) and the solvent placed in a bulb attached to the cuvette. The solvent was degassed by three freeze-pump-thaw cycles prior to the addition of an atmosphere of gas. The bulb was left in a water bath at the desired temperature for fifteen minutes and the solvent transferred to the cuvette. The initial spectrum was obtained as soon as dissolution of the solid occurred, usually within a minute of adding the solvent. The temperature was maintained by the use of a water bath which circulated the water through the system. Each spectrum was measured five times and took 0.1s to acquire. This allowed the absorbance to be determined to  $\pm 0.0001$  absorbance units. Kinetic parameters were calculated using Hewlett-Packard kinetics software, which employs a curve fitting routine for first order kinetics. The observed rate data were fitted to the following expression

$$A = A_1 + A_2 e^{-kt}$$

where  $A$  = absorbance at time  $t$ ,  $A_1$  and  $A_2$  = constants related to the initial and final absorbances at the monitoring wavelengths, and  $k$  is the observed first order rate constant



### 3.4.2.3 NMR spectral studies

All samples were analysed using a Bruker 400MHz NMR spectrophotometer

### 3.4.2.4 Thermogravimetric analysis

Thermogravimetric analysis of pure samples was executed using a Stanton-Redcroft TG750 thermogravimetric analyser.

### 3.4.2.5 Photolysis experiments

All photolyses were executed in the photoreactor presented in Figure 3 4 2.5 1 The double walled Pyrex glass vessel contains a 400W medium pressure mercury lamp which is cooled by a circulating water system.

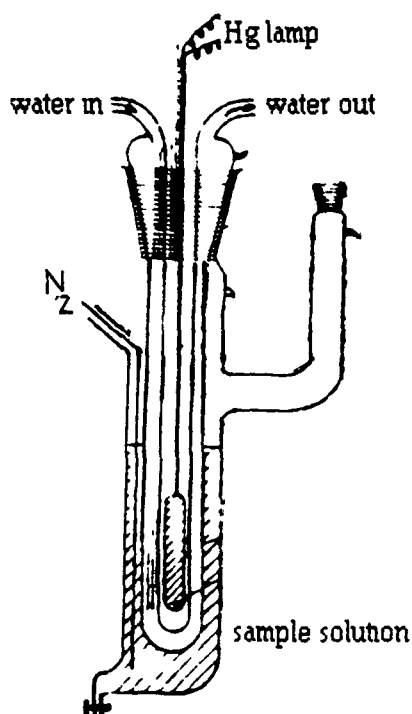


Figure 3 4 2 4.1 The photolysis apparatus

The external vessel contains the solution to be irradiated which has a continuous stream of nitrogen bubbling through, to remove carbon monoxide, which is liberated during the reactions

### 3.4.2.6 The determination of the activation parameters

The Arrhenius and Eyring plots were used to determine the Thermodynamic parameters of activation energy, enthalpy and entropy. The Arrhenius<sup>38</sup> equation is given by

$$\ln k_{\text{obs}} = -E_a/RT + \ln(A)$$

where T= temperature in kelvin

$E_a$ = activation energy in J mol<sup>-1</sup>

R= universal gas constant

The activation energy of a reaction may be determined if the rate constant is measured at a number of temperatures. A plot of  $\ln k_{\text{obs}}$  against  $1/T$  is linear and the slope is equal to  $-E_a/2.303R$ .

The Eyring equation<sup>38</sup> is given by

$$\ln(k_{\text{obs}}/T) = -(\Delta H^\ddagger/RT) + (\Delta S^\ddagger/R) + \ln(h/k)$$

A plot of  $\ln(k_{\text{obs}}/T)$  against  $1/T$  gives a slope of  $-(\Delta H^\ddagger/R)$  and an intercept of  $\Delta S^\ddagger/R + \ln(h/k)$  in J mol<sup>-1</sup>

### 3.4.3 The synthesis of the $(M(CO)_5)_x(L)$ ( $M = Cr$ or $W$ ; $x = 1$ or $2$ ; $L = dphbpy$ , $bpa$ , $ampy$ , $bipyam$ )

#### 3.4.3.1 The synthesis of $(Cr(CO)_5)_2(dphbpy)$

A sample of  $dphbpy$  ( $9.9 \times 10^{-4} m$ ) dissolved in toluene solution ( $5 cm^3$ ) was degassed prior to its addition to a degassed sample of  $Cr(CO)_5(cis\text{-cyclo-octene})$  ( $1.98 \times 10^{-3} m$ ). The solution was maintained at 273K, under an argon atmosphere, for fifteen minutes until the addition of cold pentane. The product precipitated out and was washed repeatedly with cold pentane to remove any traces of unreacted ligand or  $Cr(CO)_5(cis\text{-cyclo-octene})$ . The product was then redissolved in toluene and left to recrystallise at 248K. The product was stored at 253K under an argon atmosphere. Elemental analysis of  $(Cr(CO)_5)_2(dphbpy)$  (calculated % (experimental %)) C. 55.46 (55.34); H 2.32 (2.53); N 4.04 (4.32).

#### 3.4.3.2 The synthesis of $M(CO)_5(bpa)$ ( $M = Cr$ or $W$ )

A solution of the ligand ( $1.32 \times 10^{-3} m$ ), dissolved in toluene ( $5 cm^3$ ), was degassed and added to a sample of  $Cr(CO)_5(cis\text{-cyclo-octene})$  ( $1.32 \times 10^{-3} m$ ) at 273K under an argon atmosphere. The solution was maintained at 273K for twenty minutes and then filtered to remove any traces of unreacted ligand or  $Cr(CO)_5(cis\text{-cyclo-octene})$ . Cold pentane was added to the solution and it was stored under an argon atmosphere at 248K until crystal formation. Elemental analysis for the complex proved satisfactory (calculated % (experimental %)) C 52.17 (52.29), H 3.32 (3.47), N 10.74 (11.00).

$W(CO)_6$  ( $1.705 \times 10^{-3} m$ ) was dissolved in dry THF ( $250 cm^3$ ) and the solution transferred to the photochemical reactor. A stream of dry nitrogen gas was passed through the solution to assist the removal of carbon monoxide produced in the

photochemical reaction The solution was irradiated for three hours using a 400W medium pressure Hg lamp (Applied Photophysics) filtered through Pyrex glass Following the photolysis a solution of the bpa ligand, dissolved in the minimum volume of THF ( $1.705 \times 10^{-3}$  m) was added to the photogenerated  $\text{W(CO)}_5(\text{THF})$  and stirred under a dry nitrogen atmosphere for ten minutes. The solvent was removed under reduced pressure at room temperature and recrystallised from acetone at 248K under an argon atmosphere For the complex (calculated % (experimental %)) C 39.01 (38.68), H 2.48 (2.52), N 8.03 (8.02)

#### 3.4.3.3 The synthesis of $\text{Cr(CO)}_5(\text{ampy})$

A solution of ampy ( $2.27 \times 10^{-3}$  m) in toluene ( $5\text{cm}^3$ ) was degassed and added to a sample of  $\text{Cr(CO)}_5(\text{cis-cyclo-octene})$  ( $2.27 \times 10^{-3}$  m) at 273K under an argon atmosphere. The solution was kept at 273K for twenty minutes under an argon atmosphere and any precipitate filtered. The solution was then left at 248K to recrystallise under an argon atmosphere. Elemental analysis for the complex was satisfactory (calculated % (experimental %)) C. 44.01 (43.57), H 2.68 (2.66), N 9.33 (9.16).

#### 3.4.3.4 The synthesis of $\text{M(CO)}_5(\text{bipyam})$

An argon purged solution of bipyam ( $1.78 \times 10^{-3}$  m) in toluene ( $10\text{cm}^3$ ) was added to a sample of  $\text{Cr(CO)}_5(\text{cis-cyclo-octene})$  ( $1.78 \times 10^{-3}$  m) at 273K under an argon atmosphere After twenty minutes the solution was filtered and cold pentane added to the filtrate. The solution was left at 248K, under an argon atmosphere, until crystal formation occurred For the complex (calculated % (experimental %)) C 49.58 (49.59), H 2.47 (2.52), N 11.57 (11.79)

W(CO)<sub>6</sub> (1.42 x 10<sup>-3</sup>m) was dissolved in dry THF (200 mL) and the solution placed in a photochemical reactor. A stream of dry nitrogen gas was passed through the solution to assist the removal of carbon monoxide produced in the photochemical reaction. The solution was irradiated for three hours using a 400 W medium pressure Hg lamp filtered through pyrex glass. Following the photolysis a solution of bipyam (1.42 x 10<sup>-3</sup>m) which had been dissolved in the minimum volume of dry THF was added. The solvent was then removed under reduced pressure and the crude W(CO)<sub>5</sub>(bipyam) was recrystallised from nitromethane solution at 248K under a nitrogen atmosphere, yielding yellow needle shaped crystals of suitable quality for X-ray structural analysis. The elemental analysis for the complex is (calculated % (experimental %)) C 36.37 (36.65), H 1.82 (2.07), N 8.49 (8.50).

#### 3.4.4 The synthesis of the M(CO)<sub>x</sub>(L) (M= Cr or W; x= 3 or 4; L= dphbpy, bpa, ampy, or phen) complexes

##### 3.4.4.1 The synthesis of M(CO)<sub>x</sub>(L) (x= 3 or 4; L= dphbpy, bpa, or ampy)

A solution of M(CO)<sub>6</sub> (4.54 X 10<sup>-3</sup>m) dissolved in pentane (200cm<sup>-3</sup>) containing 4.54 x 10<sup>-3</sup>m of dphbpy, bpa or ampy was degassed and irradiated for two hours under a nitrogen atmosphere with constant stirring using a 400W medium pressure Hg lamp. The Cr(CO)<sub>4</sub>(L) (L= dphbpy or ampy) complex precipitated from the solution and was washed with acetone and chloroform to remove any traces of unreacted ligand or Cr(CO)<sub>6</sub>. The Cr(CO)<sub>4</sub>(L) complex was recrystallised from chloroform at 248K under an argon atmosphere. The M(CO)<sub>3</sub>(bpa) complexes were insoluble in most organic solvents and so were washed repeatedly with toluene to remove any unreacted ligand or M(CO)<sub>6</sub>. The complexes were dried at 353K but satisfactory elemental analysis have yet to be obtained. Elemental analysis proved satisfactory for the Cr(CO)<sub>4</sub>(ampy)

complex (calculated % (experimental %)) C 44.09 (43.98), H 2.88 (2.57), N. 10.28 (10.34).

#### 3.4.4.2 The synthesis of $\text{W}(\text{CO})_4(\text{bpa})$

The synthesis of this complex is identical to that of the  $\text{W}(\text{CO})_5(\text{bpa})$  complex except that the solvent was removed at 318K. The crude product was recrystallised from a 1:1 mixture of acetone and hexane at 248K under an argon atmosphere. The elemental analysis for this complex was satisfactory (calculated % (experimental %)) C 38.79 (39.06), H 2.42 (2.76), N 8.48 (8.77).

#### 3.4.4.3 The synthesis of $\text{Cr}(\text{CO})_4(\text{phen})$

A solution of 1,10-phenanthroline ( $1.198 \times 10^{-3}\text{M}$ ) in pentane ( $25\text{cm}^{-3}$ ) was purged with argon prior to its addition to  $\text{Cr}(\text{CO})_5(\text{cis-cyclo-octene})$  ( $2.18 \times 10^{-4}\text{M}$ ) at 273K under an argon atmosphere. The solution was transferred to a low temperature bath at 213K for twenty four hours. The solvent was decanted at 273K and the precipitate dried under argon at the same temperature. The crude product was redissolved in toluene and left to recrystallise at 248K. The elemental analysis for the complex is (calculated % (experimental %)) C 55.81 (55.11), H 2.32 (2.31), N 8.14 (7.76).

### 3.5 References

- 1 (a) Burdett, J. K., Graham, M. A , Perutz, R. N , Poliakoff, M , Turner, J J., Turner, R F. *J Am Chem Soc* 1975, **97** 4805  
(b) Perutz, R N., Turner, J J *Inorg Chem* 1975, **14** 262.  
(c) Graham, M. A , Rest, A. J , Turner, J J *J Organomet Chem* 1970, **24** C54  
(d) Graham, M A , Perutz, R. N , Poliakoff, M , Turner, J. J. *J Organomet Chem* 1972, **34** C34  
(e) Graham, M A , Poliakoff, M , Turner, J J *J Chem Soc A* 1971, p 2939
- 2 Black, J D , Braterman, P S *J Am Chem Soc* 1975, **97** 2908.
- 3 Kundig, E P , Ozin, G. A *J Am Chem Soc* 1974, **96** 3820
- 4 Perutz, R N , Turner, J J *J Am Chem Soc* 1975, **97** 4791
- 5 Wrighton, M S , Hammond, G S , Gray, H B *J Am Chem Soc* 1971, **93** 4336.
- 6 Braterman, P S , Walker, A P *Discuss Faraday Soc* 1969, **47** 121.
- 7 Wrighton, M S *Inorg Chem* 1974, **13** 905
- 8 Wrighton, M S , Morse, D L , Gray, H B ,Ottesen, D K. *J Am Chem Soc* 1976, **98** 1111
- 9 Wrighton, M. S , Abrahamson, H. B Morse, D L. *J Am Chem Soc* 1976, **98** 4105
- 10 (a) Cotton, F A , Kraihanzel, C S. *J Am Chem Soc* 1962, **84** 4430  
(b) Cotton, F A., Kraihanzel, C S *Inorg Chem* 1963, **2** 533
- 11 Nakamoto, K *J Phys Chem* 1960, **64** 1420
- 12 Creaven, B S , Grevels, F-W , Long, C *Inorg Chem* 1989, **28** 2231
- 13 Creaven, B S *Photochemical, Thermal and Spectroscopic studies of Metal Carbonyl Complexes* Ph.D. Thesis, Dublin City University, 1989.
- 14 Zulu, M M , Lees, A J *Inorg Chem* 1988, **27** 1139

- 15 Creaven, B S , Long, C , Howie, R A., Mc Quillan, G P , Low, J. *Inorg Chim Acta* 1989, **157**. 151
- 16 Kolodziej, R M., Lees, A J *Organometallics* 1986, **5** 450
- 17 Kazlauskas, R. J , Wrighton, M. S. *J Am Chem Soc* 1982, **104**. 5784
- 18 Connor, J A , Day, J P , Jones, E M., Mc Ewen, G K. *J Chem Soc , Dalton Trans* 1973, 347
- 19 Schadt, M J , Lees, A J *J Am Chem Soc* 1986, **25**. 672.
- 20 (a) Angelici, R. J., Graham, J R *J Am Chem Soc* 1965, **87** 5586  
 (b) Angelici, R J , Graham, J. R. *J Am Chem Soc* 1966, **88** 3658  
 (c) Angelici, R J , Graham, J R *Inorg Chem* 1967, **6** 988  
 (d) Angelici, R J , Graham, J. R *Inorg Chem* 1967, **6** 2082.
- 21 (a) Schadt, M J , Gresalfi, N J , Lees, A J *J Chem Soc , Chem Commun* 1984, 506  
 (b) Schadt, M J , Gresalfi, N J , Lees, A J *Inorg Chem* 1985, **24** 2942
- 22 (a) Chan, L , Lees, A J *Inorg Chim Acta* 1986, **113**. L3  
 (b) Chan, L , Lees, A J *J Chem Soc , Dalton Trans* 1987, 513  
 (c) Drolet, D P , Chan, L , Lees, A J *Organometallics* 1988, **7** 2502
- 23 Darensbourg, D J , Brown, T L *Inorg Chem* 1968, 1679
- 24 Grevels, F-W , Skibbe, V *J Chem Soc , Chem Commun* 1984, 681
- 25 Angelici, R J *J Organomet Chem Rev* 1968, **3** 173
- 26 Ingemanson, C. I., Angelici, R. J. *Inorg Chem* 1968, **7** 2646
- 27 Wrighton, M S *Chem Revs* 1974, **4** 401
- 28 Glerup, J , Goodson, P A , Hodgson, D J , Michelsen, K , Nialsen, K. M., Weihe, H *Inorg Chem* 1992, **31** 4611.
- 29 Connor, J. A., Hudson, G A. *J Chem Soc , Dalton Trans* 1975, 1025
- 30 Marx, D E., Lees, A J *Organometallics* 1986, **5** 2072
- 31 Marx, D. E., Lees, A. J. *Inorg Chem* 1987, **26**: 2254.
- 32 Darensbourg, D J , Dennenberg, R J *Inorg Chem* 1972, **11** 72



- 33    Howie, R. A., Izquierdo, G., Mc Quillan, G. P. *Inorg Chim Acta* 1983, 72, 165
- 34    Data collection by Dr R. A. Howie, University of Aberdeen, Meston Walk, Aberdeen, AB9 2VE, Scotland.
- 35    Marx, D. E., Lees, A. J. *Inorg Chem* 1987, 26, 2254
- 36    Oishi, S. *Organometallics* 1988, 7, 6 1237
- 37    *Purification of Laboratory Chemicals* Perrin, D. D., Armarego, W. L. F., Perrin, D. R. Pergamon Press, Oxford, New York, Toronto, 1980
- 38    *Basic reaction kinetics and mechanisms* Avery, H. E. Macmillan education, London, 1991

ξ

## **Chapter 4**

**The molecular structure determination of  $\text{W(CO)}_5(\text{bipyam})$  and infrared spectroscopic analysis of the complex in the solid and solution state.**

## 4.1 Introduction

With the advent of modern technology, one may question the purpose of X-ray structure determination when high resolution infrared spectroscopy can yield qualitative structural information and, in favourable circumstances, high field NMR can provide estimates of distances between identified atoms. However, crystallography is unique in providing a complete three dimensional molecular representation of the atoms in a crystal. This method of structural determination is invaluable in relating structural features to chemical reactivity. For example, molecular strain will be evident from a crystal structure which would explain the reactivity of a complex in solution. Features of the molecular geometry such as bond angles and interatomic distances may also be readily calculated.

Any crystal may be regarded as being built up by the continuing three dimensional repetition of some basic structural pattern, which may comprise one or more atoms, a molecule, or a complex assembly of molecules. In order to determine the detail of molecular structure it is necessary to use X-radiation of a wavelength comparable to the spacing of atoms in a molecule (usually  $\lambda < 2\text{\AA}$ )<sup>1</sup>. The electronic fields of X-rays interact with the electron clouds of atoms and because of their shorter wavelength, X-rays, scattered by adjacent atoms in crystals, can interfere and diffraction effects become important. The diffraction pattern reveals much about the internal arrangement of the crystal. There is a three dimensional pattern of electron density, corresponding to the three dimensional atomic pattern of the crystal, all of which takes part in the scattering of X-rays. A diffracted beam behaves as if it were being reflected from the electron layer and thus they are termed reflections. The diffracted pattern is recorded by measuring the reflections with some form of counter.

The first step in studying the diffraction pattern is to study the positions of the reflections with the objective of determining the shape and size of the unit cell. The second is to study the intensity of the reflections in the hope of deducing details of the atomic arrangements within the cell. Often a structure determination begins by computing the Patterson function of the crystal which gives the resulting function as a map of interatomic vectors. The height of a peak in the Patterson function will be proportional to the product of the number of electrons in each of the atoms. When a solution, believed to be approximately correct, has been obtained, it must be refined to give the best possible fit between observed and calculated data. The refinement procedure involves a 'crude' structure determination from the observed structure factors and the calculated electron density functions. A set of structure factors, allowing for thermal effects, is calculated and a new electron density map and structure is calculated from the observed structure factors and calculated phases.

When a reproducible model has been obtained, a difference Fourier map is produced permitting further refinement. This allows for the identification of missing atoms and the refinement of thermal parameters. Using least squares refinement, which represents the best fit with the observed data, a model of the structure is obtained. The final result is a difference map, which essentially consists of the true electron density minus the electron density resultant from the assumed structure<sup>2</sup>. If the assumed structure is correct, the difference map should be featureless. At each stage in the refinement process an R value is calculated which represents the correlation between the calculated and actual structure.

In the determination of the molecular structure of  $\text{W(CO)}_5(\text{bipyam})$ , the data was collected using a four circle diffractometer (Figure 4.1.1), in the University of Aberdeen<sup>3</sup>. This method allows the crystal to be rotated around three axes, while the detector may be rotated about a fourth angle which is the horizontal plane.

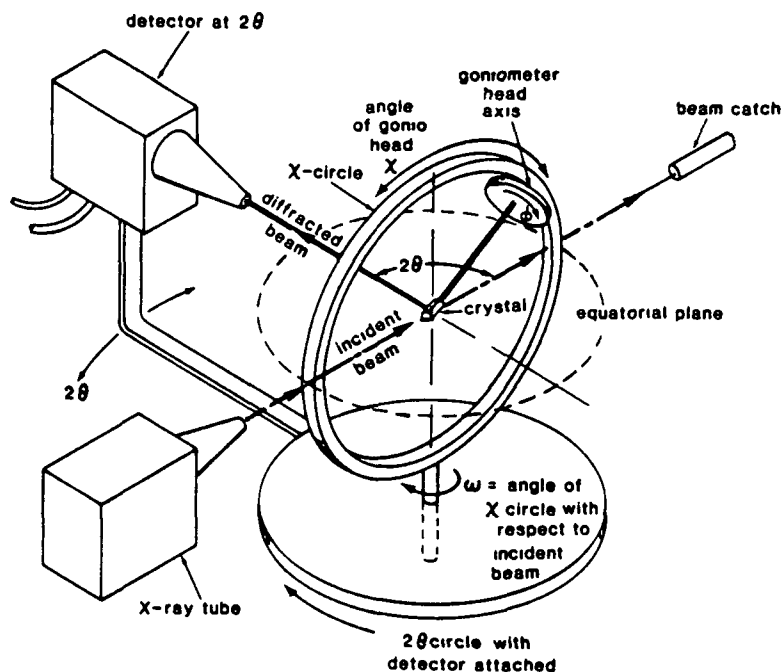


Figure 4 1 1 A schematic diagram of a four circle diffractometer

It was hoped that the determination of the molecular structure of  $\text{W(CO)}_5(\text{bipyam})$  would yield a greater insight into the nature of the amine link of the ligand. The orientation of the amine link, when the ligand was coordinated in a bidentate fashion, was known<sup>4</sup> (Figure 4 1 2), and it was anticipated that the orientation of the amine link in this complex would be different. The orientation of this amine link was important because it would reveal the suitability of this ligand to act as a bridge between two metal centres. The nature of the ligand indicated that it had the capacity to act as a bridge between two metal centres. Also, the molecular structure of

this complex could be used as a model for monodentately coordinated potentially chelating ligands of diimine complexes

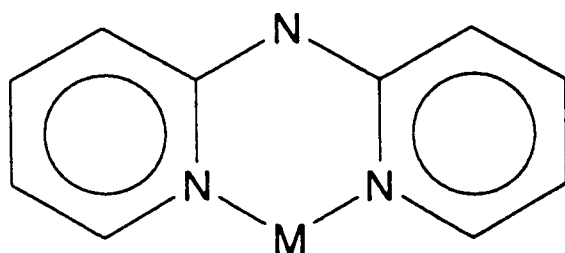


Figure 4 1.2 The orientation of the amine link in the bipyam ligand when its coordinated in a bidentate fashion<sup>4</sup>

## 4.2 Results and discussion

### 4.2.1 Data collection for $\text{W}(\text{CO})_5(\text{bipyam})$

The synthesis of  $\text{W}(\text{CO})_5(\text{bipyam})$  is described in section 3.4. The crystallographic data was collected by Dr R. A. Howie at the University of Aberdeen<sup>3</sup>. A yellow crystal of dimensions 0.26 X 0.52 X 0.26 mm was selected for unit cell determination and intensity data collection. The data was collected on a Nicolet P3 four circle diffractometer using graphite monochromatic  $\text{Mo K}\alpha$  radiation ( $\lambda = 0.7107 \text{ \AA}$ ). The unit cell was found to be monoclinic ( $z = 4$ ) with  $a = 12.812(11)$ ;  $b = 7.187(7)$ ,  $c = 17.835(15) \text{ \AA}$  and  $\beta = 99.61(7)^\circ$  giving a calculated density of  $2.03 \text{ g cm}^{-3}$  for a molecular mass of 494.45 a.m.u. The space group was uniquely defined from the systematic absences to be  $P_{21}/n$ , which is a non-standard setting of  $P_{21}/c$  No. 14. Using the  $\omega/2\theta$  scan technique, the intensities of 4208 unique reflections were measured in the range  $h$  0 to 16;  $k$  0 to 9,  $k$  -23 to 23 out to  $2\theta = 55^\circ$ . The intensities of the two reflections, measured at intervals throughout the data collection, showed no significant variation. An empirical absorption correction factor ( $\mu = 78.87 \text{ cm}^{-1}$ ) was applied (minimum and maximum transmission factors of 0.07 and 0.15 respectively).

The structure determination was completed on the basis of 2972 observed reflections ( $I > 3\sigma(I)$ ). The structure was solved by conventional Patterson and Fourier methods. All calculations were performed on a Digital Corporation VAX 6230 machine using SHELX-86<sup>5</sup> to find all non-hydrogen atoms. The atomic coordinates were refined with full matrix least square refinement using SHELX-76<sup>6</sup>, in which the  $\sum \omega |F_o - F_c|^2$  function was minimised. The maximum peak in the final difference map corresponded to an electron density of less than  $1 \text{ e \AA}^{-3}$ , and the maximum shift/e.s.d. for any non-hydrogen atom in the final stage of refinement was 0.22. R values were calculated to be  $R = 0.049$  and  $R_w = 0.061$ . Atomic scattering for

neutral atoms were obtained, where required, from the International Tables for X-ray Crystallography<sup>7</sup>. The molecular structure for  $\text{W(CO)}_5(\text{bipyam})$  is presented in Figure 4.2.1.1. Table 4.2.1.1 contains the fractional coordinates for the non-hydrogen atoms (hydrogen atom coordinates are presented in Appendix B). The bond lengths and angles for this complex are given in Tables 4.2.1.2 and 4.2.1.3, respectively. All hydrogen atoms are in positions calculated by the SHELX-76<sup>6</sup> except for H2, which was located in the final difference map. Figure 4.2.1.2 shows a representation of the unit cell.



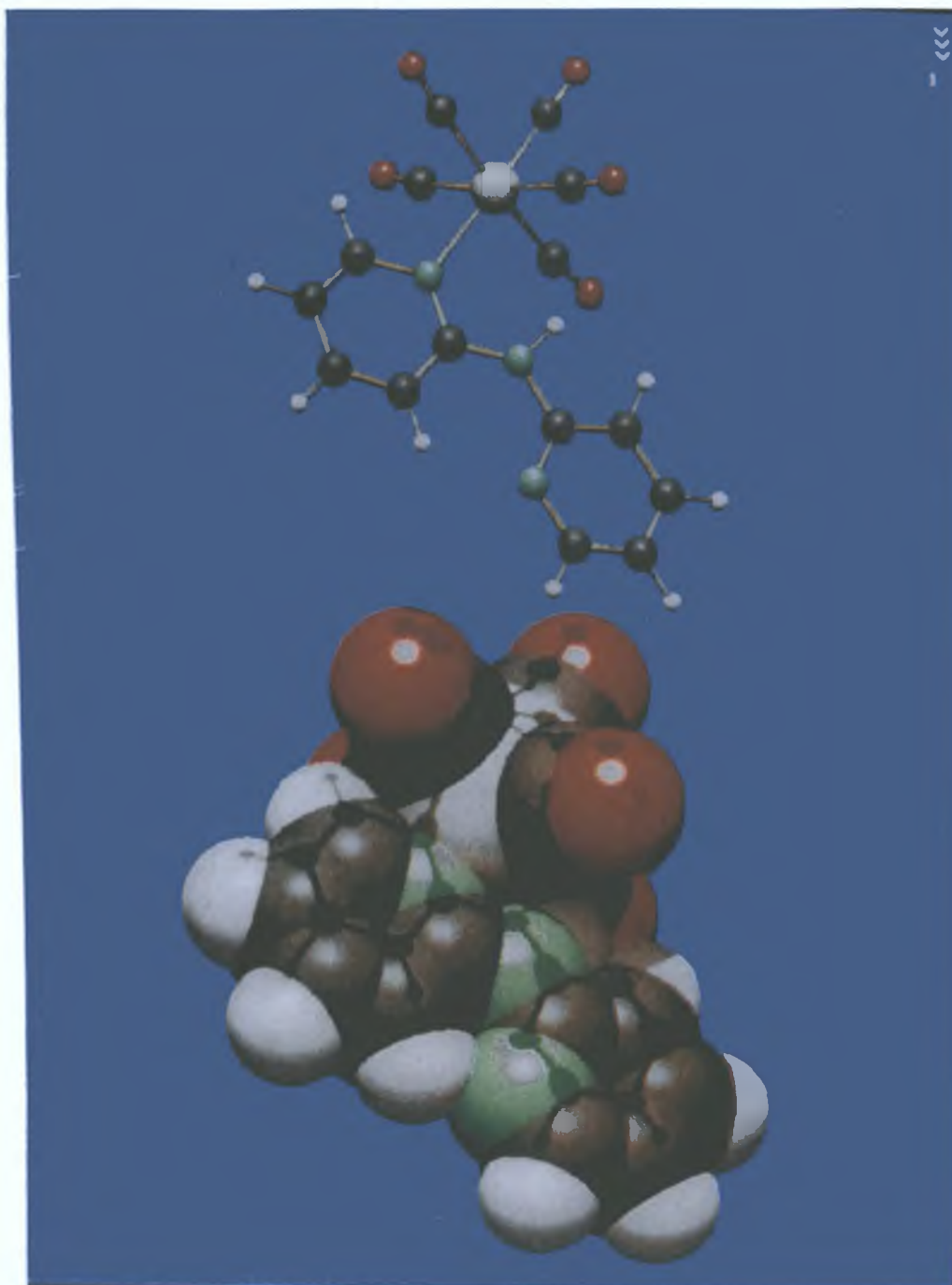


Figure 4.2.1: The molecular structure of  $\text{W(CO)}_5(\text{bipyam})$

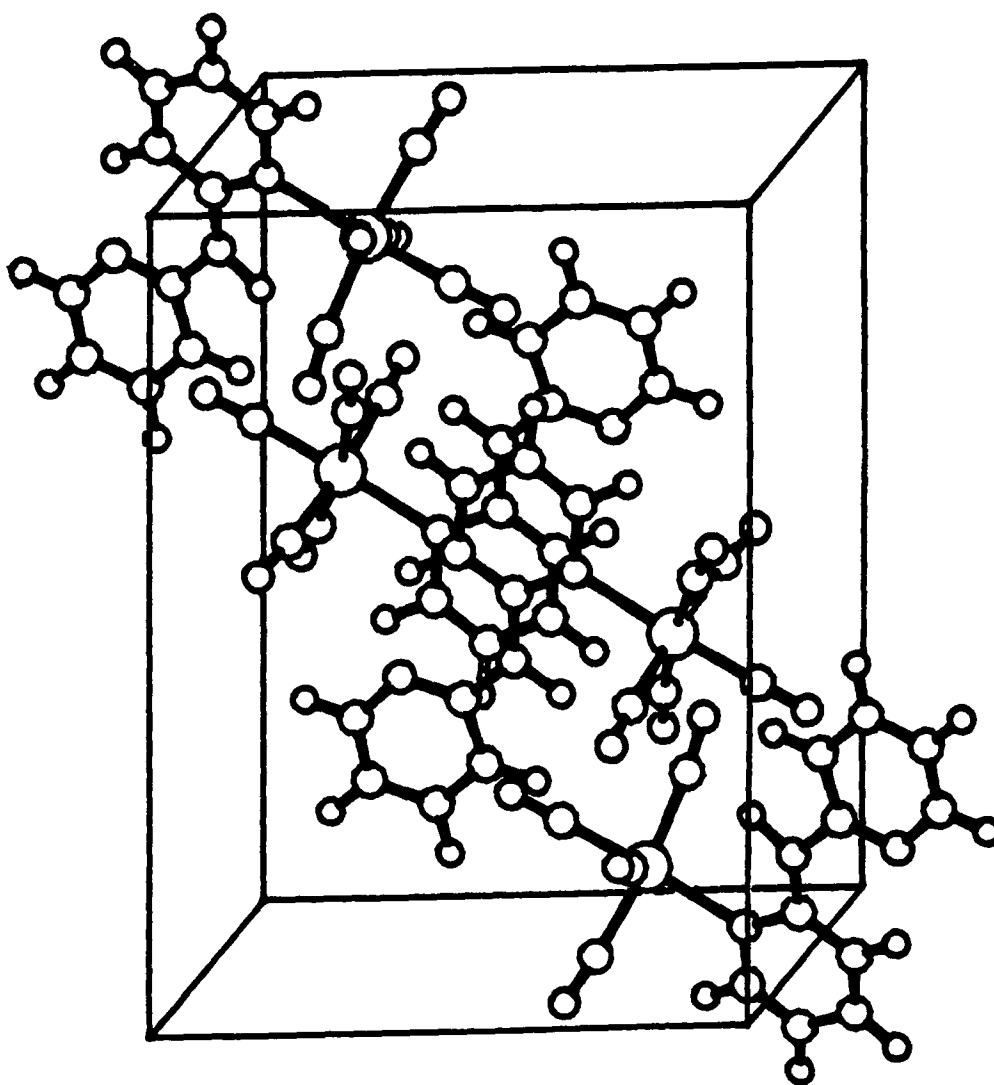


Figure 4 2 2 The representation of the unit cell of  $\text{W}(\text{CO})_5(\text{bipyam})$

Table 4 2 1 1 W(CO)<sub>5</sub>(bipyam) coordinates x 10<sup>4</sup> for non-hydrogen atoms with e s d 's in parentheses Ueq x 10<sup>3</sup>

	x/a	y/b	z/c	Ueq
W1	3185 (1)	2206 (1)	670 (1)	40 (1)
C1	2767 (8)	880 (16)	1567 (7)	48 (3)
C2	2970 (9)	4825 (15)	1094 (7)	48 (3)
C3	3792 (8)	3455 (16)	-185 (7)	44 (3)
C4	3520 (10)	-389 (18)	254 (8)	58 (4)
C5	4619 (11)	2298 (18)	1281 (8)	57 (4)
C6	594 (9)	2432 (15)	104 (7)	45 (3)
C7	-347 (10)	2488 (18)	-437 (8)	59 (4)
C8	-283 (12)	2203 (19)	-1185 (9)	66 (4)
C9	666 (12)	1832 (19)	-1402 (8)	66 (4)
C10	1544 (10)	1844 (14)	-858 (6)	46 (3)
C11	-165 (11)	2862 (16)	1299 (9)	53 (3)
C12	144 (11)	2720 (19)	209 (8)	58 (4)
C13	-1896 (13)	3105 (25)	1455(14)	89 (7)
C14	-1676 (15)	3068 (27)	2207(13)	93 (7)
C15	-600 (16)	2822 (25)	2559(12)	86 (7)
N1	1532 (8)	2166 (13)	-108 (6)	47 (2)
N2	613 (7)	2741 (13)	864 (6)	47 (2)
N3	-1189 (8)	3054 (14)	988 (8)	58 (3)
O1	2634 (7)	143 (14)	2130 (5)	72 (3)
O2	2906 (9)	6200 (13)	1347 (6)	78 (3)
O3	4184 (8)	4093 (17)	-664 (6)	81 (4)
O4	3792 (11)	-1690(17)	37 (8)	89(4)
O5	5455 (9)	2304 (16)	1619 (7)	80(4)

Table 4 2.1.2. W(CO)<sub>5</sub>(bipyam) interatomic distances (Å) e s.d.'s in parentheses.

N1-W1	2 330(10)	C3-W1	2.032(12)
C1-W1	2.011(13)	C5-W1	1.974(14)
C2-W1	2 064(11)	C4-W1	2 078(13)
C6-N1	1 333(15)	C10-N1	1.359(15)
O3-C3	1.156(14)	O1-C1	1 172(14)
C2-O2	1.095(14)	C5-O5	1 138(17)
C7-C6	1 412(17)	N2-C6	1 370(16)
C8-C7	1 368(22)	C9-C8	1 362(21)
C10-C9	1 357(18)	N3-C11	1 344(18)
N2-C11	1 366(17)	C12-C11	1 416(20)
C15-N3	1 331(20)	C14-C15	1 324(30)
C13-C14	1 428(29)	C12-C13	1 359(21)
O4-C4	1 091(16)		

Table 4 2 1 3 W(CO)<sub>5</sub>(bipyam) angles(°) and e s d 's in parentheses

C3-W1-N1	89 0(4)	C1-W1-N1	97 6(4)
C1-W1-C3	173 0(4)	C5-W1-N1	176.8(4)
C5-W1-C3	87 9(5)	C5-W1-C1	85 6(5)
C2-W1-N1	93 8(4)	C2-W1-C5	86.3(5)
C4-W1-N1	89 9(4)	C4-W1-C3	90 0(5)
C4-W1-C1	87.5(5)	C4-W1-C5	89 9(5)
C4-W1-C2	175 8(5)	C6-N1-W1	127 1(8)
C10-N1-W1	115 5(8)	C10-N1-C6	117 5(11)
O3-C3-W1	176 1(11)	O1-C1-W1	172.7(10)
O5-C5-W1	177 7(14)	O2-C2-W1	176 1(12)
C7-C6-N1	121 2(12)	N2-C6-N1	115 8(10)
N2-C6-C7	122.9(12)	C8-C7-C6	118 5(13)
C9-C8-C7	120 6(12)	C10-C9-C8	117 9(13)
C9-C10-N1	124 1(12)	N2-C11- N3	121 7(14)
C12-C11-N3	120 8(13)	C12-C11-N2	117 5(12)
C15-N3-C11	117 6(15)	C14-C15-N3	125.6(18)
C13-C14-C15	118 6(13)	C12-C13-C14	117.5(19)
C11-N2-C6	132 8(11)	C13-C12-C11	120 0(15)
O4-C4-W1	173 1(13)		

#### 4.2.2 The molecular structure of $\text{W(CO)}_5(\text{bipyam})$

The tungsten atom is coordinated to five carbonyl ligands and a bipyam ligand in a distorted octahedral configuration. The W-C bonds vary from 2.078 to 2.197 Å in length. The W-C bonds in  $\text{W(CO)}_6$ <sup>8</sup> were determined to be 2.06 Å in length. The shortest W-C bond length is that between the metal and the axial carbonyl ligand (i.e. *trans* to the ligand). The increase in electron density on the metal is donated to the carbonyl antibonding acceptor orbitals which lowers the W-C bond order. The equatorial carbonyl groups are quite noticeably bent away from the ligand pyridyl rings with CWC angles of 175.8(5) and 173.0(4)°. The presence of the ligand is responsible for the distortion of these carbonyl groups. However, the overall symmetry of the carbonyl ligands is retained to a large extent since a greater deviation from 180° would be observed if the symmetry was completely distorted. The CWN angles vary from 89.0(4) to 97.6(4)° indicative of the distortion from a perfect octahedral structure, as in  $\text{W(CO)}_6$  in which the angles are all at 90°. This crowding effect has been noted by other workers with complexes in which the ligand is coordinated in a bidentate fashion<sup>4</sup>.

The bipyam ligand is coordinated to the metal *via* one pyridyl-nitrogen (N1) atom, while the second pyridyl-nitrogen (N3) is arranged so as to point away from the metal. The central secondary nitrogen atom (N2) does not interact with the metal atom and retains the planar conformation (C11-N2-C6 = 132.8(11)°). A mean plane calculation for the bipyam ligand indicated that the ligand is essentially planar. This planar conformation is found in the free ligand<sup>9</sup> and in other complexes containing the bipyam ligand<sup>4,10-13</sup>. A comparison of the angles for these conformations is found in Table 4.2.2.1. The conformation of the dipyam ligand, with respect to the metal pentacarbonyl unit, restricts the amine bridge link to an orientation in which the

secondary amine nitrogen (N2) is forced towards the *cis*-carbonyl ligands (Figure 4.2 1 1)

Table 4 2 2 1. A comparison of the angles for the conformation of the amine link in complexes containing the bipyam ligand

Complex	Angle	Reference
W(CO) <sub>5</sub> (bipyam)	132 8(11)	this work
W(CO) <sub>4</sub> (bipyam)	126 2(1 6)	4
Mo(CO) <sub>4</sub> (bipyam)	129 3(1)	4
Cr(CO) <sub>4</sub> (bipyam)	126 4(1.3)	4
[Zn(dien)(bipyam)][NO <sub>3</sub> ] <sub>2</sub>	134 5(7)	13
bipyam	131 1(4)	9

[Zn(dien)(bipyam)][NO<sub>3</sub>]<sub>2</sub>= *Bis*-(2-aminoethyl)amine(bipyam)zinc(II)nitrates

In compounds where bipyam acts as a chelate ligand, the amine link points away from the metal centre, so as to minimise the interaction between the pyridyl ring protons (Figure 4 1 2) and to improve the 'bite' angle of the chelate ligand at the metal centre<sup>4</sup> Consequently, in this complex the amine hydrogen (H2), which was observed in the final difference map, is sufficiently close to the *cis* carbonyl group C1-O1 to be involved in an intramolecular interaction (H2-C1 distance= 2.1Å; H2-O1 distance= 2.61Å) The close proximity of the amine hydrogen and the *cis* carbonyl ligand is presented quite clearly in Figure 4 2 1.1 The usual criterion for NH-O bonding requires an O-H distance of less than about 2 4-2 6Å<sup>14</sup> The H2-O1 distance is 2 61Å for this complex which could be assumed too great for an intramolecular interaction. The existence of a hydrogen bond of any strength cannot be conclusively established or disproved using the X-ray data alone

Any hydrogen bonding interaction will tend marginally to lengthen the NH bond and cause it to bend towards O1 so that the actual H2-O1 distance is likely to be somewhat less than the calculated 2.61Å. To this end we have employed the use of infrared spectroscopy to monitor the stretching of the NH band in various solvent phases. It was found that the energy of the  $\nu_{\text{NH}}$  band in the  $\text{W}(\text{CO})_5(\text{bipyam})$  complex is lowered compared to that in the free ligand. Table 4.2.2.2 presents the  $\nu_{\text{NH}}$  stretching frequencies of the  $\text{W}(\text{CO})_5(\text{bipyam})$  complex in a variety of solvent phases. The  $\text{NH}^{15}$  stretching frequency in free, non-hydrogen-bonded bipyam is  $3425\text{cm}^{-1}$ .

Table 4.2.2.2 The infrared spectral data relating to the bipyam ligand

Compound	$\nu_{\text{NH}} (\text{cm}^{-1})$	$\nu_{\text{CO}} (\text{cm}^{-1})$	Medium
bipyam <sup>15</sup>	3425		$\text{CCl}_4$
$\text{W}(\text{CO})_6$	-	1974	Chlorobenzene
$\text{W}(\text{CO})_5(\text{bipyam})$	3332	2071, 1976, 1926	$\text{CCl}_4$
	3325		Nujol mull
	3328		kBr
			Chlorobenzene
$\text{W}(\text{CO})_4(\text{bipyam})^4$	3400	2005, 1883, 1860, 1822	$\text{CH}_2\text{Cl}_2$
	3337	2004, 1892, 1860, 1777	Nujol mull

In the  $\text{W}(\text{CO})_5(\text{bipyam})$  complex the  $\nu_{\text{NH}}$  is lowered by approximately  $100\text{cm}^{-1}$  compared to that observed for the free ligand. The insensitivity of this  $\nu_{\text{NH}}$  band to either sample phase or solvent nature provides evidence that the ligand conformation observed in the crystal is maintained in solution. In the  $\text{W}(\text{CO})_4(\text{bipyam})^4$  complex the shortest intermolecular distance, not involving hydrogen atoms, was determined to be 2.99Å, between the amine nitrogen and a carbonyl oxygen in an adjoining molecule, with a corresponding H-O distance of



2.19Å. The bipyam ligand is ideally designed for intermolecular hydrogen bond formation, when the ligand is coordinated in a bidentate manner with the acid central NH group pointing away from the metal centres. It was accepted<sup>4</sup> that the structural and spectroscopic data consistently implicated the presence of a weak but significant intermolecular bond in the crystalline W(CO)<sub>4</sub>(bipyam). The spectroscopic solution data indicated the maintenance of the weak intermolecular hydrogen bonding in the solution state also.

The C-N bonds in the amine link (C6-N2 and N2-C11) are both shorter than expected for C-N single bonds, although similar to those observed in other metal complexes containing the bipyam ligands<sup>4,10,12,13</sup>. A comparison of the C-N bond lengths in the amine link for complexes containing the bipyam ligand are presented in Table 4.2.2.3.

Table 4.2.2.3: A comparison of the C-N bond lengths in the amine link for complexes containing the bipyam ligand.

Complex	C6-N2	N2-C11	Reference
W(CO) <sub>5</sub> (bipyam)	1.37(16)	1.366(17)	this work
Mo(CO) <sub>4</sub> (bipyam)	1.39(1)	1.38(2)	4
[Zn(dien)(bipyam)][NO <sub>3</sub> ] <sub>2</sub>	1.375(12)	1.396(13)	13
Pd(C <sub>10</sub> H <sub>8</sub> N <sub>3</sub> ) <sub>2</sub>	1.373(16)	1.327(16)	12
Cu(bpa)(bipyam)(NO <sub>3</sub> ) <sub>2</sub>	1.33(16)	1.42(16)	10

Pd(C<sub>10</sub>H<sub>8</sub>N<sub>3</sub>)<sub>2</sub>= *Bis*-(2,2'-dipyridyliminato)palladium(II)

Cu(bpa)(bipyam)(NO<sub>3</sub>)<sub>2</sub>= *Bis*-(3-aminopropyl)amine(bipyam)copper(II) Nitrate

The covalent radii of carbon and nitrogen are 0.77 and 0.74Å respectively. The shortest C-N bond length in the amine link is the N2-C11 bond of 1.366(17)Å. This

distance is less than the van der Waals radius sum for carbon and nitrogen to form a single bond. A C-N bond length of 1.34 Å is normal for that in a pyridine ring and in aromatic compounds<sup>16</sup>. It appears, from the comparison of C-N bond lengths in the pyridine ring, that the C-N bonds in the amine link have considerable double bond character. Other workers have proposed this also with the complexes tabulated above, in which the bipyam ligand is coordinated in a bidentate fashion. The angle of the amine link was determined to be 132.8(11)° and this is also suggestive of the double bond character of the C-N bonds in the amine link, permitting interaction of the two pyridyl  $\pi$  systems.

The mechanism of chelate formation of complexes of the type  $M(CO)_5(L)$  ( $M = Cr, Mo, \text{ or } W$ ,  $L =$  diamine ligands), was assumed to occur *via* an intramolecular carbonyl extrusion process to yield the  $M(CO)_4(L)$  species. It would appear that these structural features preclude a facile rearrangement of the ligand to assist in an intramolecular carbonyl extrusion to form the chelate species,  $W(CO)_4(bipyam)$ . The results presented in Chapter 3 support this assumption.

### 4.3 Summary

The molecular structure of  $\text{W}(\text{CO})_5(\text{bipyam})$  was determined as a model for monodentately coordinated bpy ligands. The overall symmetry of the complex was determined to be pseudo  $\text{C}_{4v}$  which was retained despite the carbonyl groups bending away from the ligand. The bond lengths and angles at the tungsten atom are within the range reported for similar compounds. The bipyam ligand is coordinated to the metal *via* one pyridyl nitrogen atom while the second pyridyl nitrogen is arranged so as to point away from the metal.

In complexes where bipyam acts as a chelate ligand, the amine link points away from the metal centre so as to minimise the interaction between the pyridyl ring protons and to improve the 'bite' angle of the chelate ligand at the metal centre<sup>4</sup>. We have proposed intermolecular hydrogen bonding between the amine nitrogen and one of the carbonyl groups C1O1. The NH stretching frequencies of the complex were monitored in various solvent phases in an effort to determine this interaction. The  $\nu_{\text{NH}}$  of the complex was lowered compared to that of the free ligand<sup>15</sup> and the insensitivity of this band to either sample phase or solvent nature provides evidence that the ligand conformation observed in the crystal is also maintained in solution.

The C-N bonds in the amine link are both shorter than expected for C-N single bonds but similar to those observed in other metal complexes containing the bipyam ligand<sup>4,10,12,13</sup>. The angle of the amine link was found to be  $132.8(11)^\circ$ . This would suggest that the C-N bonds in the amine link possess considerable double bond character, allowing interaction of the two pyridyl  $\pi$  systems. It had been assumed, from previous investigations, that the mechanism of chelate formation occurred *via* an intramolecular carbonyl extrusion process. Together with the results presented in Chapter 3 it appears that the structural features prevent facile rearrangement of the

ligand to assist in an intramolecular carbonyl species to form the chelate species,  $W(CO)_4(bipyam)$ . Also, the observation of the regeneration of the parent hexacarbonyl complex does not support the assumption of an intramolecular carbonyl extrusion process. The results presented here indicate that the mechanism of chelate formation is not as simple as once thought.

#### 4.4 References

- 1 Glusker, J P., Trueblood, K N *Crystal Structure Analysis* Oxford University Press 1985
- 2 Glasser, L S D *Crystallography and its Applications* Van Nostrand Reinhold (UK) Co Ltd , 1977
- 3 Dr R. A Howie, University of Aberdeen, Meston Walk, Aberdeen, AB9 2VE, Scotland
- 4 Howie, R A., Izqueirido, G , Mc Quillan, G P *Inorg Chim Acta* 1983, **72** 165
- 5 Sheldrick, G M SHELX-86 Programme for Crystal Structure Determination. Instut fur Anorganische Chemie der Universitat, Tammannstrasse 4, D-3400, Gottingen, Federal Republic of Germany
- 6 Sheldrick, G M SHELX-76 Programme for Crystal Structure Determination. Cambridge University, Cambridge, England, 1976
- 7 *International Tables for X-ray Crystallography* Vol 4, Kynoch Press, Birmingham Ibers, J A , Hamilton, W C (Eds ), 1974
- 8 *Comprehensive Organometallic Chemistry* Vol. 3, Pergamon Press, Oxford. Wilkinson, G , Stone, F G A , Abel, E W (Eds ), 1982.
- 9 Johnson, J E , Jacobson, R A *Acta Cryst* 1973, **B29** 1669
- 10 Ray, N J , Hathaway, B J *Acta Cryst* 1978, **B34** 3224
- 11 Johnson, J E , Beinecke, T A , Jacobson, R A *J Chem Soc ,(A)* 1971, 1371
- 12 Freeman, H C , Snow, M R *Acta Cryst* 1965, **18** 845
- 13 Ray, N J , Hathaway, B J *J Chem Soc , Dalton Trans* 1980, 1105
- 14 Hamilton, W C , Ibers, J A. *Hydrogen Bonding in Solids* Benjamin, New York, 1968
- 15 Sobczyk, L , Koll, A , Malarski, Z *Bull Acad Pol Sci Ser Sci Chim* 1965, **13** 403
- 16 Bak, B , Hausen, L , Rastrup-Anderson, J *J Chem Phys* 1954, **22** 2013.

## **Appendix A**

Table A 1 The values obtained for the comparison of the energy difference between bpy and its conjugate acid, in various solvent polarities

Theta	D= 1	D= 2	D= 3.5	D= 5	D= 7.5	D= 10
0	24 919	35 702	40 723	42 886	44 670	45 698
15	24 933	35 704	40 720	42 882	44 665	45 603
30	24 961	35 702	40 706	42 864	44 644	45 582
45	24 988	35 695	40 685	42 837	44 614	45 549
60	25 010	35 689	40 667	43 813	44 585	45 517
75	25 027	35 689	40 657	42 797	44 562	45 491
90	25 038	35 695	40 655	42 788	44 546	45 469
105	25 044	35 706	40 661	42 788	44 535	45 452
120	25 044	35 724	40 676	42 795	44 533	45 441
135	25 039	35 744	40 696	42 809	44 535	45 436
150	25 022	35 758	40 709	42 815	44 530	45.423
165	24 990	35 751	40 701	42 800	44 505	45 390
180	24 969	35 739	40 688	42 754	44 485	45 366

Table A 2 The values obtained for the comparison of the energy difference between dimethyldimine and its conjugate acid in various solvents.

Theta	D= 1	D= 2.5	D= 5	D= 7.5	D= 10	D= infin
0	21 9782	33 327	35 1347	35 4865	35 6112	35 771
15	22 0317	33 319	35 1549	35 5024	35 6249	35.787
30	22.157	33 342	35 1935	35 5293	35 646	35 791
45	22 2907	33 414	35 2331	35 5532	35 6621	35 791
60	22 42	33 578	35 271	35 575	35 6757	35 79
75	22 52	33 634	35 2998	35 5916	35 6864	35 79
90	22 575	33 659	35 3109	35 598	35 6907	35 99
105	22.5804	33 647	35 3018	35 5921	35 6869	35 792
120	22.5437	33 604	35 2756	35 5756	35 6753	35 79
135	22 4823	33 547	35 2407	35 5528	35 659	35 786
150	22.4178	33 475	35 2074	35 5304	35 6423	35.781
165	22 3701	33 445	35 1842	35 5143	35 6299	35 776
180	22 3525	33 441	35 176	35 5086	35 6281	35 774



**Appendix B**

Table B 1 W(CO)<sub>5</sub>(bipyam) coordinates x 10<sup>4</sup> for non-hydrogen atoms with e.s d.'s in parentheses  $U_{eq} \times 10^3 U = (1/3) \sum_i \sum_j U_{ij} a_i^* a_j^* a_i a_j$

	x/a	y/b	z/c	U <sub>eq</sub>
W1	3185 (1)	2206 (1)	670 (1)	40 (1)
N1	1532 (8)	2166 (13)	-108 (6)	47 (2)
N2	613 (7)	2741 (13)	864 (6)	47 (2)
N3	-1189 (8)	3054 (14)	988 (8)	58 (3)
O1	2634 (7)	143 (14)	2130 (5)	72 (3)
O2	2906 (9)	6200 (13)	1347 (6)	78 (3)
O3	4184 (8)	4093 (17)	-664 (6)	81 (4)
O4	3792 (11)	-1690 (17)	37 (8)	89 (4)
O5	5455 (9)	2304 (16)	1619 (7)	80 (4)
C1	2767 (8)	880 (16)	1567 (7)	48 (3)
C2	2970 (9)	4825 (15)	1094 (7)	48 (3)
C3	3792 (8)	3455 (16)	-185 (7)	44 (3)
C4	3520 (10)	-389 (18)	254 (8)	58 (4)
C5	4619 (11)	2298 (18)	1281 (8)	47 (4)
C6	594 (9)	2432 (15)	104 (7)	45 (3)
C7	-347 (10)	2488 (18)	-437 (8)	59 (4)
C8	-283 (12)	2203 (19)	-1185 (9)	66 (4)
C9	666 (12)	1832 (19)	-1402 (8)	66 (4)
C10	1544 (10)	1844 (14)	-858 (6)	46 (3)
C11	-165 (11)	2862 (16)	1299 (9)	53 (3)
C12	144 (11)	2760 (19)	2098 (8)	58 (4)
C13	-600 (16)	2822 (25)	2559 (12)	86 (7)
C14	-1676 (15)	3068 (27)	2207 (13)	93 (7)
C15	-1896 (13)	3105 (25)	1455 (14)	89 (7)

Table B 2  $W(CO)_5(bipyam)$  anisotropic temperature factors  $\times 10^3$  with e.s.d.'s in parentheses

	<b>U11</b>	<b>U22</b>	<b>U33</b>	<b>U23</b>	<b>U13</b>	<b>U12</b>
W1	37 (1)	49 (1)	36 (1)	1 (1)	9 (1)	0 (1)
C1	43 (5)	46 (5)	56 (7)	-8 (5)	10 (5)	3 (4)
C2	52 (6)	41 (6)	54 (6)	-6 (5)	23 (5)	-1 (4)
C3	35 (5)	43 (5)	53 (6)	-4 (5)	7 (4)	-1 (4)
C4	64 (7)	48 (6)	62 (8)	3 (6)	17 (6)	4 (5)
C5	51 (7)	66 (7)	54 (7)	14 (6)	9 (6)	0 (5)
C6	42 (5)	45 (6)	48 (6)	10 (5)	9 (5)	-1 (4)
C7	45 (6)	73 (8)	57 (8)	4 (6)	1 (6)	0 (5)
C8	57 (8)	71 (8)	59 (8)	3 (6)	-21 (6)	-4 (6)
C9	77 (9)	60 (8)	55 (7)	-12 (6)	-5 (6)	-19 (6)
C10	66 (6)	28 (5)	44 (6)	-9 (4)	6 (5)	7 (4)
C11	54 (7)	41 (5)	64 (8)	-2 (5)	18 (6)	2 (5)
C12	47 (7)	84 (9)	44 (6)	-9 (6)	11 (5)	2 (5)
C13	53 (8)	105 (13)	116 (16)	-9 (11)	38 (10)	9 (8)
C14	69 (10)	126 (16)	93 (14)	-20 (11)	41 (10)	3 (9)
C15	80 (12)	105 (13)	82 (12)	-6 (9)	44 (11)	-3 (9)
N1	45 (5)	48 (5)	48 (5)	1 (4)	9 (4)	-2 (4)
N2	33 (4)	57 (5)	51 (5)	-1 (4)	6 (4)	3 (4)
N3	39 (5)	55 (6)	81 (8)	-7 (5)	12 (5)	11 (4)
O1	76 (6)	88 (7)	55 (5)	15 (5)	22 (5)	13 (5)
O2	109 (8)	51 (6)	78 (7)	-12 (5)	30 (6)	3 (5)
O3	90 (7)	99 (8)	60 (6)	12 (6)	31 (5)	-16 (6)
O4	105 (9)	71 (7)	99 (10)	-11 (6)	43 (8)	21 (6)
O5	53 (6)	115 (9)	67 (7)	14 (6)	-1 (5)	-13 (5)

Table B 3  $W(CO)_5(bipyam)$  coordinates  $\times 10^4$  for hydrogen atoms

	<b>x/a</b>	<b>y/b</b>	<b>z/c</b>
H2	1322	2443	1292
H7	-1098	2749	-257
H8	-994	2268	-1606
H9	717	1550	-1989
H10	2297	1561	-1030
H12	971	2625	2342
H13	-2719	3213	1198
H14	-2293	3218	2549
H15	-392	2719	3170

Table B 4  $W(CO)_5(bipyam)$  anisotropic temperature factors  $\times 10^3$  with e.s d 's in parentheses

	<b>U11</b>	<b>U22</b>	<b>U33</b>	<b>U23</b>	<b>U13</b>	<b>U12</b>
W1	37 (1)	49 (1)	36 (1)	1 (1)	9 (1)	0 (1)
N1	45 (5)	48 (5)	48 (5)	1 (4)	9 (4)	-2 (4)
C3	35 (5)	43 (5)	53 (6)	-4 (5)	7 (4)	-1 (4)
C1	43 (5)	46 (5)	56 (7)	-8 (5)	10 (5)	3 (4)
O2	109 (8)	51 (6)	78 (7)	-12 (5)	30 (6)	3 (5)
O5	53 (6)	115 (9)	67 (7)	14 (6)	-1 (5)	-13 (5)
O1	76 (6)	88 (7)	55 (5)	15 (5)	22 (5)	13 (5)
O3	90 (7)	99 (8)	60 (6)	12 (6)	31 (5)	-16 (6)
C5	51 (7)	66 (7)	54 (7)	14 (6)	9 (6)	0 (5)
C2	52 (6)	41 (6)	54 (6)	-6(5)	23 (5)	-1 (4)
C6	42 (5)	45 (6)	48 (6)	10 (5)	9 (5)	-1(4)
C7	45 (6)	73 (8)	57 (8)	4 (6)	1 (6)	0 (5)
C8	57 (8)	71 (8)	59 (8)	3 (6)	-21 (6)	-4 (6)
C9	77 (9)	60 (8)	55 (7)	-12 (6)	-5 (6)	-19 (6)
C10	66 (6)	28 (5)	44 (6)	-9 (4)	6 (5)	7 (4)
C11	54 (7)	41 (5)	64 (8)	-2 (5)	18 (6)	2 (5)
N3	39 (5)	55 (6)	81 (8)	-7 (5)	12 (5)	11 (4)
C15	53 (8)	105 (13)	116 (16)	-9 (11)	38 (10)	9 (8)
C14	69 (10)	126 (16)	93 (14)	-20 (11)	41 (10)	3 (9)
C13	80 (12)	105 (13)	82 (12)	-6 (9)	44 (11)	-3 (9)
N2	33 (4)	57 (5)	51 (5)	-1 (4)	6 (4)	3 (4)
C12	47 (7)	84 (9)	44 (6)	-9 (6)	11 (5)	2 (5)
C4	64 (7)	48 (6)	62 (8)	3 (6)	17 (6)	4 (5)
O4	105 (9)	71 (7)	99 (10)	-11 (6)	43 (8)	21 (6)